2

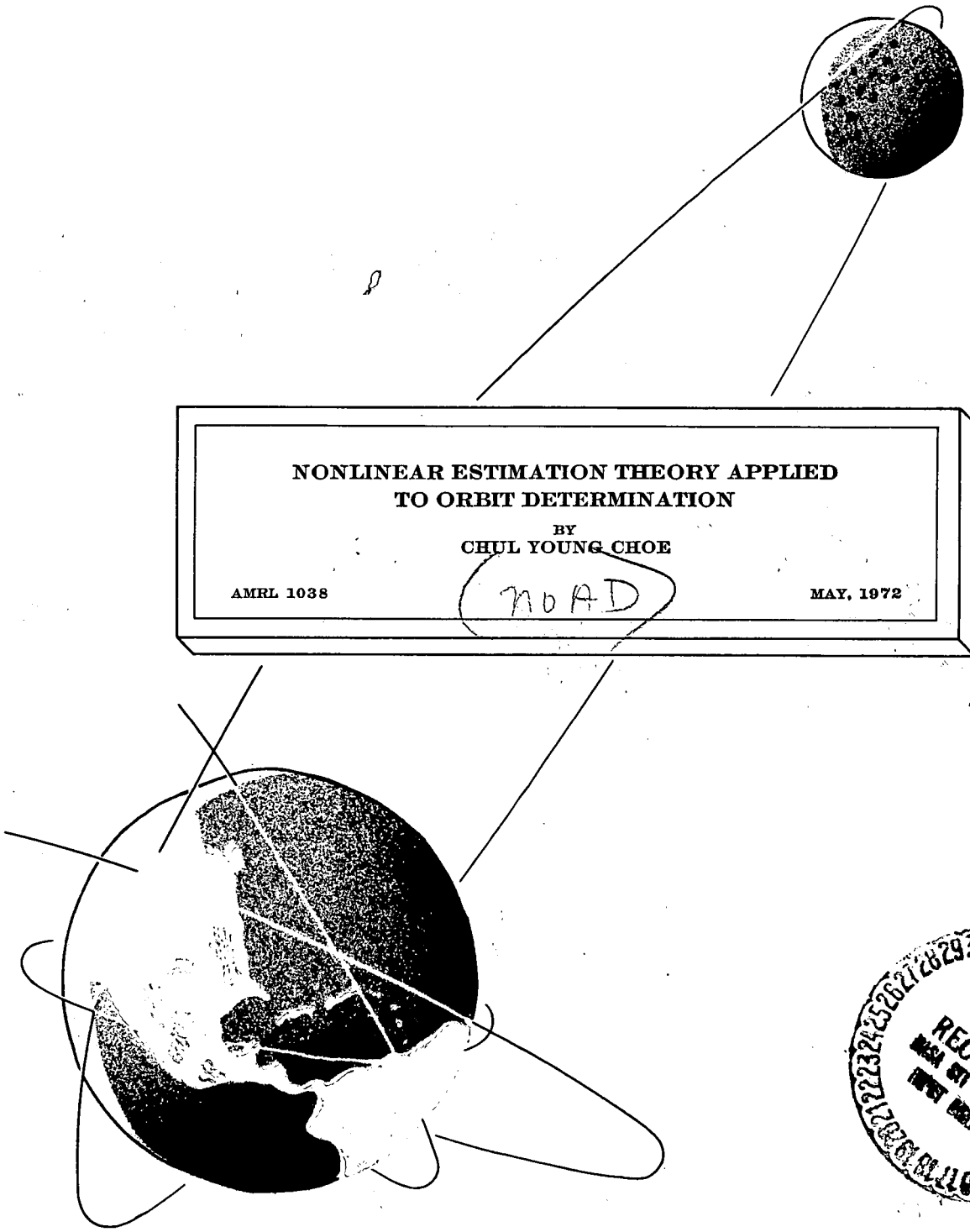

NONLINEAR ESTIMATION THEORY APPLIED TO ORBIT DETERMINATION

BY
CHUL YOUNG CHOE

AMRL 1038 MAY, 1972

NoAD

APPLIED MECHANICS RESEARCH LABORATORY
THE UNIVERSITY OF TEXAS AT AUSTIN AUSTIN, TEXAS

202

NONLINEAR ESTIMATION THEORY APPLIED TO ORBIT DETERMINATION

Chul Young Choe, B.S., M.E.
The University of Texas at Austin
Austin, Texas

AMRL 1038
May, 1972

Applied Mechanics Research Laboratory
The University of Texas at Austin
Austin, Texas

This report was prepared under

Contract No. NGL 44-012-008
for the
National Aeronautics and Space Administration
Headquarters

and

Contract No. AFOSR 72-2233
for the
Air Force Office of Scientific Research

by the

Applied Mechanics Research Laboratory
The University of Texas at Austin
Austin, Texas

under the direction of

Byron D. Tapley
Professor and Chairman

PREFACE

The practical implications of linear sequential filtering (or Kalman-Bucy filtering) theory were quickly recognized by the engineering community as an important contribution to real-time data processing. Some of its numerous successful applications have been made to aerospace engineering system. The typical examples are orbit determination and trajectory estimation problems. Since these problems generally are concerned with continuous nonlinear dynamic systems and discrete observations, nonlinear filtering has been a theme of interest in the field of orbit determination.

It has been demonstrated that the optimal nonlinear filter requires the computation of an infinite number of moments and generally its implementation is not practical. This leads one to seek an approximate solution to the optimal nonlinear filtering problem. Several approximate nonlinear filters have been proposed previously and, for the most part, these can be classified as one of two basic types of second order filters. The first is the truncated second order filter which utilizes a Taylor series expansion of the dynamic system and the state-observation relationships, followed by a truncation of the third and higher order moments. The other is the Gaussian second order filter which employs a Taylor series expansion and approximations of the fourth order moments in terms of the second order moments, under the assumption that the conditional density function is Gaussian. The unique feature of both filters is found in the fact that a random forcing term occurs in the covariance equation. The random forcing term which enters into the covariance equation in a linear manner is considered to have potential for causing the conditional covariance matrix to be negative definite over some non-zero time interval. This term is often neglected in the modified Gaussian or

truncated second order filters.

This study is concerned with the development of an approximate nonlinear filter using the Martingale theory and appropriate smoothing properties. Both the first order and the second order moments are estimated. The filter, which is developed, can be classified as a modified Gaussian second order filter. Its performance is evaluated in a simulated study of the problem of estimating the state of an interplanetary space vehicle during both a simulated Jupiter fly-by and a simulated Jupiter orbiter mission. In addition to the modified Gaussian second order filter, the modified truncated second order filter is evaluated also in the simulated study. Results obtained with each of these filters are compared with numerical results obtained with the extended Kalman filter and the performance of each filter is determined by comparison with the actual estimation errors. The simulations are designed to determine the effects of the second order terms in the dynamic state relations, the observation-state relations and in the Kalman gain compensation term. The result of an extensive simulation shows that the Kalman gain compensated filter which includes only the Kalman gain compensation term is superior to all of the other filters.

Special gratitude is expressed to Dr. B. D. Tapley for serving as supervising professor during this research. His encouragement and guidance during the author's course of study at The University of Texas at Austin are greatly appreciated. The author would also like to thank Dr. W. T. Fowler, Dr. J. R. Dickerson and Dr. D. G. Lainiotis for serving on the supervising committee. Also, special appreciation is extended to Mrs. Hope Ince for her skillful typing of the manuscript.

The author wishes to acknowledge the financial support given the

author by the National Aeronautics and Space Administration under Grant NGL 44-012-008 and the Air Force Office of Scientific Research under Grant AFOSR 72-2233 during the course of his graduate studies. The author thanks Dr. D. W. Jones and Dr. B. E. Schutz for their assistance with the development of the computer program. The encouragement of Mr. and Mrs. John L. Engvall was especially appreciated.

Finally, the author would like to express his deep appreciation to his wife, Dong-Ok, and his daughters, Caroline and Rachel, and his parents, Mr. and Mrs. Joon-Ill Choe, for their understanding, encouragement and patience during the course of his graduate studies.

Chul Young Choe

December, 1971
Austin, Texas

TABLE OF CONTENTS

LIST OF SYMBOLS

The following list tabulates all of the significant symbols used in this study and each symbol is accompanied by a brief description.

n	the number of state variables
m	the number of different types of observations
t	indicates a particular instant of time at which a discrete observation is made
x_t	state variable at time t
x_{t+s}	state variable at time $t+s$
y_i	observation at time $t = i$
Y_t	available observations at time t, that is, $Y_t \equiv \{y_i : 0 \leq i \leq t\}$ or the σ-field generated by the observations
$f(x,t)$	state dynamic equation, $n \times 1$ vector
f_x	partial derivatives of $f(\cdot)$ ω.r.t.x , $n \times n$ matrix
$h(x)$	state-observation relationship, $m \times 1$ vector
h_x	partial derivatives of $h(\cdot)\omega$.r.t.x , $m \times n$ matrix
f_i	$i^{\underline{th}}$ component of $f(\cdot)$
h_i	$i^{\underline{th}}$ component of $h(\cdot)$
$f_{ix} = \left[\frac{\partial f_i}{\partial x_1} \frac{\partial f_i}{\partial x_2} \cdots \frac{\partial f_i}{\partial x_n}\right]$	$1 \times n$ vector
$h_{ix} = \left[\frac{\partial h_i}{\partial x_1} \frac{\partial h_i}{\partial x_2} \cdots \frac{\partial h_i}{\partial x_n}\right]$	$1 \times n$ vector

$$f_{ixx} = \begin{bmatrix} \frac{\partial^2 f_i}{\partial x_1^2} & \frac{\partial^2 f_i}{\partial x_1 \partial x_2} & \cdots & \frac{\partial^2 f_i}{\partial x_1 \partial x_n} \\ \vdots & & & \vdots \\ \frac{\partial^2 f_i}{\partial x_n \partial x_1} & \frac{\partial^2 f_i}{\partial x_n \partial x_2} & \cdots & \frac{\partial^2 f_i}{\partial x_n^2} \end{bmatrix} \quad n \times n \text{ matrix}$$

$$h_{ixx} = \begin{bmatrix} \frac{\partial^2 h_i}{\partial x_1^2} & \frac{\partial^2 h_i}{\partial x_1 \partial x_2} & \cdots & \frac{\partial^2 h_i}{\partial x_1 \partial x_n} \\ \vdots & & & \vdots \\ \frac{\partial^2 h_i}{\partial x_n \partial x_1} & \frac{\partial^2 h_i}{\partial x_n \partial x_2} & \cdots & \frac{\partial^2 h_i}{\partial x_n^2} \end{bmatrix} \quad n \times n \text{ matrix}$$

$$f_{xx} : P = \begin{bmatrix} \text{trace} & (f_{1xx} P) \\ \text{trace} & (f_{2xx} P) \\ \vdots & \\ \text{trace} & (f_{nxx} P) \end{bmatrix} \quad n \times 1 \text{ vector}$$

$$h_{xx} : P = \begin{bmatrix} \text{trace} & (h_{1xx} P) \\ \text{trace} & (h_{2xx} P) \\ \vdots & \\ \text{trace} & (h_{mxx} P) \end{bmatrix} \quad m \times 1 \text{ vector}$$

where P is an $n \times n$ matrix.

LIST OF DEFINITIONS

The following definitions are used consistantly throughout this study.

$\hat{y}_{t+s/t}$	$= E[y_{t+s}/Y_t]$	predicted observation on the basis of Y_t .
$\hat{x}_{t/t}$	$= E[x_t/Y_t]$	posterior estimate of x_t on the basis of Y_t , which is the optimal estimate of x_t at time t
$\hat{x}_{t+s/t}$	$= E[x_{t+s}/Y_t]$	apriori estimate of x_{t+s} on the basis of Y_t , which is also the optimal estimate at $t+s$, provided that no other observation is made after t .
$\tilde{x}_{t/t}$	$= x_t - \hat{x}_{t/t}$	posterior estimation error
$\tilde{x}_{t+s/t}$	$= x_{t+s} - \hat{x}_{t+s/t}$	apriori estimation error, if $s = 0$ apriori estimation error becomes posterior estimation error $\tilde{x}_{t/t}$
V_t	$= \tilde{x}_{t/t}\tilde{x}^T_{t/t}$	n×n matrix of posterior estimation error square, each element in this matrix is a random variable
P_{t+s}	$= \tilde{x}_{t+s/t}\tilde{x}^T_{t+s/t}$	n×n matrix of apriori estimation error squares, each element of this matrix is a random variable
$\hat{V}_{t/t}$	$= E[V_t/Y_t]$	posterior conditional covariance matrix
$\hat{V}_{t+s/t}$	$= E[V_{t+s}/Y_t]$	apriori estimate of posterior estimation error squares V_{t+s} on the basis of Y_t , n×n matrix
$\hat{P}_{t+s/t}$	$= E[P_{t+s}/Y_t]$	apriori conditional covariance matrix, $\hat{P}_{t+s/t} = \hat{V}_{t+s/t} = \hat{V}_{t/t}$ if $s = 0$

LIST OF TABLES

C

LIST OF FIGURES

CHAPTER 1

INTRODUCTION

1.1 Preliminary Remarks

In the field of space tracking and guidance, one basic requirement for spacecraft guidance is the capability to obtain and to rapidly process observations to determine an estimate of the spacecraft trajectory. This requirement initiates the search for mathematical techniques which are computationally efficient, but which possess a high degree of accuracy. Following the precise formulations of the linear sequential estimation theory by Kalman and Bucy (6,7), the practical implications of the theory were recognized and numerous successful applications have been made in the field of orbit determination and trajectory estimation problems. However, these applications generally are concerned with nonlinear continuous dynamic systems and nonlinear state-observation relationships and, hence, the linear estimation theory cannot be applied directly. As a matter of fact, it is not a simple task to apply the linear estimation theory to orbit determination problems. Usually nonlinear dynamic systems and state-observation relationships are linearized about a nominal (or reference) trajectory under the assumption that the true trajectory is sufficiently close to the reference trajectory, and then the linear estimation theory is applied to the linearized systems. Conceptually, there are two ways to carry out the linearizations and the resulting filters are somewhat different from each other. The distinction is how the nominal trajectory is chosen. If a prescribed trajectory is chosen as a nominal trajectory, the original Kalman-Bucy linear filter can be directly applied to the linearized system which governs the state and the observation deviations from the prescribed nominal values of the state

and observation. Although this approach appears to be conceptually simple, it suffers from several points. First, if the nominal trajectory is not close enough to the true trajectory, the basic assumption used in the linearization procedure is violated and the estimate of the deviation from the nominal trajectory filter can lead to inaccurate results and often diverges. Furthermore, it is intuitively more appealing to take the current estimate, rather than a prescribed trajectory, as a nominal trajectory and conduct the linearization about the current estimate instead of a prescribed trajectory. In this case, the linearized system will involve deviation in the state and the observation from the current estimates of the state and observation instead of values related to a prescribed nominal. The original Kalman-Bucy linear filter can be applied to the above linearized system. The advantages of using the current estimate as a nominal trajectory are that a nominal which is closer to the true trajectory can be used and that the filtering procedures can be simplified due to the fact that all the propagated state deviations will become identically zero. This concept will be clearly discussed in Section 1.3. In order to represent this situation, "the extended Kalman (EK) filter" proposed by Jazwinski (2) and distinguished from the prescribed nominal trajectory filter will be used.

It is well known that all of the information about the state provided by the measurements is contained in the probability density function of the state conditioned upon the entire past history of measurements. From this conditional probability density function, one can, in principle, determine the optimal filter. In general, the optimal filter is expressed in terms of the moments of the conditional probability density function. Hence,

this conditional density function becomes a prime ingredient for studies of optimal filtering.

Several authors have considered the problem of deriving a dynamical equation for the conditional density function when the dynamic state noise and observation noise are both jointly Gaussian and white. The most recent pattern of research in this field appears to have been initiated by Stratononich (12) and Kushner (8,9). The formal character of this initial work stimulated numerous studies of nonlinear filtering which have attempted to extend, and to obtain a more rigorous verification of these initial results. The method used by Stratononich and Kushner is based on a discrete time model, and an iterative application of Bayes' rule is used to obtain a representation of the conditional density function. The solution of the continuous time problem is obtained by a limiting process.

Although the central ideas and methods were all supplied by Stratonovich and Kushner, and most other papers in this area are just concerned with extention of these basic ideas, Bucy's (4,5) approach to the optimal nonlinear filtering problem is rather unique and more mathematical than Stratonovich and Kushner's. However, the results which he obtained for the Gaussian state and observation noise case were identical to those of Kushner. An important intermediate result of Bucy's work is that of a representation theorem which demonstrates how the posterior conditional density function at some instant of time can be represented as a function of the apriori density, $P(X(t_o))$ and the conditional expectation of an exponential function of the observational data over the time interval (t_o,t) .

In addition to the above research, Mortenson (14), Cox (25) and Detchmendy et al. (21) approach the nonlinear filtering problem from the

control theoretical point of view. They formed a likely hood function and maximized the function in various ways, e.g., dynamic programming or Pontryagin's maximum principle.

Fisher (23) presented a unified and compact development of the nonlinear filtering problem for a broad class of Markov signal processes, by making use of the characteristic function technique. The idea of approaching the continuous time nonlinear estimation problem from the innovation process approach was suggested by Frost (33).

There have been a number of associated approximation methods developed. Noteable among those are those of Bucy (4,5), Kushner (10), Jazwinski (1,2,3), Bass et al. (18,20), Schwartz (19) and Athans et al. (27). Most of the references cited above utilize techniques that are closely related to the methods introduced by Kushner (10) and Bucy (4), namely, Taylor series expansion and the assumption of a Gaussian density function or Taylor series expansion and truncation. Utilizing the Taylor series expansion technique, there are two basic types of second order filters which have been developed. First, it is assumed that the third and higher order moments are negligible. The resulting filter, referred to as the truncated second order filter, was developed by Jazwinski (1,2,3) and independently by Bass, Norum and Schwartz (20) who extended the idea of Bucy (4) to the arbitrary n-dimensional case. Schwartz (19), Jazwinski (3) and Fisher (24) independently developed the Gaussian second order filter. In this approximation, the fourth order moments are approximated in terms of the second order moments under the assumption that the conditional density function is Gaussian.

A significant feature of both the truncated and the Gaussian second order filters is the presence of a random forcing term in the covariance

equation. The presence of the random forcing term is, in principle, justifiable. However, there has been considerable controversy associated with the presence of this term.

The term enters with a plus sign in one filter and with a minus sign in the other. Furthermore, the term enters in linear manner and there is a possibility that a negative variance may result due to the sign of the observation residual. These considerations suggest considering a compromise between the truncated and the Gaussian second order filters. Jazwinski (3) dropped the forcing term in the covariance equation for the compromise and defined the modified truncated second order (MTSO) filter and the modified Gaussian second order (MGSO) filter, respectively.

Athans, et al. (27) developed the modified Gaussian second order filter using an assumption based on an intuition argument and applied the filter to a simple one-dimensional free-fall reentry problem with range type of measurement. The result of the simulations indicates considerable promise for the MGSO filter.

In this report, the modified Gaussian second order filter was developed rigorously on the basis of the Martingale theory and smoothing properties of Loeve (34). The resulting algorithm was applied to a study of the Jupiter fly-by and the Jupiter orbiter missions using range, range-rate, star-planet and sun-planet angle measurements.

1.2 Kalman-Bucy Filter

Consider the linear dynamics system described by the linear vector stochastic differential equation

$$dx_t = F(t)x_t dt + G(t)d\beta_t \quad , \quad t \geq t_o \tag{1.1}$$

Eq. (1.1) can be expressed formally as (see Ref. 15)

$$\frac{dx_t}{dt} = F(t)x_t + G(t)u_t \quad , \quad t \geq t_o \tag{1.2}$$

where x_t is the n×1 state vector, $F(\cdot)$ and $G(\cdot)$ are, respectively, n×n and n×r non-random, continuous matrix functions of time, and $\{\beta_t, t \geq t_o\}$ is an r-vector Brownian motion process with the statistics

$$E[d\beta_t d\beta_t^T] = Q(t)dt$$

The r-vector u_t is a white Gaussian vector process which can be regarded as the time derivitives of β_t .

It is assumed that linear observations are taken at discrete time instants, k :

$$y_k = H(k)x_k + v_k \quad ; \quad k = 1,2,... \tag{1.3}$$

where y_k is an m-vector of observations, $H(\cdot)$ is an m×n non-random, bounded matrix function, and $\{v_k, k = 1,2,...\}$ is an m-vector, independent Gaussian sequence, i.e., $v_k \sim N(0,R_k), R_k > 0$ for all k . The distribution of x_o is Gaussian, i.e., $x_o \sim N(\hat{x}_o, P_o)$, and $x_o, \{\beta_t\}$ and $\{v_k\}$ are assumed to be independent.

The fact that the minimum variance estimate is given by the conditional expectation (see Appendix F), leads to the requirement that the conditional expectation $\hat{x}_{t/t} = E[x_t/Y_t]$ for the above system be found. The solution to this problem yields differential equations of evolution for the conditional expectation $\hat{x}_{t+s/t}$ and the covariance matrix $\hat{P}_{t+s/t}$. Between observations, these relations satisfy the differential equations given in Eqs. (1.4) and (1.5), respectively.

$$\frac{d\hat{x}_{t+s/t}}{ds} = F(t+s)\hat{x}_{t+s/t} \quad , \quad \hat{x}(t) = \hat{x}_{t/t} \tag{1.4}$$

$$\frac{d\hat{P}_{t+s/t}}{ds} = F(t+s)\hat{P}_{t+s/t} + \hat{P}_{t+s/t}F^{T}(t+s) + G(t+s)Q(t+s)G^{T}(t+s) \quad , \quad \hat{P}(t) = \hat{V}_{t/t} \tag{1.5}$$

where the superscript T indicates the transpose of matrix, t represents the time at which the last observation was made, and s represents any time segment after t and before a new observation is made. At the instant $t+s$, namely, immediately after a new observation is incorporated at $t+s$, the following difference equations are satisfied.

$$\hat{x}_{t+s/t+s} = \hat{x}_{t+s/t} + K_{t+s}(y_{t+s} - \hat{y}_{t+s/t}) \tag{1.6}$$

$$\hat{V}_{t+s/t+s} = \hat{P}_{t+s/t} - K_{t+s}H(t+s)\hat{P}_{t+s/t} \tag{1.7}$$

$$\hat{y}_{t+s/t} = H(t+s)\hat{x}_{t+s/t} \tag{1.8}$$

$$K_{t+s} = \hat{P}_{t+s/t}H^{T}(t+s)[H(t+s)\hat{P}_{t+s/t}H^{T}(t+s) + R_{t+s}]^{-1} \tag{1.9}$$

where $\hat{y}_{t+s/t}$ is the predicted observation on the basis of Y_t and K_{t+s} is the Kalman gain.

The solution of Eqs. (1.4) and (1.5) are referred to as the apriori estimate and the apriori covariance matrix, respectively. Meanwhile, the solutions of the difference Eqs. (1.6) and (1.7) are said to be the posterior estimate and the posterior covariance matrix, respectively. Once the posterior estimate $\hat{x}_{t+s/t+s}$ and the posterior covariance matrix $\hat{V}_{t+s/t+s}$ are obtained, they can be used as initial conditions for the differential Eqs. (1.4) and (1.5), respectively. By integrating these relations forward until a new observation is obtained, the apriori estimate which is the optimal estimate between observations is obtained. In order to initiate this

procedure, it is necessary to specify $\hat{x}_{o/o}$ and $\hat{V}_{o/o}$. From the statistics of a random variable x_o, $\hat{x}_{o/o}$ and $\hat{V}_{o/o}$ are given as $\hat{x}_o$ and P_o, respectively.

1.3 Linearization and the Extended Kalman Filter.

As pointed out previously, the linearization of the dynamic system and the state-observation relationships cannot be avoided, if the original Kalman-Bucy filter is applied to the orbit determination problem. The details presented in the subsequent discussion are used to obtain the extended Kalman filter.

Suppose that the equation of motion is described by the following nonlinear stochastic differential equation

$$dX_\tau = f(X_\tau,\tau)d\tau + G(\tau)d\beta_\tau \quad , \quad \tau \geq \tau_o \tag{1.10}$$

Eq. (1.10) can be expressed formally as

$$\frac{dX_\tau}{d\tau} = f(X_\tau,\tau) + G(\tau)u_\tau \tag{1.11}$$

The discrete nonlinear observations, which are taken at time instants k, can be expressed as

$$Y_k = h(X_k) + v_k \quad , \quad k = 1,2,3,... \tag{1.12}$$

In the above systems, β_τ, u_τ, v_k and x_o are assumed to have the properties described in Section 1.2. The σ-field generated by the observations Y_k is denoted by Z_t, that is $Z_t = \{Y_k; 0 \leq k \leq t\}$. Substituting $X_\tau = X^*_\tau + x_\tau$, and expanding $f(X_\tau,\tau)$ in Eq. (1.10) about the nominal X^*_τ at each point in time leads to

$$dX^*_\tau + dx_\tau = f(X^*_\tau + x_\tau,\tau)d\tau + G(\tau)d\beta_\tau$$

$$\cong f(X^*_\tau,\tau)d\tau + f_x(X^*_\tau,\tau)x_\tau d\tau + G(\tau)d\beta_\tau \tag{1.13}$$

where terms involving powers of x_τ higher than the first one are neglected. For the nominal, the following equation must be satisfied

$$dX^*_\tau = f(X^*_\tau,\tau)d\tau$$

or

$$\frac{dx^*_\tau}{d\tau} = f(X^*_\tau,\tau) \tag{1.14}$$

Hence, the state deviation x_τ can be described by the linear time varying stochastic differential equation.

$$dx_t = f_x(X^*_t,t)x_t dt + G(t)d\beta_t \tag{1.15}$$

The same procedure can be applied to the state-observation relationships (1.12), and the final result would be expressed as follows

$$Y^*_k = h(X^*_k) \tag{1.16}$$

for the nominal and

$$y_k = h_x(X^*_k)x_k + v_k \tag{1.17}$$

for the observation deviation. Here h_x is the first partial derivative of $h(\cdot)$ $\omega.r.t.X$.

Combining Eqs. (1.15) and (1.17) leads to the same model which was discussed in the previous Section. Therefore, the Kalman-Bucy linear filtering theory can be applied to the system of Eqs. (1.15) and (1.17). Hence, the optimal estimate of state deviation between observations is given by the

solution of the following linear differential equation

$$\frac{d\hat{x}_{t+s/t}}{ds} = f_x(X^*_{t+s}, t+s)\hat{x}_{t+s/t} \tag{1.18}$$

At the observation time $t + s$

$$\hat{x}_{t+s/t+s} = \hat{x}_{t+s/t} + K_{t+s}(y_{t+s} - \hat{y}_{t+s/t}) \tag{1.19}$$

where

$$\hat{y}_{t+s/t} = h_x(X^*_{t+s})\hat{x}_{t+s/t} \tag{1.20}$$

Let $\tau = t + s$; then $d\tau = ds$ and substituting these in Eq. (1.14) will yield

$$\frac{dx^*_{t+s}}{ds} = f(X^*_{t+s}, t + s) \tag{1.21}$$

Combining Eqs. (1.18) and (1.21), the following result is obtained

$$\frac{d(X^*_{t+s} + \hat{x}_{t+s/t})}{ds} = f(X^*_{t+s}, t + s) + f_x(X^*_{t+s}, t + s)\hat{x}_{t+s/t} \tag{1.22}$$

Denoting $\hat{X}_{t+s/t} = X^*_{t+s} + \hat{x}_{t+s/t}$, which is an apriori estimate of X_{t+s} based on Z_t , Eq. (1.22) can be approximated as

$$\frac{d\hat{X}_{t+s/t}}{ds} = f(\hat{X}_{t+s/t}, t + s) \tag{1.23}$$

From Eqs. (1.21) and (1.23), it follows that the same differential equation governs the nominal trajectory X^*_{t+s} as well as the apriori estimate $\hat{X}_{t+s/t}$. Therefore, selecting the same initial conditions for Eqs. (1.21) and (1.23) will lead to the conclusion that the nominal trajectory and the apriori estimate are identical. This situation is satisfied if the current optimal estimate is chosen as a nominal trajectory. In other words, if the nominal trajectory is updated with a current optimal estimate, the apriori estimate

$\hat{x}_{t+s/t}$ of state x_{t+s}, governed by Eq. (1.18) becomes identically zero, and hence, Eqs. (1.18) and (1.20) are not necessary. For this situation, the initial condition for Eq. (1.18) would be zero and, consequently, the solution becomes identically zero.

From the induction above, it follows that it would be simpler to linearize the system about the current optimal estimate instead of a certain prescribed nominal trajectory. This situation usually occurs in nature. For example, when one deals with the motion of a rigid body, it is always better to stick with the mass center, which is the analogy of the optimal estimate of position, that is, the mass center is nothing but a conditional expectation of equivalent point mass. Furthermore, it has been demonstrated, in the numerical simulations (30,43), that taking the current optimal estimate as the nominal trajectory leads to better convergence characteristics than using a certain prescribed nominal.

At observation time $t + s$, the optimal estimate $\hat{X}_{t+s/t+s}$ of X_{t+s} would be expressed as follows

$$\hat{X}_{t+s/t+s} = X^*_{t+s} + \hat{x}_{t+s/t+s} \tag{1.24}$$

If the optimal estimate is chosen as a nominal trajectory, then $X^*_{t+s} = \hat{X}_{t+s/t}$. Therefore, Eq. (1.24) becomes

$$\hat{X}_{t+s/t+s} = \hat{X}_{t+s/t} + \hat{x}_{t+s/t} + K_{t+s}(y_{t+s} - \hat{y}_{t+s/t}) \tag{1.25}$$

Since $\hat{x}_{t+s/t}$ and $\hat{y}_{t+s/t}$ are both zero for the case where the optimal estimate is chosen as a nominal, Eq. (1.25) again becomes

$$\hat{X}_{t+s/t+s} = \hat{X}_{t+s/t} + K_{t+s}(y_{t+s} + Y^*_{t+s} - Y^*_{t+s}) \tag{1.26}$$

after adding and subtracting Y^*_{t+s} . It can be easily seen from Eq. (1.16) that

$$Y^*_{t+s} = h(X^*_{t+s}) = h(\hat{X}_{t+s/t}) = \hat{Y}_{t+s/t} \tag{1.27}$$

and

$$Y_{t+s} = y_{t+s} + Y^*_{t+s} \tag{1.28}$$

Therefore, Eq. (1.26) finally becomes

$$\hat{X}_{t+s/t+s} = \hat{X}_{t+s/t} + K_{t+s}(Y_{t+s} - \hat{Y}_{t+s/t}) \tag{1.29}$$

The above expression represents the extended Kalman filter (3) and can be summarized as follows; between observations, the apriori estimate $\hat{X}_{t+s/t}$ and the apriori conditional covariance matrix $\hat{P}_{t+s/t}$ which is distinguished from the apriori covariance matrix for the linear system, must satisfy the following ordinary differential equations

$$\frac{d\hat{X}_{t+s/t}}{ds} = f(\hat{X}_{t+s/t}, t + s) \tag{1.30}$$

and

$$\frac{d\hat{P}_{t+s/t}}{ds} = f_x(\hat{X}_{t+s/t}, t+s)\hat{P}_{t+s/t} + \hat{P}_{t+s/t}f_x^T(\hat{X}_{t+s/t}, t+s) + G(t+s)Q(t+s)G^T(t+s) \tag{1.31}$$

respectively. At the observation time $t + s$, the posterior estimate $\hat{X}_{t+s/t+s}$ and the posterior conditional covariance matrix $\hat{V}_{t+s/t+s}$ are determined by the following set of difference equations.

$$\hat{X}_{t+s/t+s} = \hat{X}_{t+s/t} + K_{t+s}(Y_{t+s} - \hat{Y}_{t+s/t}) \tag{1.32}$$

$$\hat{V}_{t+s/t+s} = \hat{P}_{t+s/t} - K_{t+s}h_x(\hat{X}_{t+s/t})\hat{P}_{t+s/t} \tag{1.33}$$

$$\hat{Y}_{t+s/t} = h(\hat{X}_{t+s/t}) \tag{1.34}$$

$$K_{t+s} = \hat{P}_{t+s/t} h_x^T(\hat{X}_{t+s/t})[h_x(\hat{X}_{t+s/t})\hat{P}_{t+s/t} h_x^T(\hat{X}_{t+s/t}) + R_{t+s}]^{-1} \tag{1.35}$$

or

$$K_{t+s} = \hat{V}_{t+s/t+s} h_x^T(\hat{X}_{t+s/t}) R_{t+s}^{-1} \tag{1.36}$$

Finally, Eqs. (1.30) through (1.35) feature the extended Kalman filter and they can readily be reduced to the Kalman-Bucy filter when the systems are linear. Unlike the linear system, the covariance matrices cannot be precomputed. And, as a matter of fact, they are coupled with the optimal estimate through coefficients f_x and, hence, they are not ordinary covariance matrices, but rather they represent conditional covariance matrices.

1.4 The Problem to be Studied

The problem treated in the subsequent study is that of estimating the state of a continuous nonlinear dynamical system (1.10), influenced by Brownian motion, using discrete nonlinear observations (1.12) corrupted by an independent Gaussian noise sequence. In the previous section, the nonlinear system is linearized and the Kalman-Bucy linear filter theory is applied to the problem of estimating the state of the linearized system. This technique is based on the assumption that the state deviation is small so that the second or higher order terms in the Taylor series expansions can be neglected while retaining the first order terms. Suppose that the system is highly nonlinear or that the initial uncertainty is relatively large so that the square of the state deviation as well as the deviation itself is not negligible. In this situation, the Kalman-Bucy linear filtering theory must be abandoned and an effort must be made to develop a new theory which hopefully

applies to both linear and nonlinear systems.

Up to the present time, no sign of an exact solution to the nonlinear estimation problem is seen, unless one calculates an infinite number of moments. Therefore, some sort of an approximate solution is inevitable. With the possible exception of a scalar system, it is not practically feasible to include terms of higher order than the second order and, hence, it is desirable that the nonlinear estimation technique be defined by using only the first two moments, namely, the conditional mean and the conditional covariance. In order to do so, the second order terms are included in Taylor series expansion and a minimum variance criteria is employed to find the conditional expectation. By definition, the conditional covariance matrix is nothing more than a conditional mean of the square of the actual estimation errors and, furthermore, it is clearly understood that the square of the actual estimation errors is a random variable. Therefore, it is meaningful to interpret the conditional covariance matrix as the optimal estimate of the square of the actual estimation error and to approximate it by the same technique as the conditional mean is approximated. It is necessary to define a meaningful criteria for approximating the covariance matrix and this is accomplished by the use of the property of the trace of the matrix. This property is discussed in Appendix E.

The nonlinear estimation theory developed in this study is applied to an orbit determination problem. The actual model employed involves the investigation of the states of an interplanetary space vehicle during the planetary fly-by and planetary orbiter phases of the mission. In the simulated study, Jupiter is chosen as the main body with the Sun as the perturbing body.

1.5 Outline of Study

In Chapter 2, the nonlinear mathematical model which will be studied is discussed briefly. On the basis of a Martingale property which is presented in Appendix D, an approximate nonlinear estimation algorithm is developed. In the process of developing the algorithm, basic smoothing properties described in Appendix B are extensively used to manipulate the lengthy algebraic relations and to simplify the resulting expressions. First, a sequential nonlinear estimate is obtained and a formal limiting process is used to obtain a continuous nonlinear estimation algorithm. In the limiting process, the concept of white noise as a time derivative of Brownian motion is essential. The Brownian motion is treated separately in Appendix C.

Chapter 3 is concerned with the physical problem to be studied using the nonlinear estimation algorithm developed in Chapter 2. The problem is that of estimating the state of an interplanetary space vehicle during the planetary fly-by and planetary orbiter phase of a Jupiter mission. The equations of motion for the spacecraft are discussed briefly and expressed as a set of nonlinear state dynamic equations. Four kinds of observations are considered. They are range, range-rate, and sun-planet and star-planet angles as measured from the spacecraft. Finally, computer programs for the nonlinear and the extended Kalman filter equations are described.

In Chapter 4, the results of the numerical simulations are discussed. Several nonlinear estimation algorithms are obtained from the modified Gaussian second order filter which is developed in Chapter 2, and the modified truncated second order filter, by neglecting the second order terms in various combinations. Each nonlinear filter in conjunction with the extended Kalman filter is simulated with the problem discussed in Chapter 3 to

determine the effects of the second order terms, i.e., the dynamic second order term, the observation second order term, and the Kalman gain compensation term. The Kalman gain compensated filter obtained from the modified Gaussian second order filter by neglecting the dynamic and the observation second order terms while retaining the Kalman gain compensation term is shown to be the best filter on the basis of the simulations. The Kalman gain compensated filter is further examined through numerous simulations.

A summary of results and a list of possible extensions to this work are presented in Chapter 5.

CHAPTER 2

A NONLINEAR ESTIMATION ALGORITHM

2.1 Introduction

The state of the dynamic system is assumed to evolve as the solution of a nonlinear stochastic differential equation,

$$dx_t = f(x_t,t)dt + d\beta_t \quad , \quad t \geq t_o \tag{2.1}$$

which is expressed formally as

$$\frac{dx_t}{dt} = f(x_t,t) + u_t \quad , \quad t \geq t_o \tag{2.2}$$

In the above expression, $f(x_t,t)$ is a n-vector and $\{u_t, t > t_o\}$ is an n-vector, zero-mean, white Gaussian noise process with

$$E[u_t u_\tau^T] = Q_t \delta(t - \tau) \tag{2.3}$$

where Q_t is an n×n positive definite matrix for any t. Suppose that observations on the state are taken at discrete instants of time and s measures the time interval between a certain point in time, say $t + s$, and t, at which the last observation was made. Therefore, s will vary from zero to the maximum time span between two consecutive observations. This approach is necessary when observations are not taken regularly.

Let the observations of the state be of the form

$$y_i = h(x_i) + v_i \quad , \quad i = 1,2,... \tag{2.4}$$

where y_i and h are m-vectors, and where $\{v_i, i = 1,2,...\}$ is an m-vector, zero-mean, Gaussian noise sequence with

$$E[v_k v_\ell^T] = R_k \delta_{k\ell} \tag{2.5}$$

The covariance matrix R_k is an m×m positive definite matrix for any k. It is assumed that $\{u_t, t > t_o\}$ and $\{v_k\}$ are statistically independent. An extension to the continuous observation case can be made by simply replacing v_i with a white Gaussian noise v_t. In this case the function R_k will have an infinite magnitude. Since white noise is formally modeled as the time derivative of Brownian motion β_t (see Appendix C), it is natural to relate v_i with a white noise v_t as follows

$$v_i = \frac{\beta_{i+s} - \beta_i}{s} \tag{2.6}$$

$$v_t = \lim_{s \to o} \frac{\beta_{t+s} - \beta_t}{s} = \left.\frac{d\beta_s}{ds}\right|_{s=t} \tag{2.7}$$

With these definitions, R_k would be of the form

$$R_k = \frac{R_t}{s} \tag{2.8}$$

which approaches $R_t \delta(s)$ as s goes zero. Denoting

$$Y_t = \{y_i, i = 1,2,\ldots t\} \tag{2.9}$$

for the σ-field generated by $y_i, i = 1,2,\ldots t$, the problem of concern is that of estimating the state x_t of the dynamical system (2.2) on the basis of Y_t. In particular, the desired estimate is the minimum variance estimate and the solution is well known to be the conditional expectation $E[x_t/Y_t]$ (5). The details are discussed in Appendix F.

When both the dynamical system and the observations are linear, the exact solution yields the Kalman-Bucy linear filter. However, an exact solution does not seem to be realizable with a finite set of moments when the

models are nonlinear. Therefore, an approximate solution is inevitable. It is common practice to linearize the system dynamics $f(\cdot)$ and the observation-state relationships $h(\cdot)$, about a specified reference trajectory and then to apply the Kalman-Bucy filtering theory to the linearized system. In this chapter, an approximate nonlinear filter, which is a modified Gaussian second order filter, is derived by utilizing Martingale properties (Appendix D) and a Taylor series expansion of $f(\cdot)$ and $h(\cdot)$ about the current optimal estimate, retaining the second order terms in each expansion.

Regarding the square of the actual estimation errors as a collection of random variables, the conditional covariance is obtained by minimizing the following risk function (see Appendix E)

$$R(\hat{V}_{t+s/t+s}) = tr[(V_{t+s} - \hat{V}_{t+s/t+s})(V_{t+s} - \hat{V}_{t+s/t+s})^T] \qquad (2.10)$$

where V_{t+s} is an $n \times n$ matrix and the square of the actual estimation errors and $\hat{V}_{t+s/t+s}$ is the optimal estimate of V_{t+s} given Y_{t+s}, which is the conditional expectation of V_{t+s} given Y_{t+s}.

2.2 Apriori Estimate $\hat{x}_{t+s/t}$

Integrating the state dynamic equation (2.2) from t to $t+s$, the state at $t+s$ can be formally expressed as follows

$$x_{t+s} = x_t + \int_t^{t+s} f(x_\tau,\tau)d\tau + \int_t^{t+s} u_\tau d\tau \qquad (2.11)$$

$$\cong \hat{x}_{t/t} + (x_t - \hat{x}_{t/t}) + \int_t^{t+s} u_\tau d\tau$$

$$+ \int_t^{t+s} \{f(\hat{x}_{\tau/t},\tau) + f_x(\hat{x}_{\tau/t},\tau)(x_\tau - \hat{x}_{\tau/t}) + \frac{1}{2} f_{xx}(\hat{x}_{\tau/t},\tau) : P_\tau\}d\tau \qquad (2.12)$$

The approximate expression (2.12) is obtained by utilizing a Taylor series expansion of $f(\cdot)$ and truncating at the second order terms. In this expression t is merely a parameter and s is a variable. For the convenience of notation, τ in $f(\cdot)$, $f_x(\cdot)$ and $f_{xx}(\cdot)$ is neglected unless otherwise stated. Knowing that $u_\tau, \tau > t$ is independent of Y_t, and $(x_t - \hat{x}_{t/t})$ and $(x_\tau - \hat{x}_{\tau/t})$ have zero conditional means, the conditional expectation $\hat{x}_{t+s/t}$ which is the desired apriori estimate of x_{t+s}, is obtained after taking the conditional expectation of both sides of Eq. (2.12).

$$\hat{x}_{t+s/t} = \hat{x}_{t/t} + \int_t^{t+s} \{f(\hat{x}_{\tau/t}) + \frac{1}{2} f_{xx}(\hat{x}_{\tau/t}) : \hat{P}_{\tau/t}\} d\tau \qquad (2.13)$$

Note that $f(\hat{x}_{\tau/t})$, $f_x(\hat{x}_{\tau/t})$ and $f_{xx}(\hat{x}_{\tau/t})$ are Y_t-measurable and the smoothing property 3 (Appendix B) can be applied. The differential equation for $\hat{x}_{t+s/t}$, as a function of s, is readily obtained by differentiating Eq. (2.13) with respect to s. Since the upper limit of integration is a function of s, Leibnitz's rule is applied and the result is

$$\frac{d\hat{x}_{t+s/t}}{ds} = f(\hat{x}_{t+s/t}) + \frac{1}{2} f_{xx}(\hat{x}_{t+s/t}) : \hat{P}_{t+s/t} \qquad (2.14)$$

The above differential equation is different from that of the extended Kalman filter through the inclusion of the dynamic second order term $f_{xx}(\cdot) : \hat{P}/2$ and must be integrated in conjunction with $\hat{P}_{t+s/t}$, from t to the instant of a new observation, using $\hat{x}_{t/t}$ as the initial condition.

2.3 Apriori Conditional Covariance Matrix $\hat{P}_{t+s/t}$

Subtracting out Eq. (2.13) from Eq. (2.12), the apriori estimation errors $\tilde{x}_{t+s/t}$ at $t + s$, is obtained as follows

$$\tilde{x}_{t+s/t} = x_{t+s} - \hat{x}_{t+s/t}$$

$$= (x_t - \hat{x}_{t/t}) + \int_t^{t+s} u_\tau d\tau \qquad (2.15)$$

$$+ \int_t^{t+s} \{f_x(\hat{x}_{\tau/t})(x_\tau - \hat{x}_{\tau/t}) + \frac{1}{2} f_{xx}(\hat{x}_{\tau/t}) : (P_\tau - \hat{P}_{\tau/t})\}d\tau$$

Differentiation of Eq. (2.15) with respect to s yields the following differential equation for apriori estimation error $\tilde{x}_{t+s/t}$

$$\frac{d\tilde{x}_{t+s/t}}{ds} = f_x(\hat{x}_{t+s/t})\tilde{x}_{t+s/t} + \frac{1}{2} f_{xx}(\hat{x}_{t+s/t}) : (P_{t+s} - \hat{P}_{t+s/t}) + u_{t+s} \qquad (2.16)$$

By definition

$$P_{t+s} = \tilde{x}_{t+s/t}\, \tilde{x}^T_{t+s/t} \qquad (2.17)$$

and differentiating Eq. (2.17) with respect to s, the following relation is obtained

$$\frac{dP_{t+s}}{ds} = \frac{d\tilde{x}_{t+s/t}}{ds}\, \tilde{x}^T_{t+s/t} + \tilde{x}_{t+s/t}\, \frac{d\tilde{x}^T_{t+s/t}}{ds} \qquad (2.18)$$

Substitution of Eq. (2.16) into Eq. (2.18) yields

$$\frac{dP_{t+s}}{ds} = f_x(\hat{x}_{t+s/t})P_{t+s} + \frac{1}{2}\{f_{xx}(\hat{x}_{t+s/t}):(P_{t+s}-\hat{P}_{t+s/t})\}\tilde{x}^T_{t+s/t} + u_{t+s}\tilde{x}^T_{t+s/t}$$

$$+ P_{t+s}f^T_x(x_{t+s/t}) + \frac{1}{2}\tilde{x}_{t+s/t}\{f_{xx}(\hat{x}_{t+s/t}):(P_{t+s}-\hat{P}_{t+s/t})\}^T + \tilde{x}_{t+s/t}u^T_{t+s} \qquad (2.19)$$

Since t is merely a fixed parameter, the conditional expectation given Y_t and time derivative can be interchanged. Therefore, the following expression is obtained after taking the conditional expectation of both sides of Eq. (2.19) and interchanging the conditional expectation and the time derivative.

$$\frac{d\hat{P}_{t+s/t}}{ds} = f_x(\hat{x}_{t+s/t})\hat{P}_{t+s/t} + E[u_{t+s}\tilde{x}^T_{t+s/t}/Y_t] + \hat{P}_{t+s/t}f^T_x(\hat{x}_{t+s/t}) + E[\tilde{x}_{t+s/t}u^T_{t+s}/Y_t] \tag{2.20}$$

In the above, the symmetry of the probability density function is assumed and, hence, the third order moment is taken to be zero. The remaining terms $E[u_{t+s}\tilde{x}^T_{t+s/t}/Y_t]$ can be computed as follows

$$E[u_{t+s}\tilde{x}^T_{t+s/t}/Y_t] = E[u_{t+s}\tilde{x}^T_{t/t}/Y_t] + \int_t^{t+s} E[u_{t+s}u^T_\tau/Y_t]d\tau + \int_t^{t+s} E[u_{t+s}\{f_x(\hat{x}_{\tau/t})\tilde{x}_{\tau/t} + \tfrac{1}{2}f_{xx}(\hat{x}_{\tau/t}):(P_\tau - \hat{P}_{\tau/t})\}^T/Y_t]d\tau \tag{2.21}$$

$$E[u_{t+s}\tilde{x}^T_{t+s/t}/Y_t] = \frac{1}{2}Q_{t+s} \tag{2.22}$$

The factor $\frac{1}{2}$ comes from the property of the delta function (6). By the same token

$$E[\tilde{x}_{t+s/t}u^T_{t+s}/Y_t] = \frac{1}{2}Q_{t+s}$$

and, hence, Eq. (2.20) becomes

$$\frac{d\hat{P}_{t+s/t}}{ds} = f_x(\hat{x}_{t+s/t})\hat{P}_{t+s/t} + \hat{P}_{t+s/t}f^T_x(\hat{x}_{t+s/t}) + Q_{t+s} \tag{2.23}$$

which is the desired matrix differential equation for the apriori conditional covariance matrix $\hat{P}_{t+s/t}$. The initial condition is given as a posterior conditional covariance matrix $\hat{V}_{t/t}$.

2.4 Predicted Observation $\hat{y}_{t+s/t}$

It is apparent from Eq. (2.4) that the actual observation at $t + s$ would be

$$y_{t+s} = h(x_{t+s}) + v_{t+s} \tag{2.24}$$

Expanding $h(\cdot)$ in Taylor series about the apriori estimate $\hat{x}_{t+s/t}$ and neglecting the third or higher order terms, the following approximate expression for y_{t+s} is obtained

$$y_{t+s} = h(\hat{x}_{t+s/t}) + h_x(\hat{x}_{t+s/t})\tilde{x}_{t+s/t} + \frac{1}{2} h_{xx}(\hat{x}_{t+s/t}) : P_{t+s} + v_{t+s} \tag{2.25}$$

After taking the conditional expectation of both sides of Eq. (2.25) given Y_t, the predicted observation $\hat{y}_{t+s/t}$ is obtained.

$$\hat{y}_{t+s/t} = h(\hat{x}_{t+s/t}) + \frac{1}{2} h_{xx}(\hat{x}_{t+s/t}) : \hat{P}_{t+s/t} \tag{2.26}$$

The above relation is different from that of the extended Kalman filter through the second order term in the observation-state relation, i.e., $h_{xx}(\cdot) : \hat{P}/2$.

The expected errors between actual and predicted observations are obtained by the difference in Eq. (2.25) and (2.26). Hence, the apriori observation error (or residual) is given by

$$y_{t+s} - \hat{y}_{t+s/t} = h_x(\hat{x}_{t+s/t})\tilde{x}_{t+s/t} + \frac{1}{2} h_{xx}(\hat{x}_{t+s/t}) : (P_{t+s} - \hat{P}_{t+s/t}) + v_{t+s} \tag{2.27}$$

2.5 Posterior Estimate and the Optimal Gain K_{t+s}

According to the Theorem 2 of Appendix D, the following sequence

$$\hat{x}_{t+s/1}, \hat{x}_{t+s/2}, \cdots, \hat{x}_{t+s/t}, \hat{x}_{t+s/t+s}, \cdots \tag{2.28}$$

constitute a Martingale and if $z_1, z_2, z_3, \ldots$ are defined as

$$\begin{aligned} z_1 &= \hat{x}_{t+s/1}, z_2 = \hat{x}_{t+s/2} - \hat{x}_{t+s/1}, z_3 = \hat{x}_{t+s/3} - \hat{x}_{t+s/2}, \cdots, \\ z_t &= \hat{x}_{t+s/t} - \hat{x}_{t+s/t-1}, \cdots, z_{t+s} = \hat{x}_{t+s/t+s} - \hat{x}_{t+s/t}, \cdots \end{aligned} \tag{2.29}$$

then z_n's satisfy the following conditions

$$E[|z_n|] < \infty \quad , \quad E[z_{n+1}/z_1, z_2, \ldots, z_n] = 0 \quad , \quad n \geq 0 \qquad (2.30)$$

with probability 1. Further, the terms $\hat{x}_{t+s/n}$, $n = 1,2,\ldots$ of the sequence (2.28) are partial sums of the series $\sum_n z_n$. In other words, if z_{t+s} is so determined that the conditions (2.30) are satisfied, the term $\hat{x}_{t+s/t+s}$ of the sequence (2.28), which is the posterior estimate, is uniquely determined as a partial sum $\sum_{n=1}^{t+s} z_n$. Since z_{t+s} must be a function of observation y_{t+s} , the following linear approximation

$$z_{t+s} = K_{t+s} y_{t+s} + b_{t+s} \qquad (2.31)$$

is assumed. Where K_{t+s} and b_{t+s} are random variables which are measurable over the σ-field generated by the observations Y_t . The bias term b_{t+s} is given as

$$b_{t+s} = -K_{t+s} \hat{y}_{t+s/t}$$

from the condition (2.30) which must hold for the z_n's . From the series (2.29) and Eq. (2.31), the posterior estimate $\hat{x}_{t+s/t+s}$ is expressed, therefore, as follows

$$\hat{x}_{t+s/t+s} = \hat{x}_{t+s/t} + K_{t+s}(y_{t+s} - \hat{y}_{t+s/t}) \qquad (2.32)$$

In Eq. (2.32), the $n \times m$ matrix K_{t+s} can be chosen from a family of Y_t-measurable functions so that the minimum variance or equivalently the minimum of the trace of $E[V_{t+s}]$ is achieved. By definition,

$$\begin{aligned} \mathrm{trE}[V_{t+s}] &= \mathrm{trE}[(x_{t+s} - \hat{x}_{t+s/t+s})(x_{t+s} - \hat{x}_{t+s/t+s})^T] \\ &= \mathrm{trE}[\{x_{t+s} - \hat{x}_{t+s/t} - K_{t+s}(y_{t+s} - \hat{y}_{t+s/t})\} \\ &\qquad \{x_{t+s} - \hat{x}_{t+s/t} - K_{t+s}(y_{t+s} - \hat{y}_{t+s/t})\}^T] \end{aligned} \tag{2.33}$$

and the optimality condition (Appendix F) for the minimum of the above relation requires that

$$E[\{(x_{t+s} - \hat{x}_{t+s/t}) - K_{t+s}(y_{t+s} - \hat{y}_{t+s/t})\}\{y_{t+s} - \hat{y}_{t+s/t}\}^T/Y_t] = 0 \tag{2.34}$$

Substituting Eq. (2.27) into Eq. (2.34) and using the smoothing property 3 of Appendix B, the following relation is obtained.

$$\begin{aligned} &E[(x_{t+s}-\hat{x}_{t+s/t})\{h_x(\hat{x}_{t+s/t})(x_{t+s}-\hat{x}_{t+s/t}) + \tfrac{1}{2}h_{xx}(\hat{x}_{t+s/t}):(P_{t+s}-\hat{P}_{t+s/t})+v_{t+s}\}^T/Y_t] \\ &= K_{t+s}E[\{h_x(\hat{x}_{t+s/t})(x_{t+s}-\hat{x}_{t+s/t}) + \tfrac{1}{2}h_{xx}(\hat{x}_{t+s/t}):(P_{t+s}-\hat{P}_{t+s/t})+v_{t+s}\} \\ &\qquad \{h_x(\hat{x}_{t+s/t})(x_{t+s}-\hat{x}_{t+s/t}) + \tfrac{1}{2}h_{xx}(\hat{x}_{t+s/t}):(P_{t+s}-\hat{P}_{t+s/t})+v_{t+s}\}^T/Y_t] \end{aligned} \tag{2.35}$$

If the estimation errors are assumed to be jointly Gaussian, and if it is assumed further that

$$\begin{aligned} &E[\{h_{xx}(\hat{x}_{t+s/t}) : P_{t+s}\}\{h_{xx}(\hat{x}_{t+s/t}) : P_{t+s}\}^T/Y_t] \\ &= 3\{h_{xx}(\hat{x}_{t+s/t}) : \hat{P}_{t+s/t}\}\{h_{xx}(\hat{x}_{t+s/t}) : \hat{P}_{t+s/t}\}^T \end{aligned} \tag{2.36}$$

then, the optimal gain K_{t+s} is given by

$$\begin{aligned} K_{t+s} &= \hat{P}_{t+s/t}h_x^T(\hat{x}_{t+s/t})[h_x(\hat{x}_{t+s/t})\hat{P}_{t+s/t}h_x^T(\hat{x}_{t+s/t}) + R_{t+s} \\ &\quad + \tfrac{1}{2}\{h_{xx}(\hat{x}_{t+s/t}) : \hat{P}_{t+s/t}\}\{h_{xx}(\hat{x}_{t+s/t}) : \hat{P}_{t+s/t}^T\}^T]^{-1} \end{aligned} \tag{2.37}$$

The approximation given in (2.36) leads to the identical results obtained by Athans et al. (27) for the scalar case but yields a slightly different result for the vector case. However, in contrast to the result obtained by Athans et al. the Kalman gain compensation term

$$\frac{1}{2}\{h_{xx}(\hat{x}_{t+s/t}) : \hat{P}_{t+s/t}\}\{h_{xx}(\hat{x}_{t+s/t}) : \hat{P}_{t+s/t}\}^T$$

is always positive definite, as are the terms, $h_x \hat{P}_{t+s/t} h_x^T$ and R_{t+s} of Eq. (2.37). Hence, the matrix to be inverted in Eq. (2.37) will always be positive definite, for non-zero R_{t+s}. In the extended Kalman filter, the optimal gain K_{t+s} can be expressed in terms of either apriori or posterior conditional covariance matrix, which is given in Eqs. (1.35) and (1.36). However, this situation is not possible in Eq. (2.37), due to the Kalman gain compensation term.

2.6 Apriori Estimate $\hat{V}_{t+s/t}$ of V_{t+s}

By virtue of random variable x_{t+s}, the posterior estimation error $\tilde{x}_{t+s/t+s}$ is an n×1 vector random variable, and, hence, V_{t+s} represents an n×n matrix of random variables and its apriori estimate which is the conditional expectation of V_{t+s} given Y_t can be obtained from the definition

$$V_{t+s} = \tilde{x}_{t+s/t+s}\tilde{x}^T_{t+s/t+s}$$

$$V_{t+s} = [x_{t+s} - \hat{x}_{t+s/t} - K_{t+s}(y_{t+s} - \hat{y}_{t+s/t})] \qquad (2.38)$$

$$[x_{t+s} - \hat{x}_{t+s/t} - K_{t+s}(y_{t+s} - \hat{y}_{t+s/t})]^T$$

Substitution of Eq. (2.27) into Eq. (2.38) yields the following development.

$$V_{t+s} = [\{I - K_{t+s}h_x\}\tilde{x}_{t+s/t} - K_{t+s}\{\tfrac{1}{2}h_{xx} : (P_{t+s} - \hat{P}_{t+s/t}) + v_{t+s}\}]$$

$$[\{I - K_{t+s}h_x\}\tilde{x}_{t+s/t} - K_{t+s}\{\tfrac{1}{2}h_{xx} : (P_{t+s} - \hat{P}_{t+s/t}) + v_{t+s}\}]^T$$

or

$$\begin{aligned} V_{t+s} &= [I - K_{t+s}h_x]P_{t+s}[I - K_{t+s}h_x]^T \\ &- [\{I - K_{t+s}h_x\}\tilde{x}_{t+s/t}\{\tfrac{1}{2}h_{xx} : (P_{t+s} - \hat{P}_{t+s/t}) + v_{t+s}\}^T K_{t+s}^T \\ &- K_{t+s}\{\tfrac{1}{2}h_{xx} : (P_{t+s} - \hat{P}_{t+s/t}) + v_{t+s}\}\tilde{x}_{t+s/t}^T\{I - K_{t+s}h_x\}^T \\ &+ K_{t+s}\{\tfrac{1}{2}h_{xx} : (P_{t+s} - \hat{P}_{t+s/t}) + v_{t+s}\}\{\tfrac{1}{2}h_{xx} : (P_{t+s} - \hat{P}_{t+s/t}) + v_{t+s}\}^T K_{t+s}^T \end{aligned} \tag{2.39}$$

where the argument of h_x and h_{xx} is $\hat{x}_{t+s/t}$.

Knowing that v_{t+s} is independent of Y_t and taking the conditional expectation of both sides of Eq. (2.39) given Y_t yields the following approximate expression for the apriori estimate of V_{t+s},

$$\begin{aligned} \hat{V}_{t+s/t} &= \{I - K_{t+s}h_x(\hat{x}_{t+s/t})\}\hat{P}_{t+s/t}\{I - K_{t+s}h_x(\hat{x}_{t+s/t})\}^T \\ &+ K_{t+s}[\tfrac{1}{2}\{h_{xx}(\hat{x}_{t+s/t}) : \hat{P}_{t+s/t}\}\{h_{xx}(\hat{x}_{t+s/t}) : \hat{P}_{t+s/t}\}^T + R_{t+s}]K_{t+s}^T \end{aligned} \tag{2.40}$$

2.7 Posterior Conditional Covariance Matrix $\hat{V}_{t+s/t+s}$

As pointed out in the previous section, V_{t+s} is a collection of random variables. The conditional expectation $\hat{V}_{t+s/t+s}$ given Y_{t+s} is a posterior estimate of V_{t+s} and can be determined by estimating each element of V_{t+s} in terms of the linear combination of the apriori estimate $\hat{V}_{t+s/t}$ and a new observation y_{t+s}. The above argument is based on the Martingale properties of the sequence $\hat{V}_{t+s/1}, \hat{V}_{t+s/2}, \ldots, \hat{V}_{t+s/t}, \ldots$, and, hence, the same reasoning as that used in regard to Eq. (2.31) can be applied. Regarding V_{t+s} as an $n^2 \times 1$ vector instead of $n \times n$ matrix, the estimation problem

can be stated as follows: determine $n^2 \times m$ matrix B_{t+s} of the linear combination

$$\hat{V}_{t+s/t+s} = \hat{V}_{t+s/t} + B_{t+s}(y_{t+s} - \hat{y}_{t+s/t}) \tag{2.41}$$

such that the risk (see Appendix E)

$$R(B_{t+s}) = trE[(V_{t+s} - \hat{V}_{t+s/t+s})(V_{t+s} - \hat{V}_{t+s/t+s})^T] \tag{2.42}$$

is minimized. Substituting Eq. (2.41) into Eq. (2.42) leads to the following result

$$\begin{aligned} R(B_{t+s}) = trE[&\{V_{t+s} - \hat{V}_{t+s/t} - B_{t+s}(y_{t+s} - \hat{y}_{t+s/t})\} \\ &\{V_{t+s} - \hat{V}_{t+s/t} - B_{t+s}(y_{t+s} - \hat{y}_{t+s/t})\}^T] \end{aligned} \tag{2.43}$$

The optimality condition for the minimum of R is given by the following orthogonality condition (see Appendix F)

$$E[\{V_{t+s} - \hat{V}_{t+s/t} - B_{t+s}(y_{t+s} - \hat{y}_{t+s/t})\}\{y_{t+s} - \hat{y}_{t+s/t}\}^T / Y_t] = 0 \tag{2.44}$$

$$E[(V_{t+s} - \hat{V}_{t+s/t})(y_{t+s} - \hat{y}_{t+s/t})^T / Y_t] = B_{t+s} E[(y_{t+s} - \hat{y}_{t+s/t})(y_{t+s} - \hat{y}_{t+s/t}) / Y_t] \tag{2.45}$$

By the same argument as that used with regard to Eqs. (2.34), (2.35) and (2.36) the right hand side (R.H.S.) of Eq. (2.45) is approximated as follows

$$\begin{aligned} \text{R.H.S.} = B_{t+s}[&h_x(\hat{x}_{t+s/t})\hat{P}_{t+s/t}h_x(\hat{x}_{t+s/t}) + R_{t+s} \\ &+ \frac{1}{2}\{h_{xx}(\hat{x}_{t+s/t}) : \hat{P}_{t+s/t}\}\{h_{xx}(\hat{x}_{t+s/t}) : \hat{P}_{t+s/t}\}^T] \end{aligned} \tag{2.46}$$

Knowing that

$$E[\hat{V}_{t+s/t}[y_{t+s} - \hat{y}_{t+s/t})^T / Y_t] = 0 \tag{2.47}$$

the left hand side (L.H.S.) of Eq. (2.45) becomes

$$\text{L.H.S.} = E[V_{t+s}(y_{t+s} - \hat{y}_{t+s/t})^T/Y_t] \tag{2.48}$$

After substitution of Eqs. (2.27) and (2.39) into Eq. (2.48), it can be easily seen that all of the terms in Eq. (2.48) are of the fourth or higher order moments, under the assumption that the probability density functions of estimation errors are jointly Gaussian. Therefore, the optimal gain B_{t+s} is given as the ratio of the fourth to the second order moments and is neglected. Hence,

$$B_{t+s} = 0 \tag{2.49}$$

With this assumption, Eq. (2.41) leads to

$$\hat{V}_{t+s/t+s} = \hat{V}_{t+s/t} \tag{2.50}$$

It is interesting to note that both the posterior and the apriori estimation errors are independent of observations available for the linear model and, hence, the conditioning on the covariance matrices becomes unconditional. Therefore, there are no distinctions between $\hat{V}_{t+s/t+s}$ and $\hat{V}_{t+s/t}$. Although Eq. (2.50) shows that $\hat{V}_{t+s/t+s}$ is closely approximated by $\hat{V}_{t+s/t}$, these are conceptually two different quantities. In the linear filtering theory, these become identical and there is no distinction between them.

Since $\hat{V}_{t+s/t}$ is related to the apriori conditional covariance matrix $\hat{P}_{t+s/t}$ through Eq. (2.40), the posterior conditional covariance matrix $\hat{V}_{t+s/t+s}$ can be expressed in terms of $\hat{P}_{t+s/t}$. From Eq. (2.50)

$$\begin{aligned}\hat{V}_{t+s/t+s} = \hat{V}_{t+s/t} &= \{I - K_{t+s}h_x(\hat{x}_{t+s/t})\}\hat{P}_{t+s/t}\{I - K_{t+s}h_x(\hat{x}_{t+s/t})\}^T \\ &+ K_{t+s}\left[\frac{1}{2}\{h_{xx}(\hat{x}_{t+s/t}) : \hat{P}_{t+s/t}\}\{h_{xx}(\hat{x}_{t+s/t}) : \hat{P}_{t+s/t}\}^T + R_{t+s}\right]K_{t+s}^T\end{aligned} \tag{2.51}$$

$$\hat{V}_{t+s/t+s} = \hat{P}_{t+s/t} - K_{t+s}h_x(\hat{x}_{t+s/t})\hat{P}_{t+s/t} - \hat{P}_{t+s/t}h_x^T(\hat{x}_{t+s/t})K_{t+s}^T$$
$$+ K_{t+s}[h_x(\hat{x}_{t+s/t})\hat{P}_{t+s/t}h_x(\hat{x}_{t+s/t}) + R_{t+s} \tag{2.52}$$
$$+ \frac{1}{2}\{h_{xx}(\hat{x}_{t+s/t}) : \hat{P}_{t+s/t}\}\{h_{xx}(\hat{x}_{t+s/t}) : \hat{P}_{t+s/t}\}^T]K_{t+s}^T$$

Substitution of Eq. (2.36) into Eq. (2.52) yields the following relationships

$$\hat{V}_{t+s/t+s} = \hat{P}_{t+s/t} - K_{t+s}h_x(\hat{x}_{t+s/t})\hat{P}_{t+s/t} \tag{2.53}$$

The above relation is used to update the apriori conditional covariance matrix $\hat{P}_{t+s/t}$ to the posterior conditional covariance matrix $\hat{V}_{t+s/t+s}$ after a new observation y_{t+s} is processed. Once $\hat{V}_{t+s/t+s}$ is obtained, it can be used as an initial condition for the integration of Eq. (2.23) from $t + s$ to the instant of a new observation. Finally, the procedures required to compute the posterior estimate $\hat{x}_{t+s/t+s}$ can be summarized as follows:

$$\frac{d\hat{x}_{t+s/t}}{ds} = f(\hat{x}_{t+s/t}) + \frac{1}{2} f_{xx}(\hat{x}_{t+s/t}) : \hat{P}_{t+s/t} \tag{2.54}$$

$$\frac{d\hat{P}_{t+s/t}}{ds} = f_x(\hat{x}_{t+s/t})\hat{P}_{t+s/t} + \hat{P}_{t+s/t}f_x^T(\hat{x}_{t+s/t}) + Q_{t+s} \tag{2.55}$$

$$\hat{y}_{t+s/t} = h(\hat{x}_{t+s/t}) + \frac{1}{2} h_{xx}(\hat{x}_{t+s/t}) : \hat{P}_{t+s/t} \tag{2.56}$$

$$K_{t+s} = \hat{P}_{t+s/t}h_x^T(\hat{x}_{t+s/t})[h_x(\hat{x}_{t+s/t})\hat{P}_{t+s/t}h_x^T(\hat{x}_{t+s/t}) + R_{t+s}$$
$$+ \frac{1}{2}\{h_{xx}(\hat{x}_{t+s/t}) : \hat{P}_{t+s/t}\}\{h_{xx}(\hat{x}_{t+s/t}) : \hat{P}_{t+s/t}\}]^{-1} \tag{2.57}$$

$$\hat{x}_{t+s/t+s} = \hat{x}_{t+s/t} + K_{t+s}[y_{t+s} - \hat{y}_{t+s/t}] \tag{2.58}$$

$$\hat{V}_{t+s/t+s} = \hat{P}_{t+s/t} - K_{t+s}h_x(\hat{x}_{t+s/t})\hat{P}_{t+s/t} \tag{2.59}$$

In order to start the computation, $\hat{x}_{o/o}$ and $\hat{V}_{o/o}$ are required and they are given by

$$\hat{x}_{o/o} = E[x_o/Y_o] = E[x_o] \tag{2.60}$$

$$\hat{V}_{o/o} = P_o \tag{2.61}$$

where P_o is given as the covariance of the random variable x_o.

Depending on the particular problem, it may be possible to neglect either the dynamic or the observation second order term. This might be the case when the state dynamics are relatively smooth while the state-observation relationships are highly nonlinear or vice versa.

2.8 Computational Algorithm

The algorithm for computing the estimate $\hat{x}_{t+s/t+s}$ of x_{t+s} by processing each data point sequentially, can be summarized as follows:

1. Given $\hat{x}_{t/t}$ and $\hat{V}_{t/t}$
2. Compute $\hat{x}_{t+s/t}$ and $\hat{P}_{t+s/t}$ by integrating Eq. (2.54) and (2.55) with the given initial conditions $\hat{x}_{t/t}$ and $\hat{V}_{t/t}$ until a new observation y_{t+s} is made at $t + s$.
3. Determine $\hat{y}_{t+s/t}$ and K_{t+s} using Eqs. (2.56) and (2.57), respectively.
4. Compute $\hat{x}_{t+s/t+s}$ and $\hat{V}_{t+s/t+s}$ by updating $\hat{x}_{t+s/t}$ and $\hat{P}_{t+s/t}$ through Eq. (2.58) and (2.59), respectively.
5. Given $\hat{x}_{t+s/t+s}$ and $\hat{V}_{t+s/t+s}$, the steps 2 through 4 can be repeated.

2.9 Continuous Second Order Filter

An approximate filter for the case of continuous observation may be obtained by passing to a formal limit. In doing so, Q_{t+s} of the dynamic state noise and R_{t+s} of the observation noise have to be replaced by Q_ts

and R_t/s , respectively. This comes from the property of white noise regarded as a time derivative of Brownian motion (see Appendix C). For an infinitesimal observation interval s , it follows that

$$\hat{x}_{t+s/t} \cong \hat{x}_{t/t} + sf(\hat{x}_{t/t}) + \frac{s}{2} f_{xx}(\hat{x}_{t/t}) : \hat{V}_{t/t} \tag{2.62}$$

$$\hat{P}_{t+s/t} \cong \hat{V}_{t/t} + sf_x(\hat{x}_{t/t})\hat{V}_{t/t} + s\hat{V}_{t/t}f_x^T(\hat{x}_{t/t}) + sQ_t \tag{2.63}$$

$$K_{t+s} \cong s\hat{P}_{t+s/t}h_x^T(\hat{x}_{t+s/t})R_t^{-1} \tag{2.64}$$

Utilizing Eqs. (2.56), (2.58), (2.59), (2.62), (2.63) and (2.64) and passing to a formal limit, the following continuous second order filter is obtained, as s goes to zero.

$$\frac{d\hat{x}}{dt} = \lim_{s\to o} \frac{\hat{x}_{t+s/t+s} - \hat{x}_{t/t}}{s}$$

$$\frac{d\hat{x}}{dt} = f(\hat{x}) + \frac{1}{2} f_{xx}(\hat{x}) : \hat{V} + K[y - h(\hat{x}) - \frac{1}{2} h_{xx}(\hat{x}) : \hat{V}] \tag{2.65}$$

$$K = \hat{V}h_x(\hat{x})R^{-1} \tag{2.66}$$

$$\frac{d\hat{V}}{dt} = \lim_{s\to o} \frac{\hat{V}_{t+s/t+s} - \hat{V}_{t/t}}{s}$$

$$\frac{d\hat{V}}{dt} = f_x(\hat{x})\hat{V} + \hat{V}f_x^T(\hat{x}) + Q - \hat{V}h_x^T(\hat{x})R^{-1}h_x(\hat{x})\hat{V} \tag{2.67}$$

Note that the optimal gain K for the continuous filter is not the limit of the optimal gain K_{t+s} given in Eq. (2.64).

CHAPTER 3

DESCRIPTION OF THE ORBIT DETERMINATION PROBLEM

3.1 Introduction

In order to compare the performance of the extended Kalman filter and the various forms of the nonlinear second order filters developed in Chapter 2, the methods are compared in a simulated study of a realistic orbit determination problem. The problem considered is that of estimating the state of an interplanetary space vehicle during the orbiting and planetary fly-by stages of a Jupiter exploration mission. The reason for choosing this problem is that considerable attention has been given to the exploration of deep space and the reconnaissance of Jupiter is regarded as an important scientific objective. However, the past Jupiter encounter missions are of comparable significance and those missions are made practical by utilizing the powerful trajectory shaping capabilities of Jupiter's gravitational field. One such mission, the so-called "Grand Tour", involves successive fly-bys of the planets, Jupiter, Saturn, Uranus, and Neptune. The Grand Tour is the subject of considerable current interest, since a mission opportunity occurs in the last half of the 1970's and will not reoccur for another 179 years.

A critical problem in the design of a space vehicle to perform a deep space mission such as the Grand Tour is the accurate determination of the expected trajectory which is the basic knowledge required for the guidance correction. Because of numerous sources of error, the true trajectory is never known to us. A major contribution to those errors, access during the encounter trajectory, due to imperfect pre-encounter guidance corrections which result from pre-encounter orbit determination errors. In regard to

this situation, it is interesting to see how the nonlinear estimation procedures perform when compared with the extended Kalman filter.

3.2 Equations of Motion

The motion of a space probe relative to a given planet is closely approximated by the solution of the following vector stochastic differential equations

$$\ddot{\bar{r}} = -\mu \frac{\bar{r}}{r^3} - \mu_s \left[\frac{\bar{r}_p}{r_p^3} - \frac{\bar{r}_t}{r_t^3}\right] + \bar{u} \tag{3.1}$$

where μ and μ_s are the gravitational constants of the target planet and the Sun, respectively, and $\bar{u}$ is a vector of Gaussian process noise and where $\bar{r}$ is the position vector of the space probe relative to the target planet, $\bar{r}_t$ is the position of the target planet relative to the Sun, and $\bar{r}_p = \bar{r} + \bar{r}_t$ is the position of the probe relative to the Sun.

Eq. (3.1) can be reduced to a system of first order differential equations by the following transformation

$$\begin{aligned} \dot{\bar{r}} &= \bar{v} \\ \dot{\bar{v}} &= -\mu \frac{\bar{r}}{r^3} - \mu_s \left[\frac{\bar{r}_p}{r_p^3} - \frac{\bar{r}_t}{r_t^3}\right] + \bar{u} \end{aligned} \tag{3.2}$$

In a cartesian coordinate system centered at the target planet, the equations of motion can be expressed in component forms as

$$\begin{aligned} \dot{X} &= U \\ \dot{Y} &= V \\ \dot{Z} &= W \end{aligned} \tag{3.3}$$

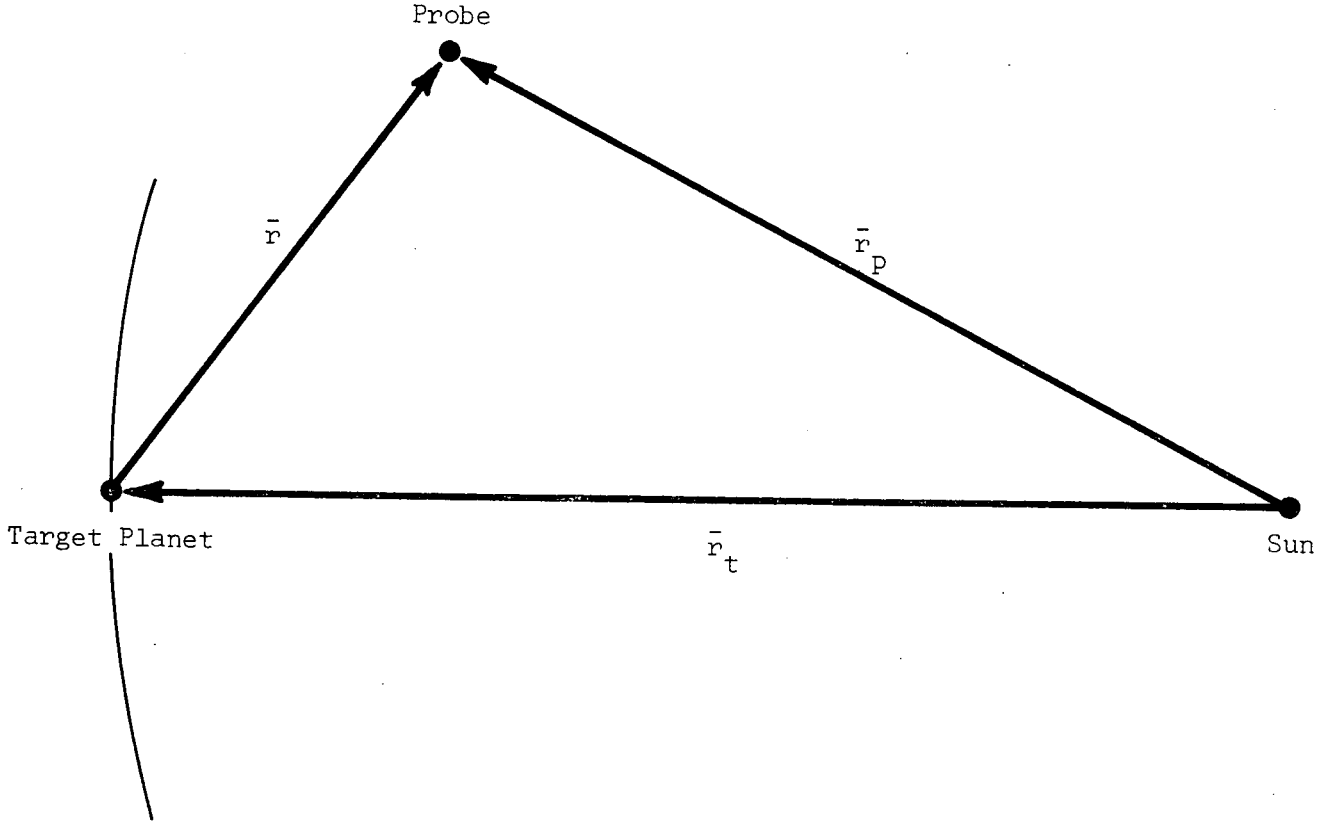

Figure 1. Problem Geometry

$$\dot{U} = -\mu \frac{X}{r^3} - \mu_s \left[\frac{X_t + X}{r_p^3} - \frac{X_t}{r_t^3}\right] + u_x \qquad (3.3)$$

$$\dot{V} = -\mu \frac{Y}{r^3} - \mu_s \left[\frac{Y_t + Y}{r_p^3} - \frac{Y_t}{r_t^3}\right] + u_y$$

$$\dot{W} = -\mu \frac{Z}{r^3} - \mu_s \left[\frac{Z_t + Z}{r_p^3} - \frac{Z_t}{r_t^3}\right] + u_z$$

The heliocentric position components of the target planet can be expressed as

$$X_t = X_t^* + b_x$$

$$Y_t = Y_t^* + b_y$$

$$Z_t = Z_t^* + b_z$$

where X_t^* , Y_t^* and Z_t^* are the components of the heliocentric position vectors obtained from the planetary ephemeris and b_x , b_y and b_z are components of bias in the position vector due to the errors in the planetary ephemeris. The components of the planetary position bias are assumed to be constant over the time period of interest. The position vector of target planet changes very slowly and this assumption appears to be reasonable.

3.3 Augmented State Vector

Since the uncertainty in the position of the outer planets (Jupiter in this study) is assumed to be an influential error source, the planetary bias vector b_x , b_y and b_z are assumed to be unknown parameters and are estimated. To achieve this objective, the original state vector given by Eq. (3.3) is expanded to include b_x , b_y and b_z and the augmented state is defined as

$$x^T = [X,Y,Z,U,V,W,b_x,b_y,b_z]$$

The augmented state vector is governed by the (9×1) vector differential equation

$$\dot{x} = f(x,t) + u \tag{3.5}$$

where

$$f_1 = U \quad , \quad f_2 = V \quad , \quad f_3 = W$$

$$f_4 = -\mu \frac{X}{r^3} - \mu_s \left[\frac{X_t + X}{r_p^3} - \frac{X_t}{r_t^3}\right] + u_x$$

$$f_5 = -\mu \frac{Y}{r^3} - \mu_s \left[\frac{Y_t + Y}{r_p^3} - \frac{Y_t}{r_t^3}\right] + u_y \tag{3.6}$$

$$f_6 = -\mu \frac{Z}{r^3} - \mu_s \left[\frac{Z_t + Z}{r_p^3} - \frac{Z_t}{r_t^3}\right] + u_z$$

$$f_7 = f_8 = f_9 = 0$$

3.4 State-Observation Relationships

There are four types of observations considered: range (ρ), range-rate $(\dot{\rho})$, sun-planet angle (α), and star-planet angle (β). The first two of these are Earth-based while the other two are onboard observations. Any combination of the above four observations can be processed at any time interval. Such a procedure is necessary if the characteristics of each type of observation are to be determined.

1. The range measurement is given by

$$\rho = (\bar{\rho} \cdot \bar{\rho})^{1/2} + v_\rho \tag{3.7}$$

where v_ρ is the random error in the range measurements and where

$$\bar{\rho} = \bar{r}_p - \bar{r}_s \quad .$$

In cartesian components

$$\rho = [(X_p - X_s)^2 + (Y_p - Y_s)^2 + (Z_p - Z_s)^2]^{1/2} + v_\rho \tag{3.8}$$

where X_s, Y_s and Z_s are the heliocentric position coordinates of the tracking station, and X_p, Y_p and Z_p are the heliocentric position coordinates of the probe.

2. Range-rate observation

Differentiation of Eq. (3.7) with respect to time yields the range-rate observation given by

$$\dot{\rho} = \frac{\dot{\bar{\rho}} \cdot \bar{\rho}}{\rho} + v_{\dot{\rho}} \tag{3.9}$$

where $v_{\dot{\rho}}$ is the random observation error. In the heliocentric cartesian coordinate system, the expression becomes

$$\dot{\rho} = [(\dot{X}_p - \dot{X}_s)(X_p - X_s) + (\dot{Y}_p - \dot{Y}_s)(Y_p - Y_s) + (\dot{Z}_p - \dot{Z}_s)(Z_p - Z_s)]/\rho + v_{\dot{\rho}} \tag{3.10}$$

3. Sun-planet angle

The onboard angle measurement α, defined as the smaller angle between the probe-planet line and the probe-sun line, is given by

$$\alpha = \cos^{-1}\left[\frac{\bar{r} \cdot \bar{r}_p}{r r_p}\right] + v_\alpha \tag{3.11}$$

where v_α is the observation error.

Since $\bar{r}_p = \bar{r}_t + \bar{r}$, Eq. (3.11) can be written as

$$\alpha = \cos^{-1}\left[\frac{\bar{r} \cdot \bar{r}_t + r^2}{r r_p}\right] + v_\alpha \tag{3.12}$$

which in component form becomes

$$\alpha = \cos^{-1} [(XX_t + YY_t + ZZ_t + r^2)/rr_p] + v_\alpha \qquad (3.13)$$

where

$$r = [X^2 + Y^2 + Z^2]^{1/2}$$

and

$$r_p = [X_p^2 + Y_p^2 + Z_p^2]^{1/2}$$

4. Star-planet angle

The last star-planet angle measurement β, defined as the smaller angle between the probe-planet line and the line from the probe to a reference star, is given by

$$\beta = \cos^{-1} [\frac{-\bar{r} \cdot \bar{S}}{r}] + v_\beta \qquad (3.14)$$

where v_β is the random observation error and $\bar{S}$ is a unit vector in the direction of the reference star. The star is assumed to be at an infinite distance so that $\bar{S}$ is a constant vector. Since the inclination of Earth and Jupiter are nearly zero, it follows that Earth, Jupiter and the space probe lie in very nearly the same plane. Hence, it is desirable to use a star which is not in this plane as a reference star to obtain information about the out-of-plane motion. Star-planet angle measurement can be expressed in cartesian components as

$$\beta = \cos^{-1} [-(XS_x + YS_y + ZS_z)/r] + v_\beta \qquad (3.15)$$

where S_x, S_y and S_z are the direction cosines of the reference star direction.

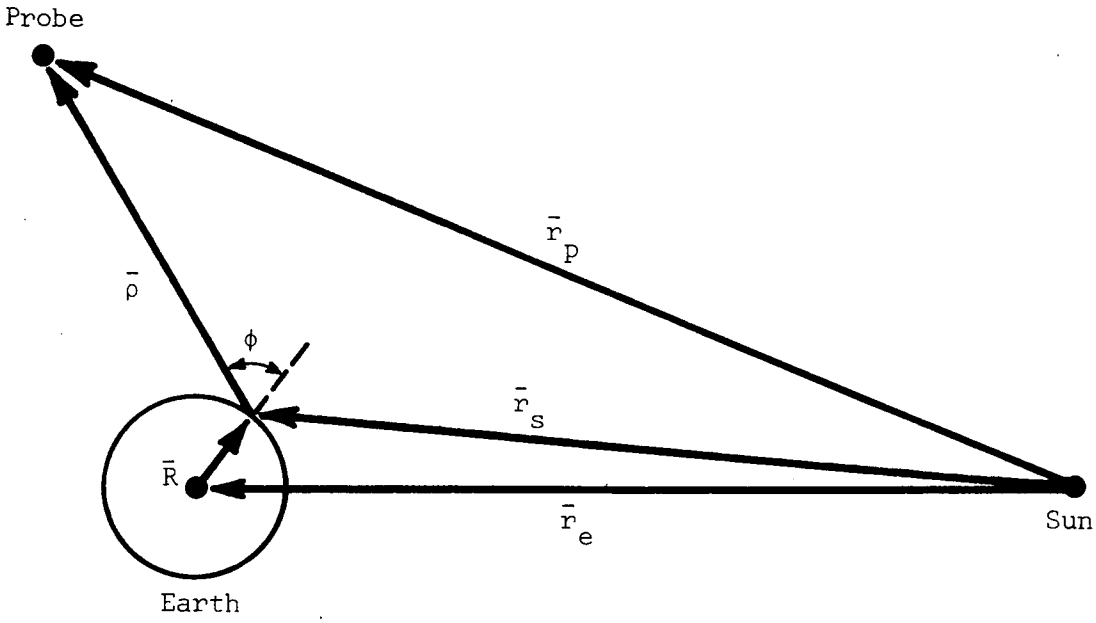

Figure 2. Earth-Based Observation Geometry

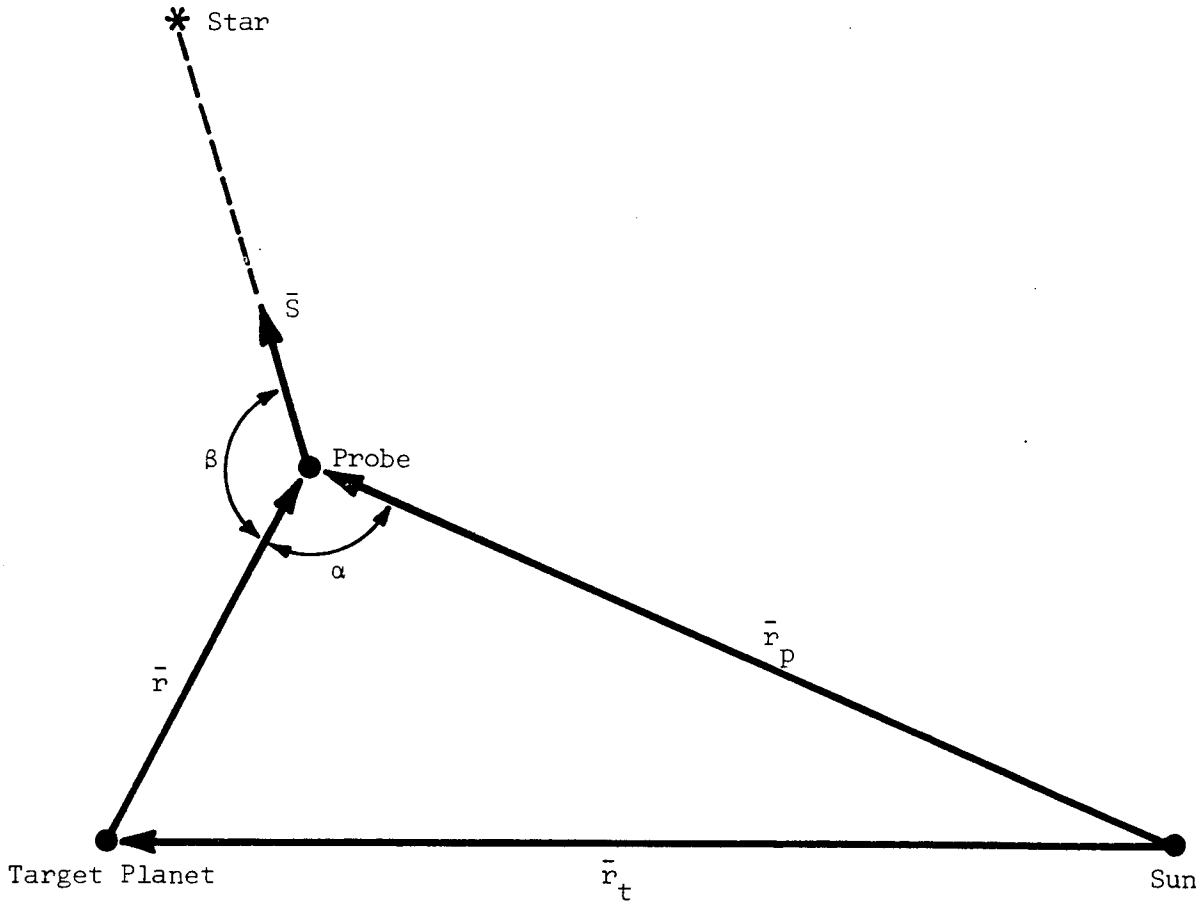

Figure 3. Onboard Observation Geometry

3.5 Motion of the Tracking Station

Range and range-rate observations are taken at a tracking station on the Earth and the heliocentric position vector of the tracking station is given by

$$\bar{r}_s = \bar{r}_e + \bar{R} \tag{3.16}$$

where $\bar{r}_e$ is the heliocentric position of the Earth and $\bar{R}$ is the geocentric position of the tracking station. The vector $\bar{R}$ is computed as a function of time from the relationship

$$\bar{R} = [T]\begin{bmatrix} R \cos \delta_s \cos \alpha_s(t) \\ R \cos \delta_s \sin \alpha_s(t) \\ R \sin \delta_s \end{bmatrix} \tag{3.17}$$

where α_s is the right ascension of the tracking station,

δ_s is the declination (latitude) of the tracking station,

R is the magnitude of the vector $\bar{R}$ and the radial distance of the tracking station from the Earth's center,

and

$$T = \begin{bmatrix} 1 & 0 & 0 \\ 0 & \cos \varepsilon & \sin \varepsilon \\ 0 & -\sin \varepsilon & \cos \varepsilon \end{bmatrix}$$

is the rotational matrix which transforms the coordinates from an equatorial to an ecliptic coordinate system which is chosen to be the heliocentric system. The argument ε is the obliquity of the ecliptic. With the assumption that the Earth's rotation is uniform, the right ascension of the tracking station can be expressed as

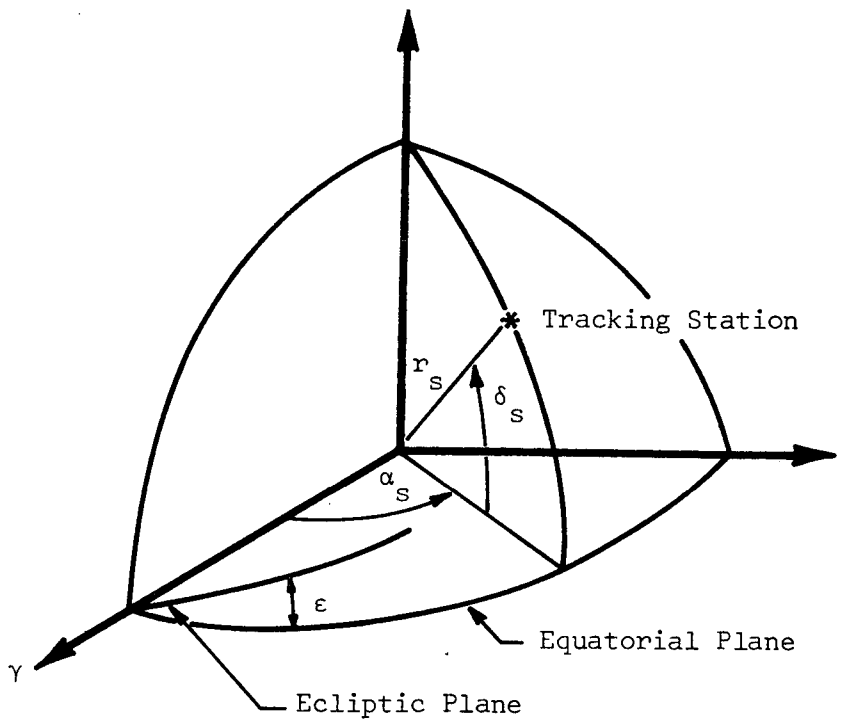

Figure 4. Tracking Station Geometry

$$\alpha_s(t) = \alpha_s(t_o) + \dot{\alpha}_s \cdot (t - t_o)$$

Differentiation of Eq. (3.16) with respect to the time yields the heliocentric velocity of the tracking station.

$$\dot{\bar{r}}_s = \dot{\bar{r}}_e + [T] \begin{bmatrix} -\dot{\alpha}_s R \cos \delta_s \sin \alpha_s(t) \\ \dot{\alpha}_s R \cos \delta_s \cos \alpha_s(t) \\ 0 \end{bmatrix} \tag{3.18}$$

The zenith angle ϕ of the probe with respect to the tracking station is given by

$$\cos \phi = \frac{\bar{R} \cdot \bar{\rho}}{R\rho} \tag{3.19}$$

The probe is assumed to be visible from the tracking station if $\cos \phi$ is positive.

3.6 Simulation of Errors

Each component of the noise in the equations of motion (3.1) and observation-state relations is modeled as a normally distributed scalar random variable with zero mean and known variance. The noises are simulated by sampling at random from a standard normal distribution function (zero mean and unit variance) and then scaling the sampled number by the given standard deviation.

The normal density function of the random variable ξ is given by

$$f(\xi) = \frac{1}{\sqrt{2\pi}\sigma} \exp \left[- \frac{(\xi - m)^2}{2\sigma^2} \right] \tag{3.20}$$

where m and σ are the mean and the standard deviation, respectively. Eq. (3.20) can be written in terms of the standard normal distribution function

$$F(z) = \frac{1}{\sqrt{2\pi}} \int_{-\infty}^{z} \exp(-\frac{\zeta^2}{2}) d\zeta \tag{3.21}$$

by the transformation

$$\zeta = \frac{\xi - m}{\sigma} \tag{3.22}$$

For the random variable of zero mean

$$\xi = \sigma\zeta \tag{3.23}$$

The inverse of Eq. (3.21) can be approximated by the curve fit equation (40)

$$z \cong \Gamma - \frac{C_o + C_1\Gamma + C_2\Gamma^2}{1 + d_1\Gamma + d_2\Gamma^2 + d_3\Gamma^3}$$

$$\Gamma = [\ell n(F^{-2})]^2 \tag{3.24}$$

where the coefficients c_i and d_i have the following values

$C_o = 2.515517$ $\quad d_1 = 1.432788$

$C_1 = 0.802853$ $\quad d_2 = 0.189269$

$C_3 = 0.010328$ $\quad d_3 = 0.001308$

Sampling of the standard normal distribution is accomplished by first sampling at random from a uniform distribution to obtain a value for $F(0 \leq F \leq 1)$ and then computing the standard normal random number z from Eq. (3.24). The simulated noise is then computed as the product of the sampled value z of the standard normal random variable ζ and the standard deviation σ by Eq. (3.23).

Observational data are simulated by adding random numbers ξ which are generated in the manner described above to the observation value computed from the true state and state-observation relationships discussed in Section 3.4, i.e.

$$Y = Y_{true} + v \tag{3.25}$$

Noise in the equation of motion is simulated in the same way as above and then added to the equation of motion at discrete points of time which correspond to the integration step.

3.7 Computer Program Description

The program NONSTEP (NONlinear STate, Estimation Program) is developed for comparison of the extended Kalman filter and the nonlinear estimation algorithms by applying each to the study of an interplanetary orbit determination problem. Special emphasis is given to the planetary fly-by mode although the planetary orbiter is considered also.

The program was written in FORTRAN IV for the CDC 6600 computer system at The University of Texas at Austin. Since this computer has a single precision word length of sixty bits, single precision arithmetic was considered to be adequate for most calculations. The initial frame of the program was founded on the existing program STEP (STate EStimation Program) developed by Jones (28) at The University of Texas at Austin.

The three basic functions of the program, i.e., simulation, estimation, and evaluation, are conducted sequentially according to a schedule specified in the input data. The program NONSTEP has a capability for carrying out the nonlinear estimation algorithms as well as the extended Kalman filter, depending on the input data IFILTER. If IFILTER = 1, the extended Kalman filter is carried out. If IFILTER = 2, the nonlinear filter is implemented and, finally, if IFILTER = 3, the nonlinear estimation procedure is first carried out and then, with the same input data and random noises, the extended Kalman filter is carried out. With this latter option,

a direct comparison of the linear and nonlinear algorithms can be made.

In order to reduce the storage space for compilation, the program NONSTEP employs OVERLAY. The main OVERLAY(0,0) controls the overall program. The OVERLAY(1,0) conducts all the plots of the output data for the case of IFILTER = 1 or 2. The OVERLAY(2,0) does the same thing for the case of IFILTER = 3. The OVERLAY(3,0) conducts all of the calculations involved in simulations, estimations, and evaluations and transfers the output data to a magnetic tape for the plot of OVERLAY(1,0) or OVERLAY(2,0).

In conjunction with the apriori conditional covariance matrix, the true trajectory and apriori estimate are generated simultaneously through parallel numerical integrations of the apriori estimate and the apriori conditional covariance matrix. A general purpose numerical integration subroutine is used to simultaneously integrate the differential equations. The routine consists of a Fourth Order Adams predictor-corrector scheme with a Runge-Kutta starter. Although the integration is carried out in single-precision, the dependent variables are carried in double-precision to minimize round-off errors.

Observational data are simulated by generating random noise and superimposing it on the true observation computed from the true state.

A simplified block diagram of the computational logic is shown in Fig. 5.

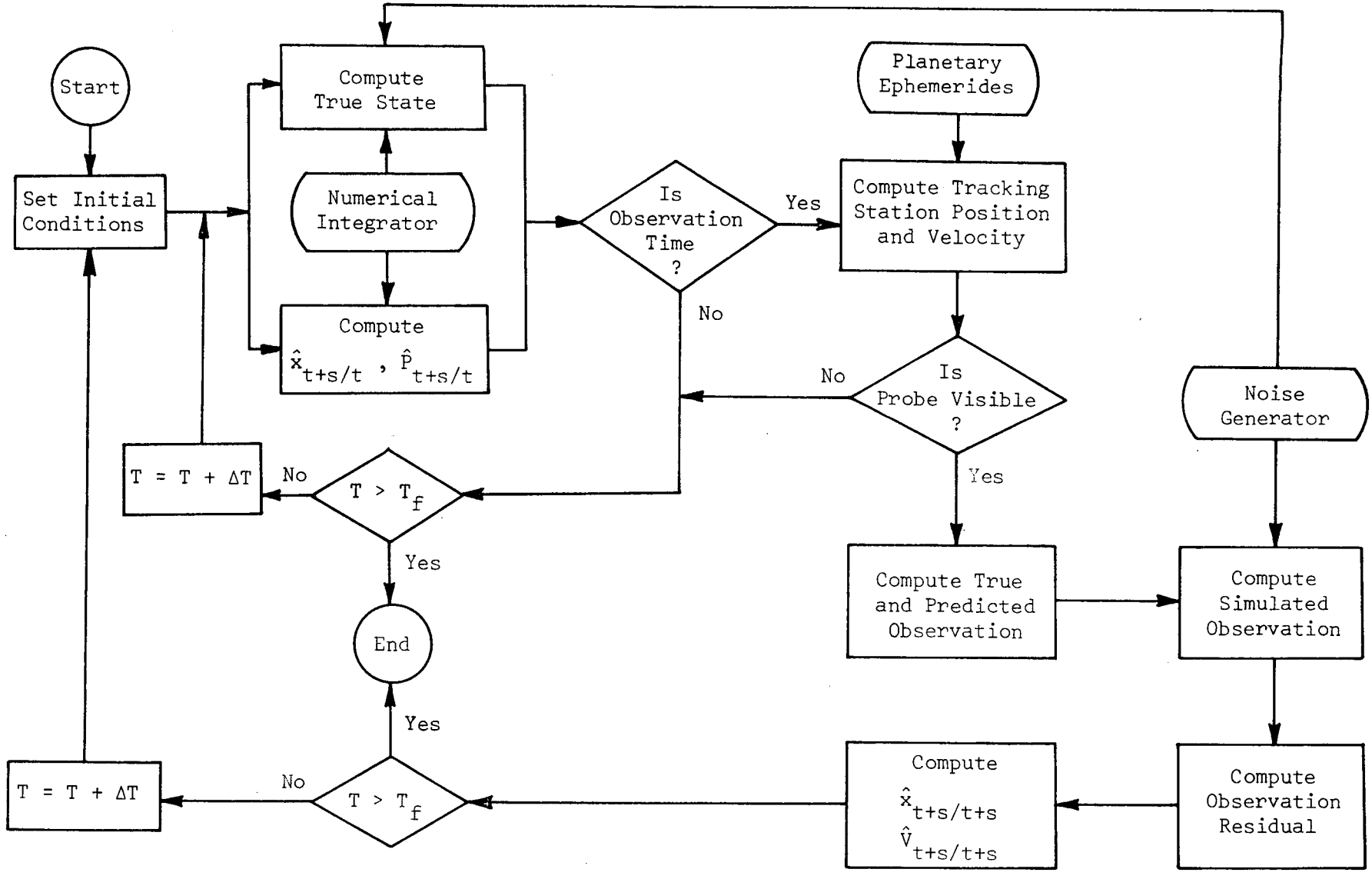

Figure 5. Block Diagram of Computational Logic

CHAPTER 4

DISCUSSION OF NUMERICAL RESULTS

The purpose of this chapter is to determine the characteristics of second order filters on the basis of a numerically simulated study. There are two basic classes of second order filters to be examined. The first is the modified Gaussian second order (MGSO) filter and the other is the modified truncated second order (MTSO) filter. The basic difference between these two filters is that the Kalman gain compensation (KGS) term enters with a plus sign of one-half in the first filter and with a minus sign of one-fourth in the later filter. Both filters include a dynamic second order (DSO) term, $(f_{xx} : \hat{P})/2$, in the dynamic equation (2.54) and an observation second order (OSO) term, $(h_{xx} : \hat{P})/2$, in the predicted observation equation (2.56).

4.1 Various Simplified Forms of Second Order Nonlinear Filters

Although the modified Gaussian second order filter and the modified truncated second order filter are developed using a model in which both state and the observation equations are nonlinear, there is a possibility that the actual problem will consist of a highly nonlinear dynamic equation and a relatively linear observation or vice versa. In this situation, the second order term in the relatively linear relation may be neglected, and, hence, several possible simplified nonlinear estimation algorithms can be obtained, depending on the presence of the dynamic second order term, observation second order term, and the Kalman gain compensation term in various combinations. The resulting filters are tabulated in Table 1. The Filters 1, 8 and 9 of Table 1 correspond to the MGSO Filter, the MTSO Filter and the extended Kalman (EK) Filter, respectively. The Filter 4 is specifically referred to

as the Kalman Gain Compensated (KGC) Filter. The performance of each of the Filters, 1 through 8, is studied through numerical simulations and compared with the EK Filter which is the most popular filter at present time. The nonlinear filter is first executed with the input data given in Tables 5 through 9, and then the EK Filter is executed under the same conditions. The same sequence of random numbers is used to simulate the state noises as well as the observation noise in both filters. The conclusions reached in this investigation are based on the results of several hundred simulations. The results obtained in eighteen of these simulations are presented in this report. These results obtained in these cases are representative of the results obtained in the remaining studies.

TABLE 1. SIMPLIFIED NONLINEAR FILTERS

	DSO = $(f_{xx} : \hat{P}_{t+s/t})/2$	OSO = $(h_{xx} : \hat{P}_{t+s/t})/2$	KGCT = $[h_{xx} : \hat{P}_{t+s/t}][h_{xx} : \hat{P}_{t+s/t}]^T$
(MGSO filter) FILTER 1	YES	YES	KGCT/2
FILTER 2	NO	YES	KGCT/2
FILTER 3	YES	YES	NO
(KGC filter) FILTER 4	NO	NO	KGCT/2
FILTER 5	NO	YES	NO
FILTER 6	NO	YES	-KGCT/4
FILTER 7	NO	NO	-KGCT/4
(MTSO filter) FILTER 8	YES	YES	-KGCT/4
(EK filter) FILTER 9	NO	NO	NO

4.2 The Nominal Trajectory and Error Sources

The nominal trajectories are generated by integrating the equations of motion (3.1) with dynamic state noise set equal to zero. In other words, the random noise u is simply set to zero. Considering the possibilities of applying the nonlinear algorithm to the problems of a near-Earth or lunar satellite, Mariner and Viking missions, simulations are conducted not only for a hypobolic orbit, but also for an elliptic orbit. The nominal trajectory of the elliptic orbit is shown in Fig. 6 and the hyperbolic orbit in Fig. 7. The periapsis and apoapsis for the elliptic orbit occur at about 4.6 and 20 days, respectively. The periapsis encounter in the hyperbolic orbit occurs at about 12.7 days.

As seen in Figs. 6 and 7, the dynamic nonlinearity in the elliptic orbit is very much concentrated near periapsis and apoapsis, but it is well distributed over the entire trajectory when compared with the hypobolic orbit. In the hypobolic orbit, the dynamic nonlinearity is concentrated almost entirely near the perigee, and the pre- and post-encounter trajectories appear to be straight lines.

The initial conditions for the hypobolic and elliptic orbits are obtained from the nominal Grand Tour mission trajectory with Earth launch date and Jupiter encounter (28). For the elliptic orbit, the velocity components are reduced so that it yields an elliptic orbit with a proper period of 30 days. The nominal trajectory initial conditions are given in Table 2 and the orbital elements of Jupiter and Earth are listed in Table 3.

The true trajectory (or state) is generated by adding a vector Gaussian random forcing term u described in Section 3.6, to the equations of motion (3.1).

The actual observations are simulated with the data given in Table 4 by using the following procedure:

1. Compute the nominal observation through the state-observation relationship with the true trajectory obtained as described above.
2. Gaussian random noise is generated as described in Section 3.6 and added to the nominal observation.

The standard deviation σ_Q of the dynamic state noise u and σ_R of observation noise v are given in Tables 5 through 9 according to the simulations. Since it is common practice to employ an adequate σ_Q for the dynamic noise u, even though there is no dynamic noise assumed, two values of σ_Q are used. σ_{QT} is designated for the true trajectory and σ_{QA} is adopted for the estimate of the state.

TABLE 2. JULIAN DATE AND TRUE STATES AT INITIAL TIME

		X COMPONENT	Y COMPONENT	Z COMPONENT
HYPOBOLIC ORBIT JD = 244802.8	POSITION (KM)	2.4700434082×10^{6}	$-1.1308760230\times10^{7}$	4.7435578173×10^{5}
	VELOCITY (KM/SEC)	-0.7804113160	9.1873486000	-0.4730900710
	BIAS (KM)	0	0	0
ELLIPTIC ORBIT JD = 244812.8	POSITION (KM)	1.5797023900×10^{6}	$-2.6660249500\times10^{6}$	4.0483584600×10^{4}
	VELOCITY (KM/SEC)	0.9227130460	5.9467835000	-0.2763467890
	BIAS (KM)	0	0	0

TABLE 3. PLANET ORBIT ELEMENTS

	EARTH	JUPITER
SEMI-MAJOR AXIS, a , (AU)	0.99999984924	5.2080609002
ECCENTRICITY, e ,	1.671330920×10^{-2}	$4.7439441265\times10^{-2}$
INCLINATION i (DEG)	$3.8534133187\times10^{-3}$	1.3066472679
RIGHT ASCENSION OF ASCENDING NODE, Ω , (DEG)	1.7545297300×10^{2}	9.9979271397×10^{1}
ARGUMENT OF PERIAPSIS ω , (DEG)	$-7.3304115746\times10^{1}$	$-8.5087384560\times10^{1}$
MEAN ANOMALY M , (DEG)	1.7589871397×10^{2}	1.1659075977×10^{2}
EPOCH OF ELEMENTS (JD)	2.4440555000×10^{6}	2.4440555000×10^{6}
SUN'S GRAVITATIONAL CONSTANT (km^3/sec^2)		$1.3271251802\times10^{11}$
JUPITER'S GRAVITATIONAL CONSTANT (km^3/sec^2)		1.2671206804×10^{8}

TABLE 4. OBSERVATIONAL DATA

REFERENCE STAR DIRECTION COSINE	ℓ	m	n
	0	-0.24192	-0.9703
TRACKING STATION LOCATION	GEOCENTRIC DISTANCE (km)	RIGHT ASCENSION (DEG)	LATITUDE (DEG)
	6376.29673	151.43676	21.99133
OBLIQUITY OF ECLIPTIC (DEG)		EARTH'S ROTATION RATE (DEG/DAY)	
23.442		360	

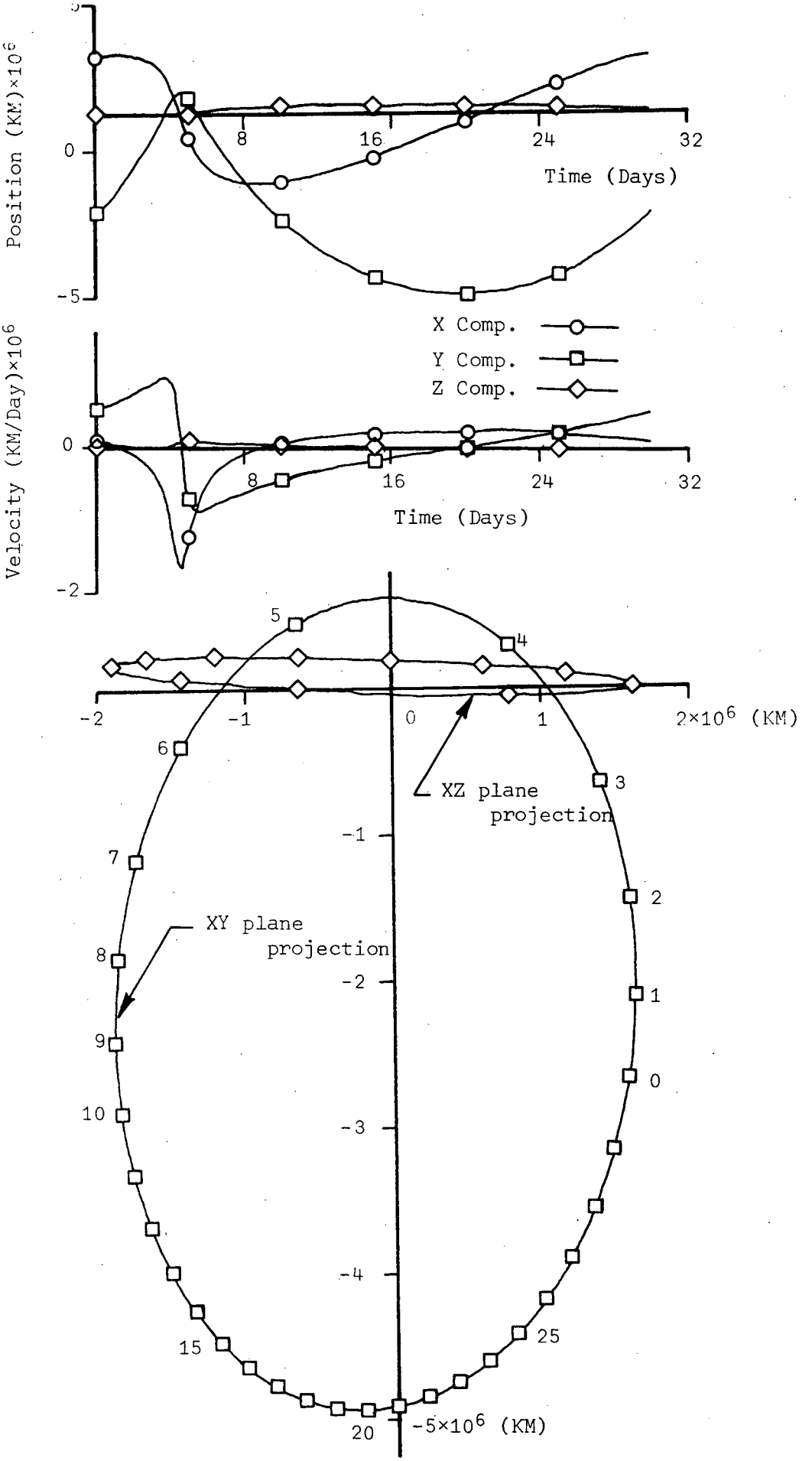

Figure 6. Nominal Trajectory (Elliptic Orbit)

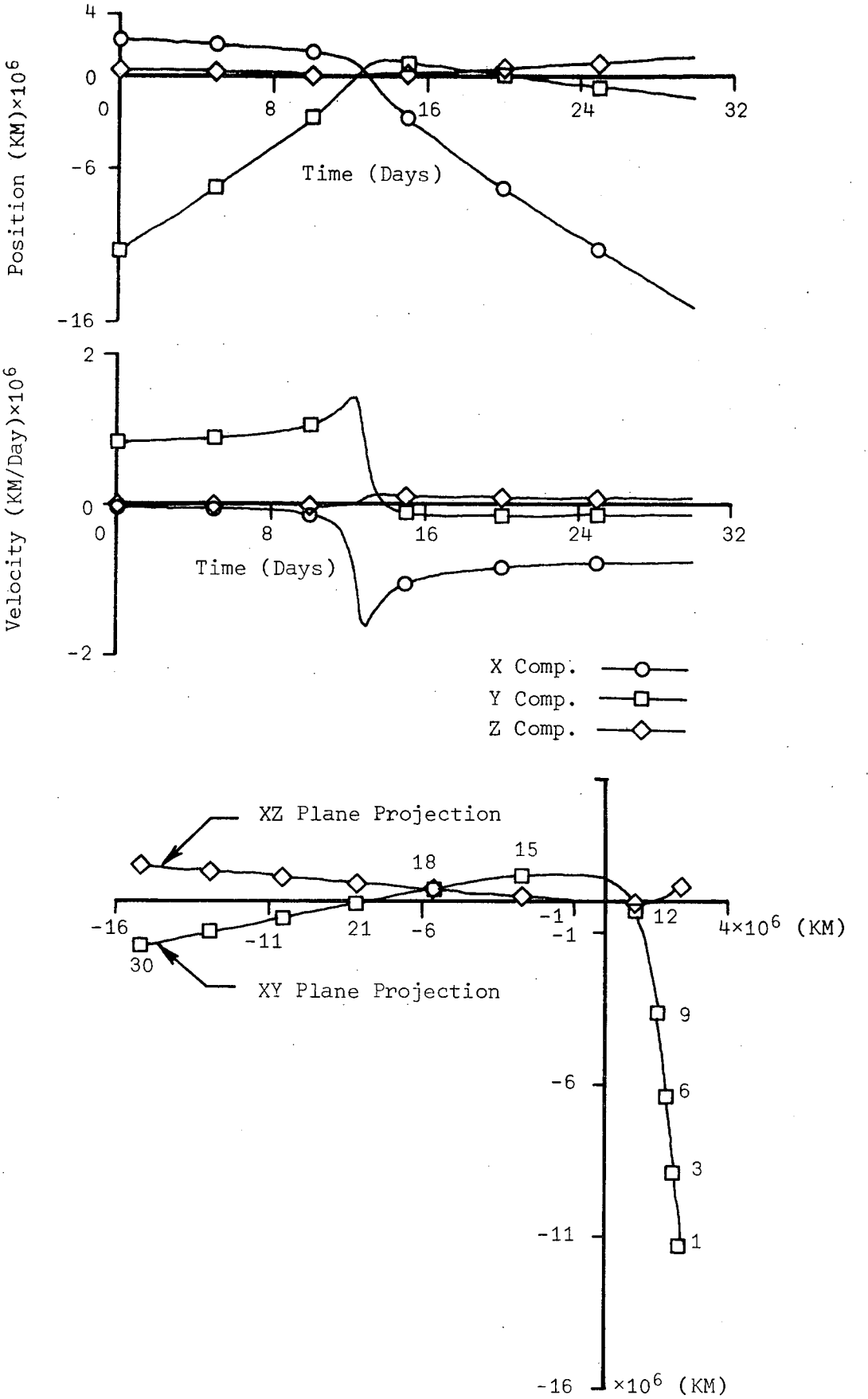

Figure 7. Nominal Trajectory (Hypobolic Orbit)

4.3 Characteristics of the Filters

The results of Simulations 1 through 8 are presented primarily for the purpose of describing the characteristics of the filter algorithms in Table 1.

For each simulation, position and velocity estimation errors are plotted and they are compared with results obtained with the extended Kalman (EK) filter which is filter 9 in Table 1. In addition to the estimation errors, the conditional variances and the observation residual which is defined as the difference between the actual observation and the predicted observation are shown. Unless stated otherwise, all figures are obtained by connecting every third data point with straight lines. There are thirty data points between two adjacent symbols. The main reason for sampling every third data point is due to the difficulty of tracing the original plot obtained from the Calcomp computer ploter when every data point is plotted.

In this study, the planetary bias is approximated as a constant parameter and its value is estimated. But, the estimation errors and the conditional variances remain virtually constant with the onboard angle measurements during the time period of interest. Furthermore, the difference between results obtained with the nonlinear filters and the EK Filter are negligible. Consequently, the estimation errors and conditional variances corresponding to the planetary bias are not presented in this report.

Since the nonlinear filters are compared with the EK filter, the estimation errors and conditional variances for the EK filter in the Simulations 1 through 8 should be identical. However, the actual figures are not identical because of scale factors.

The EK filter performs adequately up to three days and thereafter

becomes unstable. Actually, right after the three day period, the conditional variances decrease drastically and the estimation errors take several sharp oscillatory spikes during a short period of time while drifting away from zero. The sharp decrease in conditional variance is attributed to the fact that $h_x \hat{P} h_x^T$ dominates R in Eq. (1.35) and, hence, the negative term in Eq. (1.33) will be quite large. The position and velocity estimation errors and the conditional variances for the EK Filter are shown in Figs. 8-a, 8-b, 10-c, and 10-d.

Immediately after encounter (12.7 days), the velocity estimation errors remain at a relatively constant level and, hence, the position estimation errors grow linearly, in an unbounded manner, and divergences occur eventually. The velocity estimation errors become extremely unstable shortly after encounter and the magnitude oscillates several times with sharp spikes. This phenomena is not seen in the figures shown here because of the fact that every third data point, instead of every data point, is plotted. In particular, the velocity components of the conditional variances are very small after encounter, and the filter becomes saturated. Therefore, the observations taken after encounter cannot improve the estimate very much. The characteristic of poor estimation after encounter is an indication of the importance of the pre-encounter navigation.

Figs. 8-a and 8-b show the position and velocity estimation errors for the Simulation 1 which compares the Filter 1 (or MGSO Filter) and the EK Filter. Both Filters perform adequately up to three days and there are no significant differences between them. After three days, the EK Filter becomes unstable. However, the MGSO Filter performs properly up to encounter. Both Filters diverge after encounter.

It is interesting to notice that the MGSO Filter obtains a more accurate estimate of the Y and Z components and less accurate estimate of the X components after encounter than the EK Filter does.

Although the corresponding conditional variances are not specifically shown here, they are almost identical to the ones given in Figs. 11-d and 11-e. It is interesting to note that the conditional variances for the MGSO Filter are considerably larger than those of the EK Filter especially in the region from three to thirteen days, during which the MGSO Filter estimates surprisingly better than the EK Filter.

Figs. 9-a and 9-b show the position and velocity estimation errors for Simulation 2 which compares Filter 2 and the EK Filter. Filter 2 performs considerably better than the EK Filter throughout the entire region. For future discussion the oscillations around encounter are emphasized here. The conditional variances are identical to the one shown in Figs. 11-d and 11-e, which also correspond to Simulations 1 and 4.

From Table 1, it can be seen that the only difference between Filter 1 (or MGSO Filter) and Filter 2 is that the dynamic second order (DSO) term is dropped in Filter 2. Therefore, the comparison of Filter 1 and Filter 2 shows the effect of DSO term. As seen in Figs. 8-a, 8-b, 9-a, and 9-b, the effect of DSO term has a significant effect after encounter. By dropping the DSO term from the MGSO Filter (Filter 1), a far better estimate is obtained.

A number of simulations indicate that the DSO term is very sensitive to the initial covariance matrix. For the larger values of the initial variances, less satisfactory estimates are obtained. The simulations indicate that the MGSO Filter diverges while the EK Filter yields a convergent

estimate whenever large initial variances are used with relatively large state noise σ_Q . For small initial variances and small state noise σ_Q , the differences between the two Filters MGSO and EK Filters are negligible. This implies that none of the DSO, OSO and KGC terms are important. Apparently, most of the orbit determination problems which are not influenced by a state noise u fall in this category and the differences between the EK Filter and the MGSO Filter are negligible. However, there appears to be a range in which the initial variances can be so chosen that the effect of DSO term improves the filter performance. But, it may not be easy to select such an initial covariance matrix in a complex multi-dimensional problem, because the chosen set of initial covariance matrix may very well cause the DSO term to affect the filter in such a way that the estimate of some components can be improved while the estimates of other components is degraded. An example of this situation is shown in Figs. 8-a and 8-b.

Usually, if the EK Filter converges, i.e., if the conditional variances remain small, the MGSO Filter acts like the EK Filter. This is due to the fact that the effect of the DSO term can be overridden by the small variances associated with the observations. In contrast, if the covariance reduction caused by the observations cannot override the effect of the DSO term, which will occur when the initial variances and dynamic state noise are large, then the MGSO Filter diverges because of the DSO term even though the EK Filter converges. A large conditional variance allows the estimate to depart from the true trajectory because of the DSO term and cause a bad predicted observation and, consequently, large observation residual which will lead to filter instability and divergence.

Figs. 11-b and 11-c show the estimation errors for Simulation

4 which compares Filter 4 with the EK Filter. As seen in Table 1, Filter 4 includes only the KGC term and excludes the DSO and OSO terms. Filter 4 is referred to as the Kalman Gain Compensated (KGC) Filter.

The comparison of the filter performance with Filter 2 will show clearly the effect of the OSO term and the comparison with the EK Filter reflects the effects of the KGC term. From Figs. 11-b and 11-c, it is seen that the Filter 4 (KGC Filter) estimates show excellent agreement with the true trajectory throughout the entire region. Both the KGC Filter and the EK Filter appear to be identical for the first three days. After three days, the EK Filter diverges. Although the EK Filter performs poorly over almost the entire region except for the first three days, the poor performance after encounter results from the behavior which occurs from three days to encounter. The accumulated large estimation errors at encounter influence the estimate throughout the remainder of the period.

The phenomena above can be explained as follows: the conditional variances become quite small after encounter, and the filters become insensitive to observations. Therefore, a filter that can estimate accurately around encounter can retain an accurate estimate after encounter. Similarly, any filter which performs in an unsatisfactory manner around encounter will yield an inaccurate estimate after encounter.

Fig. 11-a shows the observation residuals for Simulation 4. The observation residual pattern for the EK Filter starts to grow from three days and is influenced by a large spike around encounter. After encounter the residual patterns for the EK Filter and the KGC Filter remains identical to each other.

The conditional variances are shown in Figs. 11-d and 11-e. It is

interesting to note that the conditional variances for the EK Filter undergo a sharp reduction at a time of about four days following which the estimation errors begin to drift away. The conditional variances for the KGC Filter retain a larger value for the period of time from four to twelve days during which the poor performance of the EK Filter has been accumulated.

From the simulations, it was noticed that the KGC term is negligible at the beginning in comparison with the other terms $h_x \hat{P} h_x^T$ and R in Eq. (2.57). But, it grows rapidly and becomes the dominating term from three to twelve days. As a matter of fact, the maximum value of the KGC term is about ten times larger than the other two terms. The KGC term becomes again negligible after the encounter. The above fact implies that the observation nonlinearity is very severe from three to twelve days. The observations outside this region appear to be relatively linear. The severe observation nonlinearity near encounter is seemed to be caused by the dynamic nonlinearity. The same investigation was made on the other type of observations. The sun-planet angle measurement has almost the same characteristics as the star-planet angle measurement. However, the range and range-rate observations do not appear to be influenced by the second order terms and the KGC terms for both observations are negligible. Hence, no difference between the KGC Filter and the EK Filter is seen.

From Eq. (2.57), it can be seen that a large KGC term yields a smaller optimal gain K than that which results in the EK Filter. Hence, a smaller conditional covariance reduction occurs and a larger posterior covariance matrix results, as can be seen from Eq. (2.59). In Figs. 11-d and 11-e exactly the same phenomena described above, happens in the region from four days to encounter.

Between observations, the conditional variances vary according to the differential Eq. (2.55) and the direction of change depends on the signs of the Jacobian matrix f_x. At the time of the observation, Eq. (2.59) governs the conditional covariance matrix reduction. The conditional variances increase only through the dynamics, namely, the signs of f_x and decrease by either the dynamics or observations, namely h_x. For example, the reduction for the EK Filter around four days is attributed to the observations and the one near twelve days appears to be due to the sign changes of f_x.

It appears that near encounter, the dynamic nonlinearity overrides the information gained through the observations. Physically, this means that a severe dynamic nonlinearity causes bad predicted observations and observation nonlinearity. Therefore, large observation residuals are inevitable. In this situation one can follow one of two procedures:

1. Discard the observations during this period.

2. Try to update the apriori estimates with larger gains, K.

It appears that the EK Filter follows the second course while the KGC Filter takes the first course. The KGC Filter yields a large value for the conditional covariance matrix, and hence, leads to a small value for the gain K because of the KGC term. This means that the KGC Filter places less weight on each of the observations obtained during the period of time in which dynamic nonlinearity is very severe.

In addition to the large value for K, the observation residual is so large during the brief period of time, as seen in Fig. 11-a, that the correction to the apriori estimate in the EK filter becomes excessively large and a poor posterior estimate results. The conditional variances

for the KGC Filter depend more on the state dynamics in the region of a severe dynamic nonlinearity. The sharp decrease of the conditional variances near encounter is not due to the observations but due to the sign changes of the Jacobian matrix f_x. A large integration step size often causes a negative variance near encounter. The sign change of the Jacobian matrix f_x incorporated with the large conditional variances yields a negative slope for the conditional variances which can result in negative variances.

The conditional variances for the EK Filter depend largely on the observation, namely h_x in the region where dynamic nonlinearity is high. The sharp decrease of the conditional variances for the EK Filter around four days is an indication that the reduction by the observation overrides the increase due to the state dynamics. Unusually large reductions of the conditional variance which occur in EK Filter in the early stage of application, is attributed to this phenomena. However, it can be a nuisance if the posterior estimate is still far away from the true state even after the conditional variances reduced to a zero level. The most interesting observation is that the EK Filter becomes unstable and the estimate starts to drift away from the true trajectory whenever the conditional variances are reduced sharply. Another interesting observation is that each of the Filters (1, 2 and 4) which include the KGC term have almost identical conditional variances shown in Figs. 11-d and 11-e, and have very similar observation residual patterns, as shown in Figs. 11-a.

Figs. 12-a and 12-b show that the estimation errors for the Simulation 5 which reflects the characteristics of Filter 5. Filter 5 includes only the OSO term. Filter 5 performs better than the EK Filter from three to nine days. Apparently, the observation second order improves the performance

of Filter 5 by using the proper sign. The poor performance of Filter 5 between nine and twelve days reflects the fact that the OSO term influences the filter with the wrong sign. The poor estimates of Filter 5 after encounter are due to the propagated effect of the poor estimate at encounter.

Figs. 10-a and 10-b show the estimation errors for Simulation 3 which compares Filter 3 with the EK Filter. Filter 3 contains both the DSO and the OSO terms. By comparing Figs. 10-a and 10-b with Figs. 12-a and 12-b, the effect of the DSO term is shown significantly after encounter. The estimation errors for Filter 3 are considerably larger than those of Filter 5 after encounter. The difference would be the negative contribution of the DSO term in the Filter 3, i.e., the DSO term affects the filter with the wrong sign. The conditional variances are shown in Figs. 10-c and 10-d. These figures also represent the conditional variances resulting in Simulation 5. It is interesting to note that both Filters (3 and 5) do not contain the KGC term and the conditional variances are very similar to the one given by the EK Filter and quite different from those of Filters 1, 2 and 4 which include the KGC term. Fig. 10-e represents the observation residuals of Simulation 3. This observation residual pattern which contains a large spike (even larger than that of the EK Filter) is seen also in Simulation 5. The smooth residual pattern (Fig. 11-a) of the Filters 1, 2 and 4 is primarily attributed to the presence of the KGC term and its side effects.

Simulations 6, 7 and 8 are conducted mainly to describe the characteristics of the modified truncated second order (MTSO) filter which is designated as Filter 8. For Simulations 6, 7 and 8, only the X components of the position and velocity estimation errors, observation residual and the conditional variances $\hat{V}_{11}$ and $\hat{V}_{44}$ are shown in the corresponding figures.

The other components exhibit similar characteristics and are not shown in this report to eliminate unnecessary space. The only difference between the MGSO Filter and the MTSO Filter is that the KGC term enters with a plus sign of one-half in the first Filter and with a minus sign of one-fourth in the e second. As previously pointed out, the KGC term is negligible at the beginning but grows rapidly up to ten times the value of the combination of the other terms, $h_x\hat{P}h_x^T$ and R, as shown in expression (2.57). Following encounter, the value of the KGC term reduces in value. From the above characteristics of KGC terms, it is easy to conclude that the MTSO Filter contains a potential signularity. The optimal gain K given by Eq. (2.57) with a minus sign of one-fourth of KGC term instead of plus sign approaches plus and minus infinity as the KGC term approaches the sum of the other two terms, $h_x\hat{P}h_x^T$ and R from below and above. In addition, when the optimal gain is very large with a positive sign, the posterior conditional variance becomes negative. The phenomena is clearly reflected in Filters 6, 7 and 8, and is shown in Figs. 13-a, 13-b, 14-a, 14-b, 15-a, and 15-b.

In general, the MGSO Filter keeps the conditional variances larger than those of the EK Filter. The MTSO Filter, in contrast, has a tendency to keep the conditional variances smaller than those of the EK Filter. However, the variance becomes meaningless as the KGC term drives the variance to a negative quantity in Filters 6, 7 and 8.

TABLE 5. SIMULATION DATA (1-4)

SIMULATIONS		1	2	3	4
FIGURES		8-a,b	9-a,b	10-a,b,c,d,e	11-a,b,c,d,e
FILTER TYPE		1	2	3	4
ORBIT TYPE		HYPOBOLIC	HYPOBOLIC	HYPOBOLIC	HYPOBOLIC
OBSERVATION TYPE		STAR-PLANET	STAR-PLANET	STAR-PLANET	STAR-PLANET
OBSERVATION RATE (DAY)		10^{-1}	10^{-1}	10^{-1}	10^{-1}
OBSERVATION NOISE, σ_R (DEG)		10^{-4}	10^{-4}	10^{-4}	10^{-4}
TRUE STATE NOISE, σ_{QT} (KM/DAY^2)		10^{0}	10^{0}	10^{0}	10^{0}
APRIORI STATE NOISE, σ_{QA} (KM/DAY^2)		10^{3}	10^{3}	10^{3}	10^{3}
$\tilde{x}_{o/o}$	$\tilde{X}_o = \tilde{Y}_o = \tilde{Z}_o$ (KM)	10^{3}	10^{3}	10^{3}	10^{3}
	$\tilde{U}_o = \tilde{V}_o = \tilde{W}_o$ (KM/SEC)	10^{-4}	10^{-4}	10^{-4}	10^{-4}
	$\tilde{b}_{Xo} = \tilde{b}_{Yo} = \tilde{b}_{Zo}$ (KM)	3×10^{2}	3×10^{2}	3×10^{2}	3×10^{2}
$\hat{V}_{o/o}$	$\hat{V}_{11} = \hat{V}_{22} = \hat{V}_{33}$ $(KM)^2$	4×10^{5}	4×10^{5}	4×10^{5}	4×10^{5}
	$\hat{V}_{44} = \hat{V}_{55} = \hat{V}_{66}$ $(KM/SEC)^2$	4×10^{-2}	4×10^{-2}	4×10^{-2}	4×10^{-2}
	$\hat{V}_{77} = \hat{V}_{88} = \hat{V}_{99}$ $(KM)^2$	5×10^{4}	5×10^{4}	5×10^{4}	5×10^{4}

TABLE 6. SIMULATION DATA (5-8)

SIMULATIONS		5	6	7	8
FIGURES		12-a,b	13-a,b	14-a,b	15-a,b
FILTER TYPE		5	6	7	8
ORBIT TYPE		HYPOBOLIC	HYPOBOLIC	HYPOBOLIC	HYPOBOLIC
OBSERVATION TYPE		STAR-PLANET	STAR-PLANET	STAR-PLANET	STAR-PLANET
OBSERVATION RATE (DAY)		10^{-1}	10^{-1}	10^{-1}	10^{-1}
OBSERVATION NOISE, σ_R (DEG)		10^{-4}	10^{-4}	10^{-4}	10^{-4}
TRUE STATE NOISE, σ_{QT} (KM/DAY^2)		10^{0}	10^{0}	10^{0}	10^{0}
APRIORI STATE NOISE, σ_{QA} (KM/DAY^2)		10^{3}	10^{3}	10^{3}	10^{3}
$\tilde{x}_{o/o}$	$\tilde{X}_o = \tilde{Y}_o = \tilde{Z}_o$ (KM)	10^{3}	10^{3}	10^{3}	10^{3}
	$\tilde{U}_o = \tilde{V}_o = \tilde{W}_o$ (KM/SEC)	10^{-4}	10^{-4}	10^{-4}	10^{-4}
	$\tilde{b}_{xo} = \tilde{b}_{yo} = \tilde{b}_{zo}$ (KM)	3×10^{2}	3×10^{2}	3×10^{2}	3×10^{2}
$\hat{V}_{o/o}$	$\hat{V}_{11} = \hat{V}_{22} = \hat{V}_{33}$ (KM)^2	4×10^{5}	4×10^{5}	4×10^{5}	4×10^{5}
	$\hat{V}_{44} = \hat{V}_{55} = \hat{V}_{66}$ (KM/SEC)^2	4×10^{-2}	4×10^{-2}	4×10^{-2}	4×10^{-2}
	$\hat{V}_{77} = \hat{V}_{88} = \hat{V}_{99}$ (KM)^2	5×10^{4}	$5\ 10^{4}$	$5\ 10^{4}$	$5\ 10^{4}$

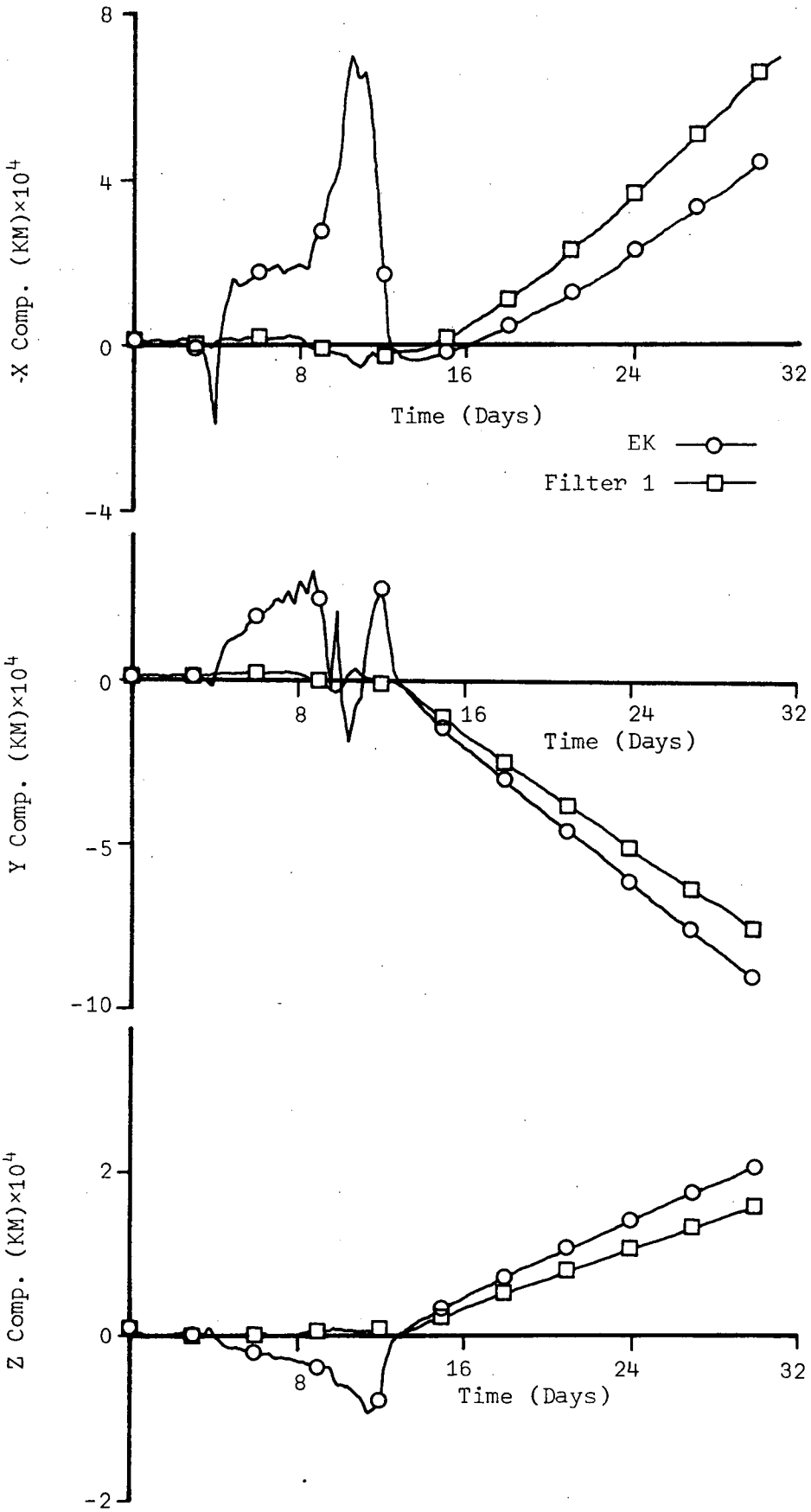

Figure 8-a. Position Estimation Errors for the Simulation 1

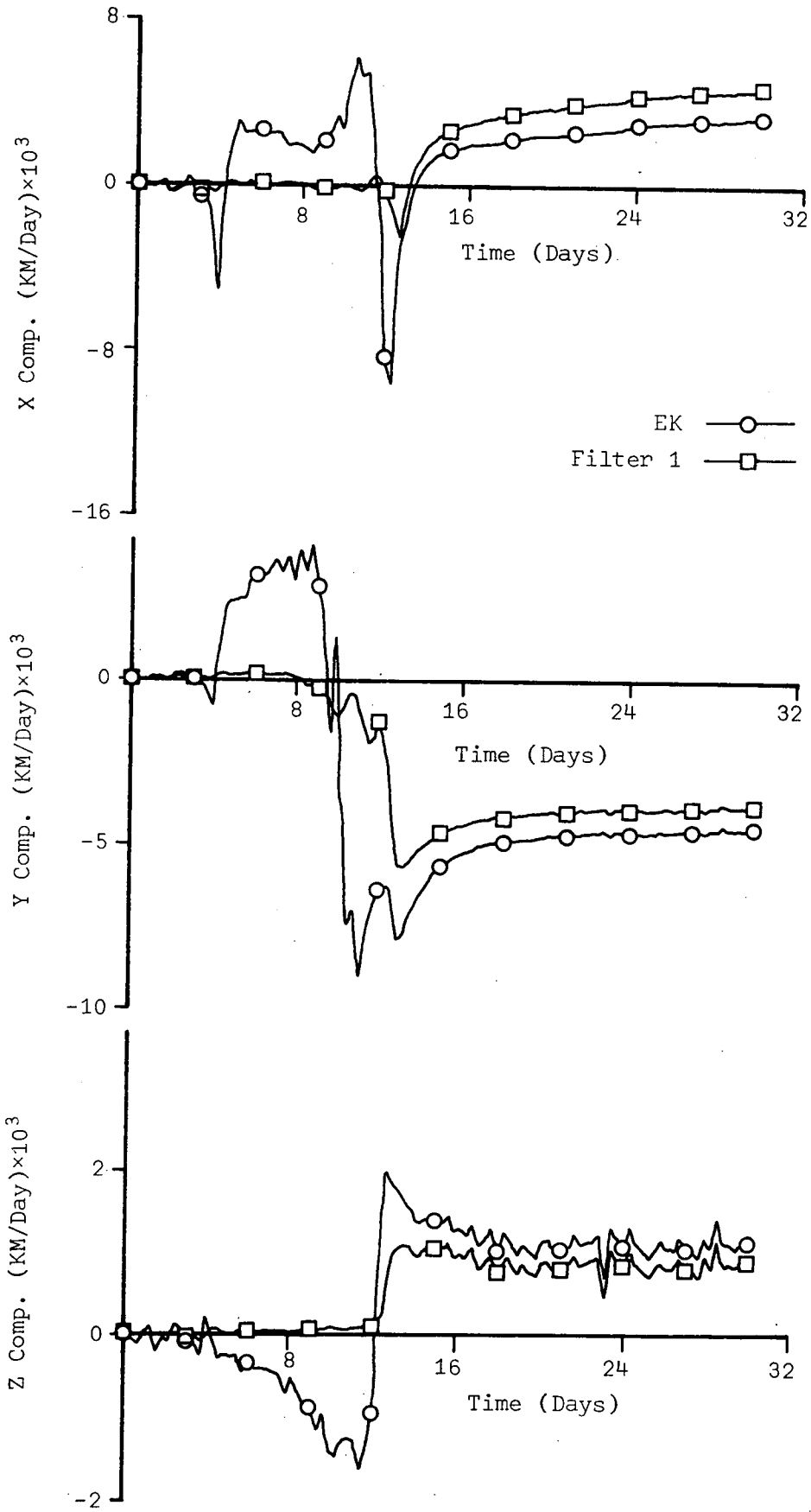

Figure 8-b. Velocity Estimation Errors for the Simulation 1

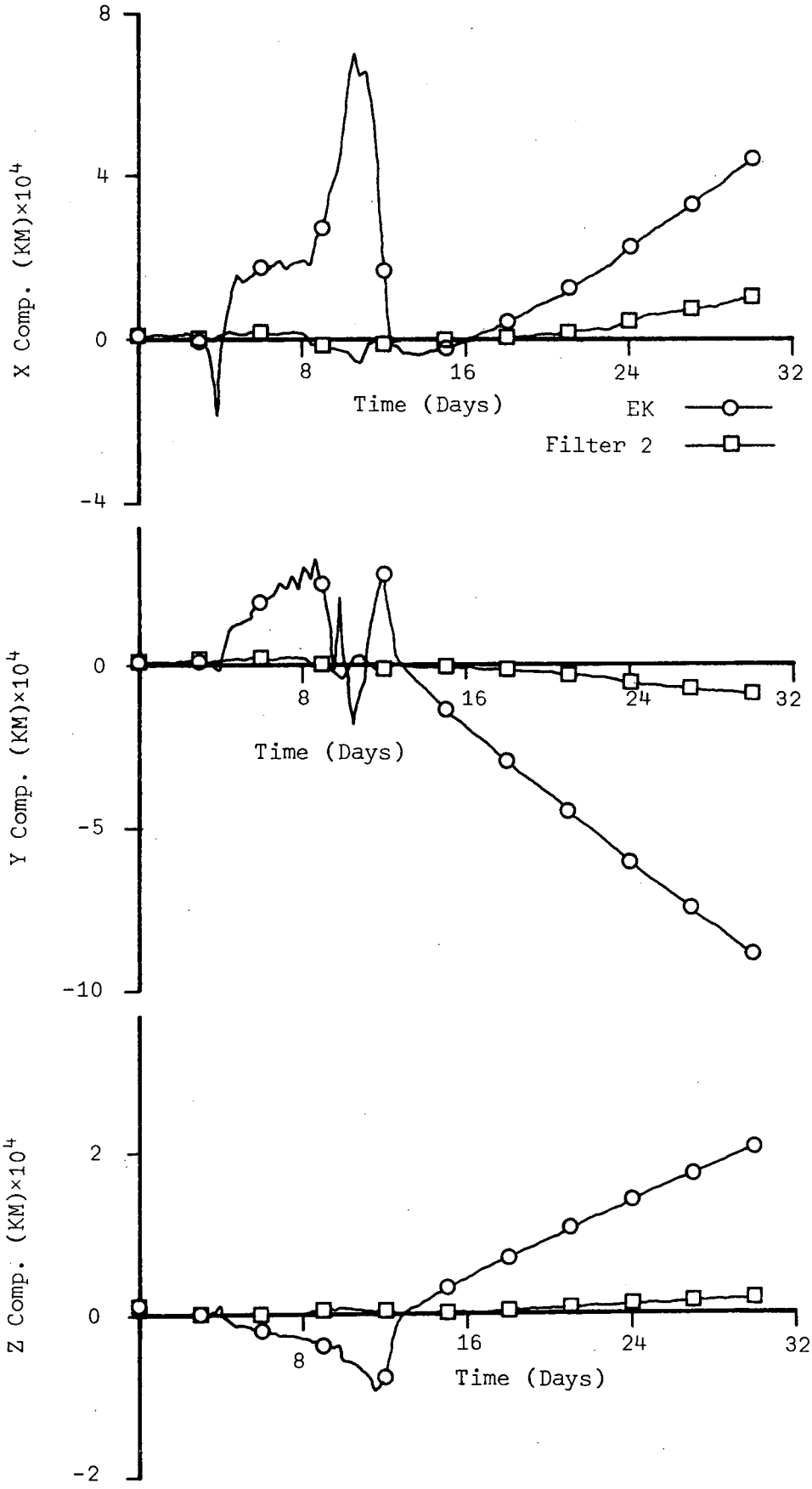

Figure 9-a. Position Estimation Errors for the Simulation 2

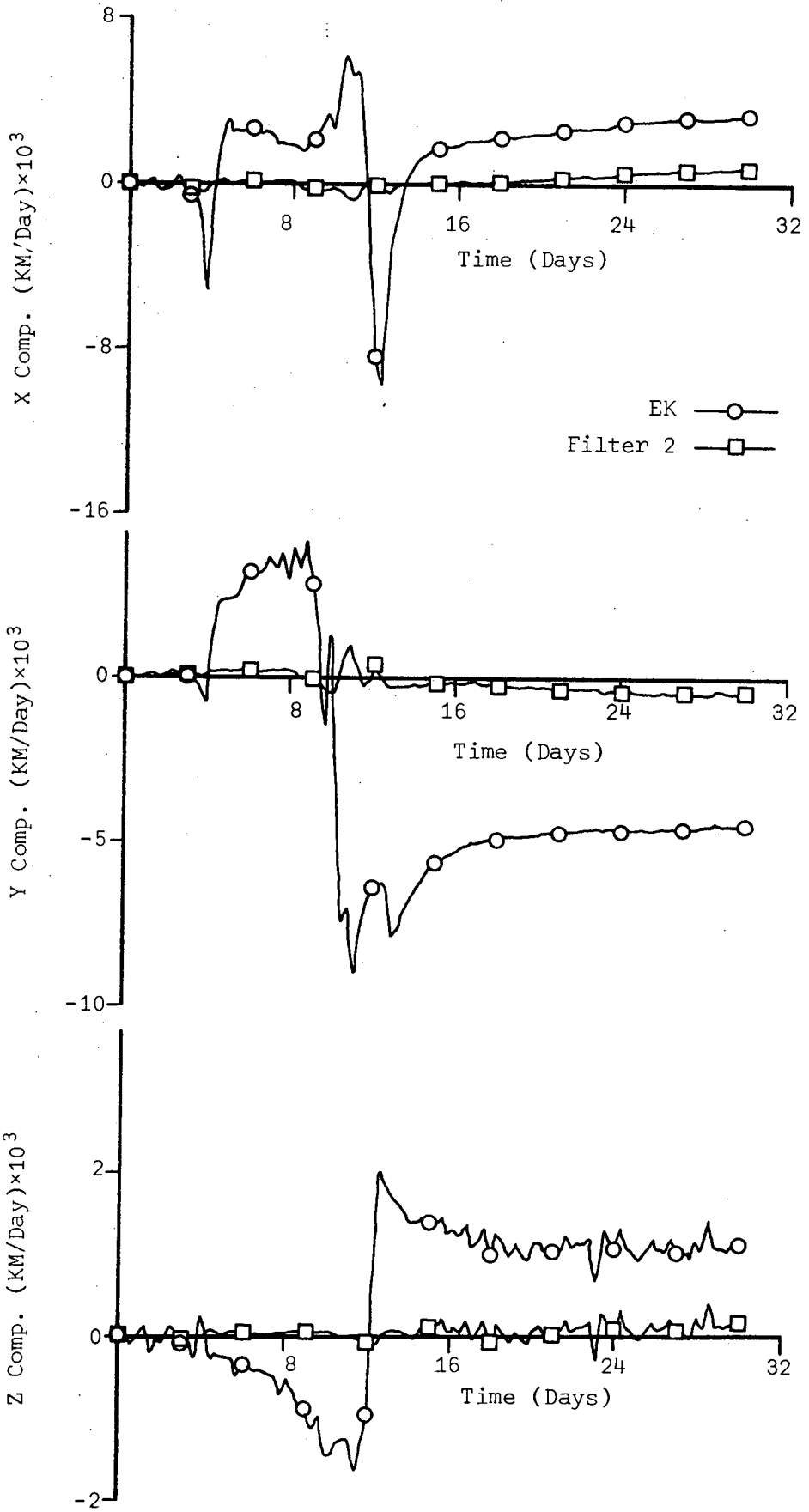

Figure 9-b. Velocity Estimation Errors for the Simulation 2

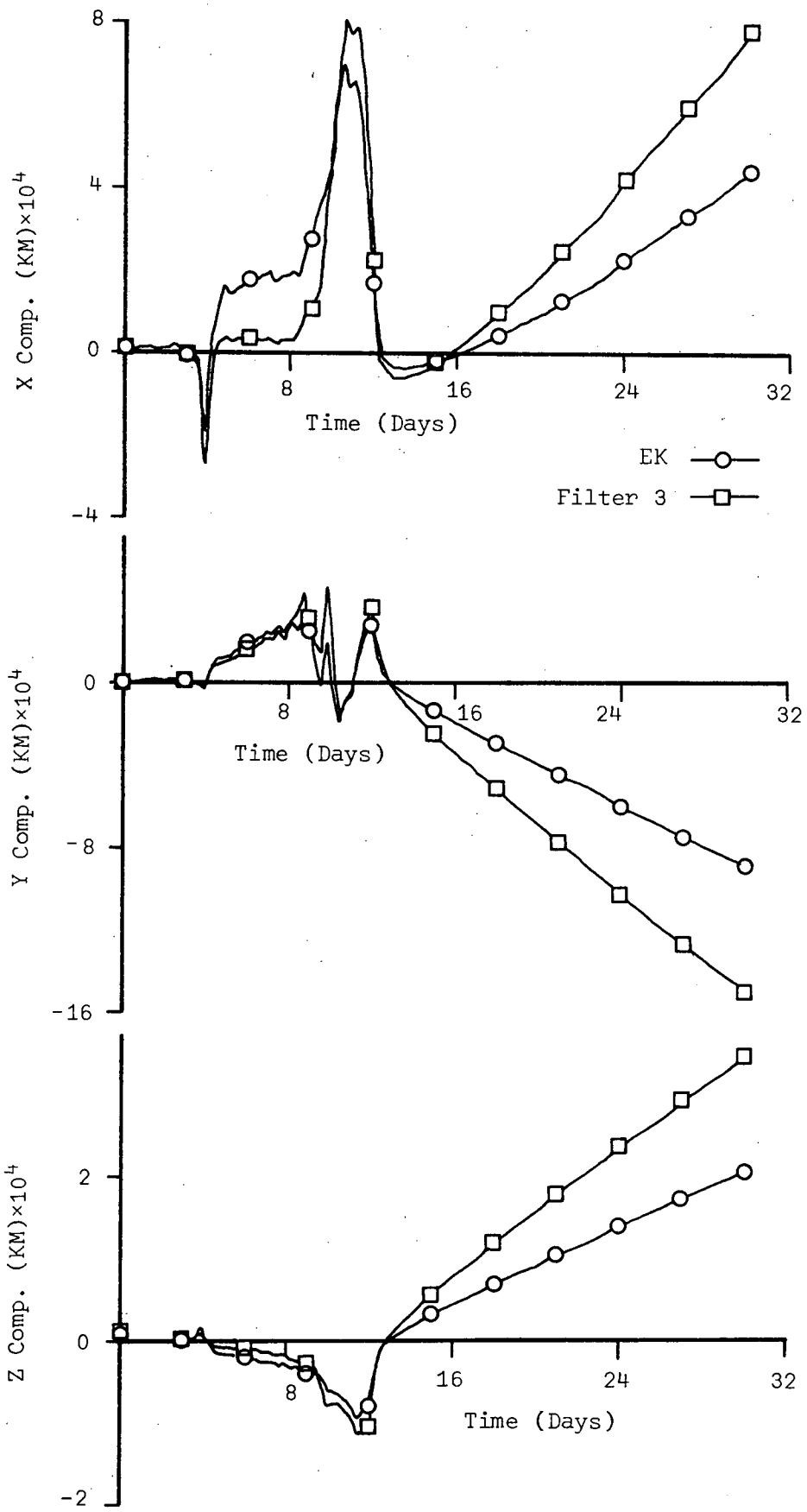

Figure 10-a. Position Estimation Errors for the Simulation 3

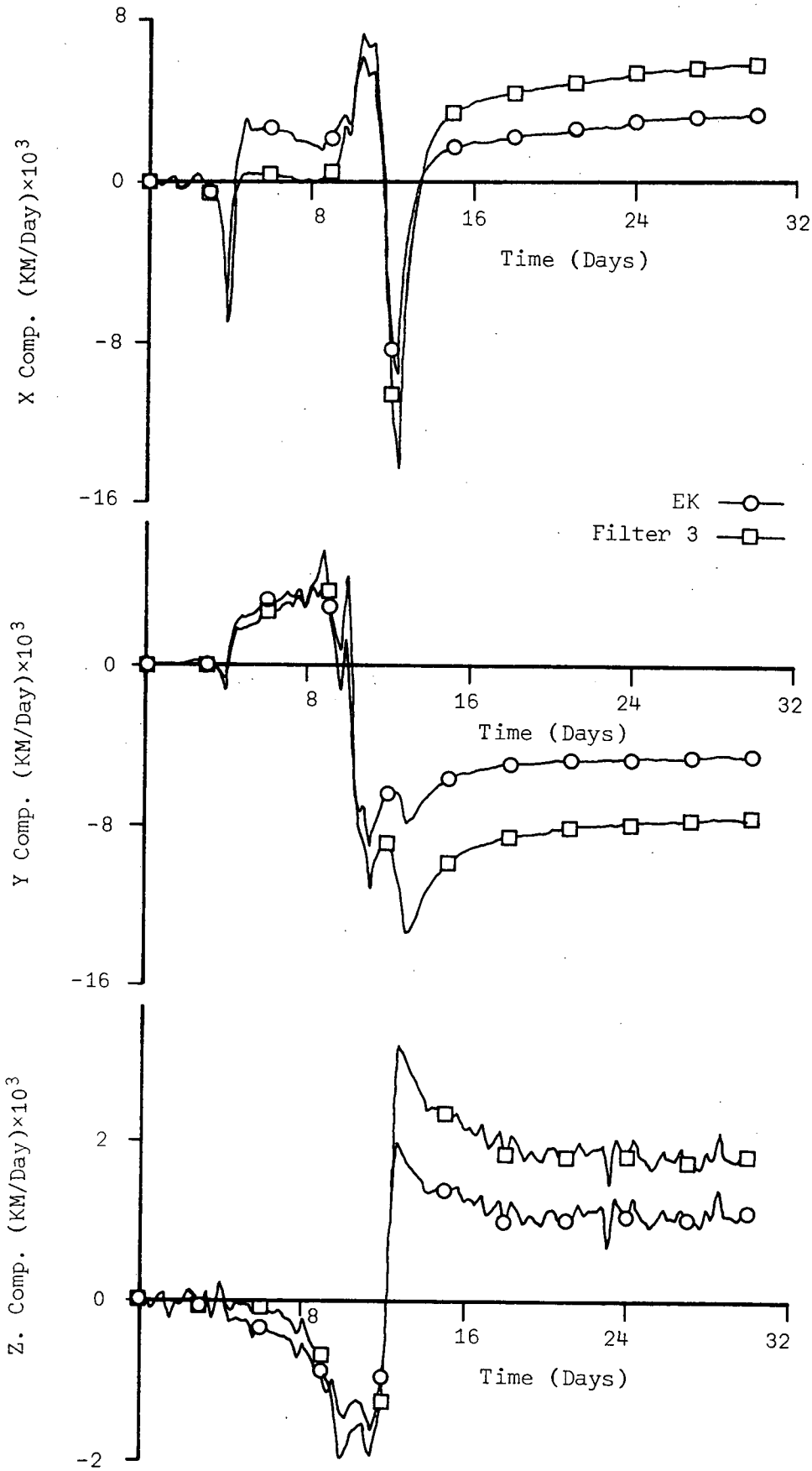

Figure 10-b. Velocity Estimation Errors for the Simulation 3

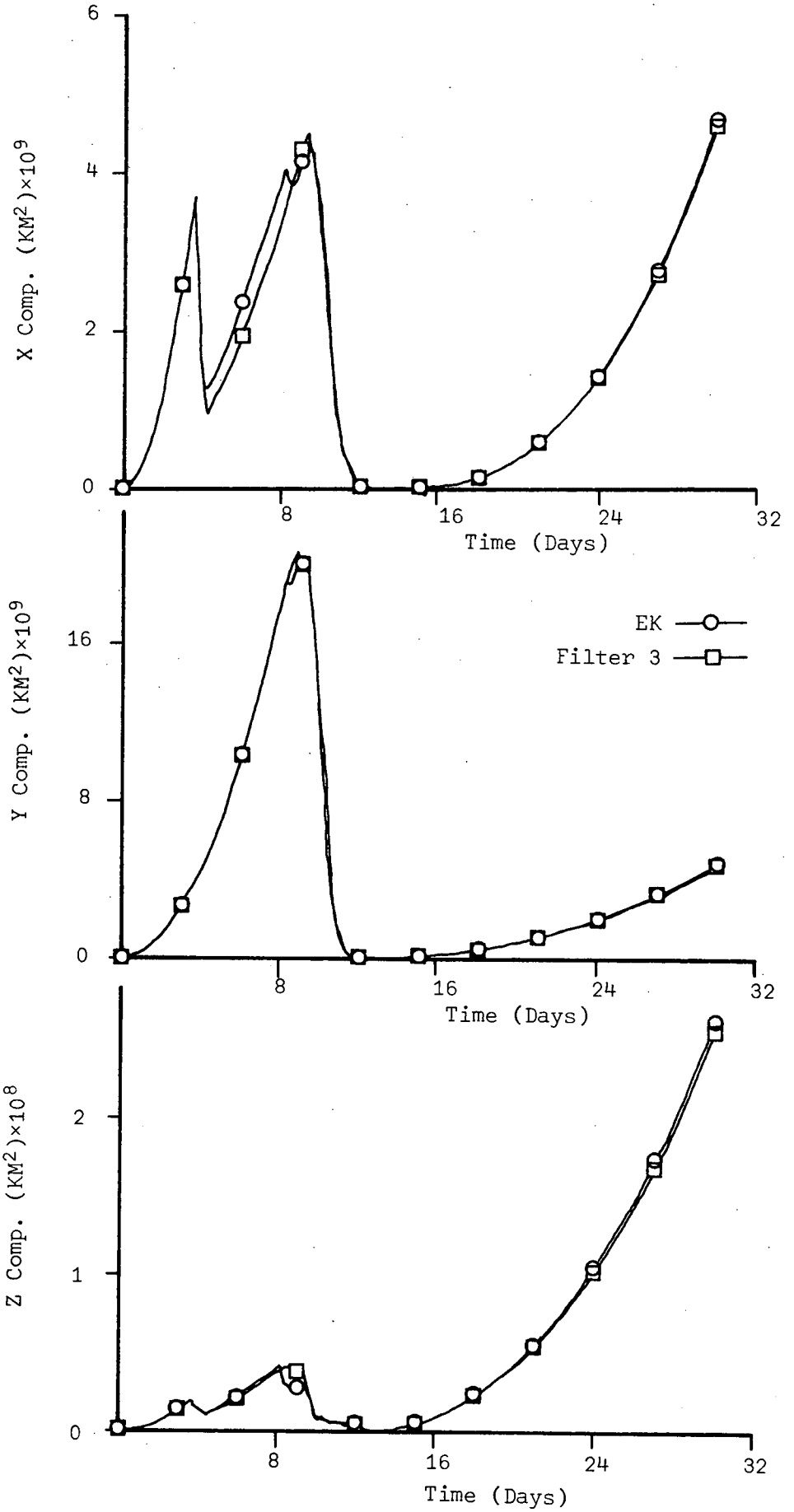

Figure 10-c. Conditional Variances of Position Estimation Errors for the Simulation 3 (and 5)

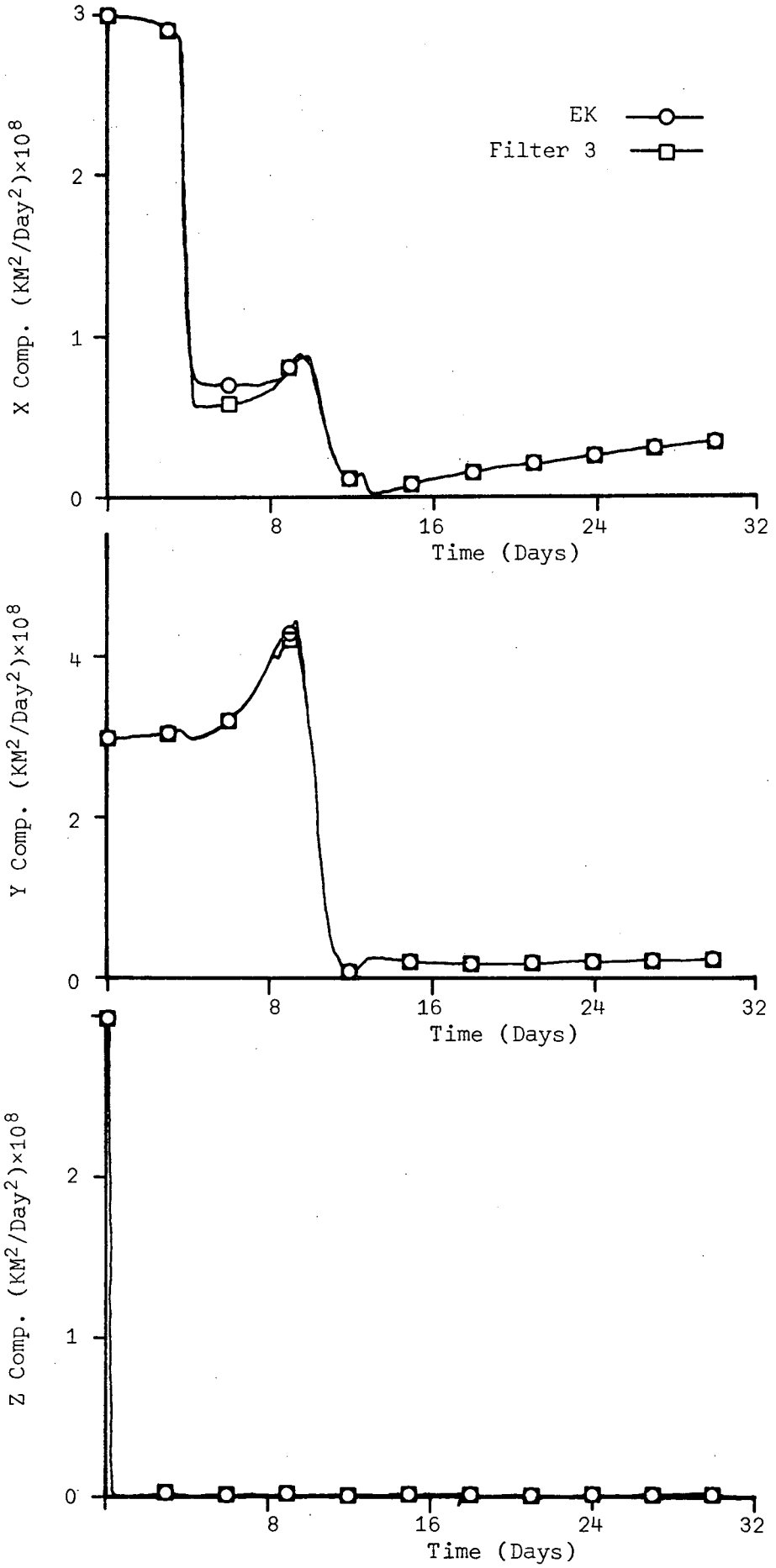

Figure 10-d. Conditional Variances of Velocity Estimation Errors for the Simulation 3 (and 5)

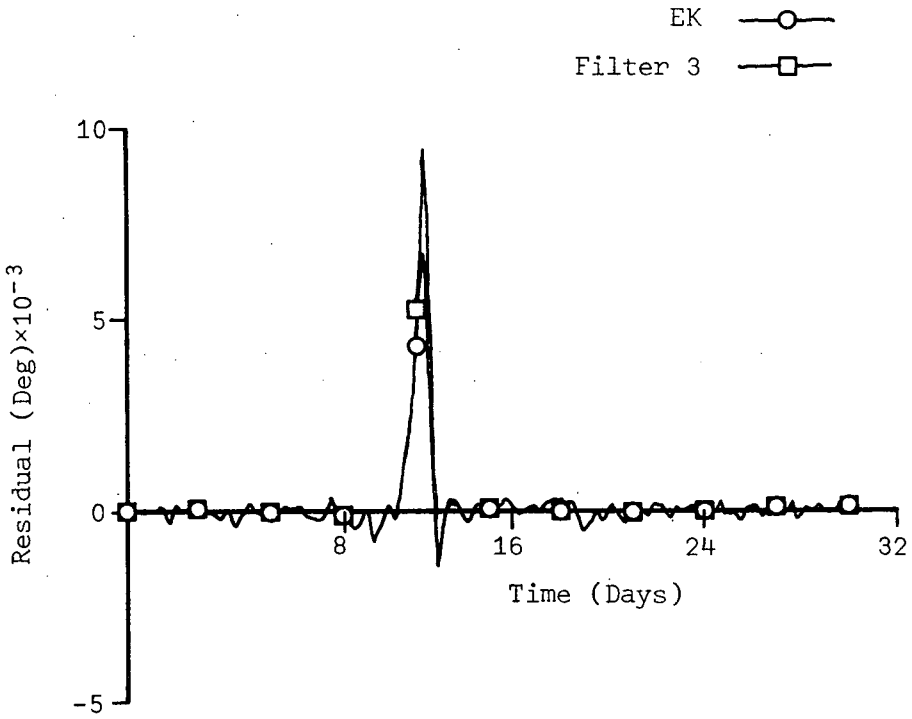

Figure 10-e. Observation Residuals for the Simulation 3

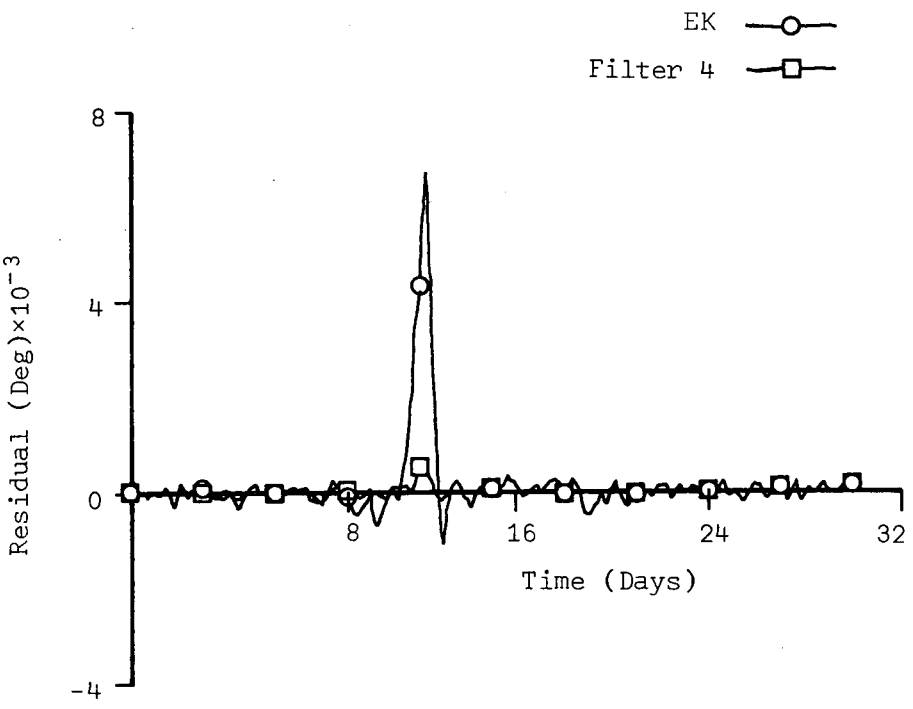

Figure 11-a. Observation Residuals for the Simulation 4

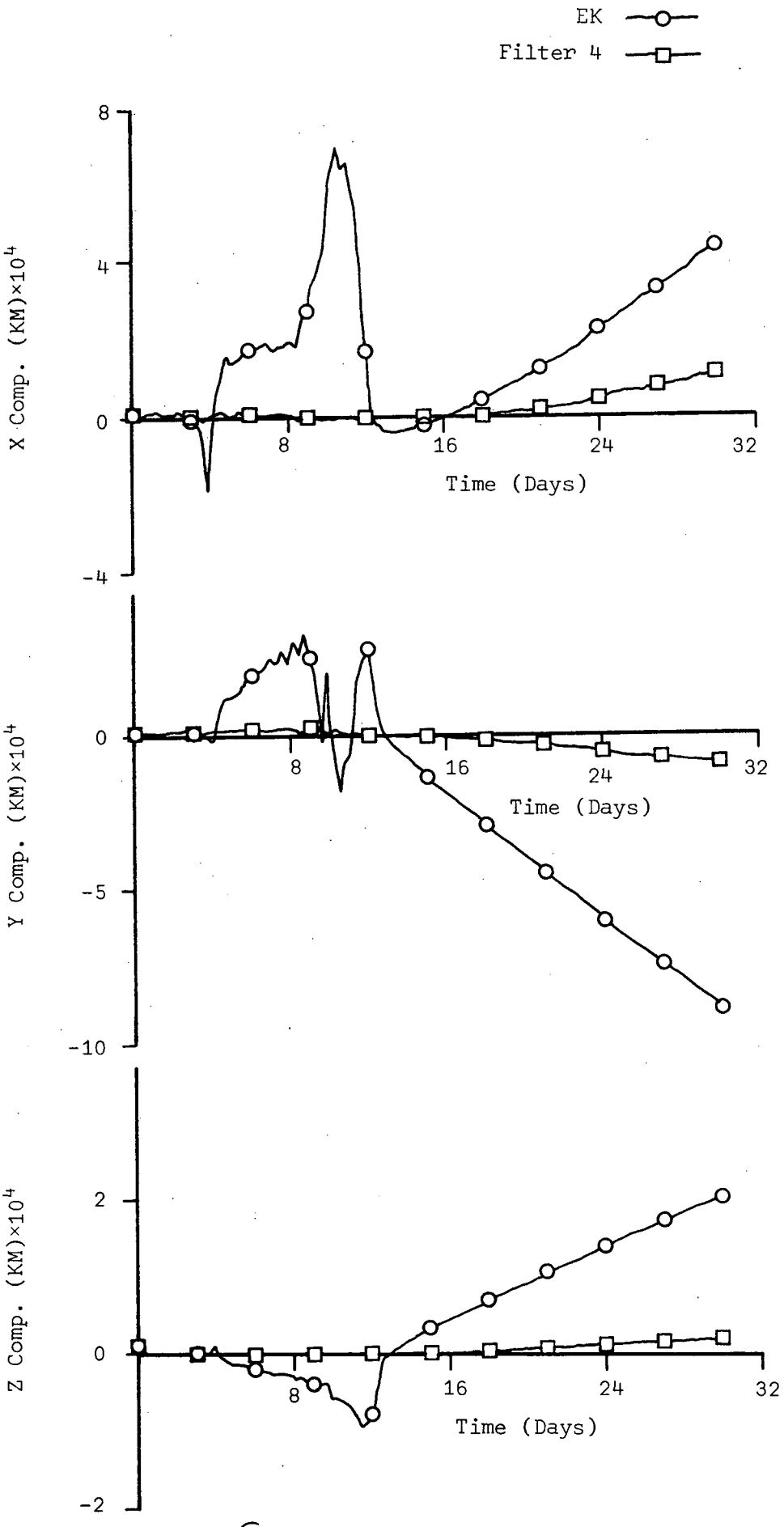

Figure 11-b. Position Estimation Errors for the Simulation 4

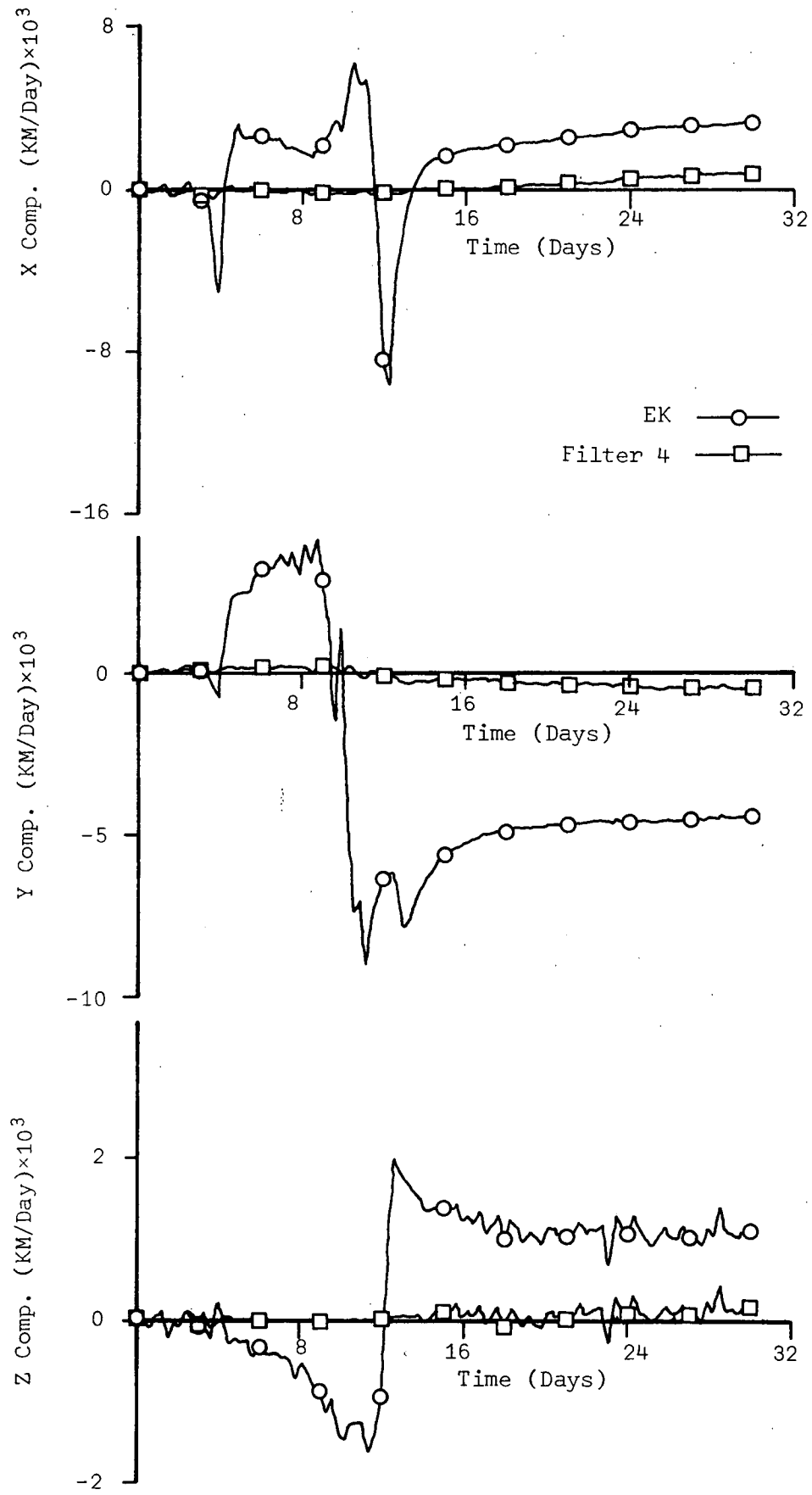

Figure 11-c. Velocity Estimation Errors for the Simulation 4

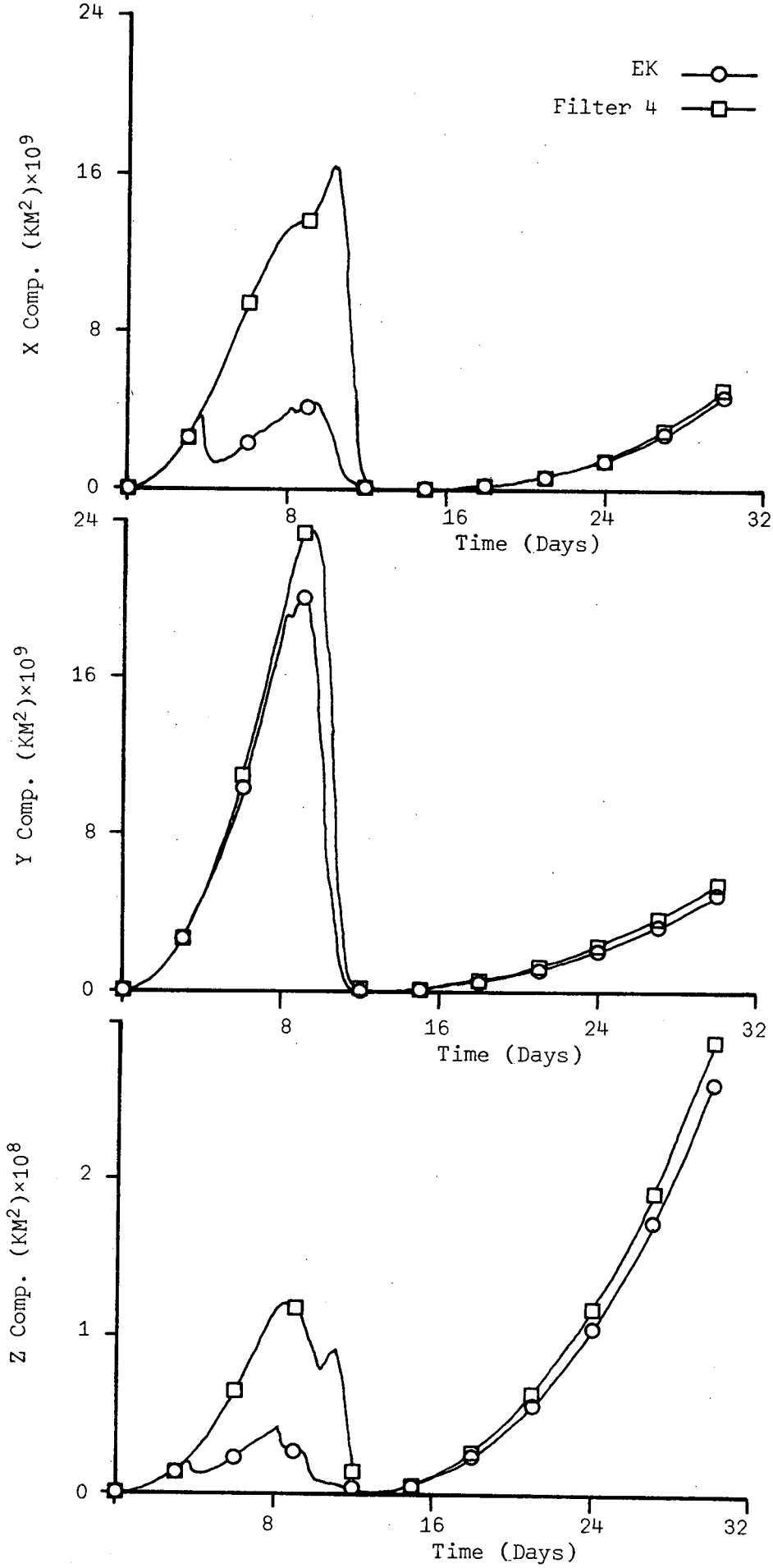

Figure 11-d. Conditional Variances of Position Estimation Errors for the Simulation 4 (Also 1 and 2)

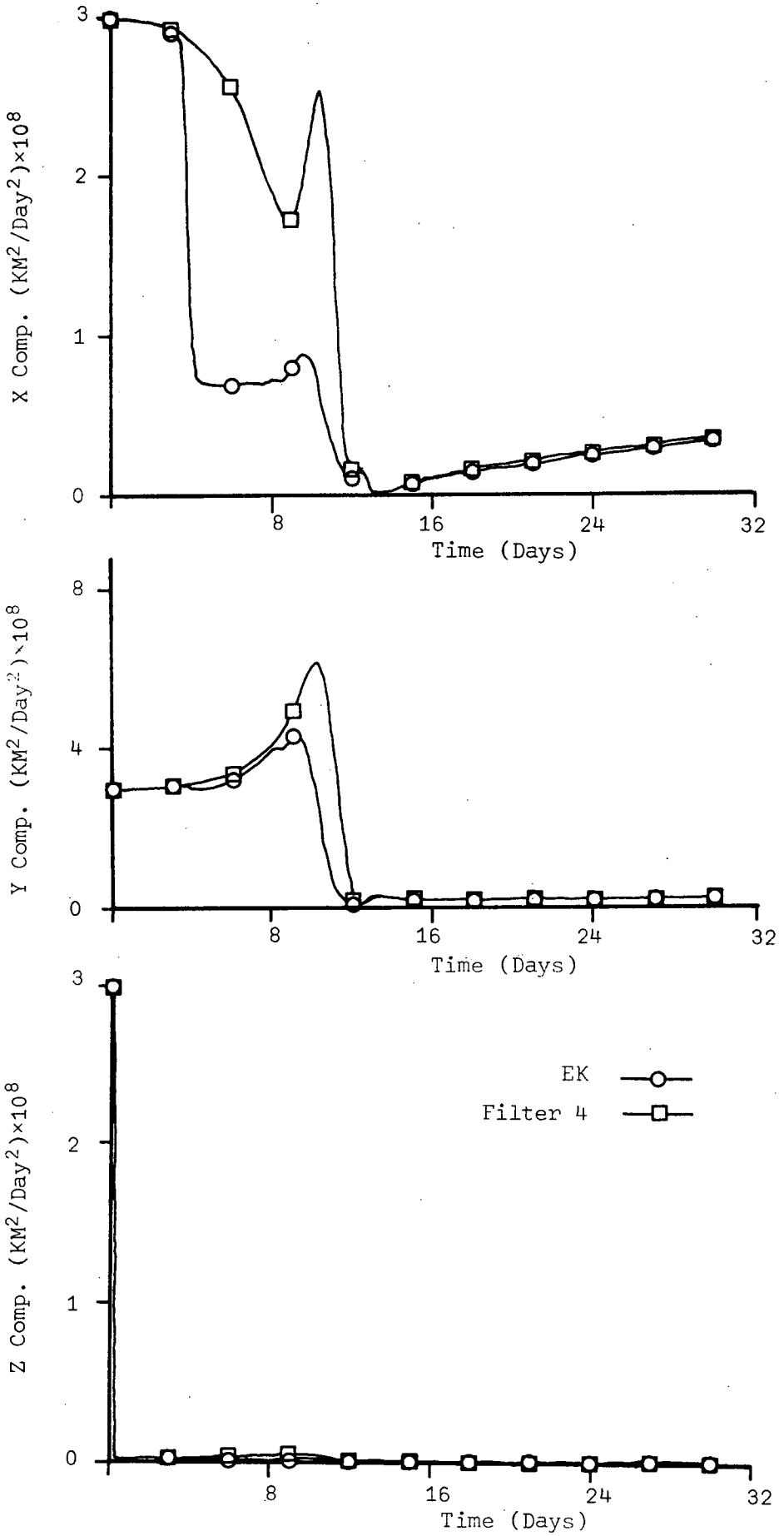

Figure 11-e. Conditional Variances of Velocity Estimation Errors for the Simulation 4 (Also 1 and 2)

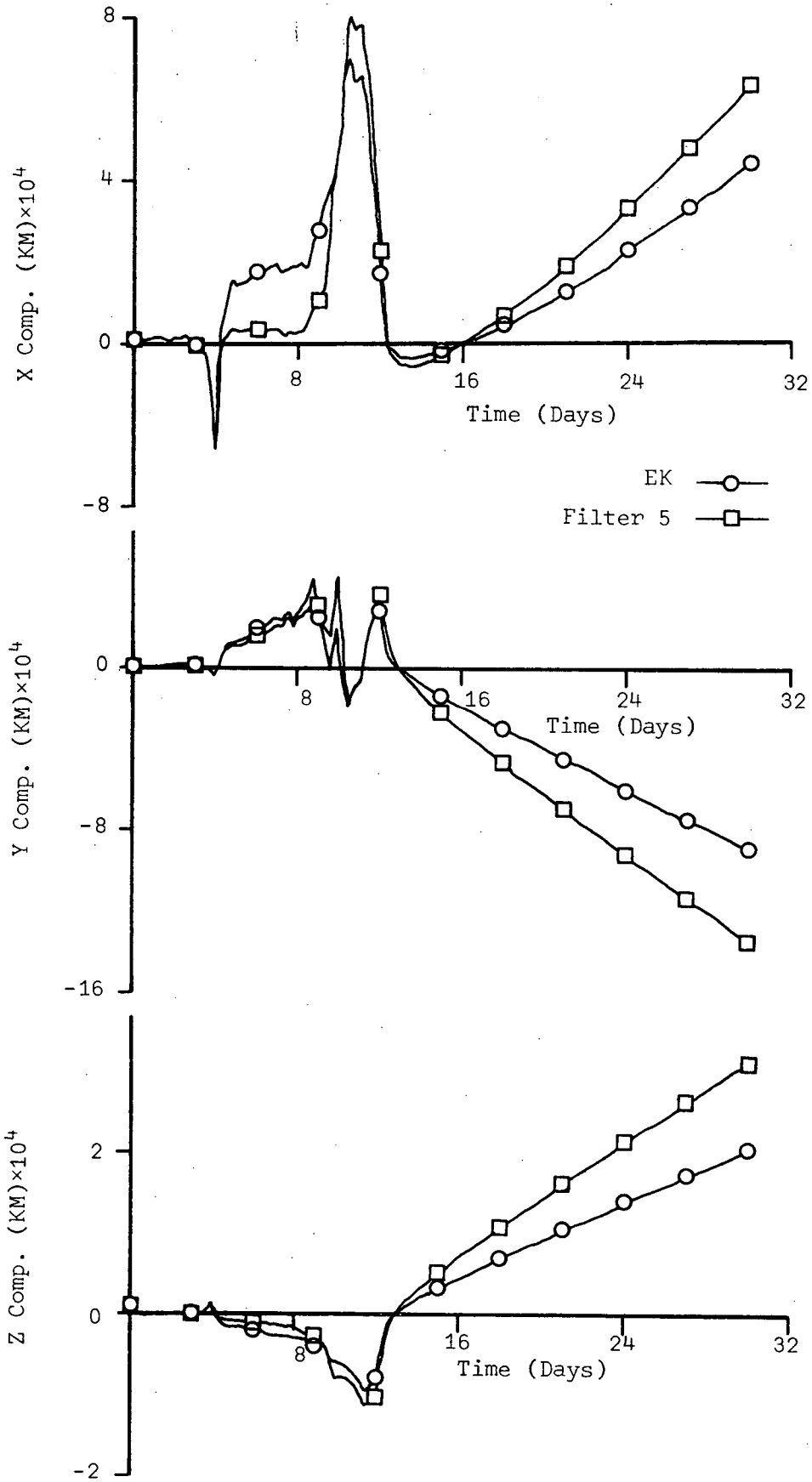

Figure 12-a. Position Estimation Errors for the Simulation 5

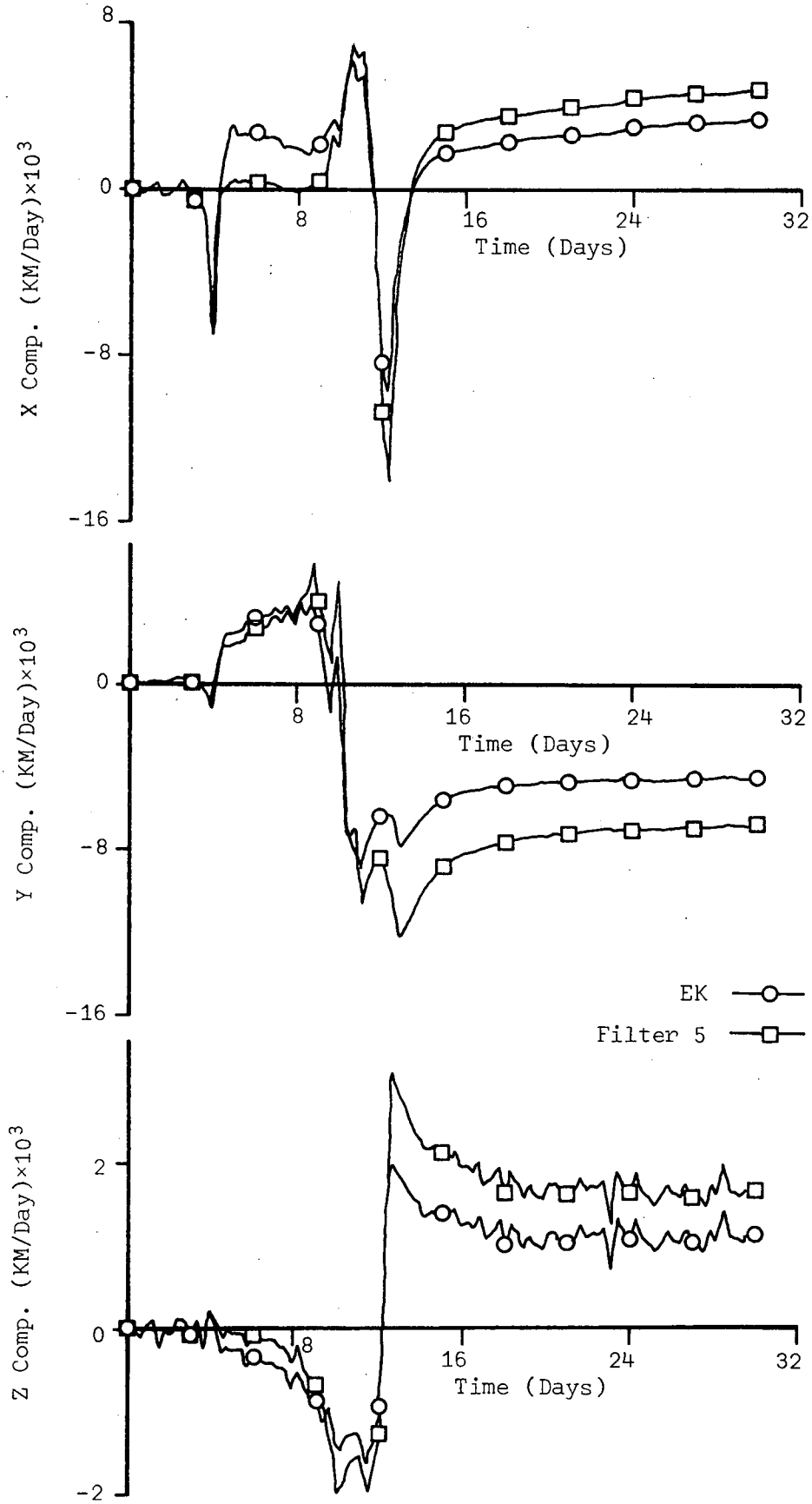

Figure 12-b. Velocity Estimation Errors for the Simulation 5

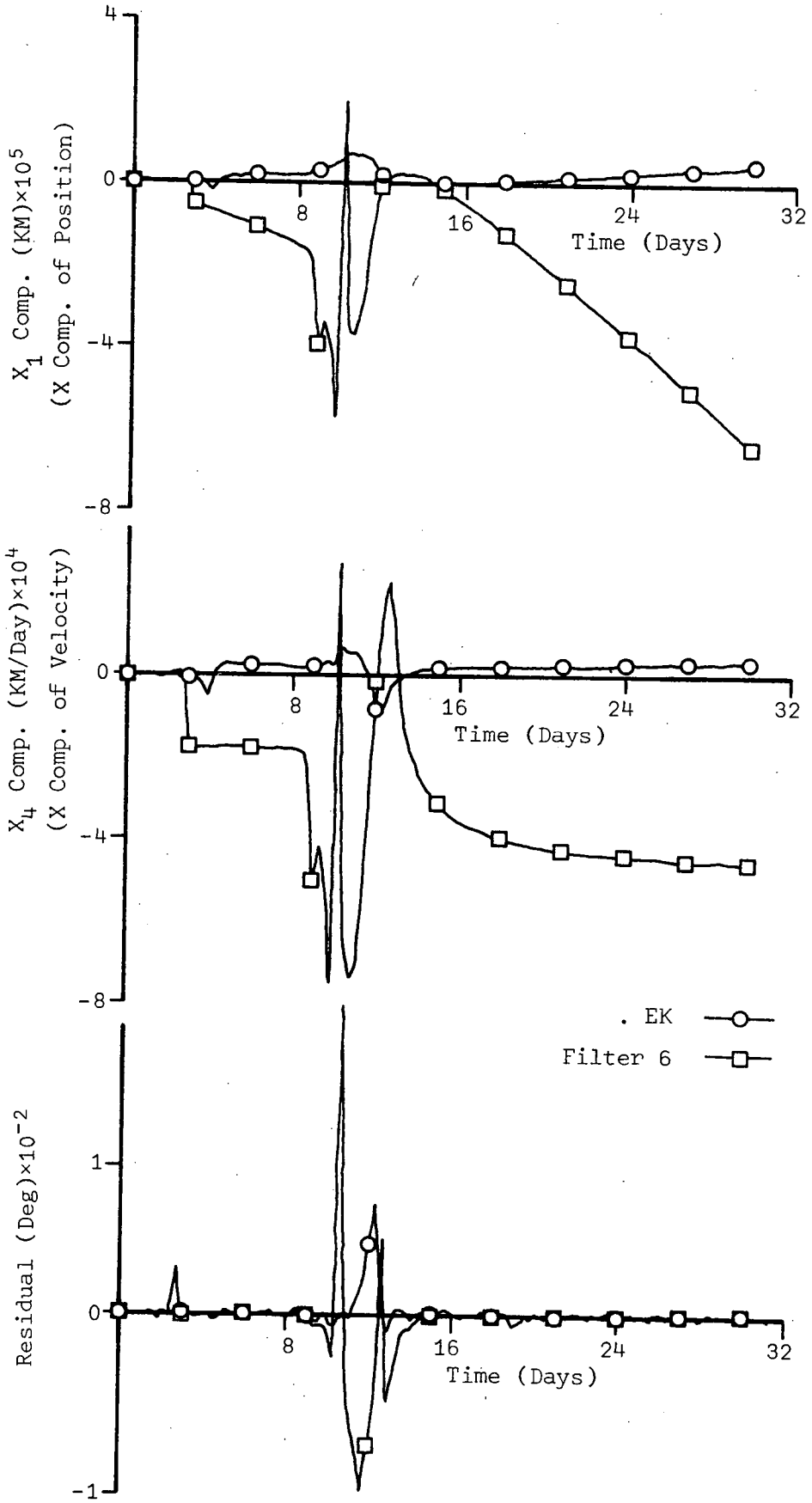

Figure 13-a. Estimation Errors (X_1,X_4) and Observation Residual for the Simulation 6

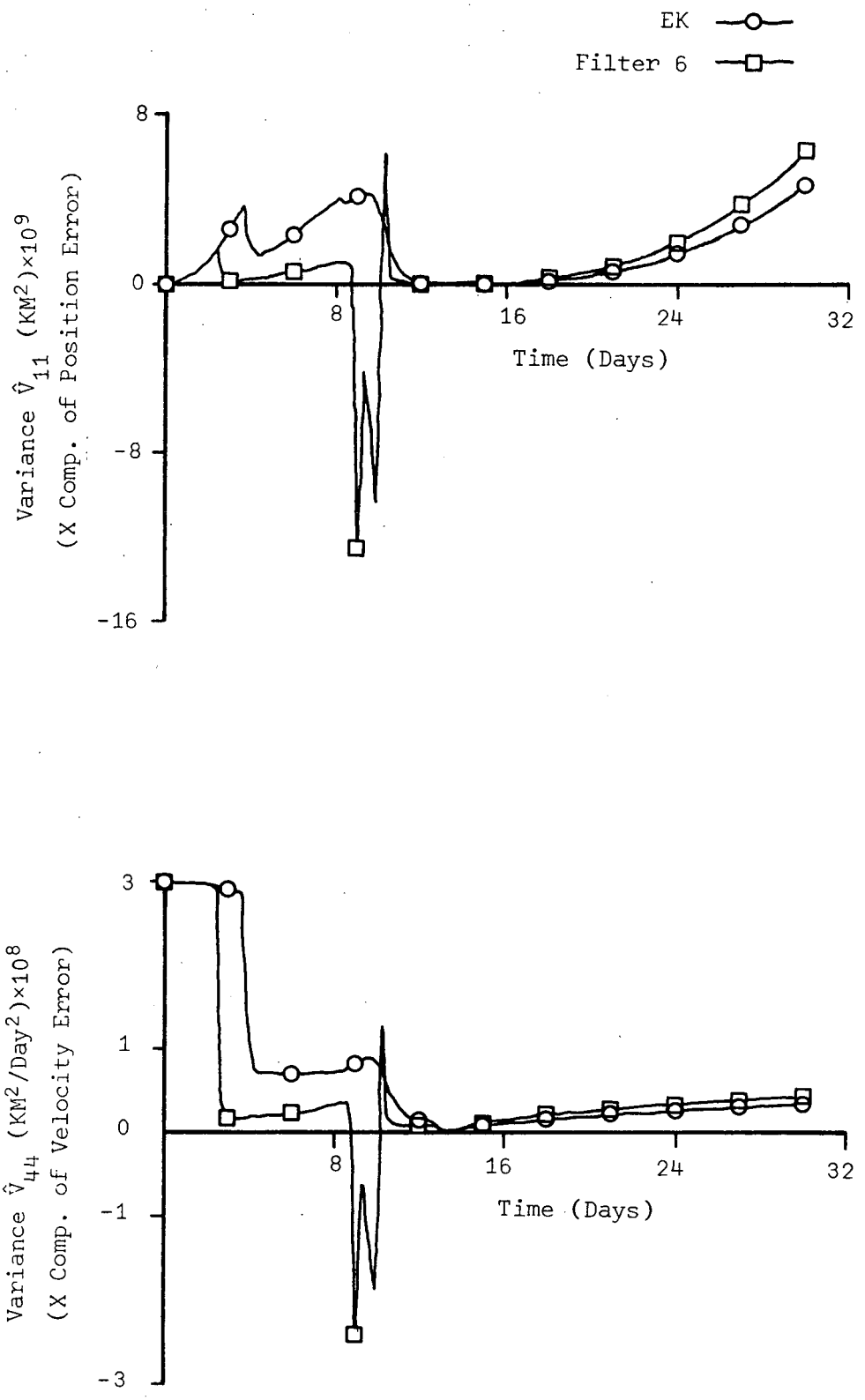

Figure 13-b. Conditional Variances ($\hat{V}_{11}$, $\hat{V}_{44}$) for the Simulation 6

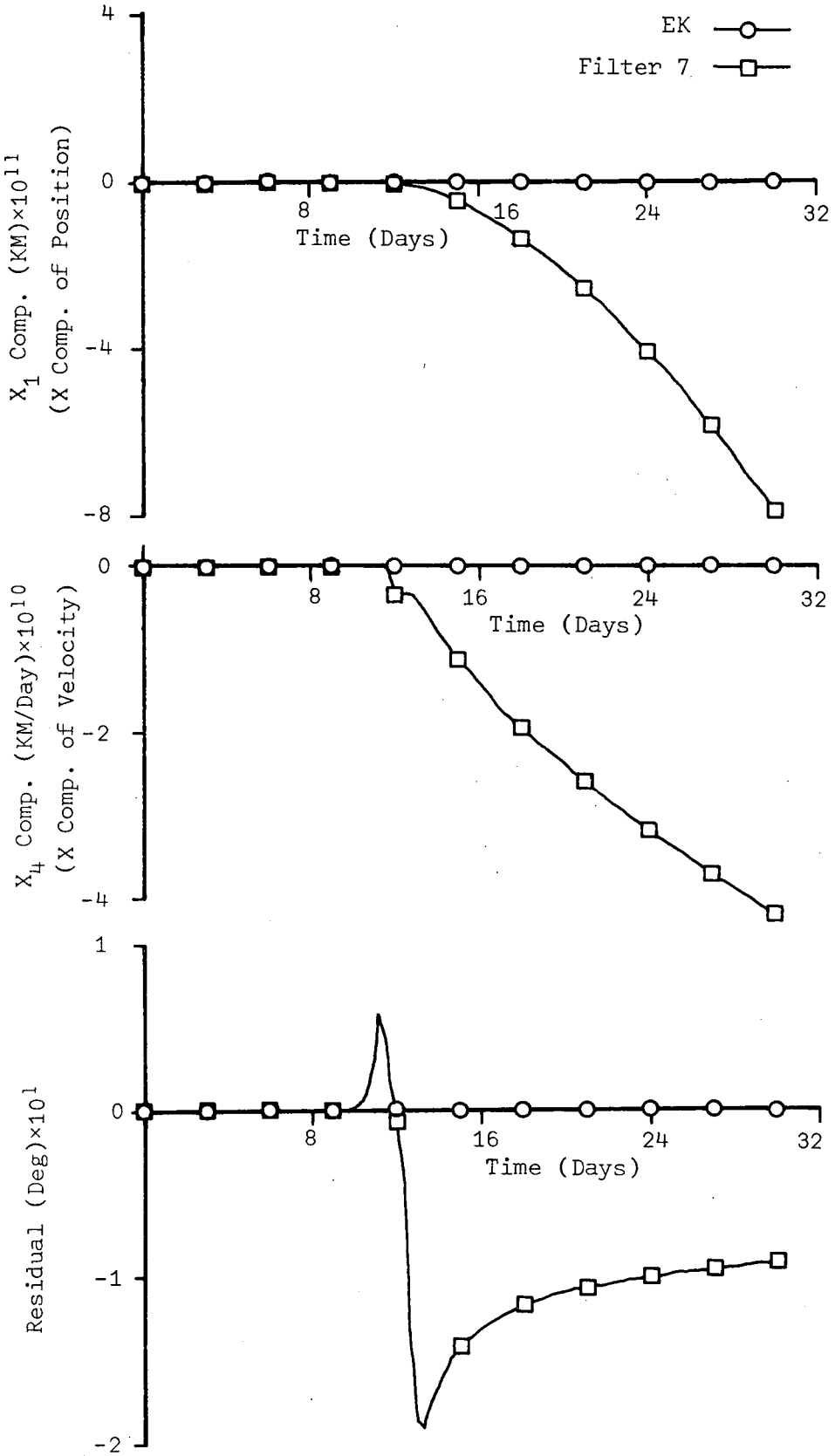

Figure 14-a. Estimation Errors (X_1,X_4) and Observation Residual for the Simulation 7

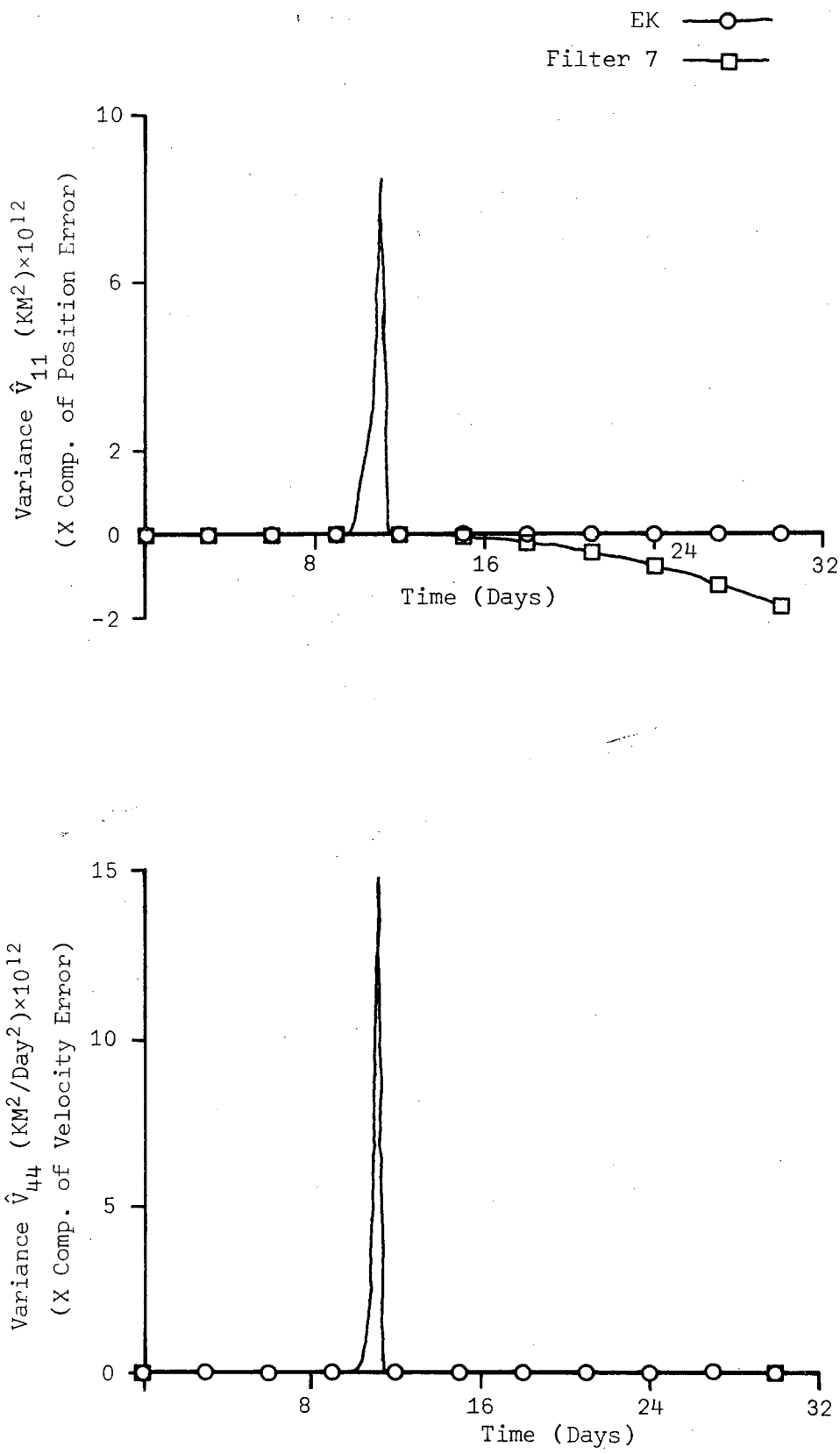

Figure 14-b. Conditional Variances ($\hat{V}_{11}$, $\hat{V}_{44}$) for the Simulation 7

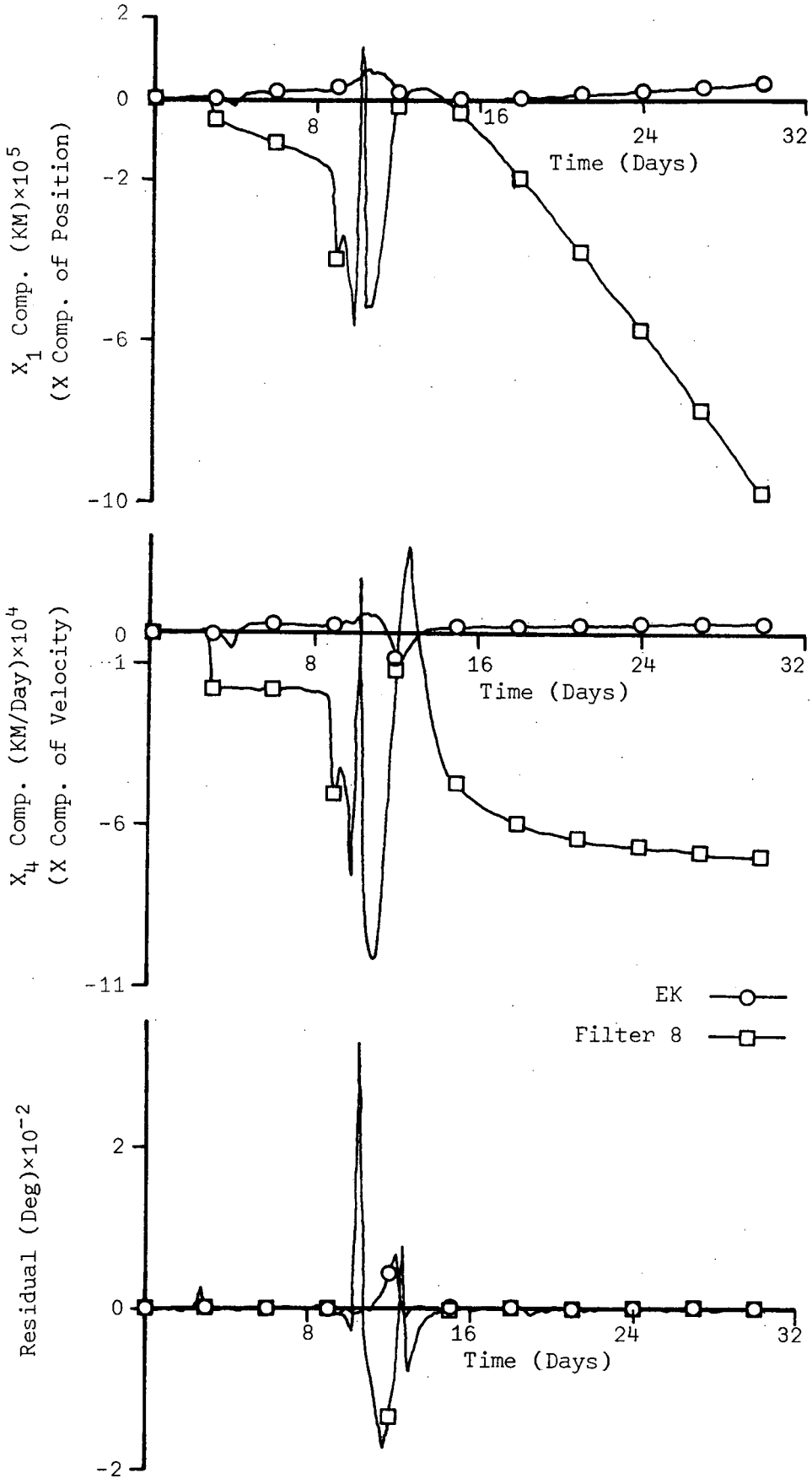

Figure 15-a. Estimation Errors (X_1,X_4) and Observation Residual for the Simulation 8

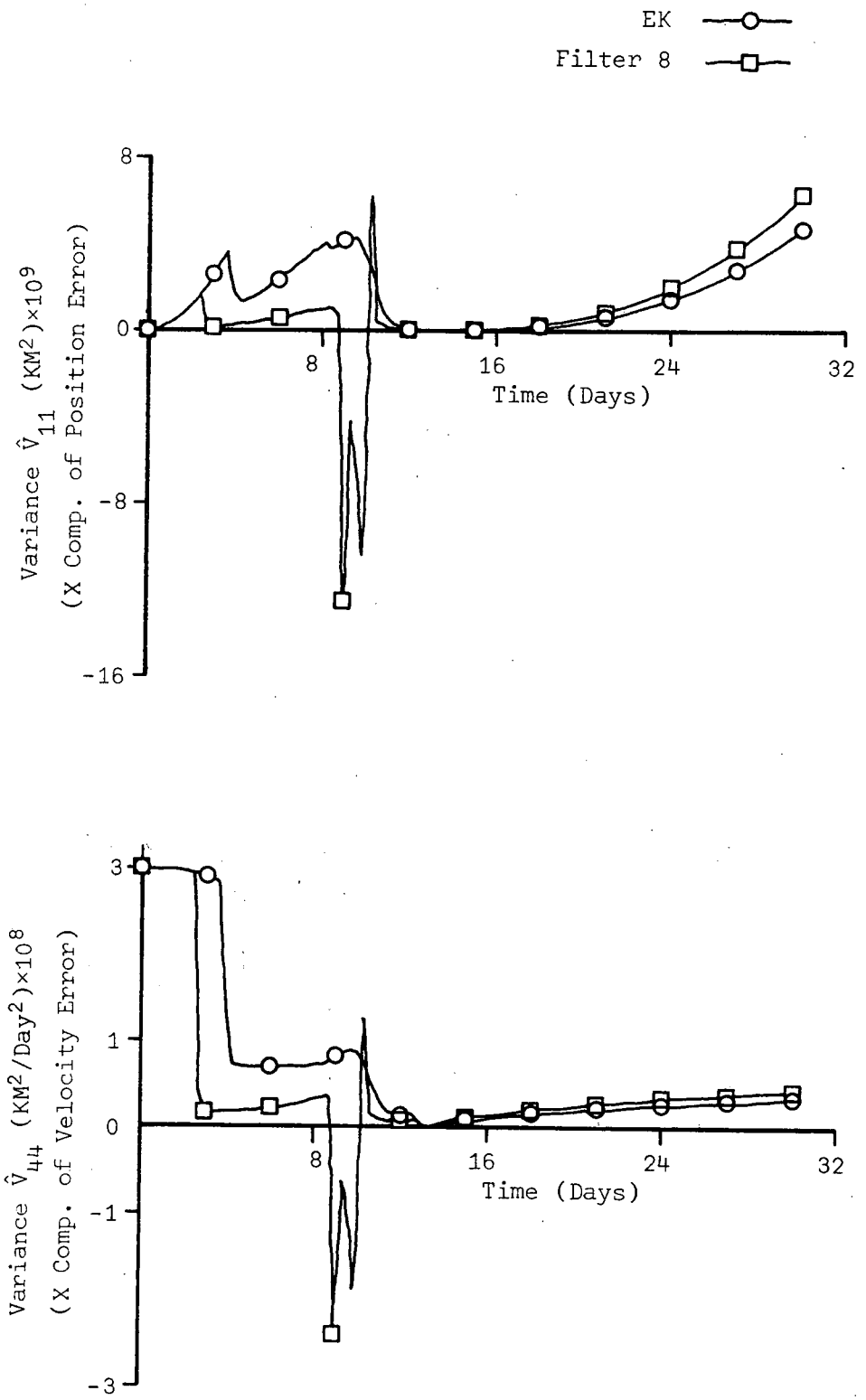

Figure 15-b. Conditional Variances ($\hat{V}_{11}$, $\hat{V}_{44}$) for the Simulation 8

4.4 Applications of the KGC Filter to the Hypobolic Orbit

In the previous section, several filters were discussed and the DSO and OSO terms were characterized in conjunction with the KGC term. Since the KGC term is the only term which improves the filter performance, the KGC filter which includes only the KGC term is designated as the best filter among those listed in Table 1.

The KGC filter is further tested through numerous simulations. The Simulations 9 through 14 are conducted on a hypobolic orbit with the sun-planet angle measurements. The simulations are designated to determine the effects of state noise covariance matrix Q, initial state errors $\tilde{x}_{o/o}$, integration step size, observation rate, initial covariance $\hat{V}_{o/o}$ and observation noise covariance matrix R. Simulation 10 is the reference case to which all other simulations are compared. The input data are given in Tables 7 and 8.

Simulation 9 is specifically designed to illustrate the effect of using two different Q's in Eq. (2.55). σ_{QT} is the true standard deviation of the state noise u which is used to compute the true trajectory. σ_{QA} is the apriori standard deviation. The square of σ_{QA} is used in Eq. (2.55) for the estimation procedure. It is common practice to include a Q in Eq. (2.55), although there may be no state noise u assumed. This procedure is followed to keep the value of the conditional variances above a certain level so that the filter can maintain a reasonable gain K and, hence, will be sensitive to the observations. Usually the EK filter reduces the conditional covariance very rapidly after a few observations are made, and, hence, the filter becomes saturated and insensitive to the observations.

Figs. 16-a and 16-b show the position and velocity estimation

errors, respectively, for Simulation 9. The conditional variances and observation residual are almost identical to the ones given in Figs. 17-c, 17-d and 17-e which are obtained by using the same σ_{QT} and σ_{QA}. The observation residual pattern should not be assumed to be zero except during the brief time interval in which the spike occurs. The non-zero value of the residuals do not show up on the scale used to plot the results.

Since the sun-planet angle measurement is restricted to the ecliptic plane, the measurement does not include very much information on the Z components of position and velocity. This fact is reflected in the figures related to the Z components from zero to ten days. Both the EK filter and the KGC filter perform reasonably well up to eight days. As a matter of fact, they are almost identical. The EK filter starts to drift away from the true trajectory after eight days. Around twelve days, the EK filter becomes extremely unstable, oscillates several times with sharp spikes during this short period of time and then diverges eventually. The oscillatory spikes near encounter are not shown in the figures simply because only every third data point is shown in the figures. As seen in Fig. 17-e, the estimate with the EK filter is influenced by a spike in the observation residual pattern around encounter. The actual observations which depend mainly on the true states and the small observation noise contain equally good informations at any time. But the predicted observation depending on the current estimate can be quite erroneous. The erroneous observation residuals around encounter are incorporated with a large optimal gain, K , during the same period and the update of the apriori estimates is, consequently, too large, causing the EK filter to diverge.

The KGC filter keeps the conditional variances large in the critical

period of time from eight to twelve days. As a result, the KGC term dominates the other two terms, $h_x \hat{P} h_x^T$ and R, and the values of the optimal gain, K, remain small. Through this effect, the KGC term makes the filter insensitive to the observations which could be erroneous, in the region where the dynamic nonlinearity is very severe.

Simulation 10 shows the effect of using the same values for σ_{QT} and σ_{QA}. It is noticeable that Simulation 9 which uses two different values for σ_{QT} and σ_{QA}, yields slightly smaller estimation errors for both the EK and KGC filters than those of the Simulation 10 which uses the same value. Since the sun-planet angle measurement is restricted to the ecliptic plane, the EK filter experiences severe nonlinearity effects on the Z components. The effect can be seen in the Z components of the conditional variances shown in Figs. 17-c and 17-d.

Simulation 11 shows the effect of the initial state errors. The errors are chosen ten times larger than those of Simulation 10. The convergence characteristics, except the Z components, appear to be well behaved for both filters immediately after taking the observations. However, the EK filter displays instability and divergence characteristics around encounter, although the KGC filter continues with an accurate estimate throughout this extremely nonlinear region.

Overall, the estimation error patterns shown in Figs. 18-b and 18-c are very much the same as those of Simulations 9 and 10, except during the first few days. The observation residual pattern is shown in Fig. 18-a and the conditional variances are almost identical to the one given in Figs. 17-c and 17-d. Again, the residuals outside the spike zone do not show up because of the relatively small size compared with the spike.

Since the nominal trajectory changes very rapidly around encounter in the hypobolic orbit and near periapsis in the elliptic orbit, the dynamic nonlinearity appears to be very severe in these regions and, consequently, so is the observation nonlinearity. In order to minimize the effects of the nonlinearities, a variable integration step size and observation rate are adopted in the Simulation 12. Initially, the integration step size and the observation intervals are set to 1/10 day, and then the actual integration step size, ΔT_i, and observation interval, ΔT_o, are determined as follows:

$$\Delta T_i = \Delta T_o = (1/10) \cdot \text{Integer Value of } (r/r_o) \quad , \quad r \geq r_o$$

or

$$\Delta T_i = \Delta T_o = (1/10) \; / \; \text{Integer Value of } (r_o/r) \quad , \quad r_o > r$$

where r_o is the initial distance between the spacecraft and the target planet, Jupiter, and r is the current distance. As seen in Fig. 7, ΔT_i and ΔT_o, for example, become nearly 1/20 of the initial step size, 1/10 day near encounter in the hypobolic orbit.

Figs. 19-a and 19-b show the estimation errors for the position and velocity components. An interesting fact about the error pattern of Simulation 12 is that the signs are reversed when compared with those of Simulation 10. Figs. 19-c and 19-d show the conditional variances and a slightly different pattern is seen near encounter when compared with those in Figs. 17-c and 17-d.

Simulation 13 is conducted with a ten-times larger initial conditional variances of the velocity components than those of Simulation 10. Due to the larger initial conditional variances, the KGC term starts influencing the KGC filter earlier than it does in Simulation 10. Figs. 20-c, 20-d and

20-e represent the conditional variances and observation residuals, respectively. Estimation errors are shown in Figs. 20-a and 20-b.

Simulation 14 shows the effect of a large observation noise standard deviation σ_R in the KGC filter. A value ten times larger than the value of σ_R which was used in Simulation 10 was adopted as an observation noise standard deviation in Simulation 14.

It is found in the EK filter which does not include the KGC term that $h_x \hat{P} h_x^T$ dominates R in Eq. (1.35) during the early stage of estimation. Later the values of R dominate. From the above observation, it is understood that the KGC term which is negligible when compared with the other two terms, $h_x \hat{P} h_x^T$ and R in Eq. (2.57), cannot affect the performance of the KGC filter very much. But in the region where the KGC term dominates the other two terms and R is larger than $h_x \hat{P} h_x^T$, the effect of a large R shows up. For example, consider the period from nine to thirteen days in Figs. 21-b and 21-c. After encounter, the value of the KGC term diminishes due to the combined effect of small conditional variances and observation second partials h_{xx} and thereafter the KGC term has virtually no influence on the KGC filter. Therefore, the KGC filter performs like the EK filter after thirteen days. For a small σ_R, the effect of the KGC term becomes very significant and the KGC filter is very desirable whenever a smaller σ_R, or equivalently accurate observation, is available.

The corresponding conditional variances and observation residuals are shown in Figs. 21-d, 21-e and 21-a, respectively.

TABLE 7. SIMULATION DATA (9-11)

SIMULATIONS		9	10	11
FIGURES		16-a,b	17-a,b,c,d,e	18-a,b,c
FILTER TYPE		4	4	4
ORBIT TYPE		HYPOBOLIC	HYPOBOLIC	HYPOBOLIC
OBSERVATION TYPE		SUN-PLANET	SUN-PLANET	SUN-PLANET
OBSERVATION RATE (DAY)		10^{-1}	10^{-1}	10^{-1}
OBSERVATION NOISE, σ_R (DEG)		10^{-4}	10^{-4}	10^{-4}
TRUE STATE NOISE, σ_{QT} (KM/DAY^2)		10^{0}	10^{2}	10^{2}
APRIORI STATE NOISE, σ_{QA} (KM/DAY^2)		10^{2}	10^{2}	10^{2}
$\tilde{x}_{o/o}$	$\tilde{X}_o = \tilde{Y}_o = \tilde{Z}_o$ (KM)	10^{3}	10^{3}	10^{4}
	$\tilde{U}_o = \tilde{V}_o = \tilde{W}_o$ (KM/SEC)	10^{-4}	10^{-4}	10^{-3}
	$\tilde{b}_{xo} = \tilde{b}_{yo} = \tilde{b}_{zo}$ (KM)	3×10^{2}	3×10^{2}	3×10^{2}
$\hat{V}_{o/o}$	$\hat{V}_{11} = \hat{V}_{22} = \hat{V}_{33}$ (KM)	4×10^{5}	4×10^{5}	4×10^{5}
	$\hat{V}_{44} = \hat{V}_{55} = \hat{V}_{66}$ $(KM/SEC)^2$	4×10^{-3}	4×10^{-3}	4×10^{-3}
	$\hat{V}_{77} = \hat{V}_{88} = \hat{V}_{99}$ $(KM)^2$	5×10^{4}	5×10^{4}	4×10^{4}

TABLE 8. SIMULATION DATA (12-14)

SIMULATIONS		12	13	14
FIGURES		19-a,b,c,d	20-a,b,c,d,e	21-a,b,c,d,e
FILTER TYPE		4	4	4
ORBIT TYPE		HYPOBOLIC	HYPOBOLIC	HYPOBOLIC
OBSERVATION TYPE		SUN-PLANET	SUN-PLANET	SUN-PLANET
OBSERVATION RATE (DAY)		*SEE FOOT NOTE	10^{-1}	10^{-1}
OBSERVATION NOISE, σ_R (DEG)		10^{-4}	10^{-4}	10^{-3}
TRUE STATE NOISE, σ_{QT} (KM/DAY^2)		10^2	10^2	10^2
APRIORI STATE NOISE, σ_{QA} (KM/DAY^2)		10^2	10^2	10^2
$\tilde{x}_{o/o}$	$\tilde{X}_o = \tilde{Y}_o = \tilde{Z}_o$ (KM)	10^3	10^3	10^3
	$\tilde{V}_o = \tilde{V}_o = \tilde{W}_o$ (KM/SEC)	10^{-4}	10^{-4}	10^{-4}
	$\tilde{b}_{xo} = \tilde{b}_{yo} = \tilde{b}_{zo}$ (KM)	3×10^2	3×10^2	3×10^2
$\hat{V}_{o/o}$	$\hat{V}_{11} = \hat{V}_{22} = \hat{V}_{33}$ $(KM)^2$	4×10^5	4×10^5	4×10^5
	$\hat{V}_{44} = \hat{V}_{55} = \hat{V}_{66}$ $(KM/SEC)^2$	4×10^{-3}	4×10^{-2}	4×10^{-3}
	$\hat{V}_{77} = \hat{V}_{88} = \hat{V}_{99}$ $(KM)^2$	4×10^4	5×10^4	5×10^4

*Integration step size and observation rate are chosen such that

$$\Delta T = \frac{1}{10} \cdot \text{INTEGER}\,(r/r_o) \quad , \quad r \geq r_o \quad \text{or} \quad \Delta T = \frac{1}{10} / \text{INTEGER}\,(r_o/r) \quad , \quad r_o > r \quad .$$

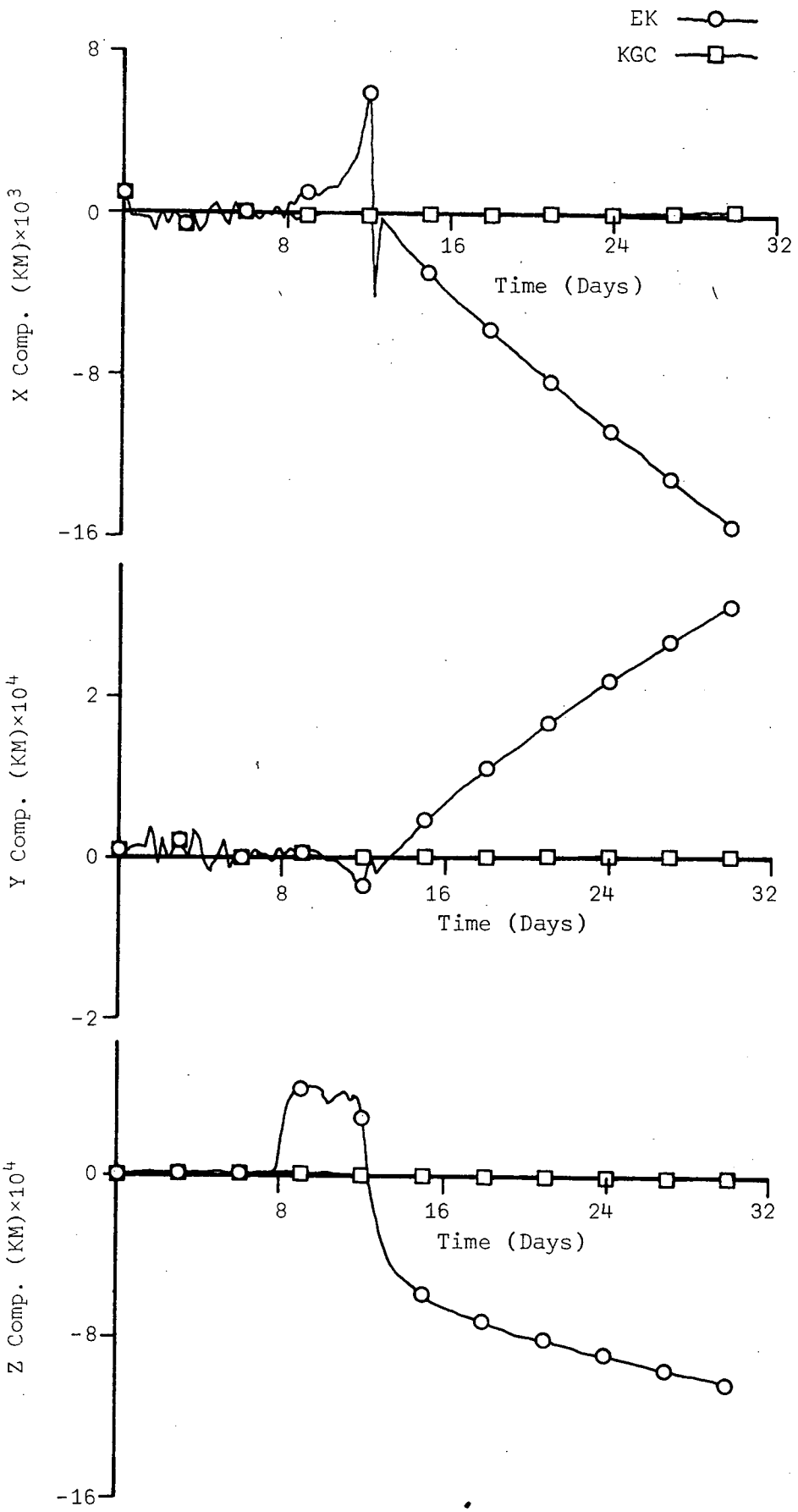

Figure 16-a. Position Estimation Error for the Simulation 9

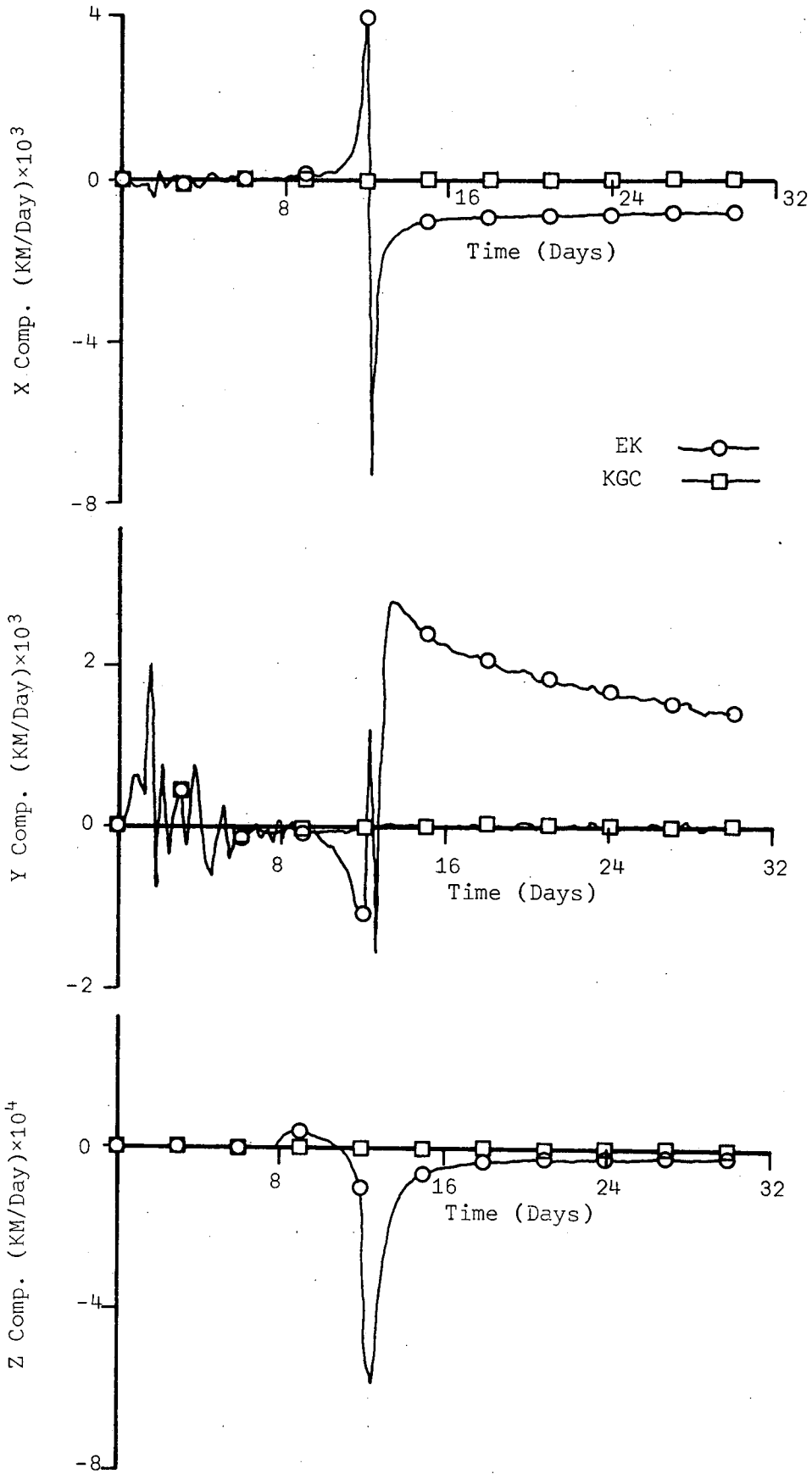

Figure 16-b. Velocity Estimation Errors for the Simulation 9

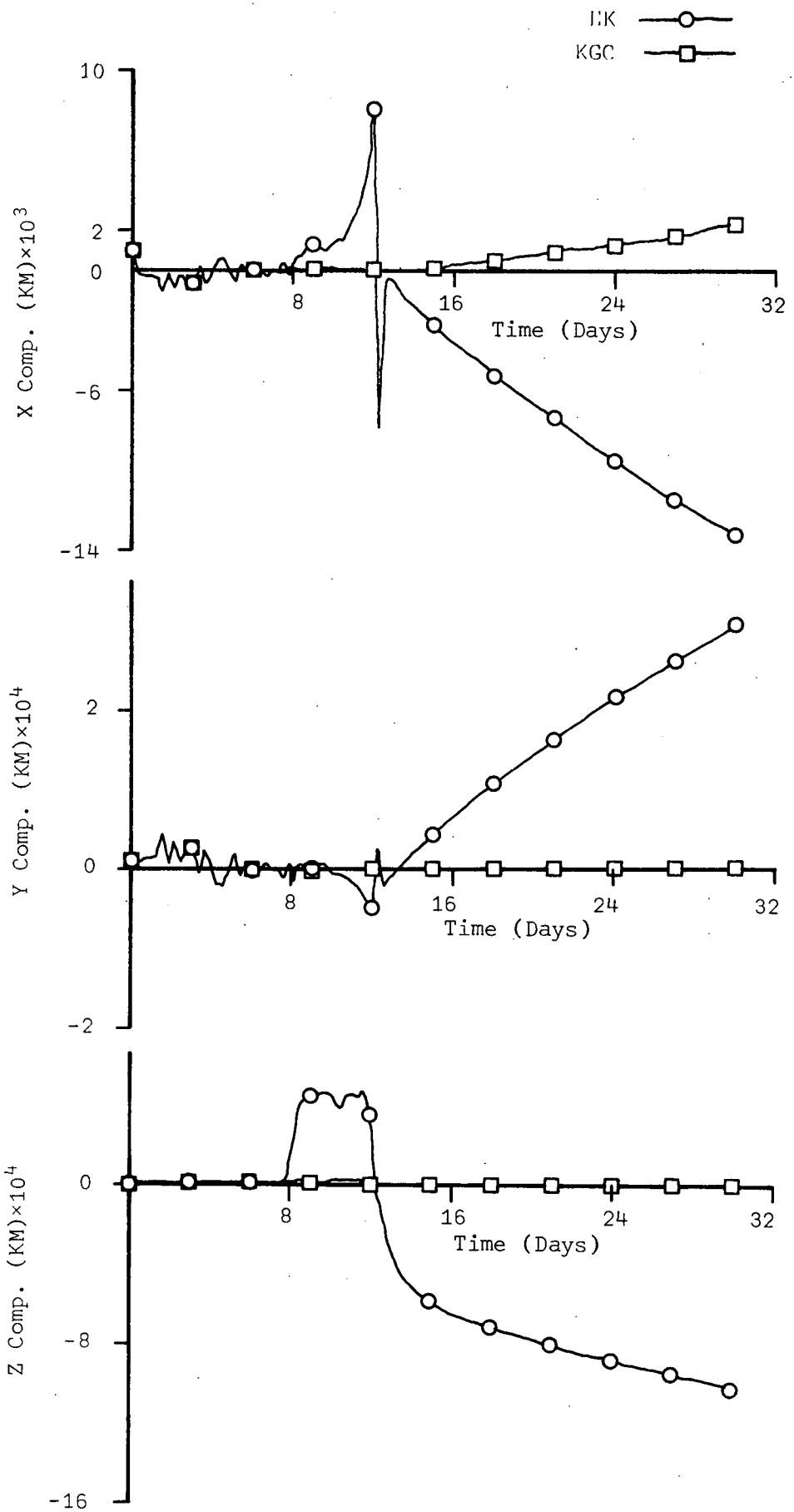

Figure 17-a. Position Estimation Errors for the Simulation 10

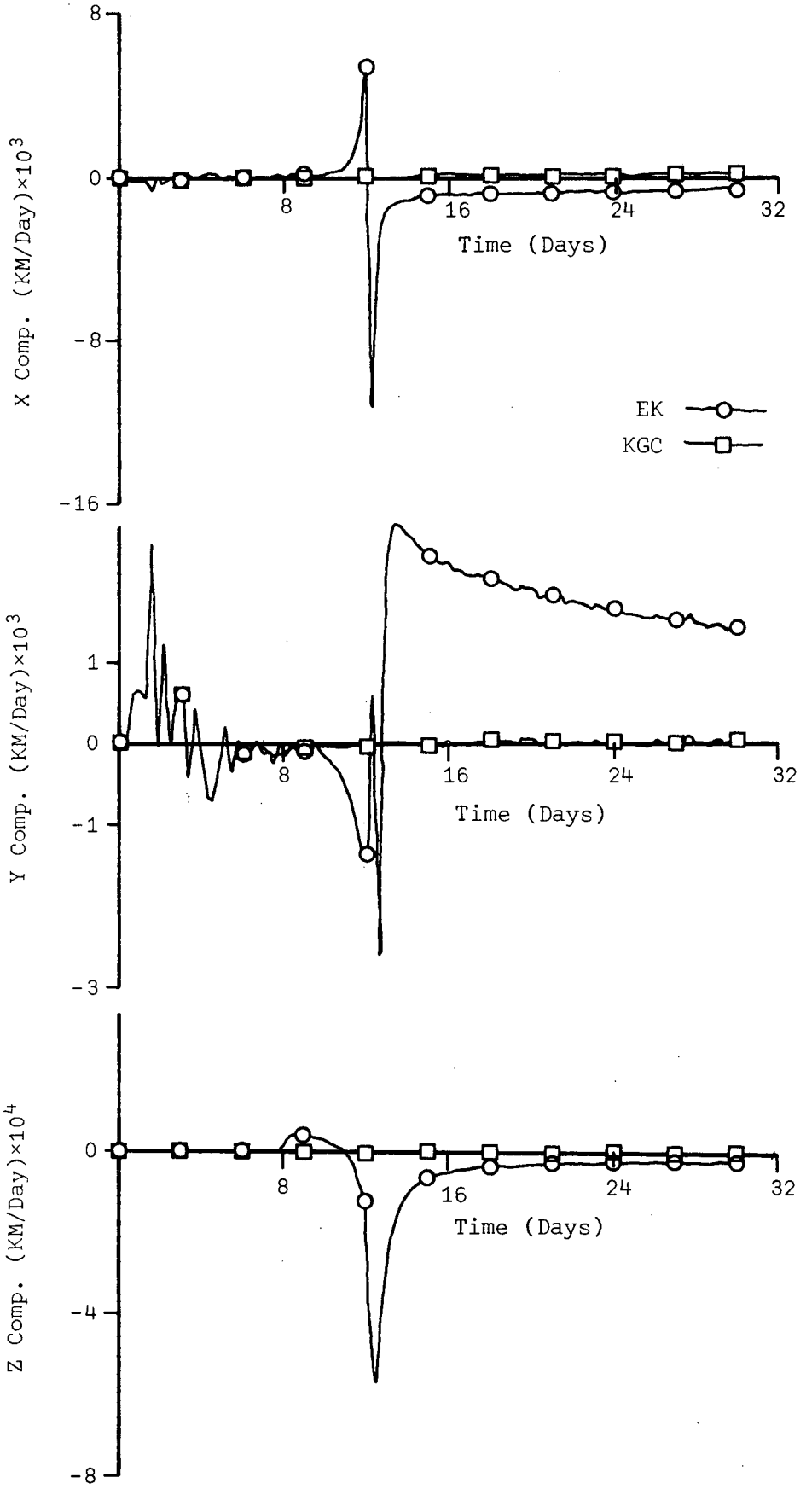

Figure 17-b. Velocity Estimation Errors for the Simulation 10

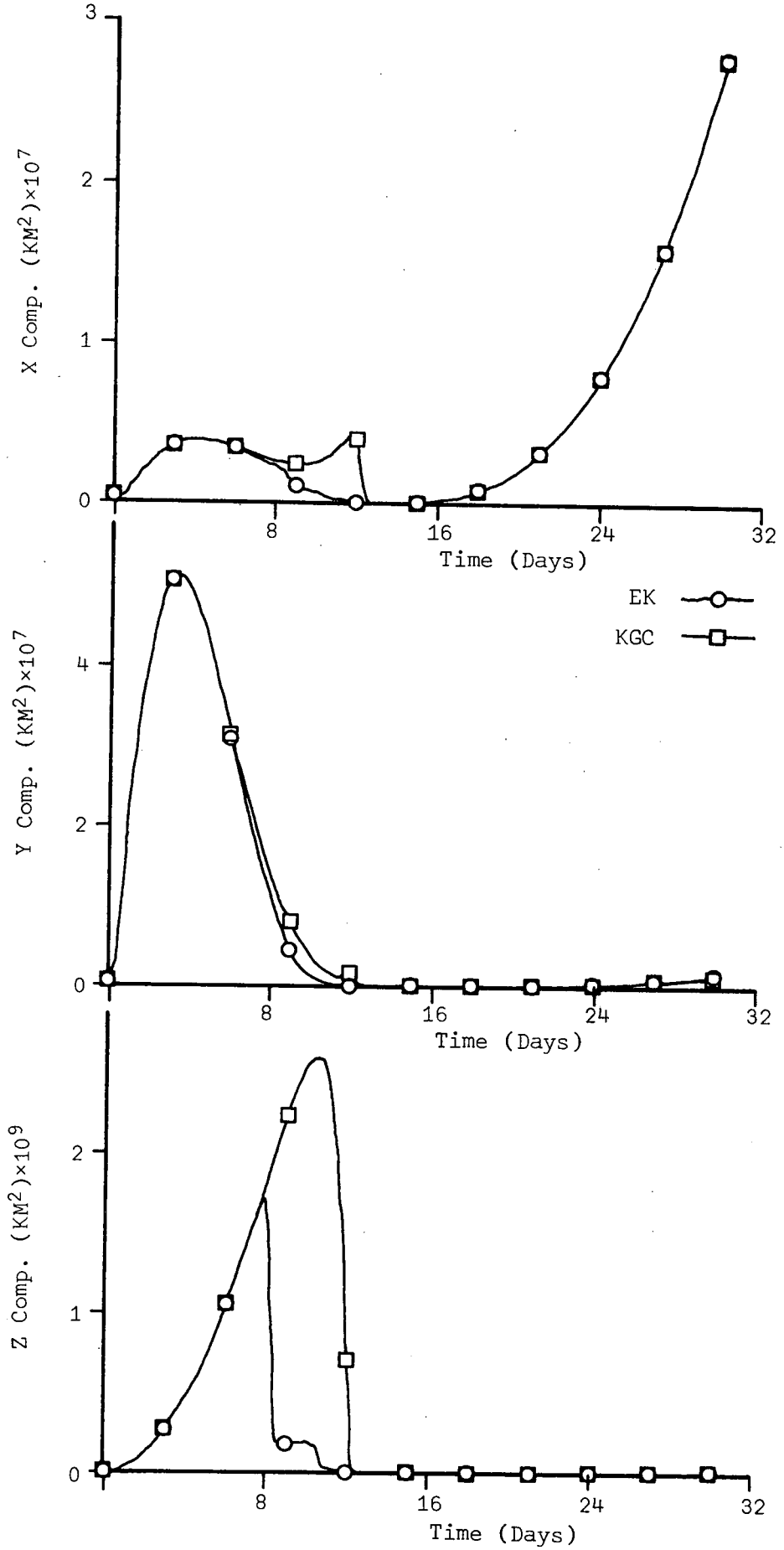

Figure 17-c. Conditional Variances of Position Estimation Errors for the Simulation 10

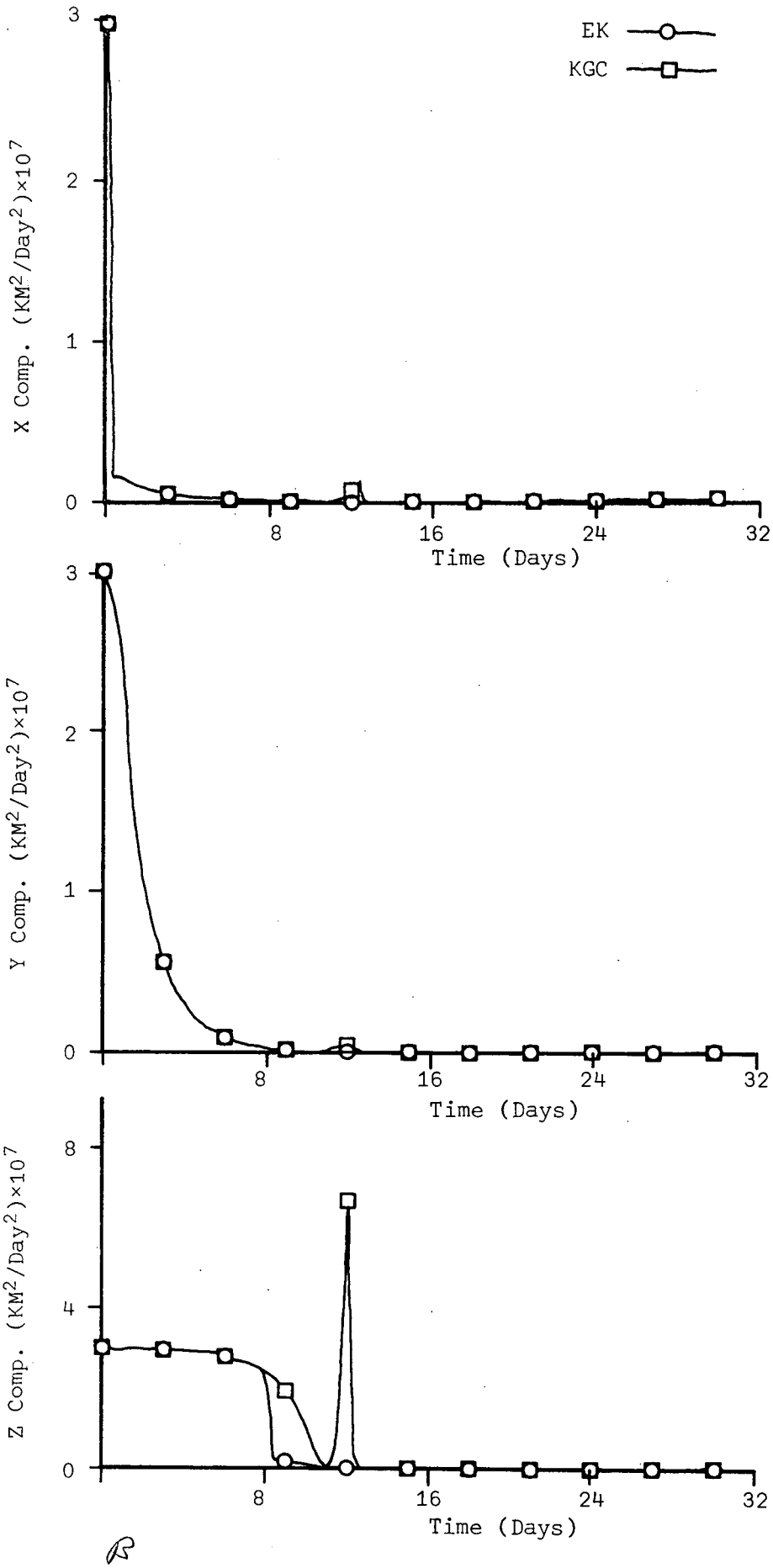

Figure 17-d. Conditional Variances of Velocity Estimation Errors for the Simulation 10

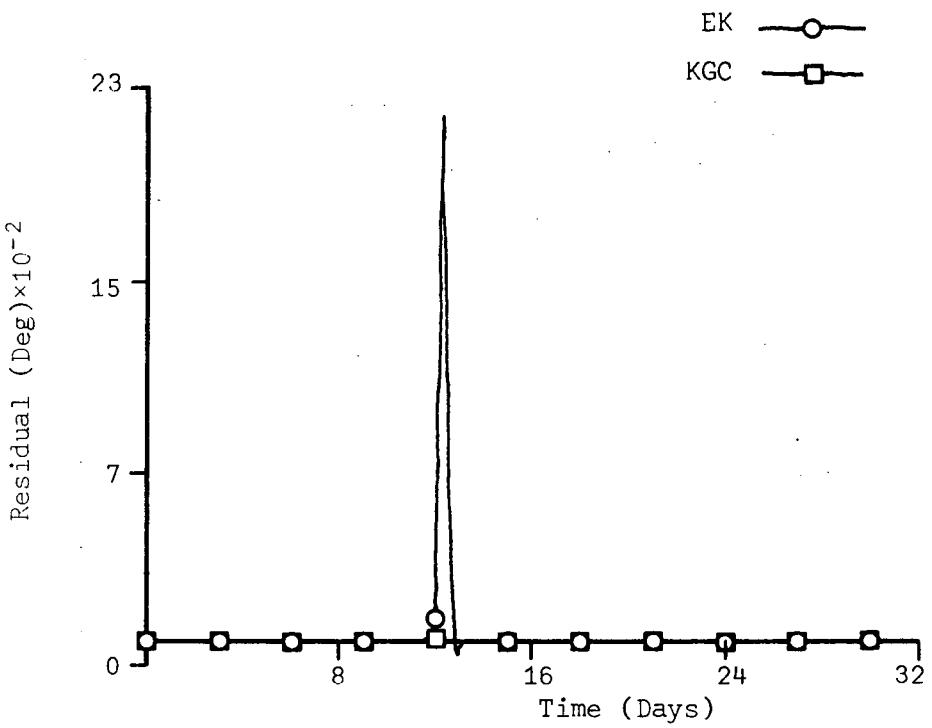

Figure 17-e. Observation Residual for the Simulation 10

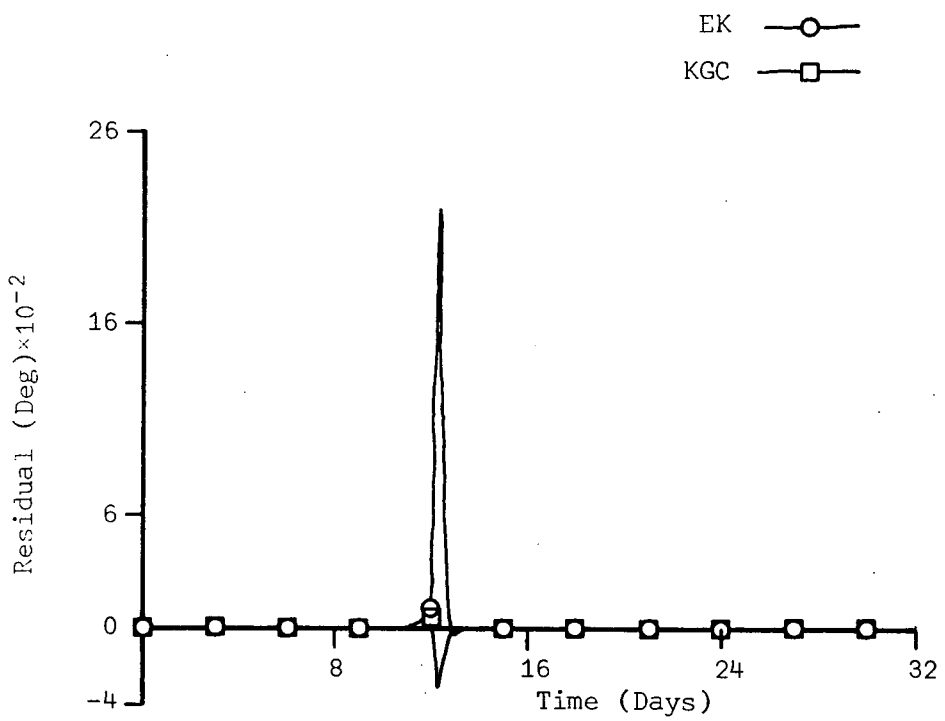

Figure 18-a. Observation Residual for the Simulation 11

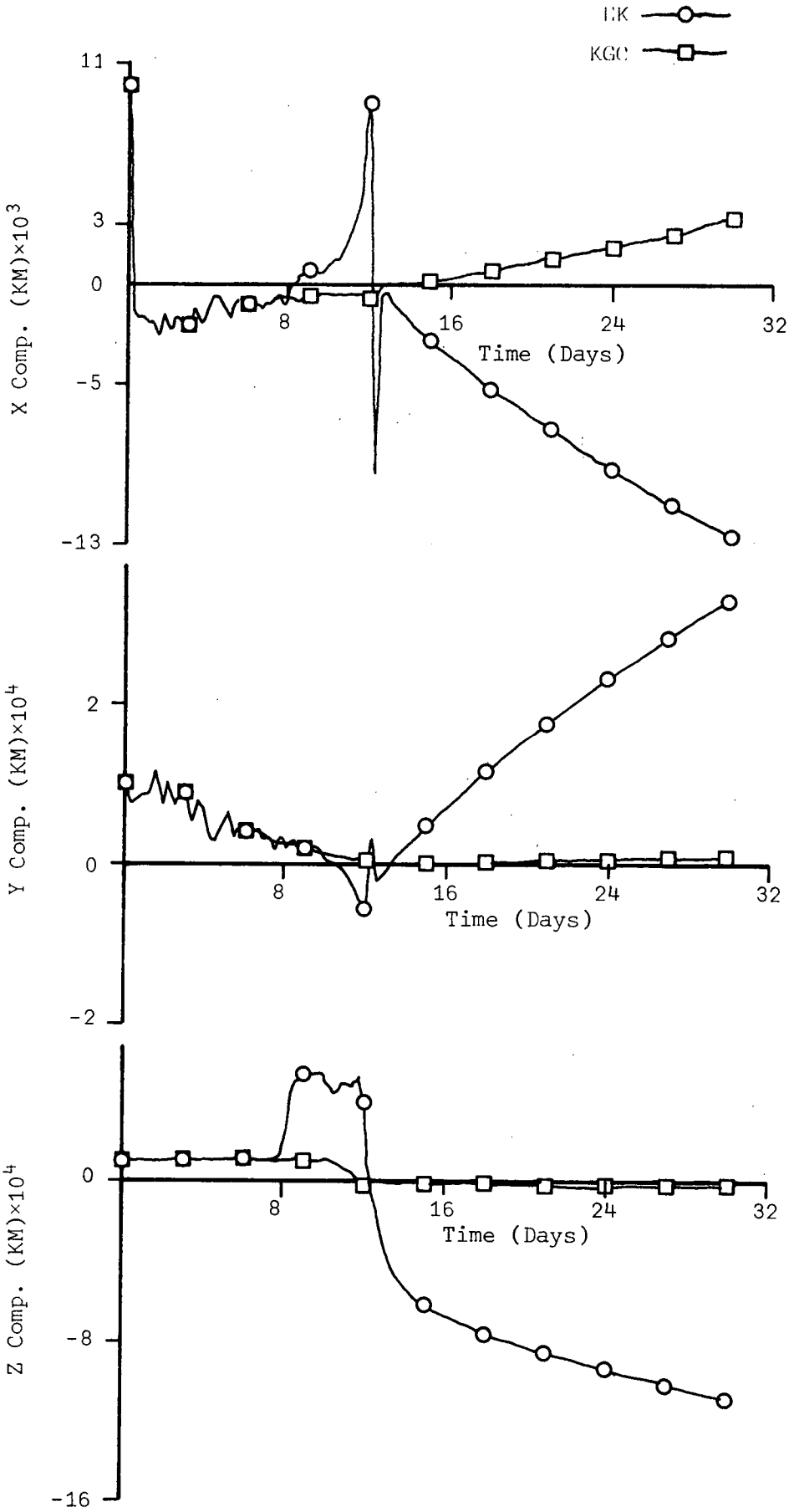

Figure 18-b. Position Estimation Errors for the Simulation 11

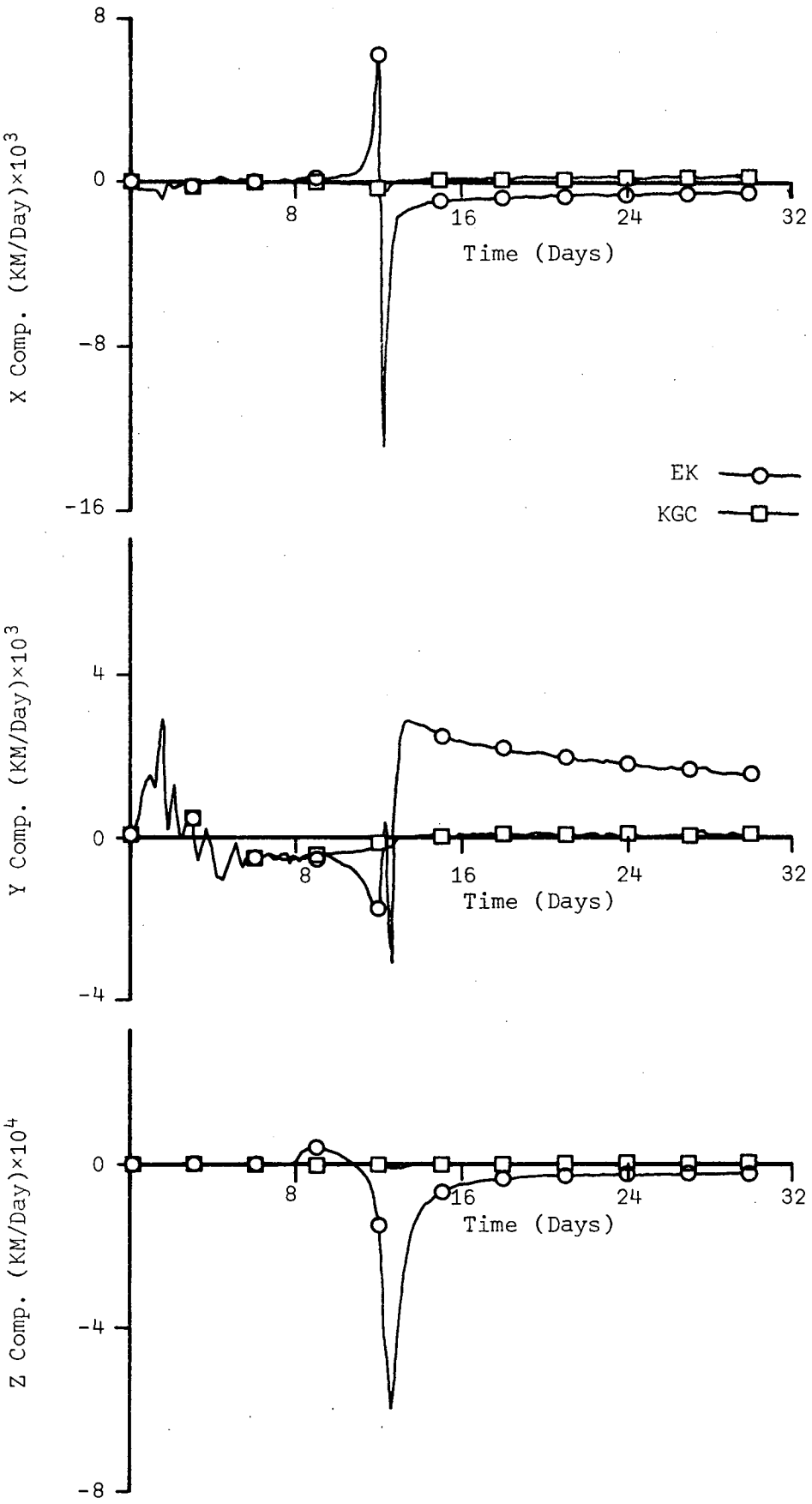

Figure 18-c. Velocity Estimation Errors for the Simulation 11

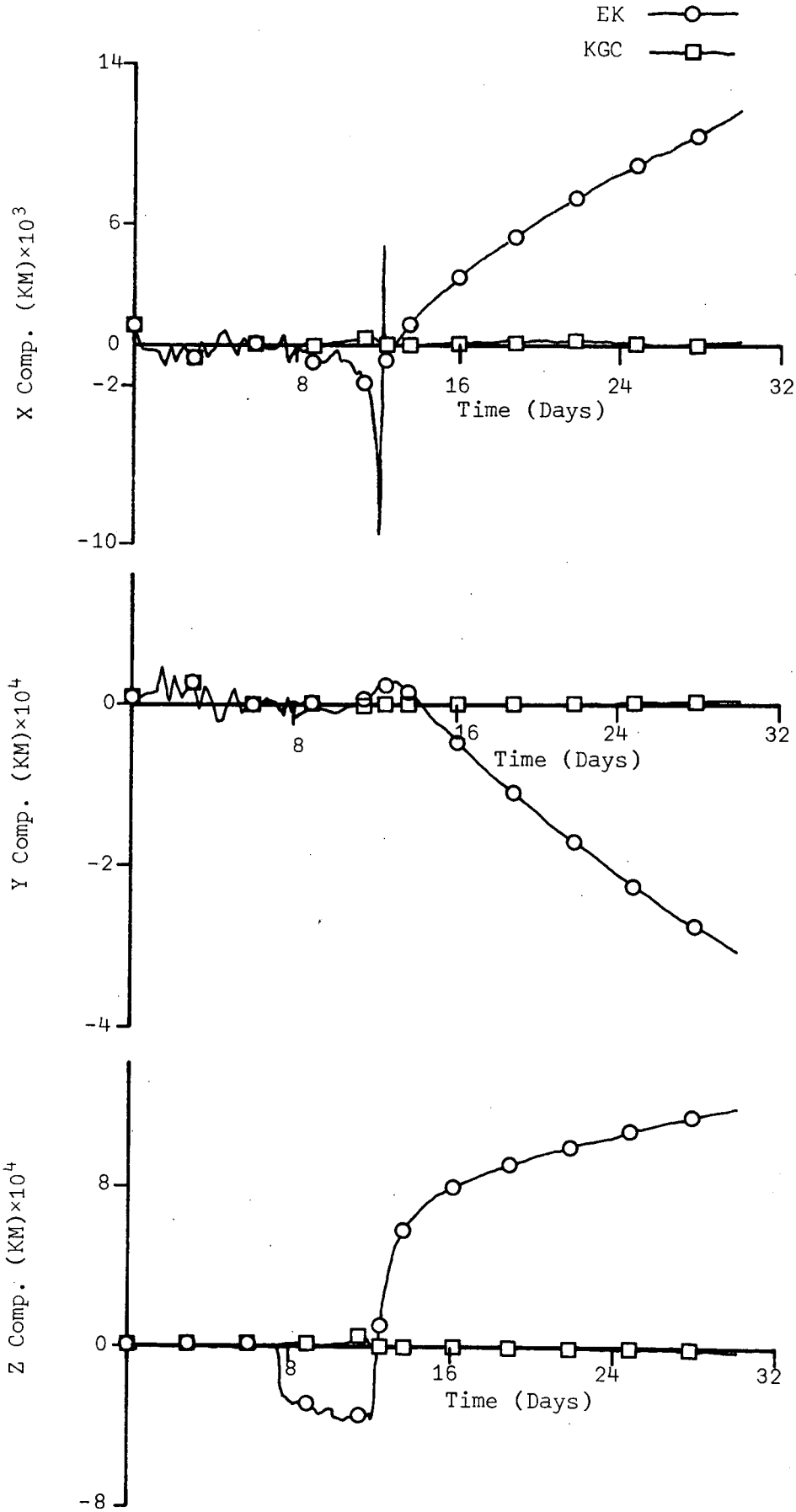

Figure 19-a. Position Estimation Errors for the Simulation 12

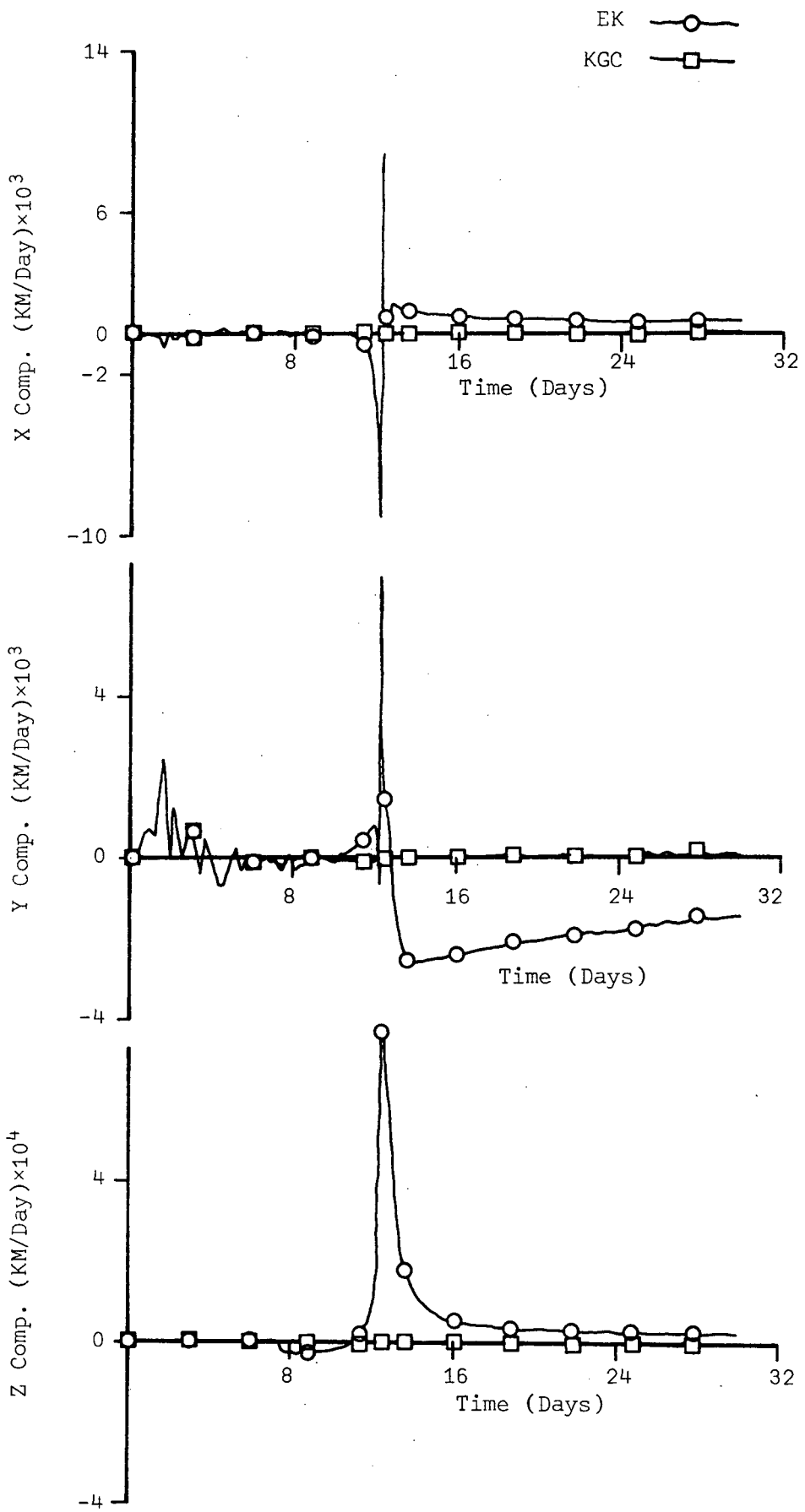

Figure 19-b. Velocity Estimation Errors for the Simulation 12

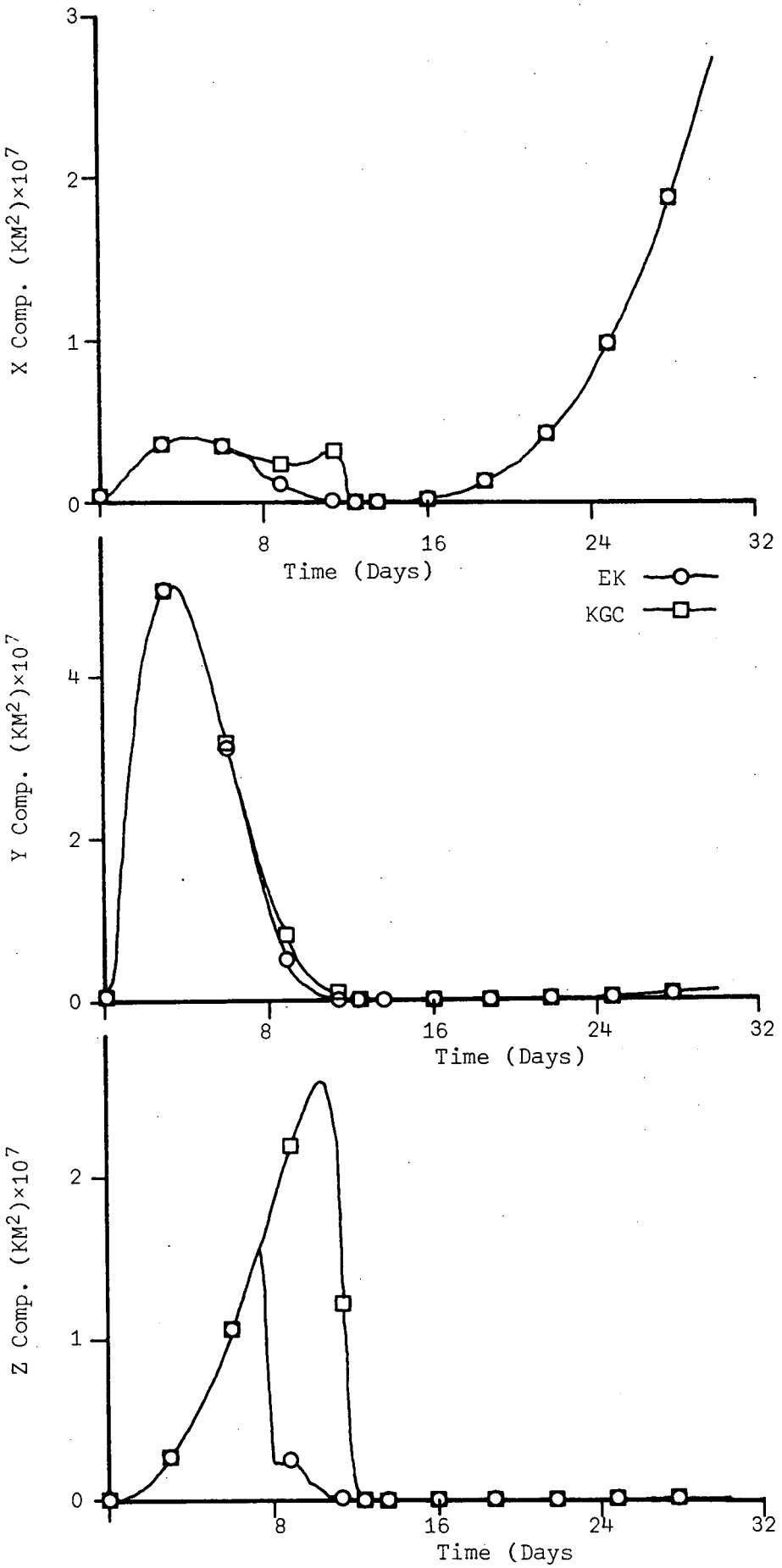

Figure 19-c. Conditional Variances of Velocity Estimation Errors for the Simulation 12

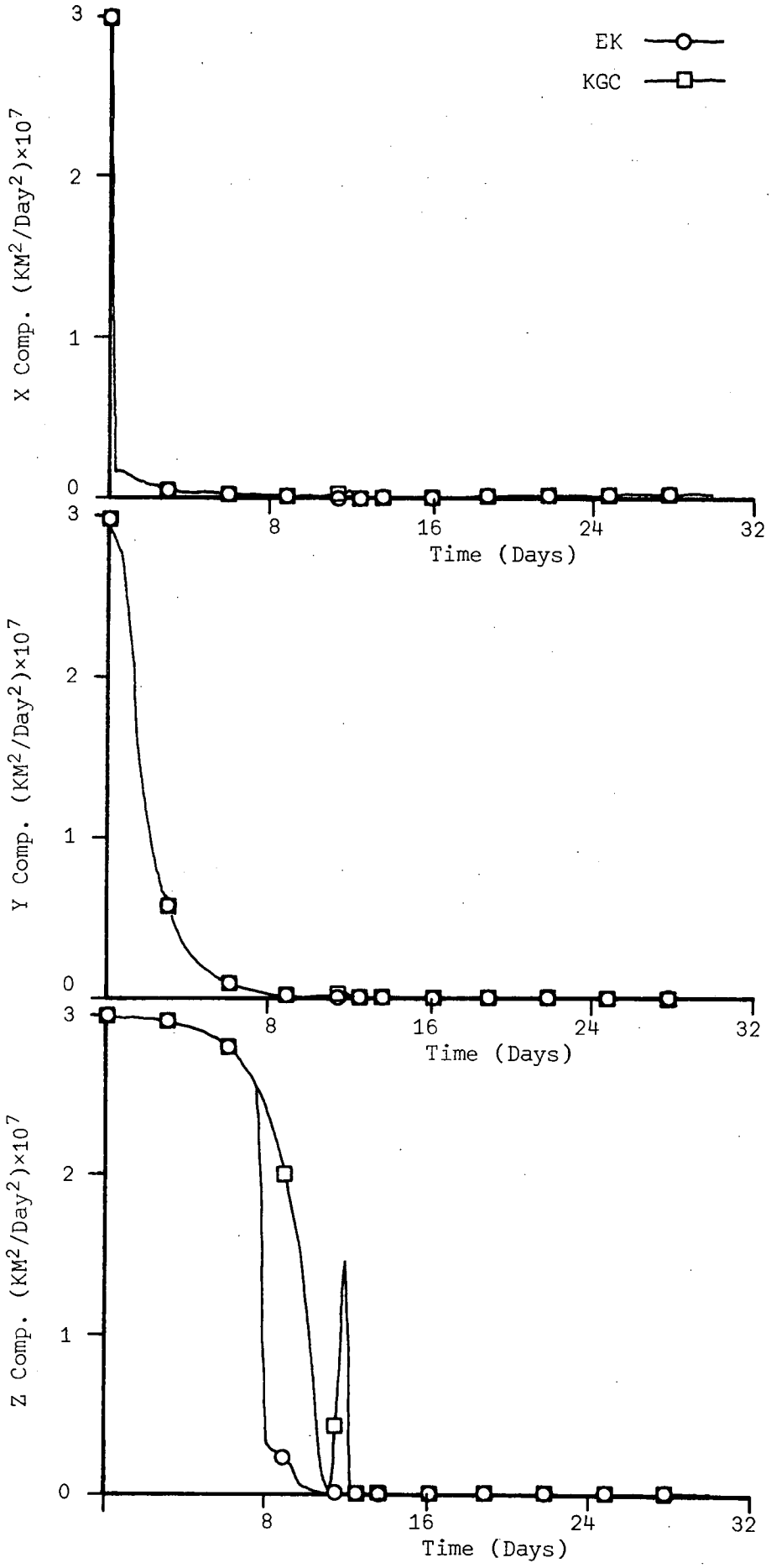

Figure 19-d. Conditional Variances of Velocity Estimation Errors for the Simulation 12

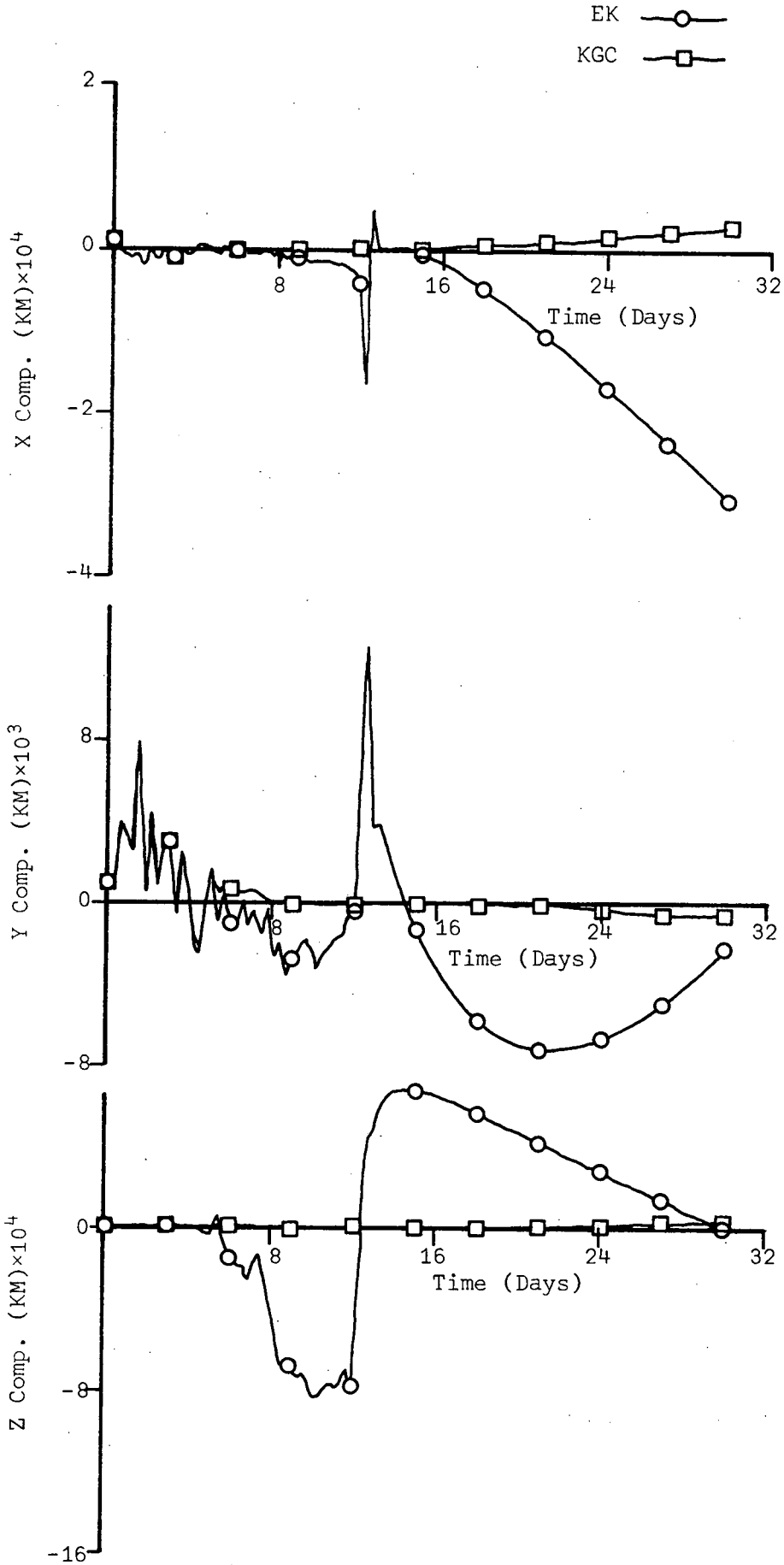

Figure 20-a. Position Estimation Errors for the Simulation 13

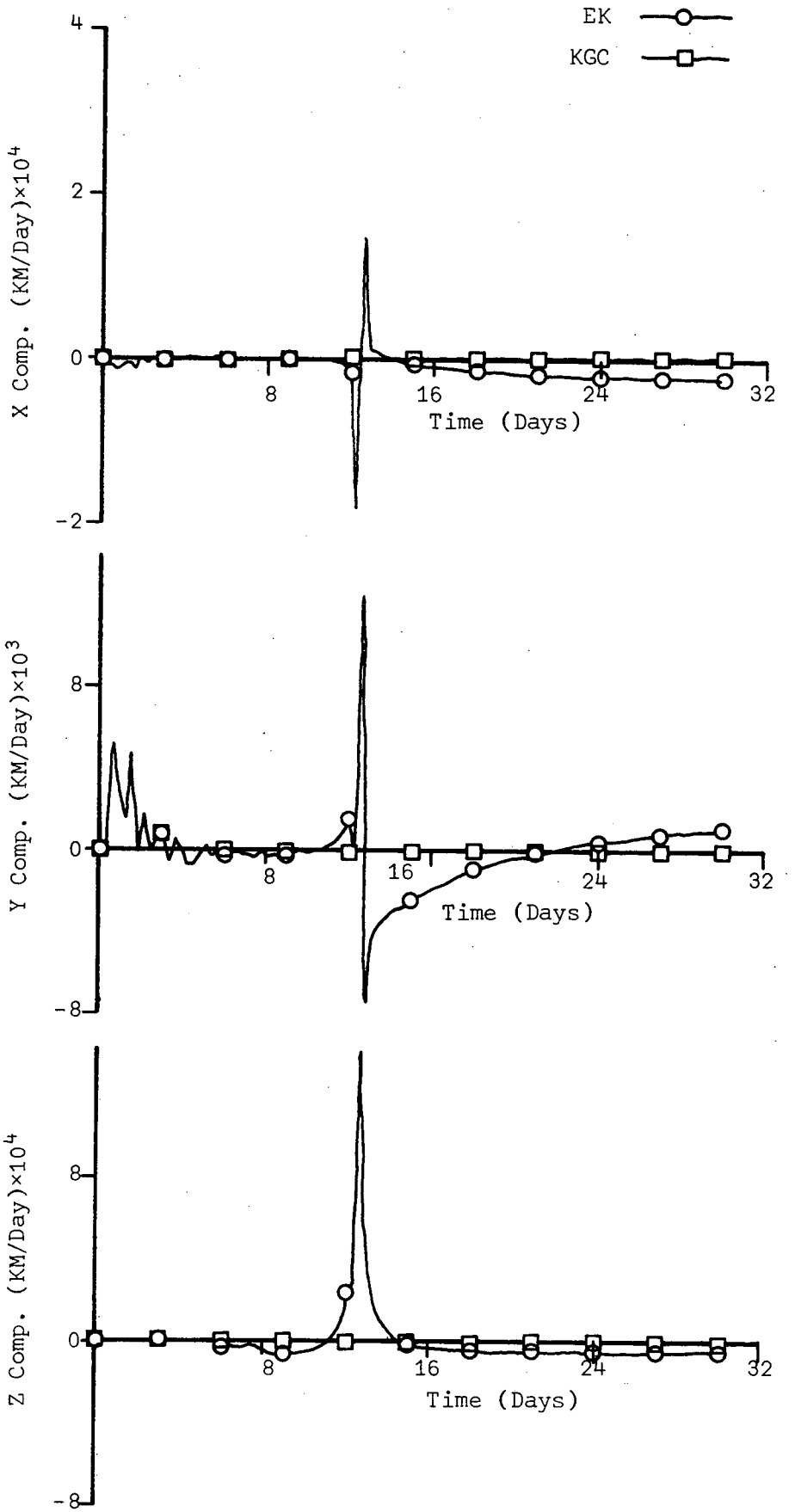

Figure 20-b. Velocity Estimation Errors for the Simulation 13

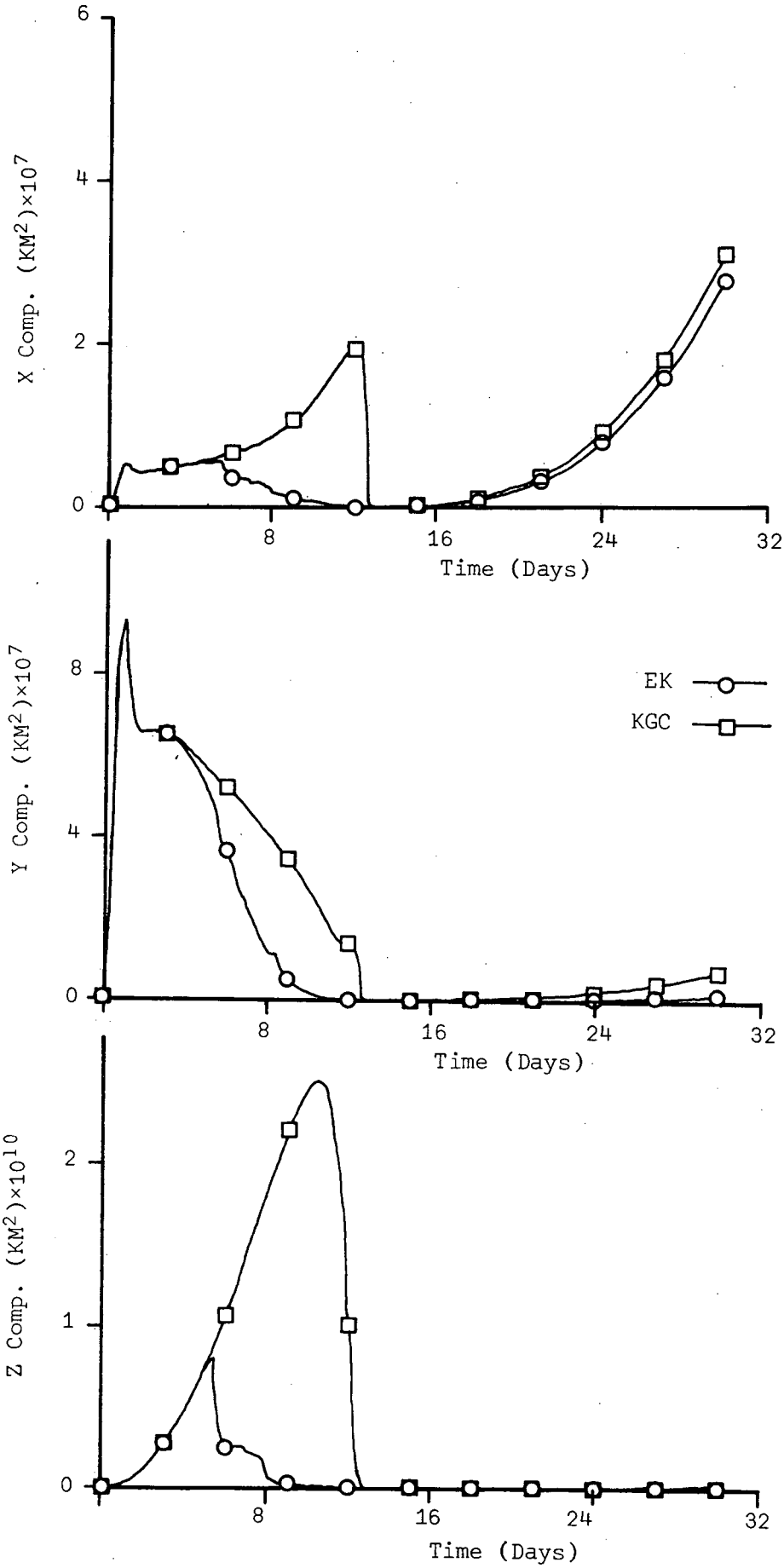

Figure 20-c. Conditional Variances of Position Estimation Errors for the Simulation 13

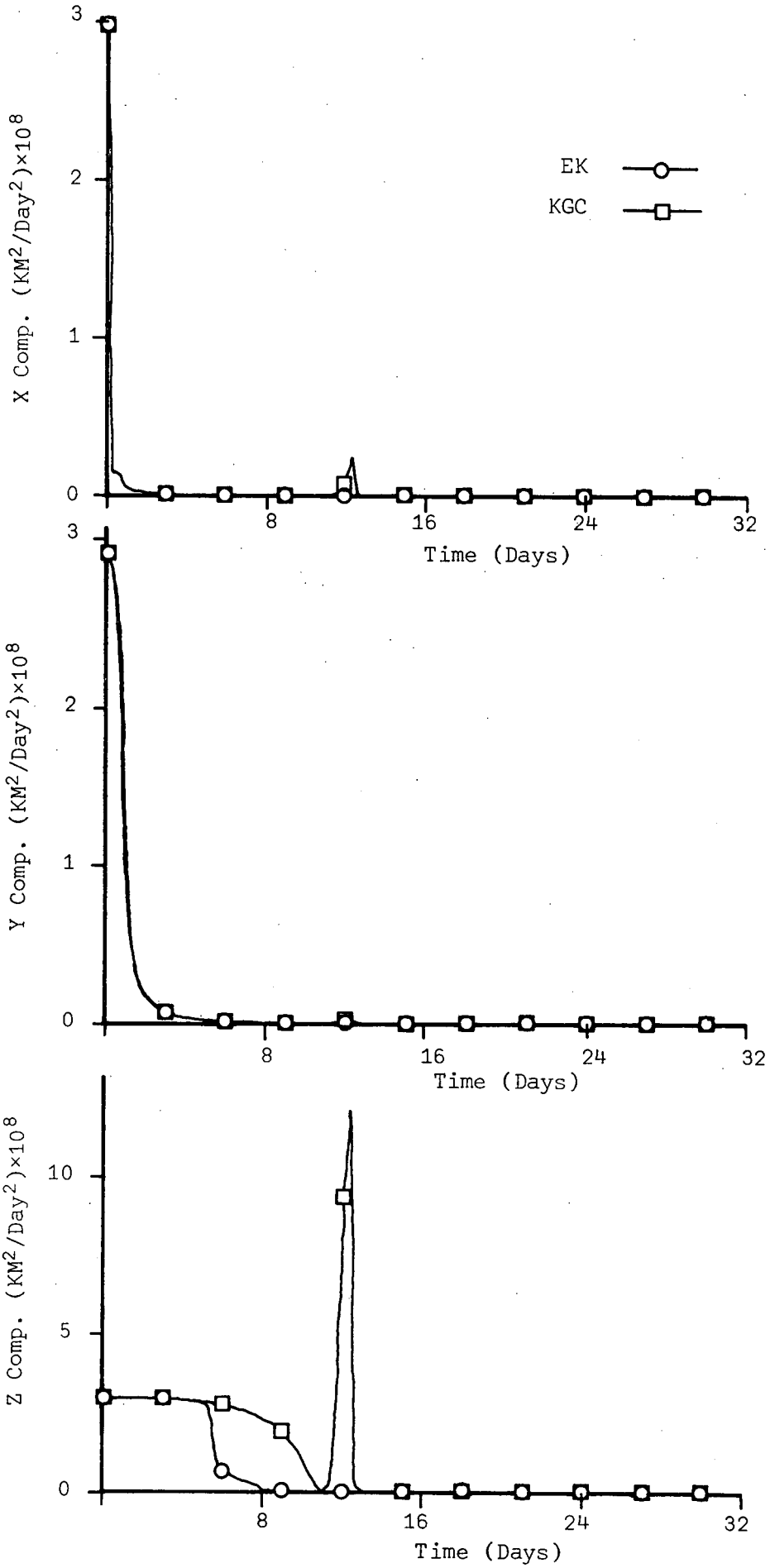

Figure 20-d. Conditional Variances of Velocity Estimation Errors for the Simulation 13

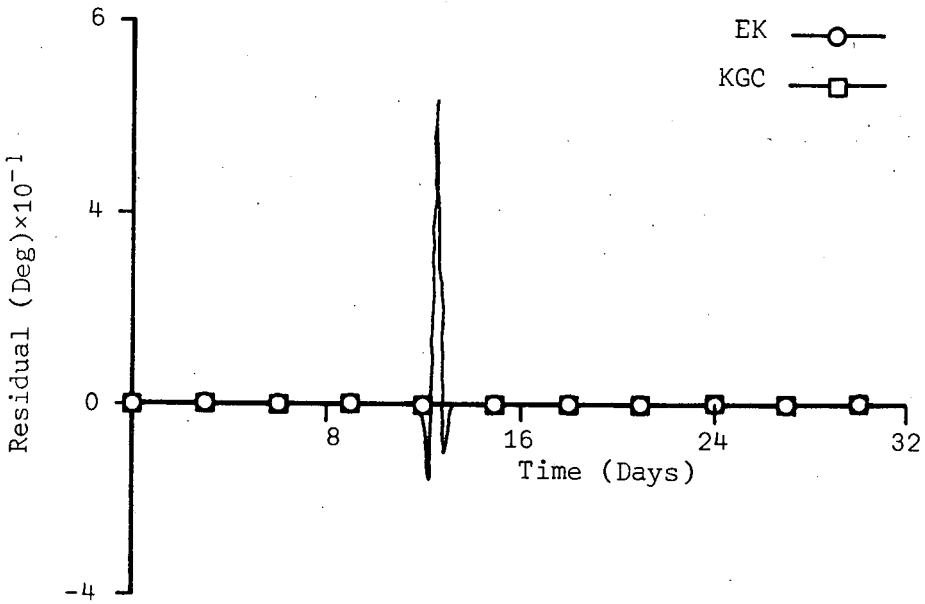

Figure 20-e. Observation Residual for the Simulation 13

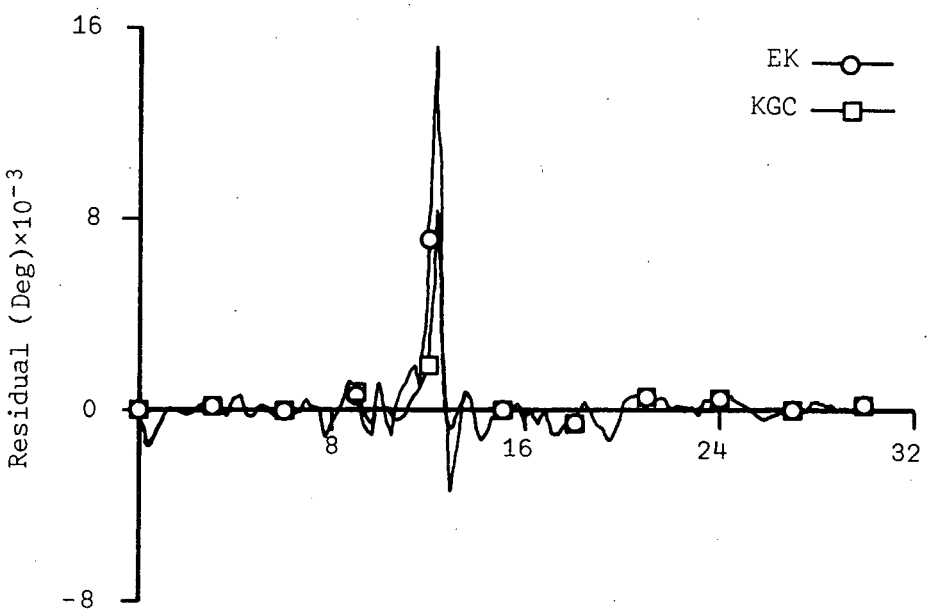

Figure 21-a. Observation Residual for the Simulation 14

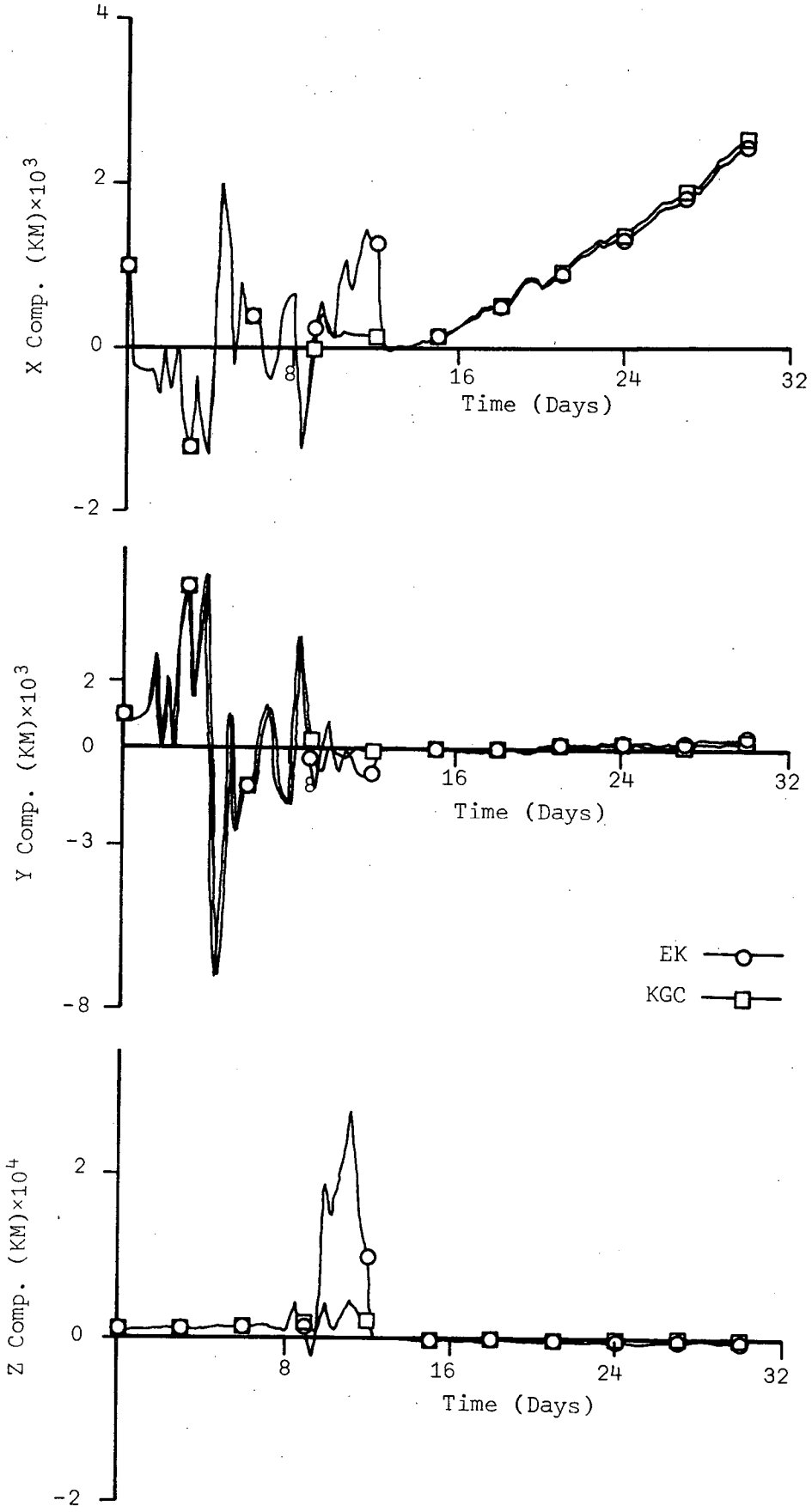

Figure 21-b. Position Estimation Errors for the Simulation 14

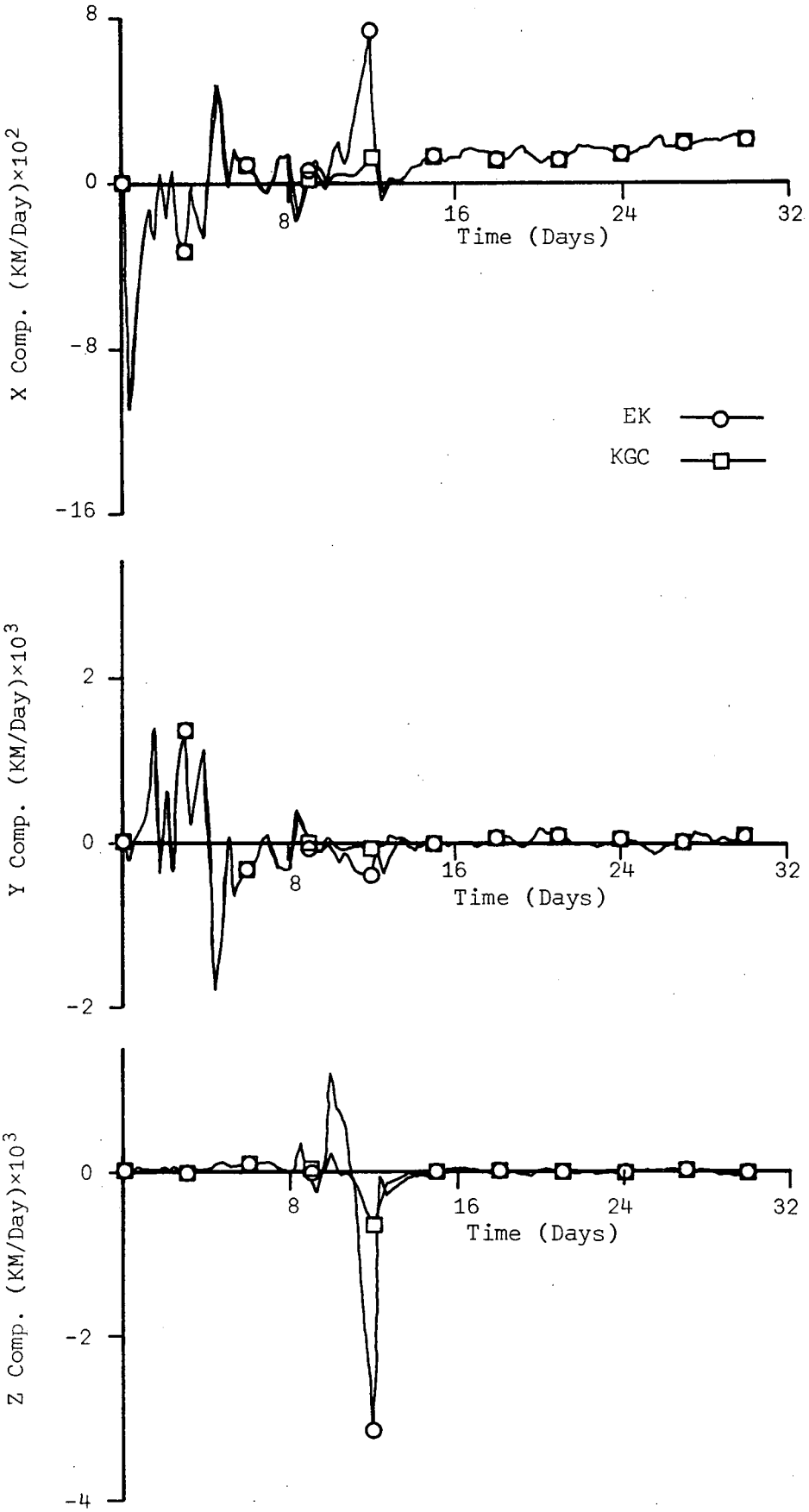

Figure 21-c. Velocity Estimation Errors for the Simulation 14

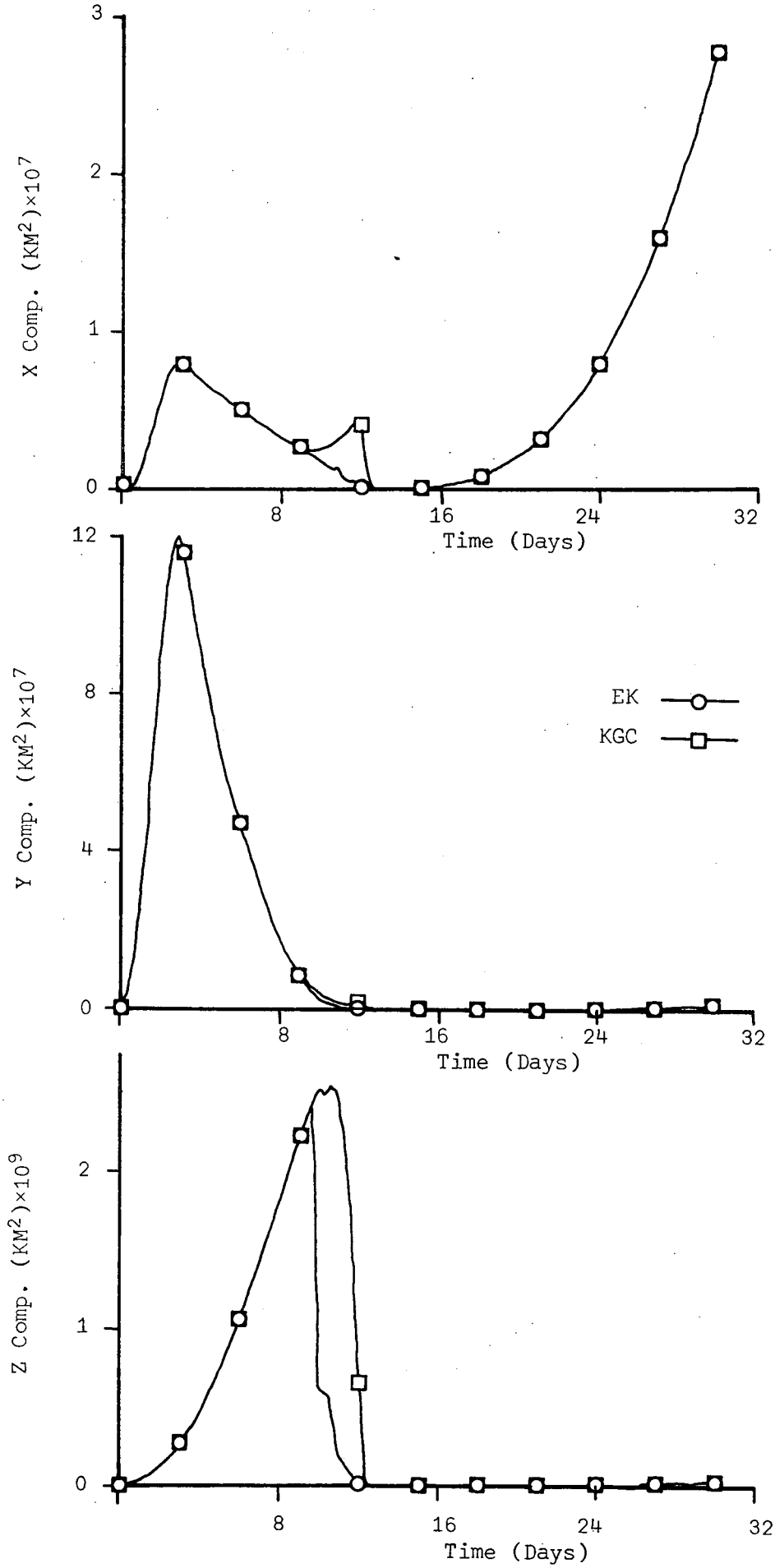

Figure 21-d. Conditional Variances of Position Estimation Errors for the Simulation 14

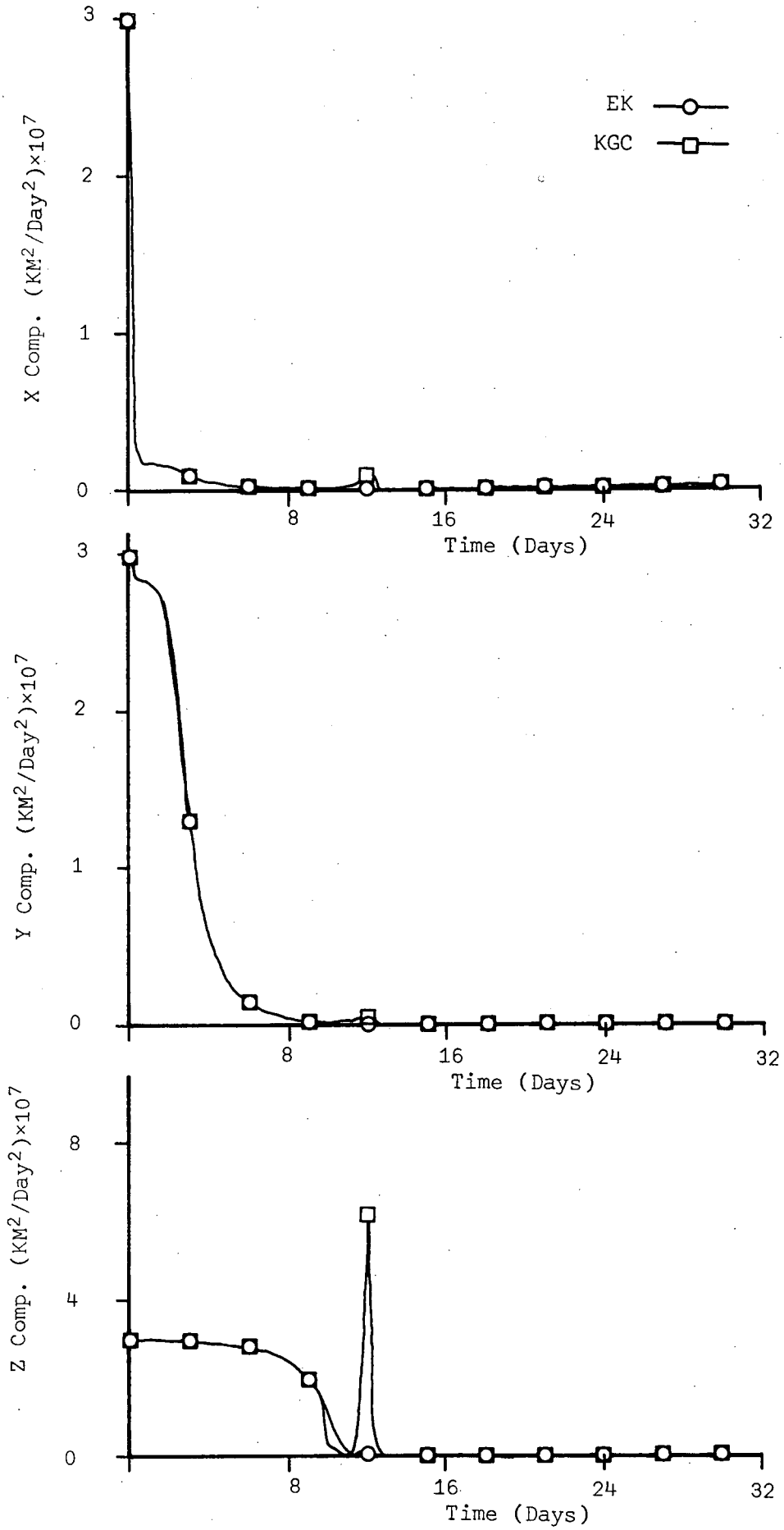

Figure 21-e. Conditional Variances of Velocity Estimation Errors for the Simulation 14

4.5 Application of the KGC Filter to the Elliptic Orbit

The KGC Filter is applied to the problem of determining an elliptic orbit around Jupiter with sun-planet, star-planet and range-rate plus sun-planet angle measurements. Since the variation of the Z components in the nominal trajectory shown in Fig. 6 is very small compared with the X and Y components, the initial state errors for the Z components of position and velocity are chosen as one-tenth of those of X and Y components, i.e., X and Y components of position and velocity estimation errors are initially chosen as 10^3 km and 10^{-4} km/sec , respectively, and Z components as 10^2 km and 10^{-5} km/sec , respectively.

Figs. 22-a and 22-b show the estimation errors for Simulation 15. Unlike the hypobolic orbit, the EK Filter gradually drifts away after fifteen days during which time the dynamic nonlinearity affects grow large. The conditional variances are shown in Figs. 22-c and 22-d. Fig. 22-e shows the observation residual pattern which consists of every tenth data point connected with straight lines. Simulation 18 is designed to see the performance of the KGC Filter for a long period of time. The period of estimation is extended to 62 days which is more than two revolutions of the elliptic orbit. The same input data as that used in Simulation 15 are used for Simulation 18. The estimation errors for the position and velocity are shown in Figs. 25-a and 25-b. For the first 30 days, the estimation error patterns of Figs. 25-a and 25-b match identically with the ones shown in Figs. 22-a and 22-b. An interesting fact is that both the EK Filter and the KGC Filter exhibit a periodicity in the estimation errors. However, the errors for the EK Filter grow larger during the second revolution and reach an unacceptable value. However, the KGC Filter realizes a very accurate estimate throughout the entire period and, as a matter of fact, the estimation errors are considerably

smaller during the second revolution than those during the first revolution. Around the second periapsis, the EK Filter estimation errors exhibit spikes in the velocity estimation error components and the numerical value of the position changes sign. The conditional variances are shown in Figs. 25-c and 25-d.

From the examination of Figs. 25-a, 25-b, 25-c and 25-d, it can be seen that the KGC Filter is superior to the EK Filter in the region where the conditional variances of the KGC Filter are larger than those of the EK Filter. The improvement achieved in the KGC Filter is strictly due to the effect of the KGC term in the optimal gain K. Fig. 25-e shows the observation residual. It shows a couple of spikes around the second periapsis. For the blown up scale, the residual pattern of every tenth data point for the first 30 days matches with the one shown in Fig. 22-e.

Simulation 16 is conducted with sun-planet angle measurements. The estimation errors shown in Figs. 23-b and 23-c reflect the characteristics of the sun-planet angle measurement. Since the sun, Jupiter and the spacecraft are all almost on the ecliptic plane, the information about the Z components is poor and the EK Filter determines a poor estimate of the Z components of position and velocity. Figs. 23-d, 23-e and 23-a show the conditional variances and the observation residual pattern, respectively. The residual pattern is obtained by connecting every tenth data point with a straight line.

The Simulation 17 is conducted with two kinds of observations, i.e., range-rate plus sun-planet angle measurements. Figs. 24-a and 24-b show the estimation errors and the conditional variances are given in Figs. 24-d and 24-e. The Z components are estimated poorly again. Fig. 24-e shows the

two observation residuals, one for the range-rate and the other for the sun-planet angle measurement. With the data of Simulations 16 and 17, the filters were examined for 62 days. The same characteristics discussed in Simulation 18 can be found. The conditional variances vary periodically and large spikes can be found in the observation residual and velocity estimation errors for the EK Filter. The EK Filter estimation errors are incomparable at the second revolution. Actually, they diverge after the second periapsis. However, the KGC Filter performs exceptionally well through out the entire period and even better at the second revolution.

Simulations 1 through 8 are re-examined by using the variable integration step size and observation rate discussed in Section 4.4. The characteristics discussed in the Section 4.3 are unchanged.

It is found that variable integration step size and rapid observation rate do not change the characteristics of Simulations 15, 16, 17 and 18 except that over all estimation errors are smaller than those of the constant integration step size and observation rate. However, the improvement is not significant considering the computer time. Usually, for this case, the EK Filter reduces the estimation errors more significantly than the KGC Filter does, but the EK Filter solution will diverge still.

TABLE 9. SIMULATION DATA (15-18)

SIMULATIONS		15	16	17	18*
FIGURES		22-a,b,c,d,e	23-a,b,c,d,e	24-a,b,c,d,e	25-a,b,c,d,e
FILTER TYPE		4	4	4	4
ORBIT TYPE		ELLIPTIC	ELLIPTIC	ELLIPTIC	ELLIPTIC
OBSERVATION TYPE		STAR-PLANET	SUN-PLANET	RANGE-RATE SUN-PLANET	STAR-PLANET
OBSERVATION RATE (DAY)		2×10^{-1}	10^{-1}	10^{-1}	2×10^{-1}
OBSERVATION NOISE, σ_R (DEG) or (KM/SEC)		10^{-4}	10^{-4}	R-R = 10^{-6} S-P = 10^{-4}	10^{-4}
TRUE STATE NOISE, σ_{QT} (KM/DAY^2)		10^0	10^0	10^0	10^0
APRIORI STATE NOISE, σ_{QA}		10^3	10^3	10^3	10^3
$\tilde{x}_{o/o}$	$\tilde{X}_o = \tilde{Y}_o , \tilde{Z}_o$ (KM)	$10^3, 10^2$	$10^3, 10^2$	$10^3, 10^2$	$10^3, 10^2$
	$\tilde{U}_o = \tilde{V}_o , \tilde{W}_o$ (KM/SEC)	$10^4, 10^5$	$10^4, 10^5$	$10^4, 10^5$	$10^4, 10^5$
	$\tilde{b}_{xo} = \tilde{b}_{yo} = \tilde{b}_{zo}$ (KM)	3×10^2	3×10^2	3×10^2	3×10^2
$\hat{V}_{o/o}$	$\hat{V}_{11} = \hat{V}_{22} = \hat{V}_{33}$ (KM)^2	4×10^5	$V_{11} = V_{22} = 4\times10^5$ $V_{33} = 4\times10^4$	4×10^5	4×10^5
	$\hat{V}_{44} = \hat{V}_{55} = \hat{V}_{66}$ (KM/SEC)^2	4×10^{-2}	$V_{44} = V_{55} = 4\times10^{-4}$ $V_{66} = 4\times10^{-5}$	4×10^{-3}	4×10^{-2}
	$\hat{V}_{77} = \hat{V}_{88} = \hat{V}_{99}$ (KM)	5×10^4	5×10^4	5×10^4	5×10^4

*Estimation performed for 62 days which is about two revolutions.

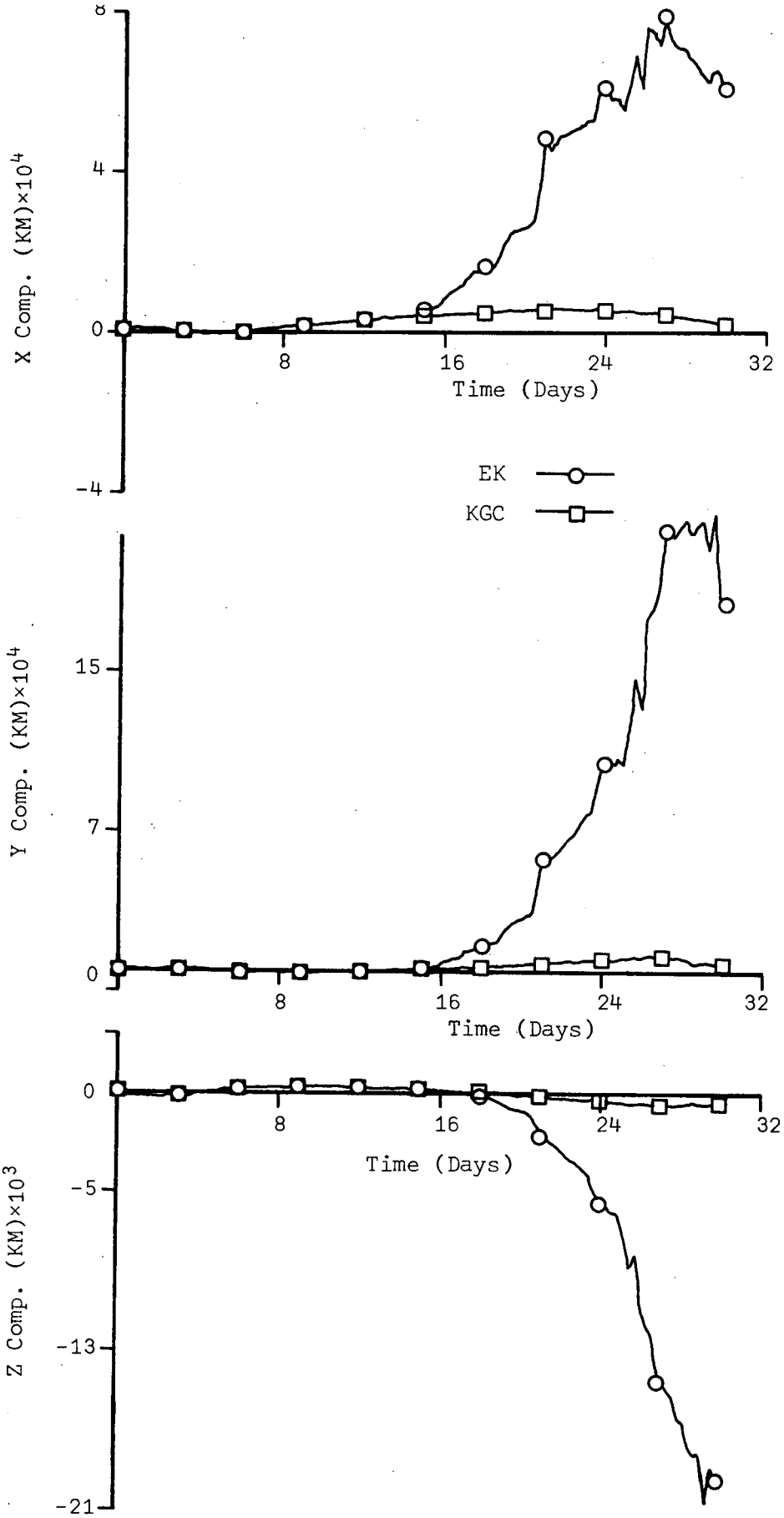

Figure 22-a. Position Estimation Errors for the Simulation 15

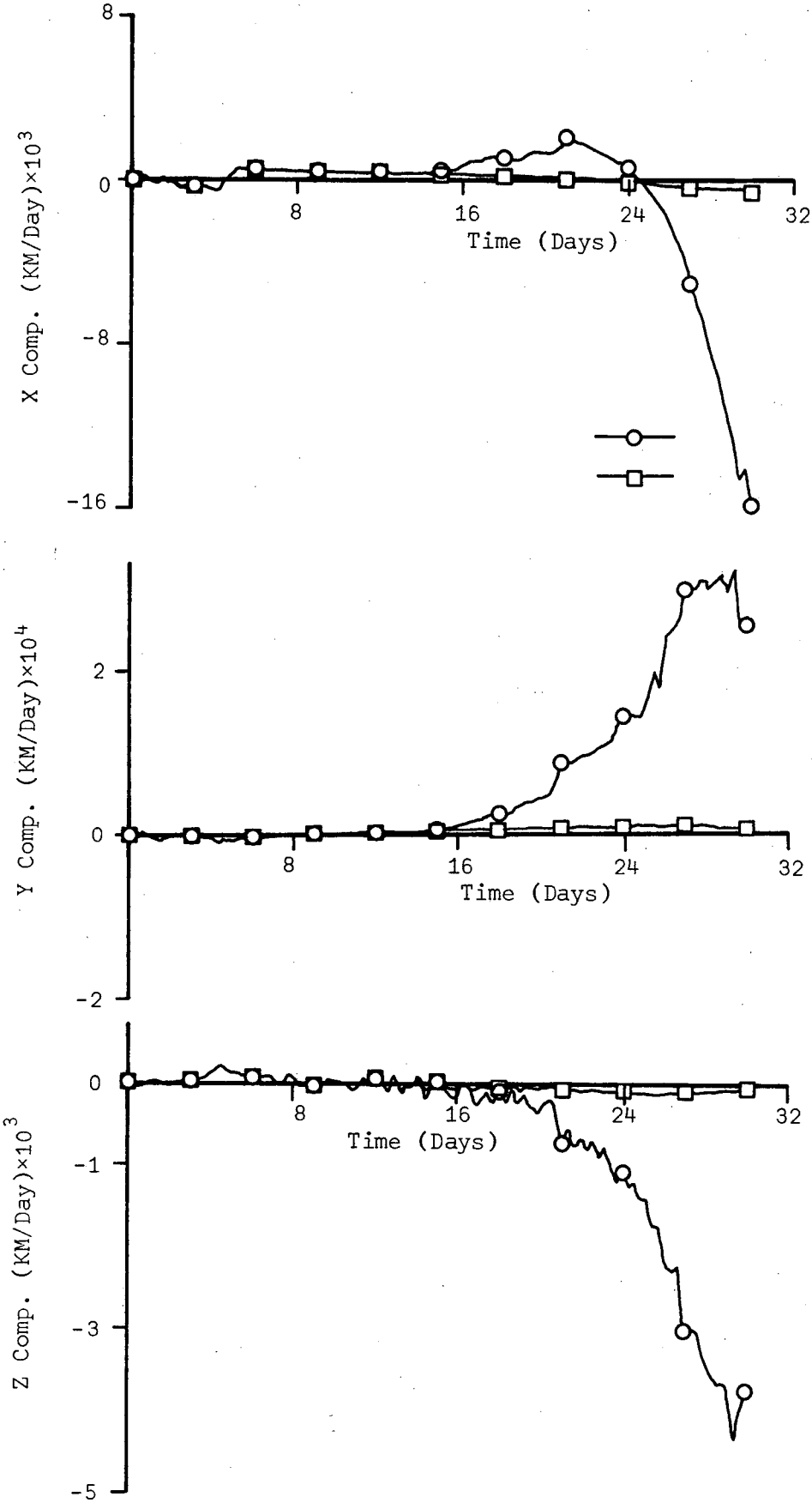

Figure 22-b. Velocity Estimation Errors for the Simulation 15

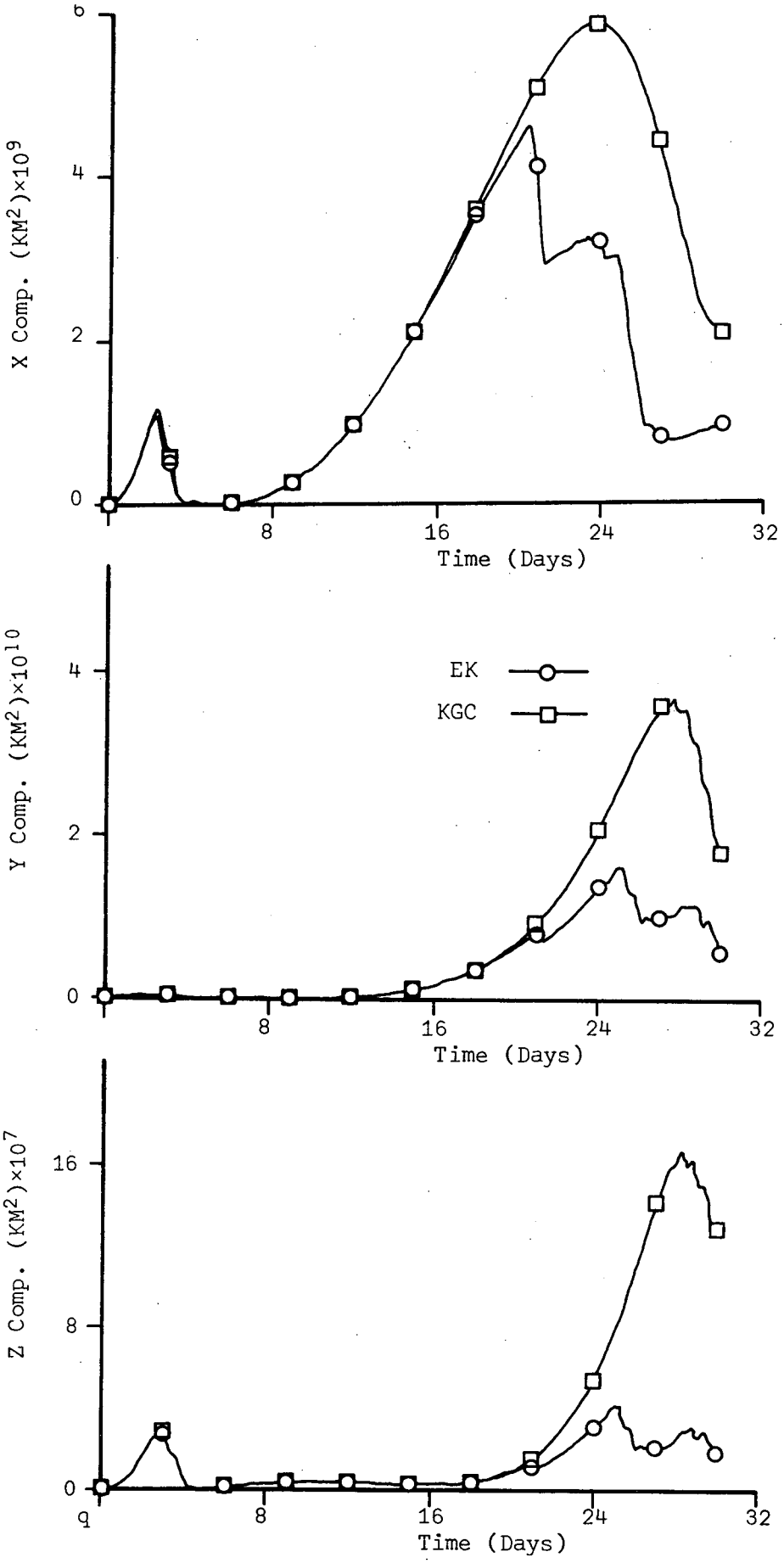

Figure 22-c. Conditional Variances of Position Estimation Errors for the Simulation 15

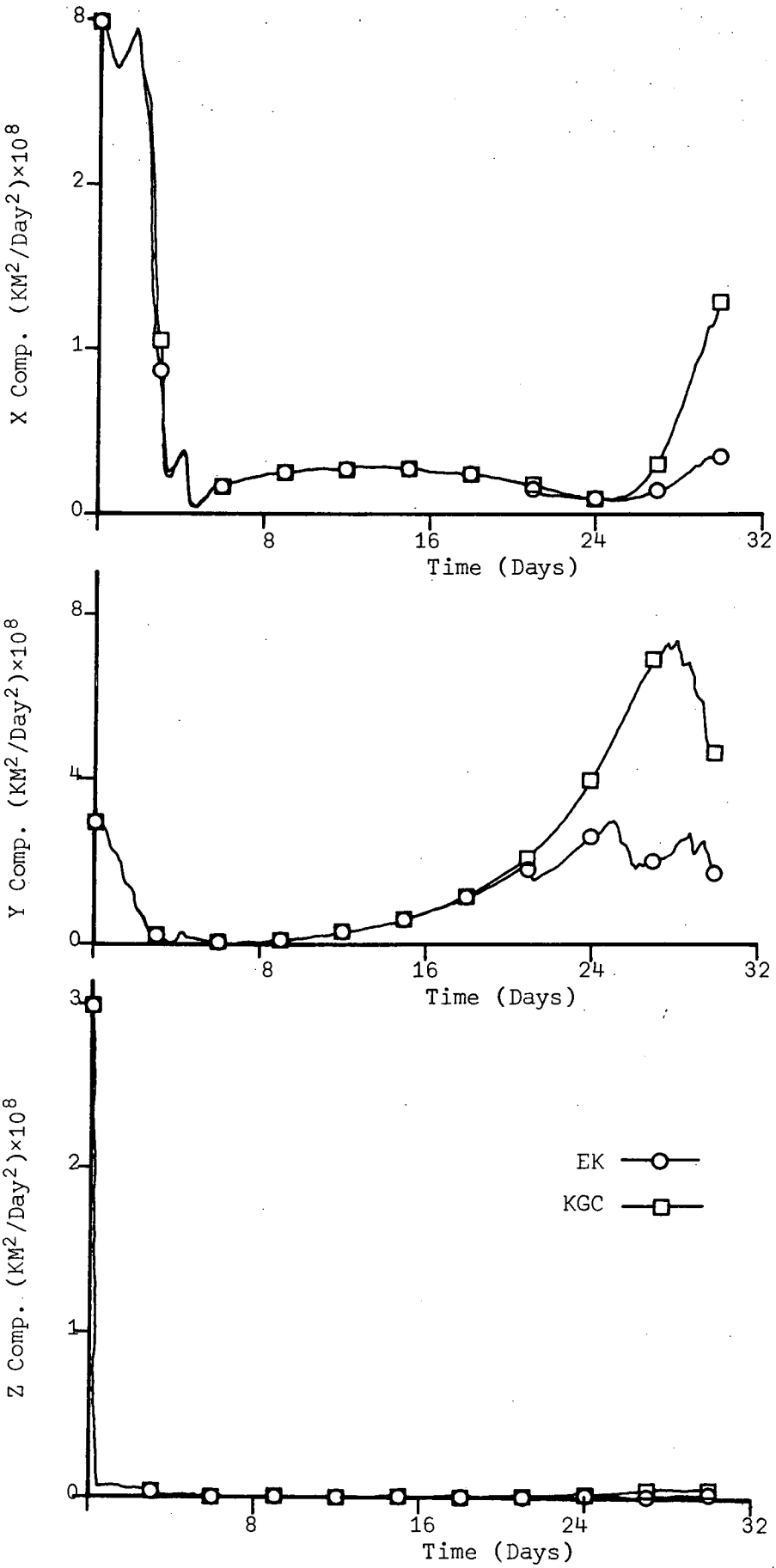

Figure 22-d. Conditional Variances of Velocity Estimation Errors for the Simulation 15

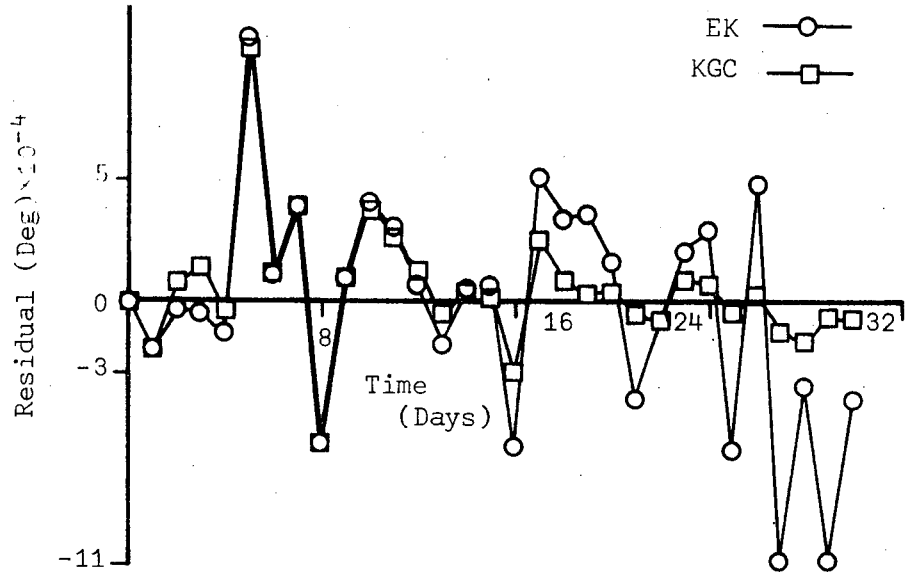

Figure 22-e. Observation Residual for the Simulation 15

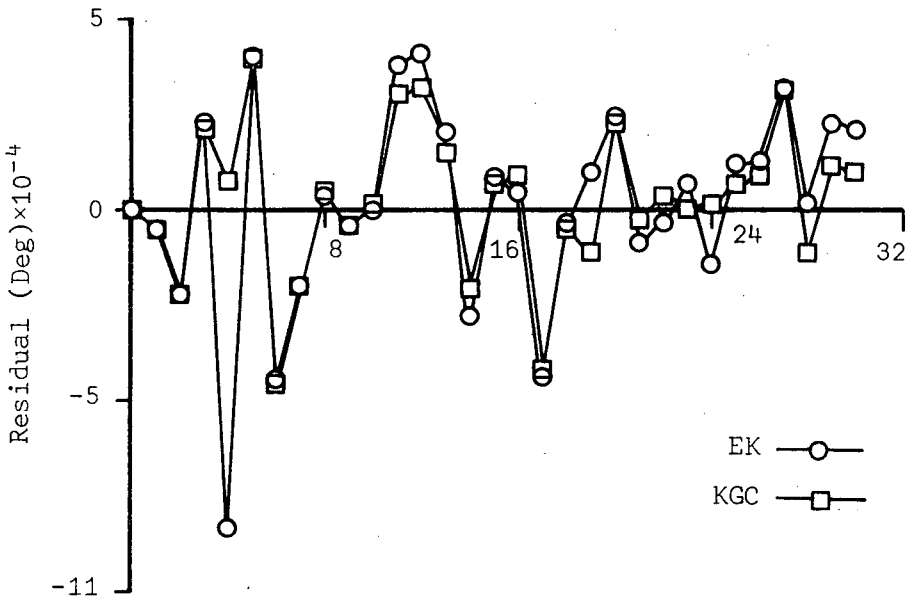

Figure 23-a. Observation Residual for the Simulation 16

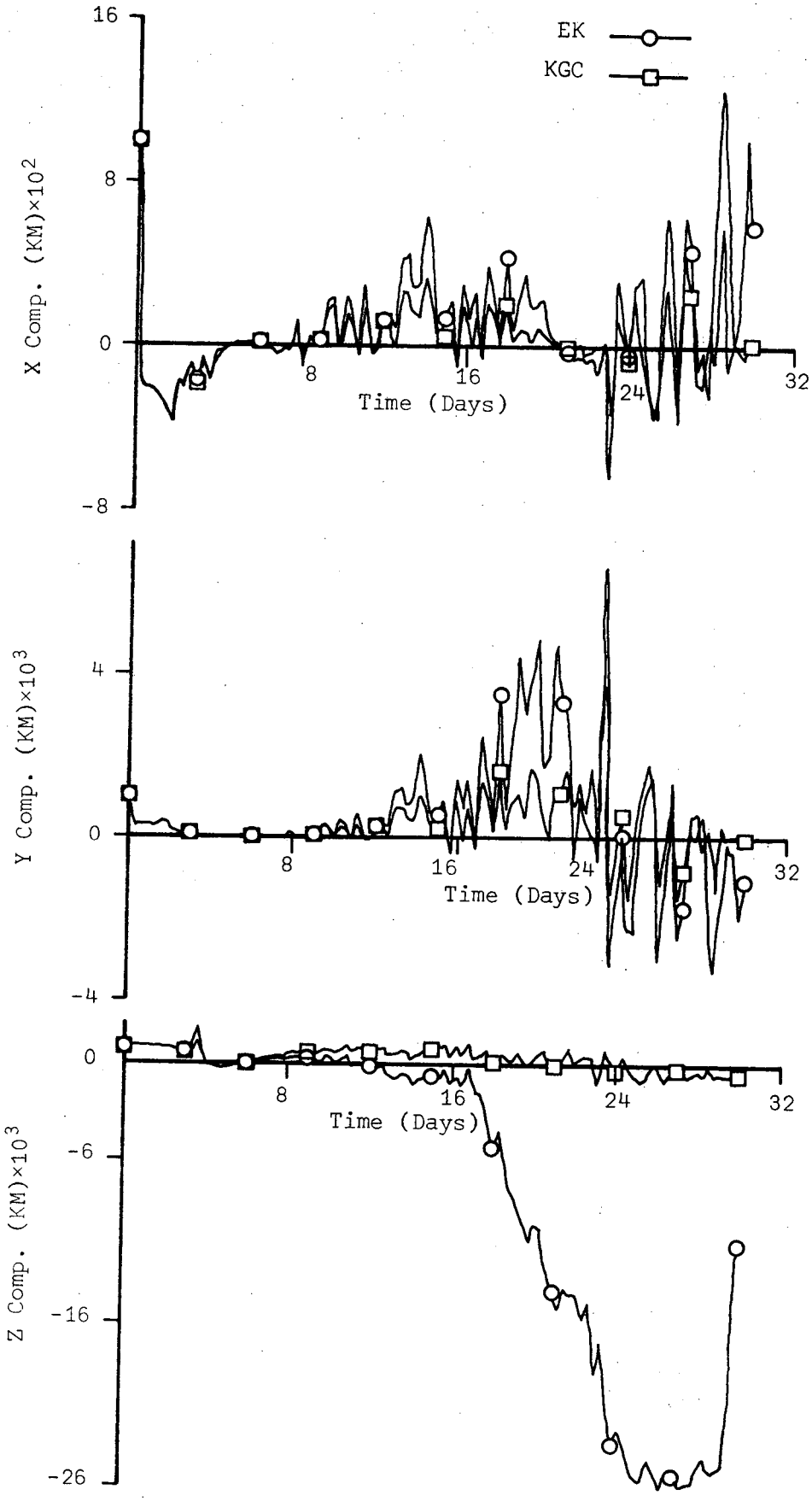

Figure 23-b. Position Estimation Errors for the Simulation 16

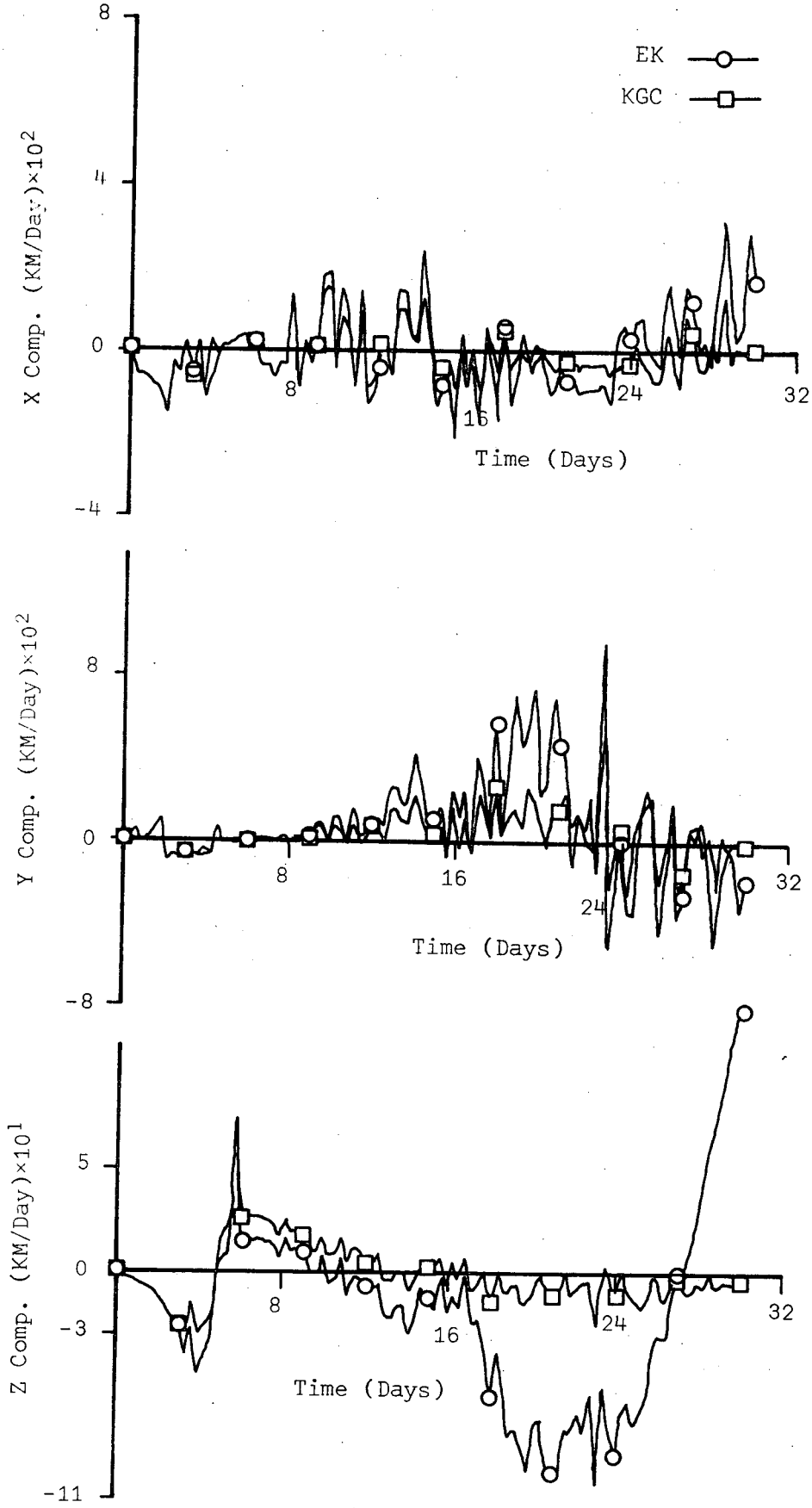

Figure 23-c. Velocity Estimation Errors for the Simulation 16

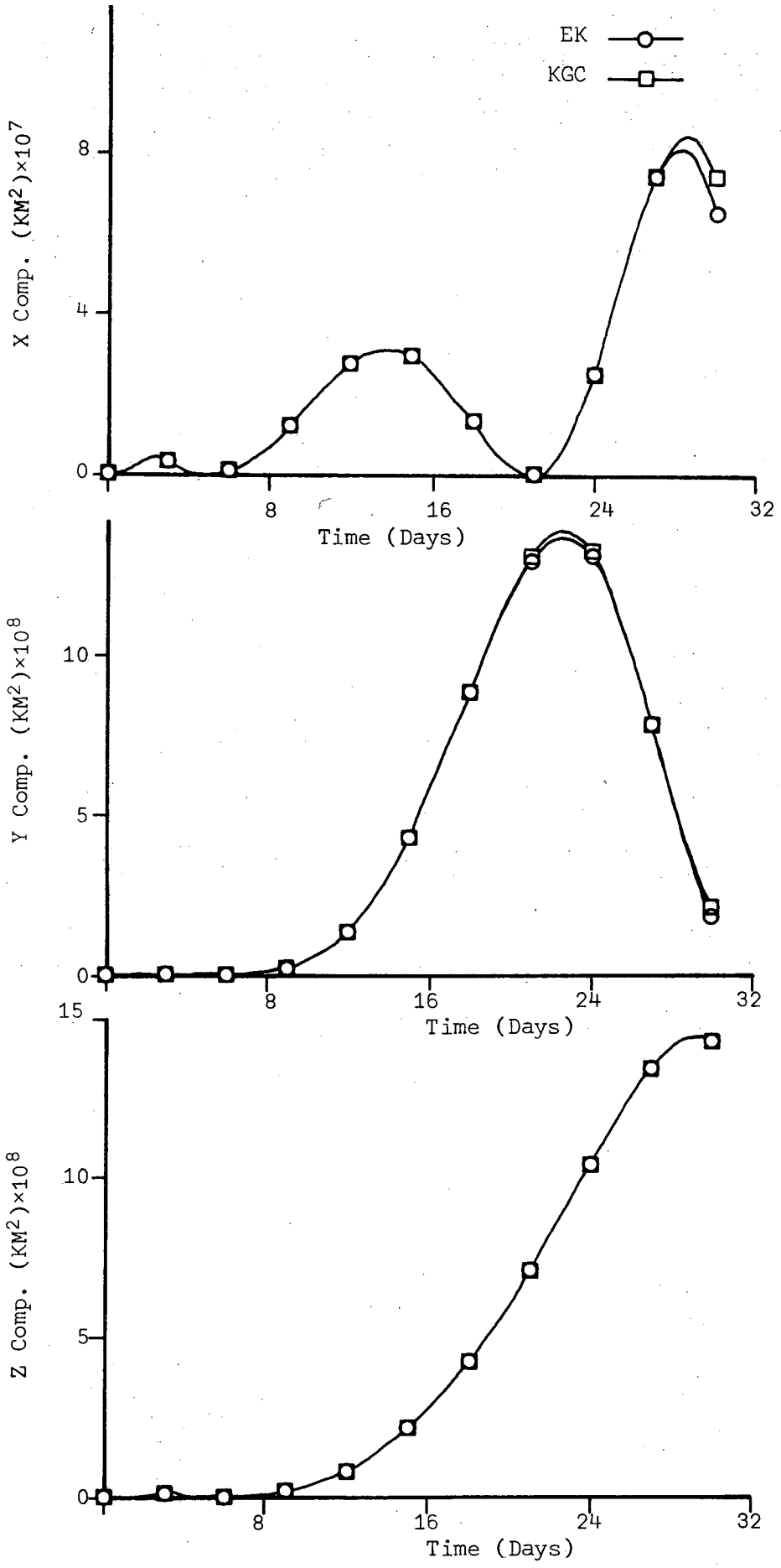

Figure 23-d. Conditional Variances of Position Estimation Errors for the Simulation 16

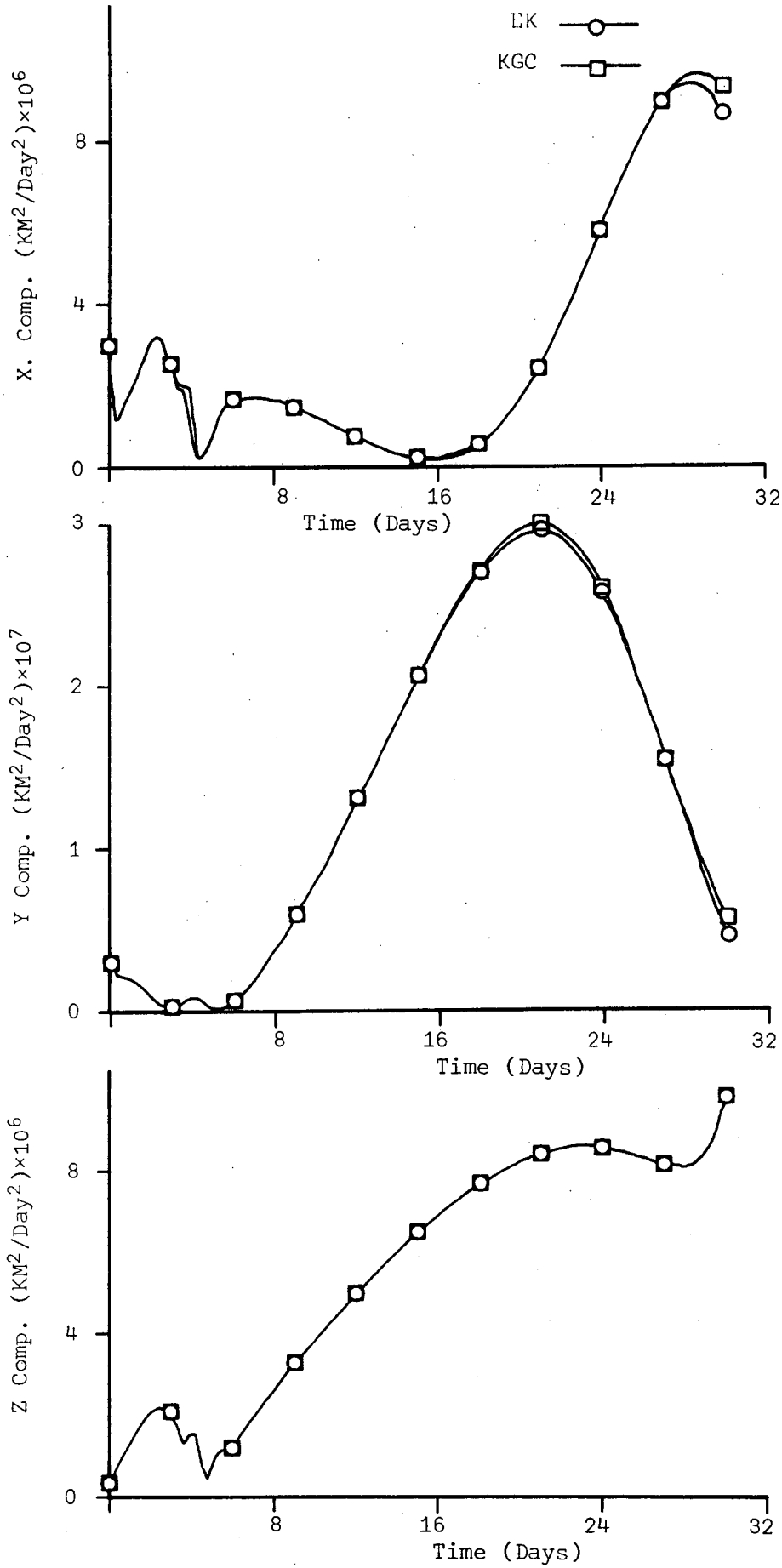

Figure 23-e. Conditional Variances of Velocity Estimation Errors for the Simulation 16

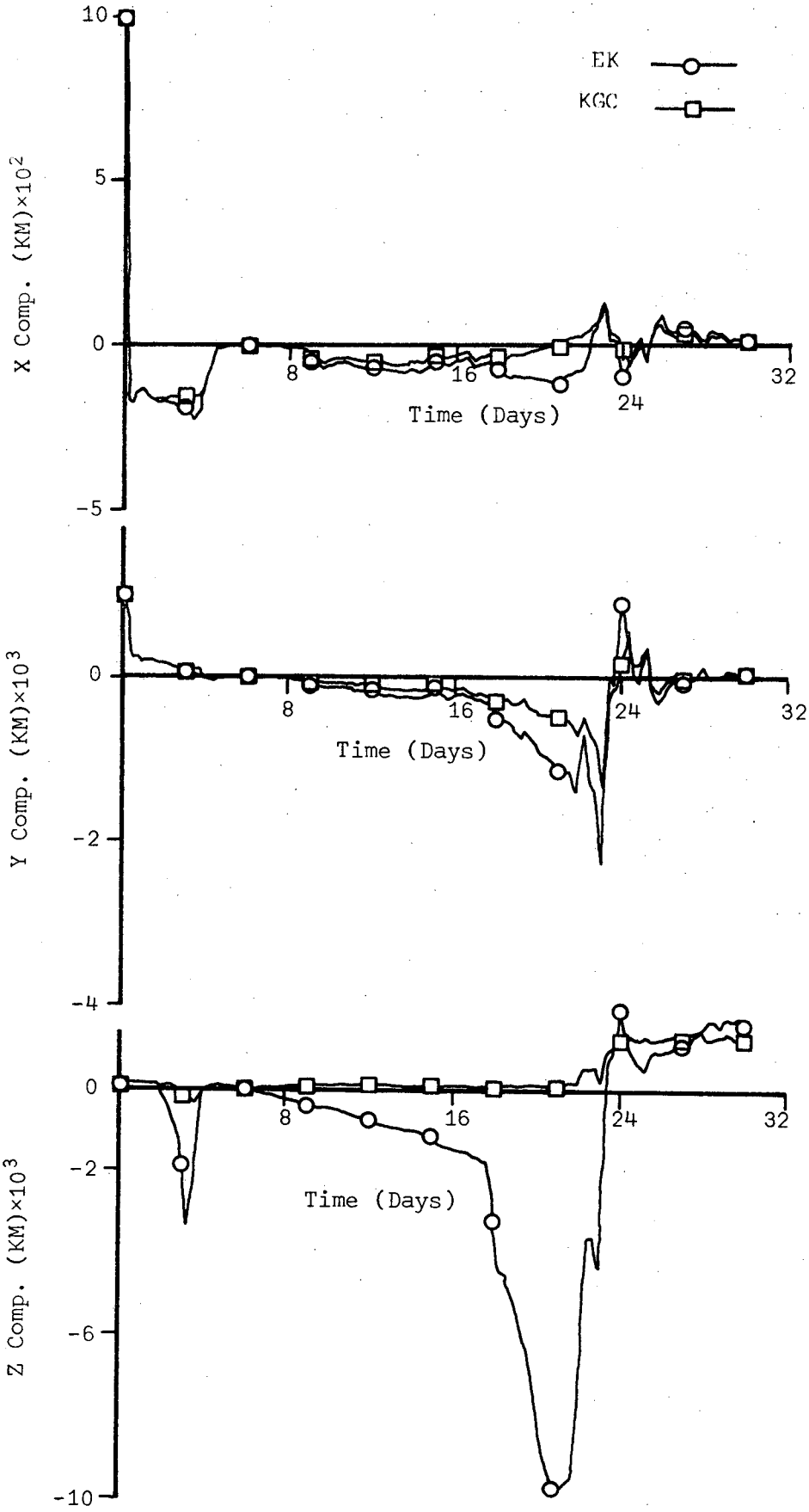

Figure 24-a. Position Estimation Errors for the Simulation 17

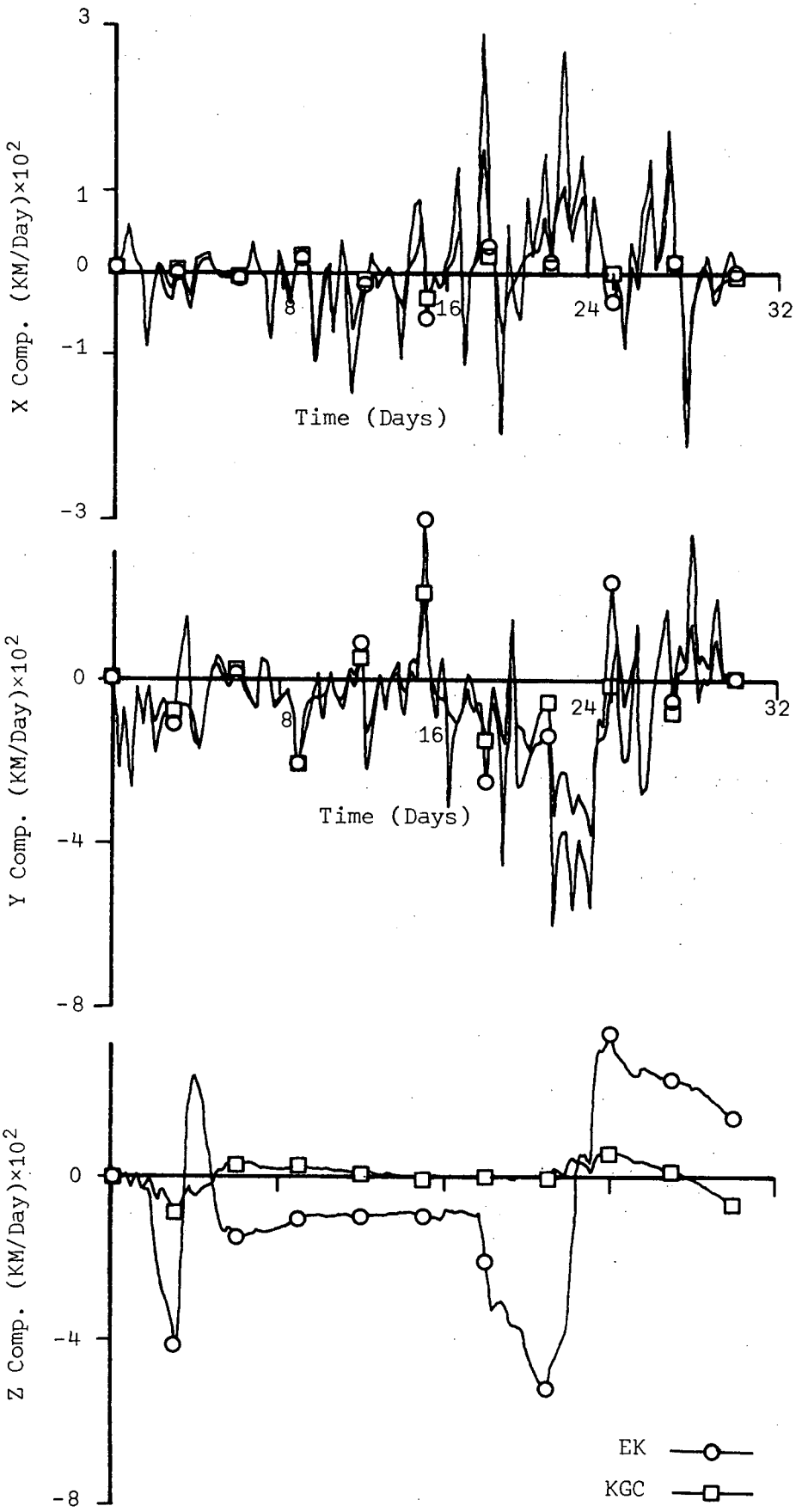

Figure 24-b. Velocity Estimation Errors for the Simulation 17

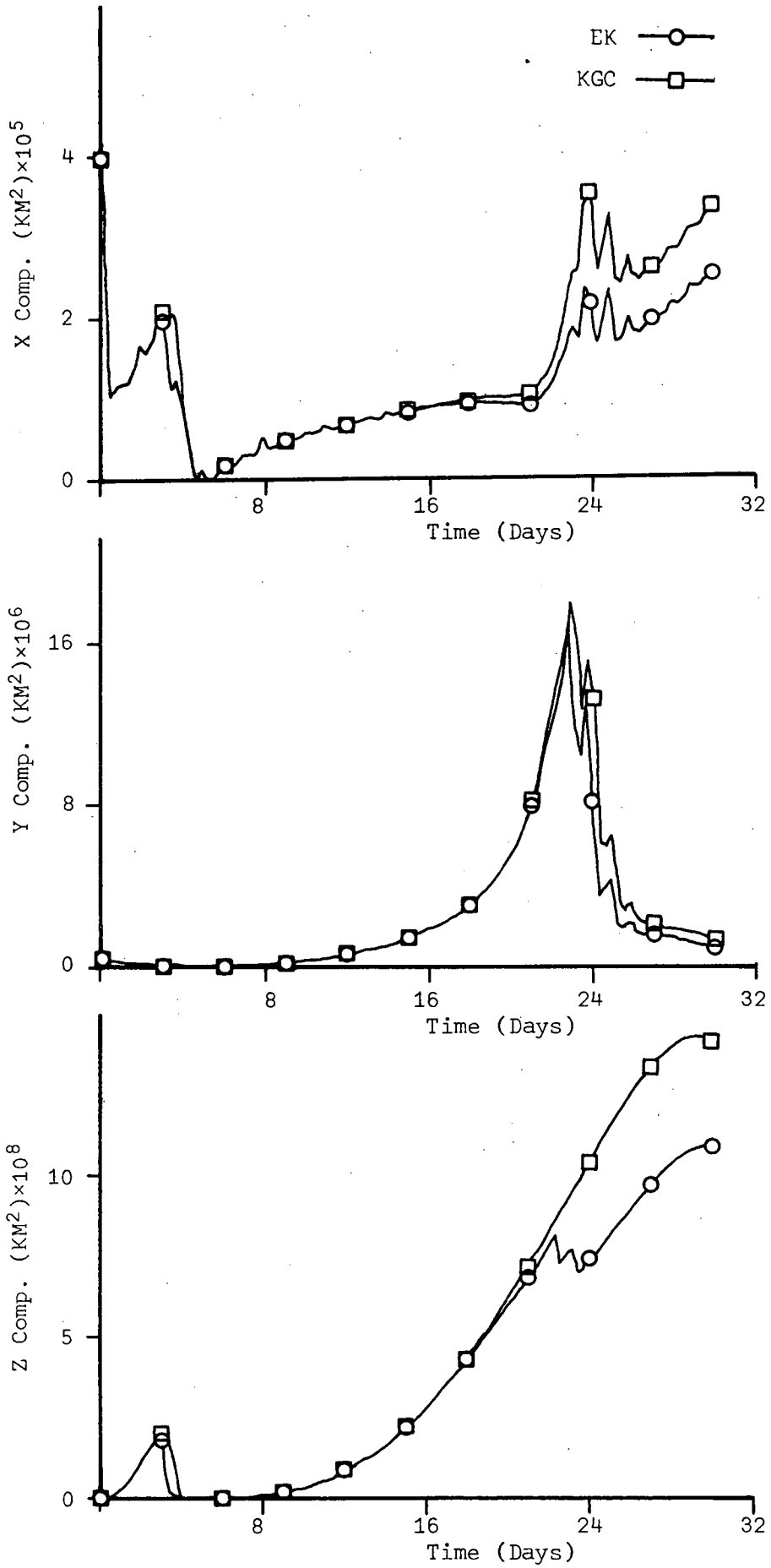

Figure 24-c. Conditional Variances of Position Estimation Errors for the Simulation 17

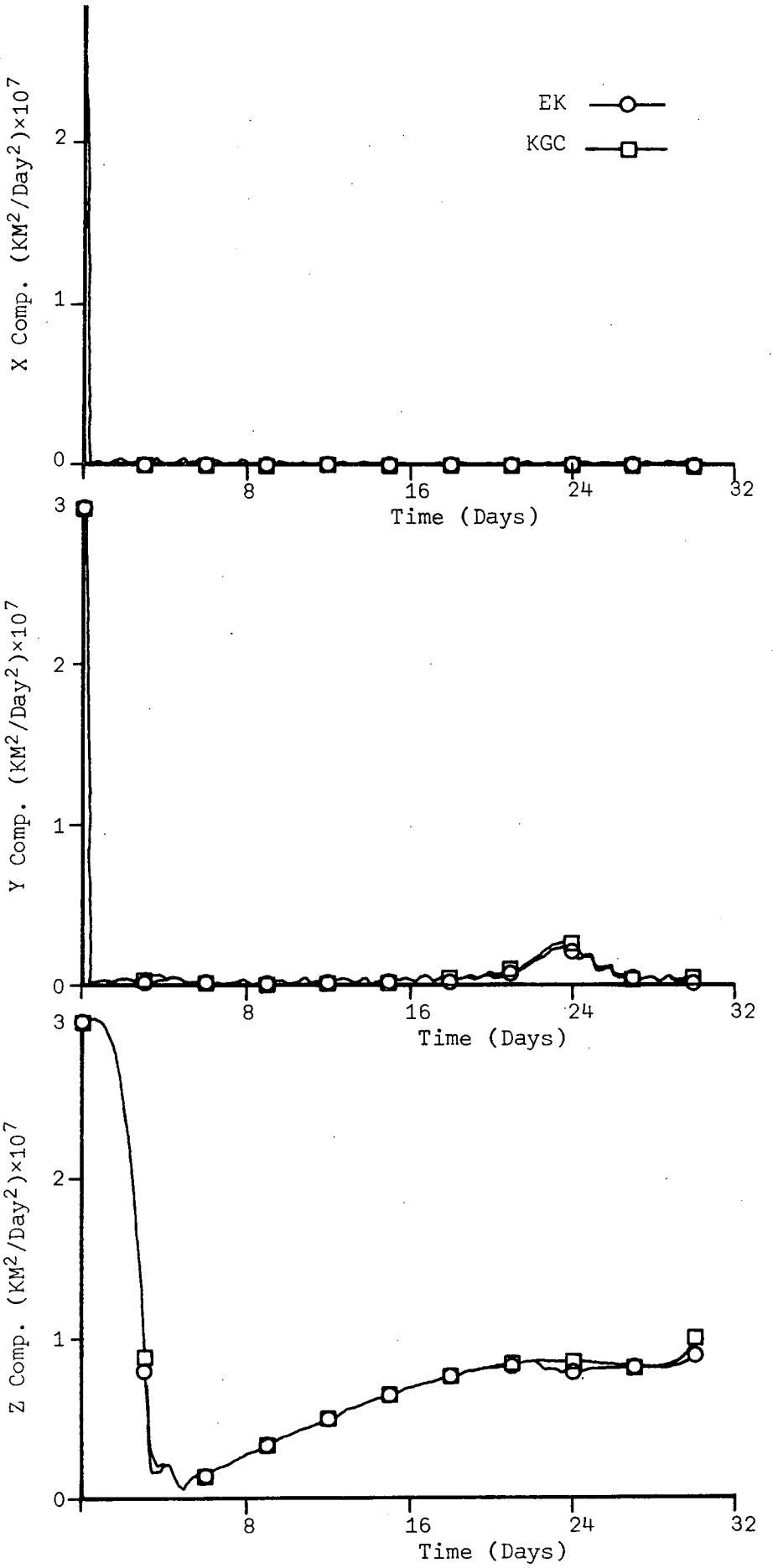

Figure 24-d. Conditional Variances of Velocity Estimation Errors for the Simulation 17

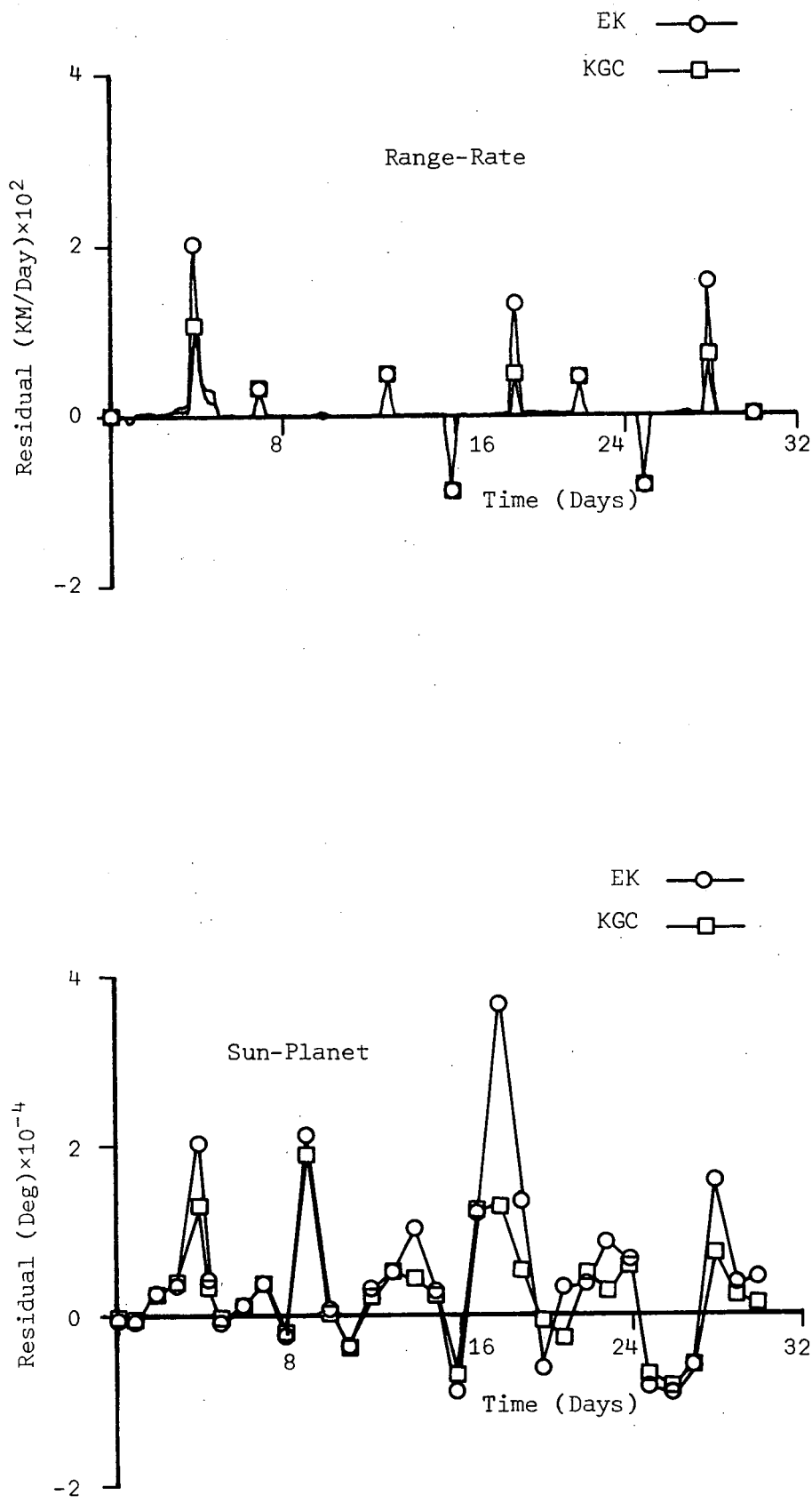

Figure 24-e. Observation Residuals for the Simulation 17

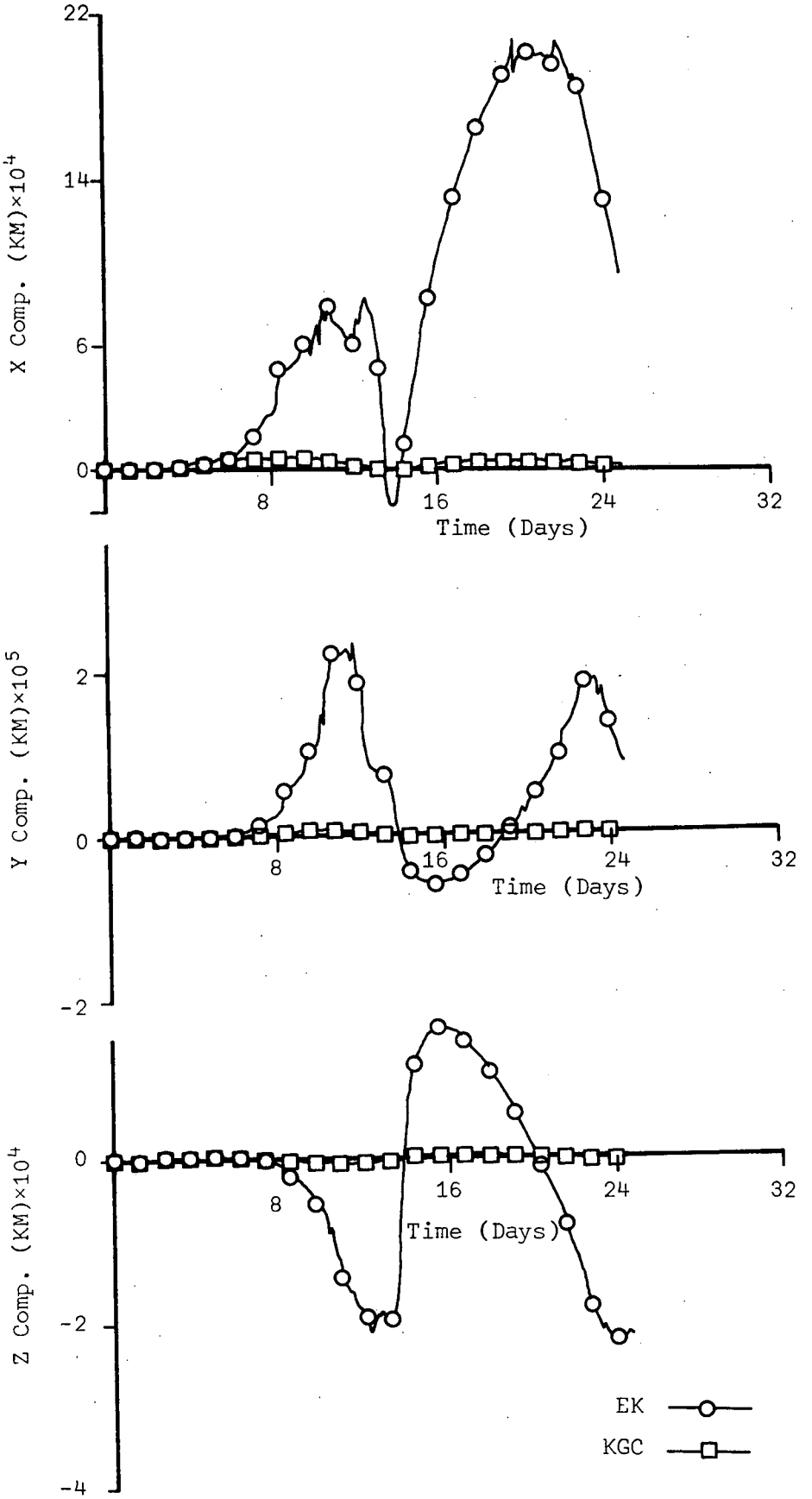

Figure 25-a. Position Estimation Errors for the Simulation 18

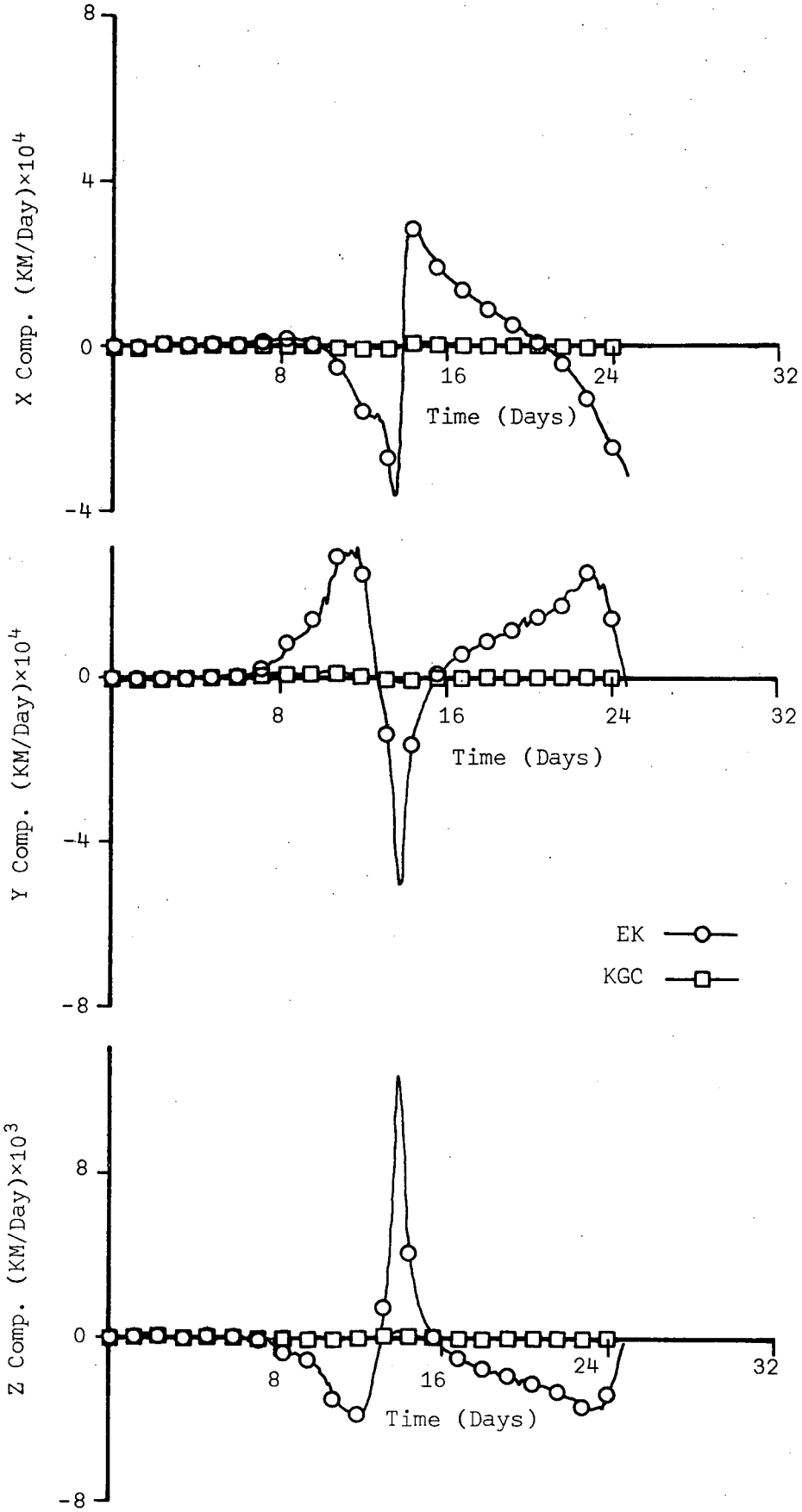

Figure 25-b. Velocity Estimation Error for the Simulation 18

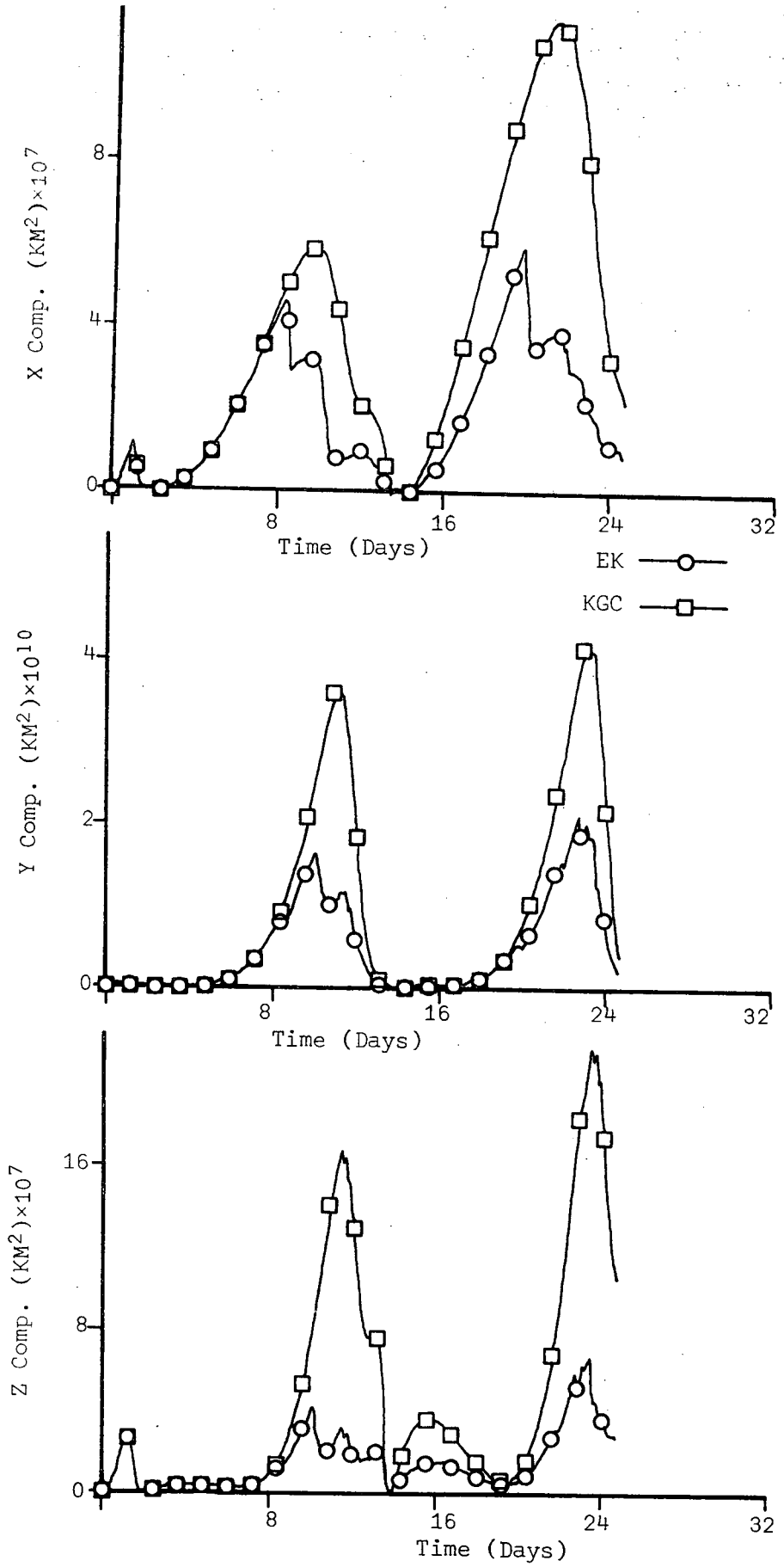

Figure 25-c. Conditional Variances of Position Estimation Errors for the Simulation 18

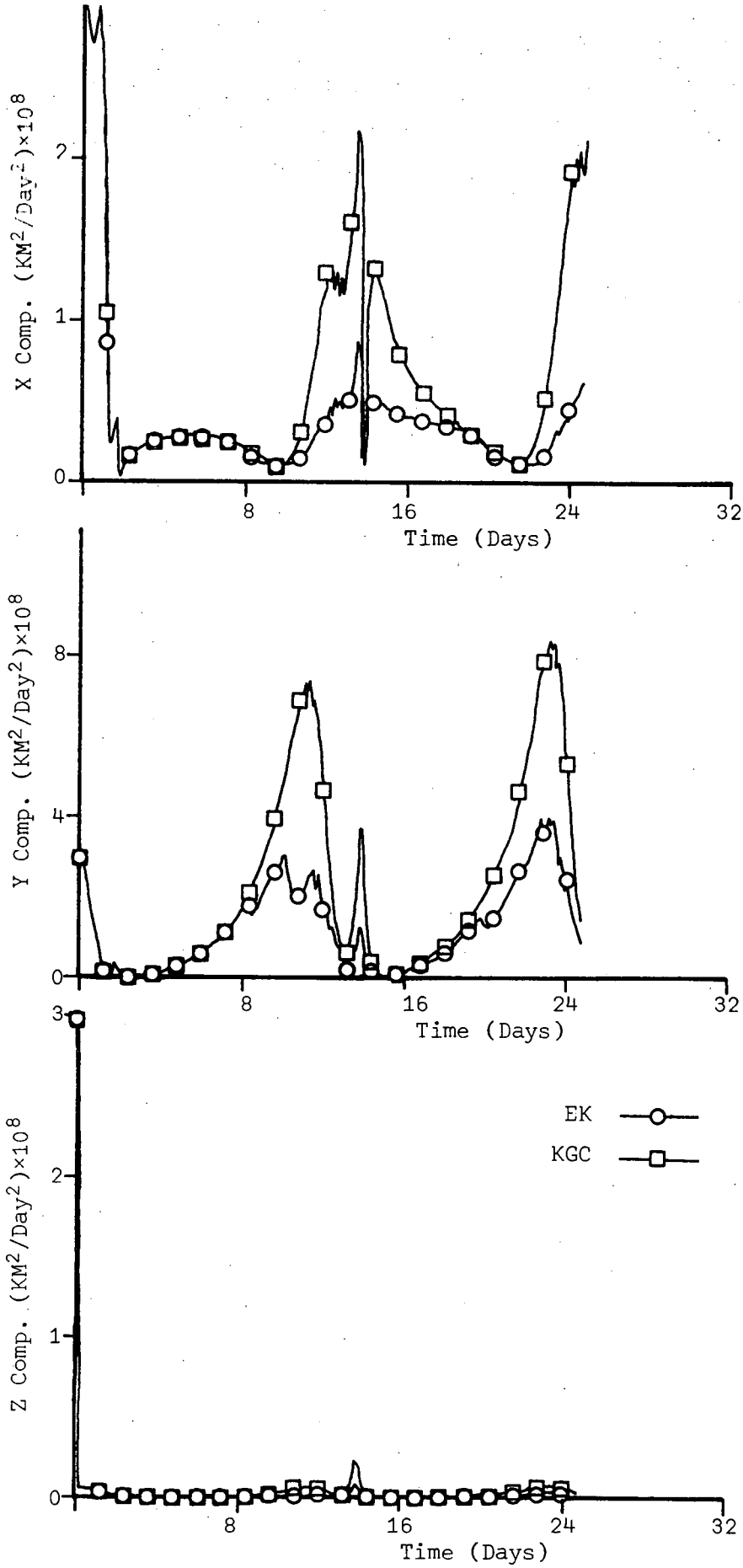

Figure 25-d. Conditional Variances of Velocity Estimation Errors for the Simulation 18

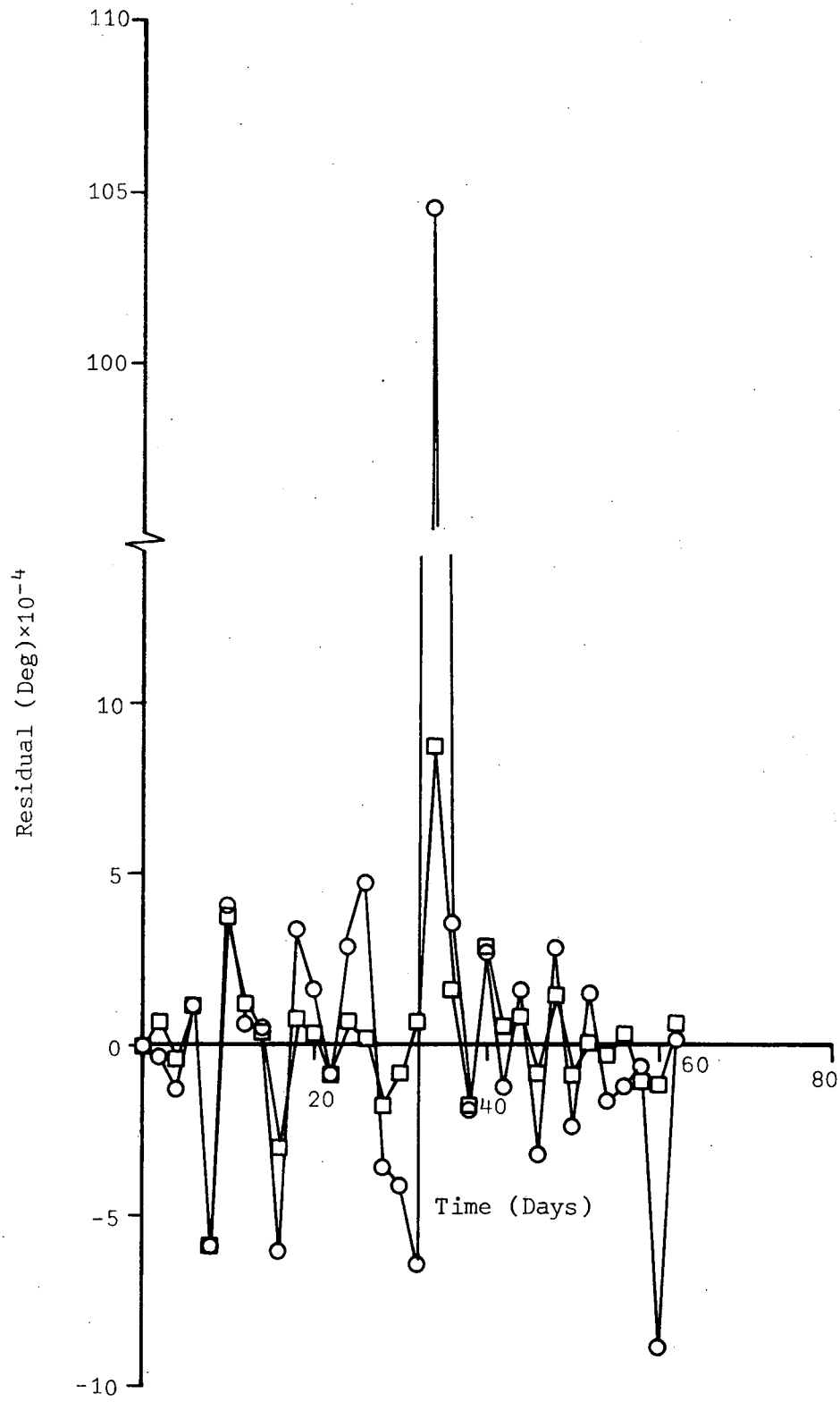

Figure 25-e. Observation Residual for the Simulation 18

CHAPTER 5

CONCLUSIONS AND RECOMMENDATIONS

5.1 Summary

In the investigation described in the previous discussion, a comparative study has been made of nonlinear estimation algorithms and their application to the orbit determination problem for interplanetary spacecraft. By using the properties of a Martingale series and Loeve's smoothing properties, a second order nonlinear estimation algorithm is derived. The algorithm is shown to be of the Gaussian second-order class as distinguished from the truncated second-order class. Both classes of second order filters retain a second order term in the state dynamics, the observation state relation and in the optimal weighting matrix (Kalman gain), respectively. The merits of each of the algorithms as well as the influence of each second order term is evaluated by a numerical simulation of the orbit determination for a Jupiter fly-by and Jupiter orbiter missions.

5.2 Conclusions

Based on the results of extensive numerical simulations on the Jupiter fly-by and Jupiter orbiter missions, the following conclusions can be drawn for the class of problems considered here:

1. The system dynamic influences the performance of the EK Filter through

   i) initial conditions

   ii) conditional covariance matrices

   iii) predicted observations

The effect of the initial conditions is considered to effect the system dynamics directly, in contrast to the effects of the other two factors, which are regarded as an indirect effect on the performance of the filter. It is concluded that the indirect effects of the system dynamics are more severe than the direct effects, especially when the system dynamics are highly nonlinear.

2. The effect of the dynamic second order (DSO) term cannot be isolated. If the conditional variances are large, which means that the extended Kalman Filter does not perform adequately, the effect of DSO term is very severe and causes the second order filters (MGSO and MTSO) to diverge, in a situation when the EK Filter performs reasonably well. In contrast, the small conditional variances, which imply that the EK Filter works very well, do not reveal any differences between the second order filters (MGSO and MTSO) and the EK Filter. As a matter of fact, there is no reason for using a second order filter if the conditional variances are small and the EK Filter performs adequately. By including the dynamic second order (DSO) term, approximately 30% more computer time is required than that required by the EK Filter. Furthermore, any filter including the DSO term is very sensitive to the initial covariance matrix, if a dynamic nonlinearity is significant at the beginning. It is interesting to note that Athans et al. (27), based on a different example problem, concluded that the DSO term is the major factor in improving the performance of the MGSO Filter. Hence, the conclusions reached in this investigation regarding the DSO term should be regarded as problem dependent.

3. The observation nonlinearity depends on the type of observations and the dynamic nonlinearity. The range and range-rate observation in the Jupiter fly-by problem are regarded as relatively linear observations.

Like the DSO term, the effect of the observation second order (OSO) term cannot be determined for all problems. The same conclusions as those reached for the DSO term can be stated for the OSO term. But the effect of the OSO term is not as severe as the effect of the DSO term for the MGSO Filter.

4. The Kalman Gain Compensated (KGC) Filter appears to give a quite acceptable behavior based on the following observations:

i) In the region where dynamic nonlinearity is not significant, the KGC Filter acts like the extended Kalman filter.

ii) In the region where dynamic nonlinearity is very severe and, consequently, the observation residuals are large, the KGC Filter down weights the large observation residuals.

iii) The effect of the KGC Filter becomes more significant when the observation noise R is small and the state noise Q is large. This fact implies that the KGC Filter is more desirable when the observations are measured accurately and when the dynamic noise is large or equivalently when the dynamic process is poorly modeled.

iv) The KGC Filter is very stable and insensitive to the dynamic nonlinearity as compared with the EK Filter.

v) The KGC Filter maintains an accurate estimate for the highly nonlinear type of observations while acting like the extended Kalman Filter for the relatively linear type of observations.

vi) In contrast to any other second order filter, implementation of the KGC Filter is as feasible for complex problems as the extended Kalman Filter is.

5. If no state noise is assumed, the EK Filter works adequately

and the differences between the two filters (EK and KGC) are negligible. The absence of state noise implies that the conditional variances cannot be too large.

7. For the Jupiter fly-by, the extended Kalman Filter determines an adequate estimate up to a period of encounter minus three days. However, the estimate diverges around encounter, when the dynamic state noise is included while the KGC Filter yields accurate estimates.

8. For the Jupiter orbiter, the estimate of the extended Kalman Filter drifts away gradually from the true trajectory and diverges at the second revolution, when the dynamic state noise is included while the KGC Filter yields an accurate estimate.

5.3 Recommendations for Future Study

The research reported here is an indication of a successful application of an approximate nonlinear filter and indicates the possibility that the Kalman Gain Compensated Filter can be applied to other problems. The following studies are recommended:

1. Application of the KGC Filter to the orbit determination problems associated with re-entry, near-Earth and lunar satellites, Mariner and Viking missions, should be carried out. In particular, application of the KGC Filter to the re-entry and ascent phases of the shuttle navigation problem is recommended.

2. The applicability of the square root covariance and the consider filter versions of the Kalman Gain Compensated Filter should be developed.

3. An extended study of nonlinear estimation algorithms and their applicability to the orbit determination problems should be made. The comparative study should be made in the frame-work of the applicability of the

methods to anticipated orbit determination problems. In the study, particular attention should be given to those data types which undergo significant geometrical changes during a mission. The objective of such a study would be to define particular missions and data types for which nonlinear orbit determination algorithms will yield a significant improvement over the estimate obtained with the extended Kalman Filter.

4. Further study of the effects of the dynamic second order (DSO) term and the observation second order (OSO) term should be made.

5. An extensive study of the Gaussian second order filter and the truncated second order filter should be made in the direction of determining the characteristics of the random forcing term in the covariance equation.

APPENDIX A

THE PARTIAL DERIVATIVES

The first order partial derivatives f_x and h_x and the second order partial derivatives f_{xx} and h_{xx} which appear in the nonlinear estimation algorithm are defined in this appendix.

From Eq. (3.5), the (9×9) matrix f_x can be partitioned as follows:

$$f_x = \left[\begin{array}{c|c|c} \phi & I & \phi \\ \hline A_{21} & \phi & A_{23} \\ \hline \phi & \phi & \phi \end{array}\right]$$

where ϕ is the 3×3 null matrix and I is the 3×3 identity. The symmetric submatrices A_{21} and A_{23} are defined as follows:

$$A_{21} = \begin{bmatrix} F_{41} & F_{42} & F_{43} \\ F_{51} & F_{52} & F_{53} \\ F_{61} & F_{62} & F_{63} \end{bmatrix} \qquad A_{23} = \begin{bmatrix} F_{47} & F_{48} & F_{49} \\ F_{57} & F_{58} & F_{59} \\ F_{67} & F_{68} & F_{69} \end{bmatrix}$$

where

$$F_{41} = \frac{\partial f_4}{\partial X} = \mu\left[\frac{3X^2}{r^5} - \frac{1}{r^3}\right] + \mu_s\left[\frac{3X_p^2}{r_p^5} - \frac{1}{r_p^3}\right]$$

$$F_{42} = \frac{\partial f_4}{\partial Y} = \mu\left[\frac{3XY}{r^5}\right] + \mu_s\left[\frac{3X_pY_p}{r_p^5}\right]$$

$$F_{43} = \frac{\partial f_4}{\partial Z} = \mu\left[\frac{3XZ}{r^5}\right] + \mu_s\left[\frac{3X_pZ_p}{r_p^5}\right]$$

$$F_{51} = \frac{\partial f_5}{\partial X} = F_{42}$$

$$F_{52} = \frac{\partial f_5}{\partial Y} = \mu\left[\frac{3Y^2}{r^5} - \frac{1}{r^3}\right] + \mu_s\left[\frac{3Y_p^2}{r_p^5} - \frac{1}{r_p^3}\right]$$

$$F_{53} = \frac{\partial f_5}{\partial Z} = \mu\left[\frac{3YZ}{r^5}\right] + \mu_s\left[\frac{3Y_p Z_p}{r_p^5}\right]$$

$$F_{61} = \frac{\partial f_6}{\partial X} = F_{43}$$

$$F_{62} = \frac{\partial f_6}{\partial Y} = F_{53}$$

$$F_{63} = \frac{\partial f_6}{\partial Z} = \mu\left[\frac{3Z^2}{r^5} - \frac{1}{r^3}\right] + \mu_s\left[\frac{3Z_p^2}{r_p^5} - \frac{1}{r_p^3}\right]$$

$$F_{47} = \frac{\partial f_4}{\partial b_x} = \mu_s\left[\frac{3X_p^2}{r_p^5} - \frac{3X_t^2}{r_t^5} - \frac{1}{r_p^3} - \frac{1}{r_t^3}\right]$$

$$F_{48} = \frac{\partial f_4}{\partial b_y} = \mu_s\left[\frac{3X_p Y_p}{r_p^5} - \frac{3X_t Y_t}{r_t^5}\right]$$

$$F_{49} = \frac{\partial f_4}{\partial b_z} = \mu_s\left[\frac{3X_p Z_p}{r_p^5} - \frac{3X_t Z_t}{r_t^5}\right]$$

$$F_{57} = \frac{\partial f_5}{\partial b_x} = F_{48}$$

$$F_{58} = \frac{\partial f_5}{\partial b_y} = \mu_s\left[\frac{3Y_p^2}{r_p^5} - \frac{3Y_t^2}{r_t^5} - \frac{1}{r_p^3} + \frac{1}{r_t^3}\right]$$

$$F_{59} = \frac{\partial f_5}{\partial b_z} = \mu_s\left[\frac{3Y_p Z_p}{r_p^5} - \frac{3Y_t Z_t}{r_t^5}\right]$$

$$F_{67} = \frac{\partial f_6}{\partial b_x} = F_{49}$$

$$F_{68} = \frac{\partial f_6}{\partial b_y} = F_{59}$$

$$F_{69} = \frac{\partial f_6}{\partial b_z} = \mu_s\left[\frac{3Z_p^2}{r_p^5} - \frac{3Z_t^2}{r_t^5} - \frac{1}{r_p^3} + \frac{1}{r_t^3}\right]$$

where $r = \sqrt{X^2 + Y^2 + Z^2}$, $r_p = \sqrt{X_p^2 + Y_p^2 + Z_p^2}$ and $r_t = \sqrt{X_t^2 + Y_t^2 + Z_t^2}$

The first order partial derivative matrix h_x is defined as follows:

$$h_x = \begin{bmatrix} H_{11} & H_{12} & \cdots & H_{19} \\ H_{21} & H_{22} & \cdots & H_{29} \\ H_{31} & H_{32} & \cdots & H_{39} \\ H_{41} & H_{42} & \cdots & H_{49} \end{bmatrix}$$

where

$$H_{11} = \frac{\partial \rho}{\partial X} = (X_p - X_s)/\rho$$

$$H_{12} = \frac{\partial \rho}{\partial Y} = (Y_p - Y_s)/\rho$$

$$H_{13} = \frac{\partial \rho}{\partial Z} = (Z_p - Z_s)/\rho$$

$$H_{14} = \frac{\partial \rho}{\partial U} = 0$$

$$H_{15} = \frac{\partial \rho}{\partial V} = 0$$

$$H_{16} = \frac{\partial \rho}{\partial W} = 0$$

$$H_{17} = \frac{\partial \rho}{\partial b_x} = h_{11}$$

$$H_{18} = \frac{\partial \rho}{\partial b_y} = h_{12}$$

$$H_{19} = \frac{\partial \rho}{\partial b_x} = h_{13}$$

$$H_{21} = \frac{\partial \dot{\rho}}{\partial X} = [(\dot{X}_p - \dot{X}_s) - (X_p - X_s)(\dot{\rho}/\rho)]/\rho$$

$$H_{22} = \frac{\partial \dot{\rho}}{\partial X} = [(\dot{Y}_p - \dot{Y}_s) - (Y_p - Y_s)(\dot{\rho}/\rho)]/\rho$$

$$H_{23} = \frac{\partial \dot{\rho}}{\partial Z} = [(\dot{Z}_p - \dot{Z}_s) - (Z_p - Z_s)(\dot{\rho}/\rho)]/\rho$$

$$H_{24} = \frac{\partial \dot{\rho}}{\partial U} = h_{11}$$

$$H_{25} = \frac{\partial \dot{\rho}}{\partial V} = h_{12}$$

$$H_{26} = \frac{\partial \dot{\rho}}{\partial W} = h_{13}$$

$$H_{27} = \frac{\partial \dot{\rho}}{\partial b_x} = h_{21}$$

$$H_{28} = \frac{\partial \dot{\rho}}{\partial b_y} = h_{22}$$

$$H_{29} = \frac{\partial \dot{\rho}}{\partial b_z} = h_{23}$$

$$H_{31} = \frac{\partial \alpha}{\partial X} = \left[\cos\alpha \left[\frac{X}{r^2} + \frac{X_p}{r_p^2}\right] - \frac{(X + X_p)}{rr_p}\right] \frac{1}{\sin\alpha}$$

$$H_{32} = \frac{\partial \alpha}{\partial Y} = \left[\cos\alpha \left[\frac{Y}{r^2} + \frac{Y_p}{r_p^2}\right] - \frac{(Y + Y_p)}{rr_p}\right] \frac{1}{\sin\alpha}$$

$$H_{33} = \frac{\partial \alpha}{\partial Z} = \left[\cos\alpha \left[\frac{Z}{r^2} + \frac{Z_p}{r_p^2}\right] - \frac{(Z + Z_p)}{rr_p}\right] \frac{1}{\sin\alpha}$$

$$H_{34} = \frac{\partial \alpha}{\partial U} = 0 \qquad H_{35} = \frac{\partial \alpha}{\partial V} = 0 \qquad H_{36} = \frac{\partial \alpha}{\partial W} = 0$$

$$H_{37} = \frac{\partial \alpha}{\partial b_x} = \left[\cos\alpha \frac{X_p}{r_p^2} - \frac{X}{rr_p}\right] \frac{1}{\sin\alpha}$$

$$H_{38} = \frac{\partial \alpha}{\partial b_y} = \left[\cos\alpha \frac{Y_p}{r_p^2} - \frac{Y}{rr_p}\right] \frac{1}{\sin\alpha}$$

$$H_{39} = \frac{\partial \alpha}{\partial b_z} = \left[\cos \alpha \frac{Z_p}{r_p^2} - \frac{Z}{r r_p}\right] \frac{1}{\sin \alpha}$$

$$H_{41} = \frac{\partial \beta}{\partial X} = \left[S_x + \frac{X \cos \beta}{r}\right] \frac{1}{r \sin \beta}$$

$$H_{42} = \frac{\partial \beta}{\partial Y} = \left[S_y + \frac{Y \cos \beta}{r}\right] \frac{1}{r \sin \beta}$$

$$H_{43} = \frac{\partial \beta}{\partial Z} = \left[S_z + \frac{Z \cos \beta}{r}\right] \frac{1}{r \sin \beta}$$

$$H_{44} = \frac{\partial \beta}{\partial U} = 0 \quad , \quad H_{45} = \frac{\partial \beta}{\partial V} = 0 \quad , \quad H_{46} = \frac{\partial \beta}{\partial W} = 0$$

$$H_{47} = \frac{\partial \beta}{\partial b_x} = 0 \quad , \quad H_{48} = \frac{\partial \beta}{\partial b_y} = 0 \quad , \quad H_{49} = \frac{\partial \beta}{\partial b_z} = 0$$

The second order partial derivatives f_{xx} are defined as a (9×9×9) three-dimensional array and each layer is defined as a symmetric (9×9) matrix. The three-dimensional array can be pictured as shown in Fig. 26.

Each layer is further partitioned into (3×3) matrices and they are as follows:

$$F^i = \begin{bmatrix} F^i_{11} & \phi & F^i_{13} \\ \phi & \phi & \phi \\ F^{iT}_{13} & \phi & F^i_{33} \end{bmatrix} \qquad i = 4,5,6$$

$$F^i = \begin{bmatrix} \phi & \phi & \phi \\ \phi & \phi & \phi \\ \phi & \phi & \phi \end{bmatrix} \qquad i = 1,2,3,7,8,9$$

where ϕ is a (3×3) matrix with identically zero elements. The submatrices F^i_{11}, F^i_{13}, and F^i_{33} are redefined as follows:

$$F^i_{11} = \begin{bmatrix} F_{i11} & F_{i12} & F_{i13} \\ F_{i12} & F_{i22} & F_{i23} \\ F_{i13} & F_{i23} & F_{i33} \end{bmatrix} \qquad F^i_{13} = \begin{bmatrix} F_{i17} & F_{i18} & F_{i19} \\ F_{i27} & F_{i28} & F_{i29} \\ F_{i37} & F_{i38} & F_{i39} \end{bmatrix}$$

$$F^i_{33} = \begin{bmatrix} F_{i77} & F_{i78} & F_{i79} \\ F_{i78} & F_{i88} & F_{i89} \\ F_{i79} & F_{i89} & F_{i99} \end{bmatrix} \qquad i = 4,5,6$$

where

$$F_{411} = \frac{\partial^2 f_4}{\partial X \partial X} = \mu\left[-15\,\frac{X^2 X}{r^7} + 3\,\frac{2X}{r^5}\right] + \mu_s\left[-15\,\frac{X^2_p X_p}{r^7_p} + 3\,\frac{2X_p}{r^5_p}\right] + \mu\left[3\,\frac{X}{r^5}\right] + \mu_s\left[3\,\frac{X_p}{r^5_p}\right]$$

$$F_{412} = \frac{\partial^2 f_4}{\partial X \partial Y} = \mu\left[-15\,\frac{X^2 Y}{r^7} + 3\,\frac{Y}{r^5}\right] + \mu_s\left[-15\,\frac{X^2_p Y_p}{r^7_p} + 3\,\frac{Y_p}{r^5_p}\right]$$

$$F_{413} = \frac{\partial^2 f_4}{\partial X \partial Z} = \mu\left[-15\,\frac{X^2 Z}{r^7} + 3\,\frac{Z}{r^5}\right] + \mu_s\left[-15\,\frac{X^2_p Z_p}{r^7_p} + 3\,\frac{Z_p}{r^5_p}\right]$$

$$F_{417} = \frac{\partial^2 f_4}{\partial X \partial b_x} = \mu_s\left[-15\,\frac{X^2_p X_p}{r^7_p} + 3\,\frac{2X_p}{r^5_p}\right] + \mu_s\left[3\,\frac{X_p}{r^5_p}\right]$$

$$F_{418} = \frac{\partial^2 f_4}{\partial X \partial b_y} = \mu_s\left[-15\,\frac{X^2_p Y_p}{r^7_p}\right] + \mu_s\left[3\,\frac{Y_p}{r^5_p}\right]$$

$$F_{419} = \frac{\partial^2 f_4}{\partial X \partial b_z} = \mu_s\left[-15\,\frac{X^2_p Z_p}{r^7_p}\right] + \mu_s\left[3\,\frac{Z_p}{r^5_p}\right]$$

$$F_{422} = \frac{\partial^2 f_4}{\partial Y \partial Y} = \mu\left[-15\,\frac{XYZ}{r^7} + 3\,\frac{X}{r^5}\right] + \mu_s\left[-15\,\frac{X_p Y_p Y_p}{r^7_p} + 3\,\frac{X_p}{r^5_p}\right]$$

$$F_{423} = \frac{\partial^2 f_4}{\partial Y \partial Z} = \mu\left[-15\,\frac{XYZ}{r^7}\right] + \mu_s\left[-15\,\frac{X_p Y_p Z_p}{r^7_p}\right]$$

$$F_{427} = \frac{\partial^2 f_4}{\partial Y \partial b_x} = \mu_s\left[-15\,\frac{X_p Y_p X_p}{r_p^7} + 3\,\frac{Y_p}{r_p^5}\right]$$

$$F_{428} = \frac{\partial^2 f_4}{\partial Y \partial b_y} = \mu_s\left[-15\,\frac{X_p Y_p Y_p}{r_p^7} + 3\,\frac{X_p}{r_p^5}\right]$$

$$F_{429} = \frac{\partial^2 f_4}{\partial Y \partial b_z} = \mu_s\left[-15\,\frac{X_p Y_p Z_p}{r_p^7}\right]$$

$$F_{433} = \frac{\partial^2 f_4}{\partial Z \partial Z} = \mu\left[-15\,\frac{XZZ}{r^7} + 3\,\frac{X}{r^5}\right] + \mu_s\left[-15\,\frac{X_p Z_p Z_p}{r_p^7} + 3\,\frac{X_p}{r_p^5}\right]$$

$$F_{437} = \frac{\partial^2 f_4}{\partial Z \partial b_x} = \mu_s\left[-15\,\frac{X_p Z_p X_p}{r_p^7} + 3\,\frac{Z_p}{r_p^5}\right]$$

$$F_{438} = \frac{\partial^2 f_4}{\partial Z \partial b_y} = \mu_s\left[-15\,\frac{X_p Z_p Y_p}{r_p^7}\right]$$

$$F_{439} = \frac{\partial^2 f_4}{\partial Z \partial b_z} = \mu_s\left[-15\,\frac{X_p Z_p Z_p}{r_p^7} + 3\,\frac{X_p}{r_p^5}\right]$$

$$F_{477} = \frac{\partial^2 f_4}{\partial b_x \partial b_x} = \mu_s\left[-15\,\frac{X^2 X_p}{r_p^7} + 3\,\frac{2X_p}{r_p^5}\right] - \mu_s\left[-15\,\frac{X_t^2 X_t}{r_t^7} + 3\,\frac{2X_t}{r_t^5}\right] + \mu_s\left[3\,\frac{X_p}{r_p^5}\right]$$

$$- \mu_s\left[3\,\frac{X_t}{r_t^5}\right]$$

$$F_{478} = \frac{\partial^2 f_4}{\partial b_x \partial b_y} = \mu_s\left[-15\,\frac{X^2 Y_p}{r_p^7} + 3\,\frac{Y_p}{r_p^5}\right] - \mu_s\left[-15\,\frac{X_t^7 Y_t}{r_t^7} + 3\,\frac{Y_t}{r_t^5}\right]$$

$$F_{479} = \frac{\partial^2 f_4}{\partial b_x \partial b_y} = \mu_s\left[-15\,\frac{X^2 Z_p}{r_p^7} + 3\,\frac{Z_p}{r_p^5}\right] - \mu_s\left[-15\,\frac{X_t^7 Z_t}{r_t^7} + 3\,\frac{Z_t}{r_t^5}\right]$$

$$F_{488} = \frac{\partial^2 f_4}{\partial b_y \partial b_y} = \mu_s\left[-15\,\frac{X_p Y_p Y_p}{r_p^7} + 3\,\frac{X_p}{r_p^5}\right] - \mu_s\left[-15\,\frac{X_t Y_t Y_t}{r_t^7} + 3\,\frac{X_t}{r_t^5}\right]$$

$$F_{489} = \frac{\partial^2 f_4}{\partial b_y \partial b_z} = \mu_s\left[-15\,\frac{X_p Y_p Z_p}{r_p^7}\right] - \mu_s\left[-15\,\frac{X_t Y_t Z_t}{r_t^7}\right]$$

$$F_{499} = \frac{\partial^2 f_4}{\partial b_z \partial b_z} = \mu_s \left[-15 \frac{X_p Z_p Z_p}{r_p^7} + 3 \frac{X_p}{r_p^5} \right] - \mu_s \left[\frac{X_t Z_t Z_t}{r_t^7} + 3 \frac{X_t}{r_t^5} \right]$$

$$\left.\begin{aligned} F_{51j} &= F_{42j} \\ F_{57j} &= F_{48j} \end{aligned}\right\} \quad j = 1,2,3,7,8,9$$

$$F_{51J} = F_{42J} \ , \ F_{59J} = F_{48J} \ , \ J = 1,2,3,7,8,9$$

$$F_{522} = \frac{\partial^2 f_5}{\partial Y \partial Y} = \mu_s \left[-15 \frac{Y_p^2 Y_p}{r_p^7} + 3 \frac{2Y_p}{r_p^5} \right] + \mu \left[-15 \frac{Y^2 Y}{r^7} + 3 \frac{2Y}{r^5} \right] + \mu_s \left[3 \frac{Y_p}{r_p^5} \right] + \mu \left[3 \frac{Y}{r^5} \right]$$

$$F_{523} = \frac{\partial^2 f_5}{\partial Y \partial Z} = \mu_s \left[-15 \frac{Y_p^2 Z_p}{r_p^7} + 3 \frac{Z_p}{r_p^5} \right] + \mu \left[-15 \frac{Y^2 Z}{r^7} + 3 \frac{Z}{r^5} \right]$$

$$F_{528} = \frac{\partial^2 f_5}{\partial Y \partial b_y} = \mu_s \left[-15 \frac{Y_p^2 Y_p}{r_p^7} + 3 \frac{2Y_p}{r_p^5} \right] + \mu_s \left[3 \frac{Y_p}{r_p^5} \right]$$

$$F_{529} = \frac{\partial^2 f_5}{\partial Y \partial b_z} = \mu_s \left[-15 \frac{Y_p^2 Z_p}{r_p^7} \right] + \mu_s \left[3 \frac{Y_p}{r_p^5} \right]$$

$$F_{533} = \frac{\partial^2 f_5}{\partial Z \partial Z} = \mu_s \left[-15 \frac{Y_p Z_p Z_p}{r_p^7} + 3 \frac{Y_p}{r_p^5} \right] + \mu \left[-15 \frac{YZZ}{r^7} + 3 \frac{Y}{r^5} \right]$$

$$F_{538} = \frac{\partial^2 f_5}{\partial Z \partial b_z} = \mu_s \left[-15 \frac{Y_p Z_p Y_p}{r_p^7} + 3 \frac{Z_p}{r_p^5} \right]$$

$$F_{539} = \frac{\partial^2 f_5}{\partial Z \partial b_z} = \mu_s \left[-15 \frac{Y_p Z_p Z_p}{r_p^7} + 3 \frac{Y_p}{r_p^5} \right]$$

$$F_{588} = \frac{\partial^2 f_5}{\partial b_y \partial b_y} = \mu_s \left[-15 \frac{Y_p^2 Y_p}{r_p^7} + 3 \frac{3Y_p}{r_p^5} \right] - \mu_s \left[-15 \frac{Y_t^2 Y_t}{r_t^7} + 3 \frac{3Y_t}{r_t^5} \right]$$

$$F_{589} = \frac{\partial^2 f_5}{\partial b_y \partial b_y} = \mu_s \left[-15 \frac{Y_p^2 Z_p}{r_p^7} + 3 \frac{Z_p}{r_p^5} \right] - \mu_s \left[-15 \frac{Y_t^2 Z_t}{r_t^7} + 3 \frac{Z_t}{r_t^5} \right]$$

$$F_{599} = \frac{\partial^2 f_5}{\partial b_z \partial b_z} = \mu_s \left[-15 \frac{Y_p Z_p Z_p}{r_p^7} + 3 \frac{Y_p}{r_p^5} \right] - \mu_s \left[-15 \frac{Y_t Z_t Z_t}{r_t^7} + 3 \frac{Y_t}{r_t^5} \right]$$

$$\left.\begin{aligned} F_{61j} &= F_{43j} \\ F_{62j} &= F_{53j} \\ F_{67j} &= F_{49j} \\ F_{68j} &= F_{59j} \end{aligned}\right\} \quad j = 1,2,3,7,8,9$$

$$F_{639} = \frac{\partial^2 f_6}{\partial z \partial b_z} = \mu_s\left[-15\,\frac{Z_p^2 Z_p}{r_p^7} + 3\,\frac{2Z_p}{r_p^5}\right] + \mu_s\left[3\,\frac{Z_p}{r_p^5}\right]$$

$$F_{699} = \frac{\partial^2 f_6}{\partial b_z \partial z} = \mu_s\left[-15\,\frac{Z_p^2 Z_p}{r_p^7} + 3\,\frac{2Z_p}{r_p^5}\right] - \mu_s\left[-15\,\frac{Z_t^2 Z_t}{r_t^7} + 3\,\frac{2Z_t}{r_t^5}\right] + \mu_s\left[3\,\frac{Z_p}{r_p^5}\right] - \mu_s\left[3\,\frac{Z_t}{r_t^5}\right]$$

The second order partial derivative h_{xx} is a (4×9×9) three-dimensional array shown in Fig. 27 and each layer is a (9×9) symmetric matrix.

Each layer is partitioned into (3×3) matrices and they are as follows:

$$H^1 = \left[\begin{array}{c|c|c} A & \phi & A \\ \hline \phi & \phi & \phi \\ \hline A & \phi & A \end{array}\right] \qquad H^2 = \left[\begin{array}{c|c|c} B & A & B \\ \hline A & \phi & A \\ \hline B & A & B \end{array}\right]$$

$$H^3 = \left[\begin{array}{c|c|c} C & \phi & 0 \\ \hline \phi & \phi & 0 \\ \hline D^T & \phi & E \end{array}\right] \qquad H^4 = \left[\begin{array}{c|c|c} F & \phi & \phi \\ \hline \phi & \phi & \phi \\ \hline \phi & \phi & \phi \end{array}\right]$$

All submatrices with the exception of D are (3×3) symmetric matrices and they are defined as follows:

f_{xx} =

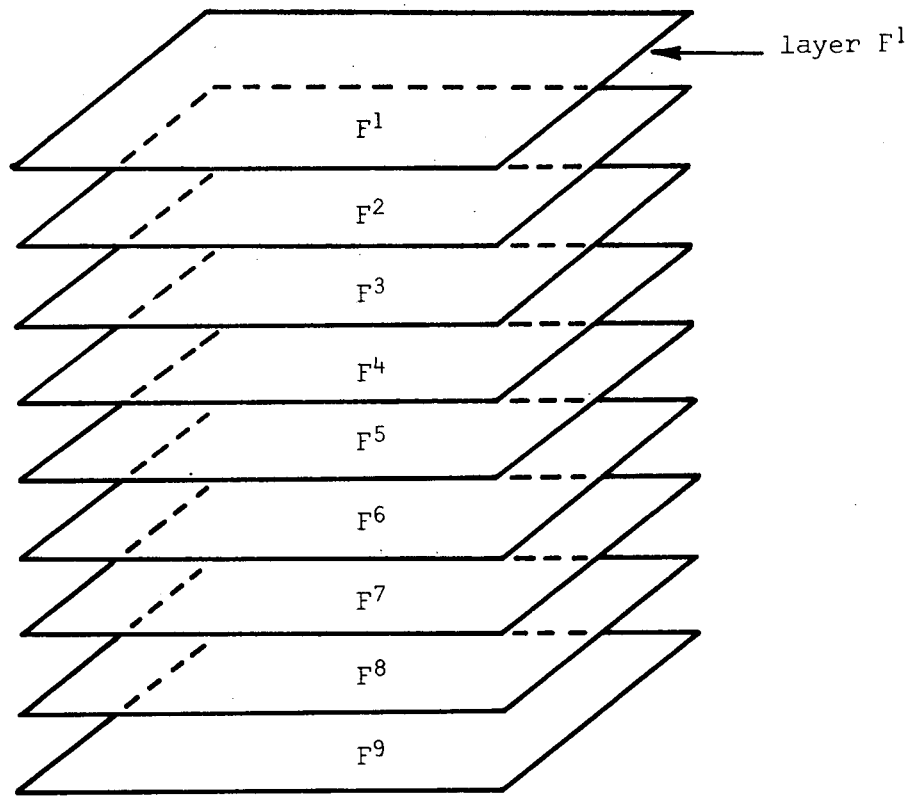

Figure 26. Three-Dimensional Array f_{xx}

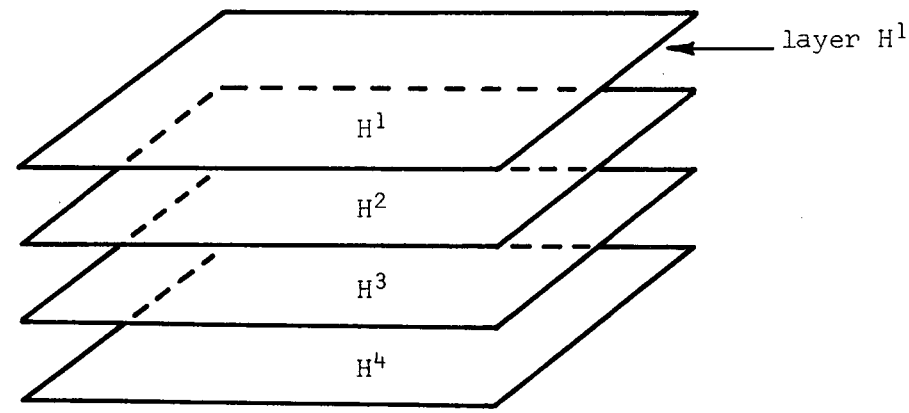

Figure 27. Three-Dimensional Array h_{xx}

$$A = \begin{bmatrix} h_{111} & h_{112} & h_{113} \\ h_{112} & h_{122} & h_{123} \\ h_{113} & h_{123} & h_{133} \end{bmatrix} \qquad B = \begin{bmatrix} h_{211} & h_{212} & h_{213} \\ h_{212} & h_{222} & h_{223} \\ h_{213} & h_{223} & h_{233} \end{bmatrix}$$

$$C = \begin{bmatrix} h_{314} & h_{312} & h_{313} \\ h_{312} & h_{322} & h_{323} \\ h_{313} & h_{332} & h_{333} \end{bmatrix} \qquad D = \begin{bmatrix} h_{317} & h_{318} & h_{319} \\ h_{327} & h_{328} & h_{329} \\ h_{337} & h_{338} & h_{339} \end{bmatrix}$$

$$E = \begin{bmatrix} h_{377} & h_{378} & h_{379} \\ h_{378} & h_{388} & h_{389} \\ h_{397} & h_{398} & h_{399} \end{bmatrix} \qquad F = \begin{bmatrix} h_{411} & h_{412} & h_{413} \\ h_{412} & h_{422} & h_{423} \\ h_{413} & h_{423} & h_{433} \end{bmatrix}$$

where

$$h_{111} = \frac{\partial^2 \rho}{\partial X \partial X} = -\frac{(X_p - X_s)(X_p - X_s)}{\rho^3} + \frac{1}{\rho}$$

$$h_{112} = \frac{\partial^2 \rho}{\partial X \partial Y} = -\frac{(X_p - X_s)(Y_p - Y_s)}{\rho^3}$$

$$h_{113} = \frac{\partial^2 \rho}{\partial X \partial Z} = -\frac{(X_p - X_s)(Z_p - Z_s)}{\rho^3}$$

$$h_{122} = \frac{\partial^2 \rho}{\partial Y \partial Y} = -\frac{(Y_p - Y_s)(Y_p - Y_s)}{\rho^3} + \frac{1}{\rho}$$

$$h_{123} = \frac{\partial^2 \rho}{\partial Y \partial Z} = -\frac{(Y_p - Y_s)(Z_p - Z_s)}{\rho^3}$$

$$h_{133} = \frac{\partial^2 \rho}{\partial Z \partial Z} = -\frac{(Z_p - Z_s)(Z_p - Z_s)}{\rho^3} + \frac{1}{\rho}$$

$$h_{211} = \frac{\partial^2 \dot{\rho}}{\partial X \partial X} = -\frac{2(\dot{X}_p - \dot{X}_s)(X_p - X_s)}{\rho^3} + \frac{3(X_p - X_s)^2(\bar{\rho} \cdot \dot{\bar{\rho}})}{\rho^5} - \frac{(\bar{\rho} \cdot \dot{\bar{\rho}})}{\rho^3}$$

$$h_{212} = \frac{\partial^2 \rho}{\partial X \partial Y} = -\frac{(\dot{X}_p - \dot{X}_s)(Y_p - Y_s)}{\rho^3} + \frac{3(X_p - X_s)(Y_p - Y_s)(\bar{\rho} \cdot \dot{\bar{\rho}})}{\rho^5} - \frac{(X_p - X_s)(\dot{Y}_p - \dot{Y}_s)}{\rho^3}$$

$$h_{213} = \frac{\partial^2 \dot{\rho}}{\partial X \partial Z} = -\frac{(\dot{X}_p - \dot{X}_s)(Z_p - Z_s)}{\rho^3} + \frac{3(X_p - X_s)(Z_p - Z_s)(\bar{\rho}\cdot\dot{\bar{\rho}})}{\rho^5} - \frac{(X_p - X_s)(\dot{Z}_p - \dot{Z}_s)}{\rho^3}$$

$$h_{222} = \frac{\partial^2 \dot{\rho}}{\partial Y \partial Y} = -\frac{2(\dot{Y}_p - \dot{Y}_s)(Y_p - Y_s)}{\rho^3} + \frac{3(Y_p - Y_s)^2(\bar{\rho}\cdot\dot{\bar{\rho}})}{\rho^5} - \frac{\dot{\bar{\rho}}\cdot\dot{\bar{\rho}}}{\rho^3}$$

$$h_{223} = \frac{\partial^2 \dot{\rho}}{\partial Y \partial Z} = -\frac{(\dot{Y}_p - \dot{Y}_s)(Z_p - Z_s)}{\rho^3} - \frac{(Y_p - Y_s)(\dot{Z}_p - \dot{Z}_s)}{\rho^3} + \frac{3(Y_p - Y_s)(Z_p - Z_s)}{\rho^5}$$

$$h_{233} = \frac{\partial^2 \dot{\rho}}{\partial Z \partial Z} = -\frac{2(\dot{Z}_p - \dot{Z}_s)(Z_p - Z_s)}{\rho^3} + \frac{3(Z_p - Z_s)^2(\bar{\rho}\cdot\dot{\bar{\rho}})}{\rho^5} - \frac{\dot{\bar{\rho}}\cdot\dot{\bar{\rho}}}{\rho^3}$$

$$h_{311} = \frac{\partial^2 \alpha}{\partial X \partial X} = -h_{31}h_{31}\cot\alpha - h_{31}\left(\frac{X}{r^2} + \frac{X_p}{r_p^2}\right) - 2\left(\frac{X^2}{r^4} + \frac{X_p^2}{r_p^4}\right)\cot\alpha$$
$$+ \frac{X+X_p}{rr_p}\left(\frac{X_p}{r_p^2} + \frac{X}{r^2}\right)\csc\alpha + \left(\frac{1}{r^2} + \frac{1}{r_p^2}\right)\cot\alpha - \frac{2}{rr_p}\csc\alpha$$

$$h_{312} = \frac{\partial^2 \alpha}{\partial X \partial Y} = -h_{31}h_{32}\cot\alpha - h_{32}\left(\frac{X}{r^2} + \frac{X_p}{r_p^2}\right) - 2\left(\frac{XY}{r^4} + \frac{X_pY_p}{r_p^4}\right)\cot\alpha$$
$$+ \frac{X+X_p}{rr_p}\left(\frac{Y_p}{r_p^2} + \frac{Y}{r^2}\right)\csc\alpha$$

$$h_{313} = \frac{\partial^2 \alpha}{\partial X \partial Z} = -h_{31}h_{33}\cot\alpha - h_{33}\left(\frac{X}{r^2} + \frac{X_p}{r_p^2}\right) - 2\left(\frac{XZ}{r^4} + \frac{X_pZ_p}{r_p^4}\right)\cot\alpha$$
$$+ \frac{X+X_p}{rr_p}\left(\frac{Z_p}{r_p^2} + \frac{Z}{r^2}\right)\csc\alpha$$

$$h_{322} = \frac{\partial^2 \alpha}{\partial Y \partial Y} = -h_{32}h_{32}\cot\alpha - h_{32}\left(\frac{Y}{r^2} + \frac{Y_p}{r_p^2}\right) - 2\left(\frac{Y^2}{r^4} + \frac{Y_p^2}{r_p^4}\right)\cot\alpha$$
$$+ \frac{Y+Y_p}{rr_p}\left(\frac{Y_p}{r_p^2} + \frac{Y}{r^2}\right)\csc\alpha + \left(\frac{1}{r^2} + \frac{1}{r_p^2}\right)\cot\alpha - \frac{2}{rr_p}\csc\alpha$$

$$h_{323} = \frac{\partial^2 \alpha}{\partial Y \partial Z} = -h_{32}h_{33}\cot\alpha - h_{33}\left(\frac{Y}{r^2} + \frac{Y_p}{r_p^2}\right) - 2\left(\frac{YZ}{r^4} + \frac{Y_pZ_p}{r_p^4}\right)\cot\alpha$$
$$+ \frac{Y+Y_p}{rr_p}\left(\frac{Z_p}{r_p^2} + \frac{Z}{r^2}\right)\csc\alpha$$

$$h_{333} = \frac{\partial^2\alpha}{\partial Z \partial Z} = -h_{33}h_{33}\cot\alpha - h_{33}\left(\frac{Z}{r^2} + \frac{Z_p}{r_p^2}\right) - 2\left(\frac{Z^2}{r^4} + \frac{Z_p^2}{r_p^4}\right)\cot\alpha$$

$$+ \frac{Z+Z_p}{rr_p}\left(\frac{Z_p}{r_p^2} + \frac{Z}{r^2}\right)\csc\alpha + \left(\frac{1}{r^2} + \frac{1}{r_p^2}\right)\cot\alpha - \frac{2}{rr_p}\csc\alpha$$

$$h_{317} = \frac{\partial^2\alpha}{\partial X \partial b_x} = -h_{37}h_{31}\cot\alpha - h_{37}\left(\frac{X}{r^2} + \frac{X_p}{r_p^2}\right) - 2\frac{X_p^2}{r_p^4}\cot\alpha$$

$$+ \frac{X+X_p}{rr_p}\left(\frac{X_p}{r_p^2}\right)\csc\alpha + \frac{1}{r_p^2}\cot\alpha - \frac{1}{rr_p}\csc\alpha$$

$$h_{318} = \frac{\partial^2\alpha}{\partial X \partial b_y} = -h_{38}h_{31}\cot\alpha - h_{38}\left(\frac{X}{r^2} + \frac{X_p}{r_p^2}\right) - 2\frac{X_p Y_p}{r_p^4}\cot\alpha$$

$$+ \frac{X+X_p}{rr_p}\frac{Y_p}{r_p^2}\csc\alpha$$

$$h_{319} = \frac{\partial^2\alpha}{\partial X \partial b_z} = -h_{39}h_{31}\cot\alpha - h_{39}\left(\frac{X}{r^2} + \frac{X_p}{r_p^2}\right) - 2\frac{X_p Z_p}{r_p^4}\cot\alpha$$

$$+ \frac{X+X_p}{rr_p}\frac{Z_p}{r_p^2}\csc\alpha$$

$$h_{327} = \frac{\partial^2\alpha}{\partial Y \partial b_x} = -h_{37}h_{32}\cot\alpha - h_{37}\left(\frac{Y}{r^2} + \frac{Y_p}{r_p^2}\right) - 2\frac{Y_p X_p}{r_p^4}\cot\alpha$$

$$+ \frac{Y+Y_p}{rr_p}\frac{X_p}{r_p^2}\csc\alpha$$

$$h_{328} = \frac{\partial^2\alpha}{\partial Y \partial b_y} = -h_{38}h_{32}\cot\alpha - h_{38}\left(\frac{Y}{r^2} + \frac{Y_p}{r_p^2}\right) - 2\frac{Y_p^2}{r_p^4}\cot\alpha$$

$$+ \frac{Y+Y_p}{rr_p}\frac{Y_p}{r_p^2}\csc\alpha + \frac{1}{r_p^2}\cot\alpha - \frac{1}{rr_p}\csc\alpha$$

$$h_{329} = \frac{\partial^2\alpha}{\partial Y \partial b_z} = -h_{39}h_{39}\cot\alpha - h_{39}\left(\frac{Y}{r^2} + \frac{Y_p}{r_p^2}\right) - 2\frac{Y_p Z_p}{r_p^4}\cot\alpha$$

$$+ \frac{Y+Y_p}{rr_p}\frac{Z_p}{r_p^2}\csc\alpha$$

$$h_{337} = \frac{\partial^2\alpha}{\partial Z \partial b_x} = -h_{37}h_{33}\cot\alpha - h_{37}\left(\frac{Z}{r^2} + \frac{Z_p}{r_p^2}\right) - 2\frac{Z_p X_p}{r_p^4}\cot\alpha$$

$$+ \frac{Z+Z_p}{rr_p}\frac{X_p}{r_p^2}\csc\alpha$$

$$h_{338} = \frac{\partial^2\alpha}{\partial Z \partial b_y} = -h_{38}h_{33}\cot\alpha - h_{38}\left(\frac{Z}{r^2} + \frac{Z_p}{r_p^2}\right) - 2\frac{Z_p X_p}{r_p^4}\cot\alpha$$

$$+ \frac{Z+Z_p}{rr_p}\frac{Y_p}{r_p^2}\csc\alpha$$

$$h_{339} = \frac{\partial^2\alpha}{\partial Z \partial b_z} = -h_{39}h_{33}\cot\alpha - h_{39}\left(\frac{Z}{r^2} + \frac{Z_p}{r_p^2}\right) - 2\frac{Z_p}{r_p^4}\cot\alpha$$

$$+ \frac{Z+Z_p}{rr_p}\frac{Z_p}{r_p^2}\csc\alpha + \frac{1}{r_p^2}\cot\alpha - \frac{1}{rr_p}\csc\alpha$$

$$h_{377} = \frac{\partial^2\alpha}{\partial b_x \partial b_x} = -h_{37}h_{37}\cot\alpha - h_{37}\frac{X_p}{r_p^2} - 2\frac{X_p^2}{r_p^4}\cot\alpha$$

$$+ \frac{X}{rr_p}\frac{X_p}{r_p^2}\csc\alpha + \frac{1}{r_p^2}\cot\alpha$$

$$h_{378} = \frac{\partial^2\alpha}{\partial b_x \partial b_y} = -h_{37}h_{38}\cot\alpha - h_{38}\frac{X_p}{r_p^2} - 2\frac{X_p Z_p}{r_p^4}\cot\alpha + \frac{X}{rr_p}\frac{Y_p}{r_p^2}\csc\alpha$$

$$h_{379} = \frac{\partial^2\alpha}{\partial b_x \partial b_z} = -h_{37}h_{39}\cot\alpha - h_{39}\frac{X_p}{r_p^2} - 2\frac{X_p Z_p}{r_p^4}\cot\alpha + \frac{X}{rr_p}\frac{Z_p}{r_p^2}\csc\alpha$$

$$h_{388} = \frac{\partial^2\alpha}{\partial b_y \partial b_y} = -h_{38}h_{38}\cot\alpha - h_{38}\frac{Y_p}{r_p^2} - 2\frac{Y_p^2}{r_p^4}\cot\alpha + \frac{Y}{rr_p}\frac{Y_p}{r_p^2}\csc\alpha$$

$$+ \frac{1}{r_p^2}\cot\alpha$$

$$h_{389} = \frac{\partial^2\alpha}{\partial b_y \partial b_z} = -h_{38}h_{39}\cot\alpha - h_{39}\frac{Y_p}{r_p^2} - 2\frac{Y_p Z_p}{r_p^4}\cot\alpha + \frac{Y}{rr_p}\frac{Z_p}{r_p^2}\csc\alpha$$

$$h_{399} = \frac{\partial^2\alpha}{\partial b_z \partial b_z} = -h_{39}h_{39}\cot\alpha - h_{39}\frac{Z_p}{r_p^2} - 2\frac{Z_p}{r_p^4}\cot\alpha + \frac{2}{rr_p}\frac{Z_p}{r_p^2}\csc\alpha + \frac{1}{r_p^2}\cot\alpha$$

$$h_{411} = \frac{\partial^2\beta}{\partial X \partial X} = -h_{41}\frac{X}{r^2} - h_{41}h_{41}\cot\beta - 2\frac{X^2}{r^4}\cot\beta - \frac{S_x X}{r^3}\csc\beta + \frac{1}{r^2}\cot\beta$$

$$h_{412} = \frac{\partial^2\beta}{\partial X \partial Y} = -h_{42}\frac{X}{r^2} - h_{41}h_{42}\cot\beta - 2\frac{XY}{r^4}\cot\beta - \frac{S_x Y}{r^3}\csc\beta$$

$$h_{413} = \frac{\partial^2\beta}{\partial X \partial Z} = -h_{43}\frac{X}{r^2} - h_{41}h_{43}\cot\beta - 2\frac{XZ}{r^4}\cot\beta - \frac{S_x Z}{r^3}\csc\beta$$

$$h_{422} = \frac{\partial^2\beta}{\partial Y \partial Y} = -h_{42}\frac{Y}{r^2} - h_{42}h_{42}\cot\beta - 2\frac{YY}{r^2}\cot\beta - \frac{S_x Y}{r^3}\csc\beta + \frac{1}{r^2}\cot\beta$$

$$h_{423} = \frac{\partial^2\beta}{\partial Y \partial Z} = -h_{43}\frac{Y}{r^2} - h_{42}h_{43}\cot\beta - 2\frac{YZ}{r^2}\cot\beta - \frac{S_y Z}{r^3}\csc\beta$$

$$h_{433} = \frac{\partial^2\beta}{\partial Z \partial Z} = -h_{43}\frac{Z}{r^2} - h_{43}h_{43}\cot\beta - 2\frac{Z^2}{r^2}\cot\beta - \frac{S_z Z}{r^3}\csc\beta + \frac{1}{r^2}\cot\beta$$

APPENDIX B

CONDITIONAL EXPECTATION AND SMOOTHING PROPERTY

Loeve (34) introduced the concept of "conditioning" in terms of sub σ-fields of events, and further conditional probabilities of events and conditional expectations of random variables "given a σ-field $\mathcal{B}$" as $\mathcal{B}$-measurable functions defined up to an equivalence. The conditional probability of an event A "given an event B" corresponds to that of the frequencies of the occurrence of A in the repeat trials where B occurs. For every event A, the relation

$$PB \cdot P_B A = PAB \tag{B-1}$$

defines the conditional probability $P(A/B)$ of A given B as the ratio PAB/PB , provided B is a nonnull event. In a more mathematical form, the function P_B on the σ-field $\mathcal{A}$ of events, whose values are $P_B A$, $A \epsilon \mathcal{A}$, is called the conditional probability of A given B . Since P on $\mathcal{A}$ is normed, nonnegative and σ-additive, so is P_B on $\mathcal{A}$; and P_B satisfies the following condition

$$P_B \Omega = 1 \quad , \quad P_B \geq 0 \quad , \quad P_B \Sigma A_i = \Sigma P_B A_i$$

Thus, the conditioning expressed by "given B" means that the initial probability space $(\Omega, \mathcal{A}, P)$ is replaced by the probability space $(\Omega, \mathcal{A}, P_B)$. The expectation of a random variable X on this new probability space is called the conditional expectation given B and is denoted by

$$E[X/B] = \int X dP_B = \int_B X dP_B + \int_{B^C} X dP_B \tag{B-2}$$

where B^C is the complement of B . Knowing that $P_B = 0$ on $\{AB^C, A \epsilon \mathcal{A}\}$ and that $P_B = \frac{1}{P_B} P$ on $\{AB, A \epsilon \mathcal{A}\}$ from Eq. B-1, Eq. B-2 becomes

$$E[X/B] = \frac{1}{PB}\int_B XdP \qquad (B\text{-}3)$$

which is the definition of the conditional expectation of X given B. The conditional expectation acquires its full meaning when interpreted as values of functions as follows: the number $E[X/B]$ is no longer assigned to B but to every point of B, and similarly for $E[X/B^C]$, so that we have a two-valued function on Ω, with values $E[X/B]$ for $\omega\epsilon B$ and $E[X/B^C]$ for $\omega\epsilon B^C$. More generally, let $\{B_j\}$ be a countable partition of Ω and let $\mathcal{B}$ be the minimum σ-field over this partition. Let Σ be the family of all random variables X whose expectation, $E[X]$, exists so that their indefinite integrals, hence conditional expectations given any nonnull event, exist. Then the conditional expectation of X given $\mathcal{B}$ is defined as the following elementary functions (see page 64 of Loeve for the definition) up to an equivalence

$$E[X/B] = \Sigma(\frac{1}{PB_j}\int_{B_j} XdP)I_{B_j}\ ;\ X\epsilon\Sigma \qquad (B\text{-}4)$$

The above is the constructive definition and is different from (B-3) in the sense that conditioning is given as a σ-field, $\mathcal{B}$, instead of an event B, $B\epsilon\mathcal{B}$. It can be easily seen further that the conditioning can be either as a random variable which is $\mathcal{B}$-measurable function or as an output of the random variable. If the partition $\{B_j\}$ is not countable, the above constructive definition is not applicable and rather powerful tool, namely, the Radon-Nikodym theorem is employed and the descriptive definition is followed. Let $P_{\mathcal{B}}$ be the restriction of P to $\mathcal{B}$, defined by

$$P_{\mathcal{B}}B = PB\ ,\ B\epsilon\mathcal{B}\ , \qquad (B\text{-}5)$$

then the conditional expectation $E[X/\mathcal{B}]$ of X given $\mathcal{B}$ is any $\mathcal{B}$-measurabel function whose indefinite integral with respect to $P_{\mathcal{B}}$ is the restriction

to $\mathcal{B}$ of the indefinite integral of X with respect to P. This definition means precisely that, for every $X\varepsilon\Sigma$, $E[X/\mathcal{B}]$ is defined by

$$\int_B E[X/\mathcal{B}]dP_{\mathcal{B}} = \int_B XdP \quad , \quad B\varepsilon\mathcal{B} \tag{B-6}$$

up to an equivalence. Loosely speaking, the operation $E[X/\mathcal{B}]$ is a $\mathcal{B}$-smoothing and some of its important properties are quoted from Loeve without proof.

1. On every nonnull atom* $B\varepsilon\mathcal{B}$, $E[X/\mathcal{B}]$ is constant and its value $E[X/B]$ is the average of the values of X on B with respect to P.
2. For every $\mathcal{B}$ independent of the σ-field $\mathcal{B}_X$ of events induced by X

$$E[X/\mathcal{B}] = EX \quad \text{a.s.}$$

3. Conditional expectation operator $E[\cdot/\mathcal{B}]$ and $\mathcal{B}$-measurable factors commute, that is, if X is $\mathcal{B}$-measurable, then

$$E[XY/\mathcal{B}] = XE[Y/\mathcal{B}] \quad \text{a.s.}$$

4. If $\mathcal{B}\subset\mathcal{B}'$, then

$$E[E[X/\mathcal{B}']/\mathcal{B}] = E[X/\mathcal{B}] = E[E[X/\mathcal{B}]/\mathcal{B}'] \quad \text{a.s.}$$

It is interesting to note that for the "least fine" or "smallest" of all possible σ-fields $\mathcal{B}\subset\mathcal{A}$, that is, for $\mathcal{B}_o = \{\phi,\Omega\}$, $E[X/\mathcal{B}_o] = E[X]$ almost surely, which means that unconditional expectation is a special case of conditional expectation whose conditioning is merely the least fine σ-field. It is noted also that any deterministic quantity is a random variable which is measurable over the least fine σ-field.

---

*B is a nonnull atom of $\mathcal{B}$, if $PB > 0$, and B contains no other sets belonging to $\mathcal{B}$ than itself and the empty set.

The σ-field $\mathcal{A}$ is induced by the atom set A_1 and A_2 and a finer σ-field $\mathcal{B}$ containing $\mathcal{A}$ is induced by the atom set B_1, B_2, B_3, B_4 and B_5 in Figure 28. From the figure, it is apparent that the finer the σ-field $\mathcal{B}$ is, the closer to $X(\omega)$ the conditional expectation $E[X/\mathcal{B}]$ is. If a σ-field $\mathcal{B}$ is identical to the σ-field induced by $X(\omega)$, then $E[X/\mathcal{B}]$ is identical to $X(\omega)$ almost surely. The variance $E[\{X - E(X/\mathcal{B})\}^2]$ is proportional to the area between two random variables $X(\omega)$ and $E[X/\mathcal{B}]$ and the conditional variance $E[\{X - E[X/\mathcal{B}]\}^2/\mathcal{B}]$ is constant on every nonnull atom set B of $\mathcal{B}$ and is the average of $\{X - E(X/\mathcal{B})\}^2$ on B.

Since the conditional expectation is defined in an equivalence sense, the area under the conditional expectation $E[X/\mathcal{B}]$ for various σ-field $\mathcal{B}$ must be identical to the area under the random variable $X(\omega)$, which is the unconditional expectation $E[X]$. The conditional expectation $E[X/\mathcal{B}]$ is the closest approximation of $X(\omega)$ within the class of $\mathcal{B}$-measurable functions in the sense that the variance is minimized.

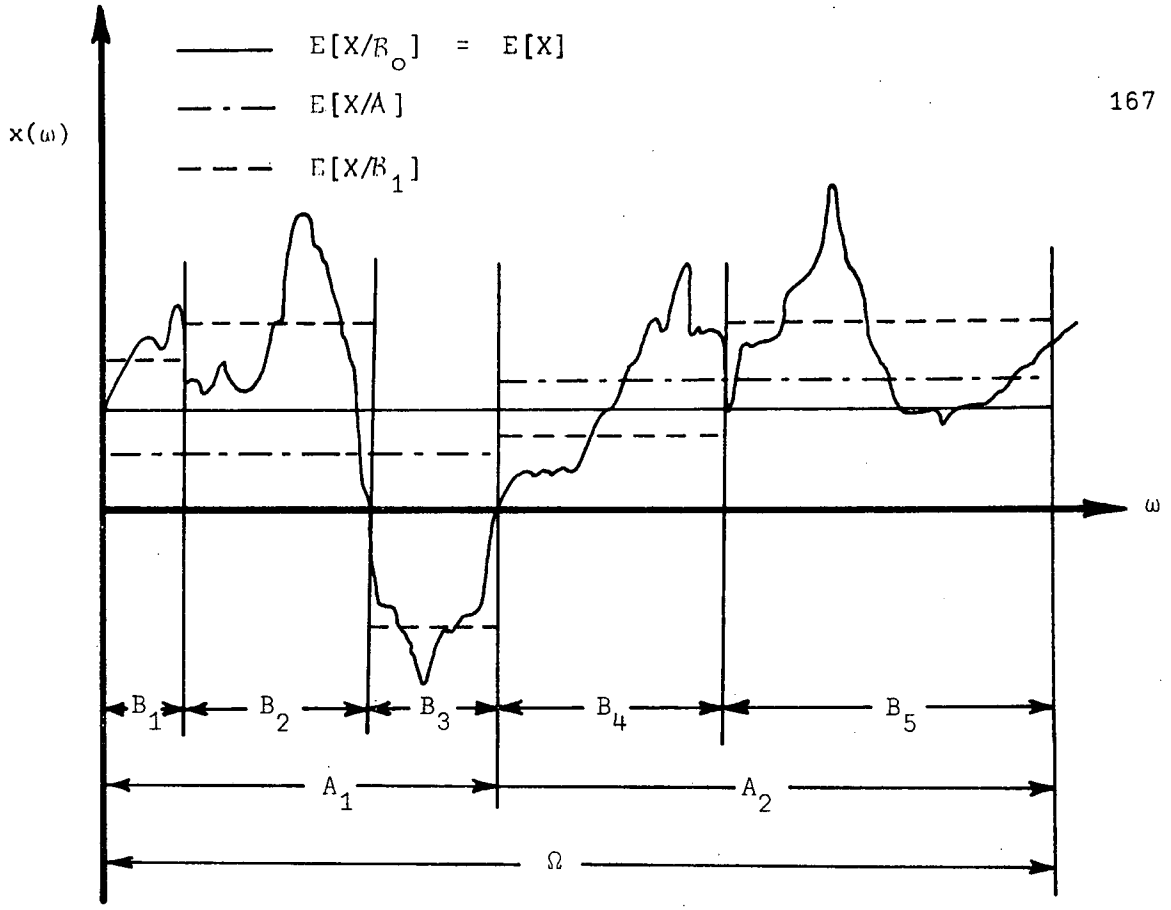

Figure 28. Conditional Expectation $E[X/\mathcal{B}]$

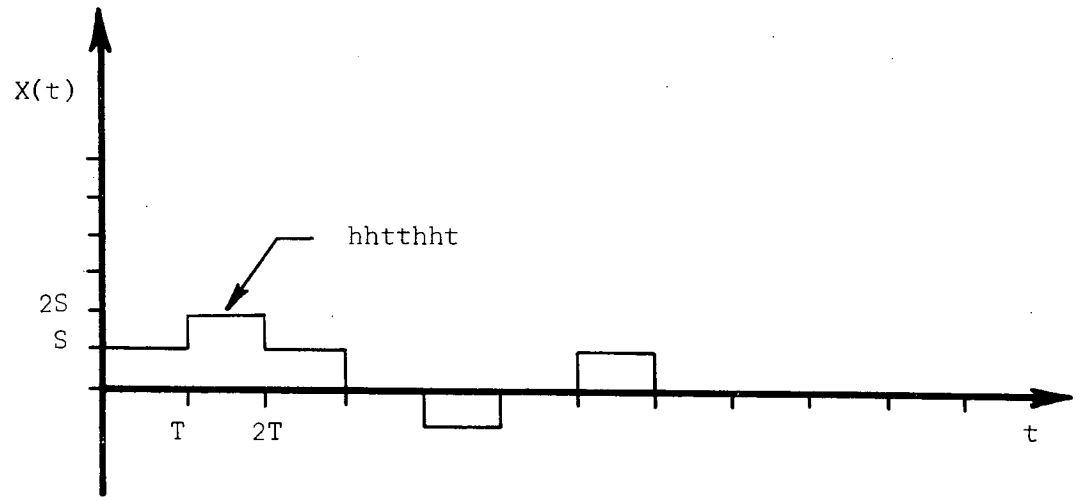

Figure 29. A Sample Function of Random Walk

APPENDIX C

RANDOM WALK, BROWNIAN MOTION AND WHITE NOISE

Historically random-walk models serve as a first approximation to the theory of diffusion and brownian motion, where small particles are exposed to a tremendous number of molecular shocks. Each shock has a negligible effect, but the superposition of many small actions produces an observable motion. Accordingly we want to present a random walk where the individual steps are extremely small and occur in very rapid succession. In the limit, the process will appear as a continuous motion, i.e., the so-called Brownian motion. Once we have grasped the concept of Brownian motion, the white noise, which is fictitious and nonexsiting but enables human beings to handle many mathematical problems, can be formally defined as a time derivative of Brownian motion. Here a brief summary of Papoulis' (36) discussion on the subject is presented.

The underlying experiment is the tossing of a fair coin an infinite number of times, and each tossing occurs every T seconds. At each tossing we take a step, to the right if heads show, to the left if tails show. Our position at t will be denoted by $X(t)$. Clearly, $X(t)$ depends on the experimental outcome, i.e. on the particular sequence of heads and tails. We have thus created a stochastic process known as random walk. Each sample function of this process is of stair-case form as in Fig. 29 with discontinuities at the points $t = nT$ the steps occur instantly and their length equals S.

We denote by x_i a random variable equal to $\pm S$, if our $i^{\underline{th}}$ step is to the right or left, i.e. heads or tails. Thus

$$P\{x_i = S\} = P = \tfrac{1}{2}$$

$$P\{x_i = -S\} = q = \tfrac{1}{2}$$

$$E\{x_i\} = 0$$

$$E\{x_i^2\} = S^2$$

Note that the random variable x_i is independent and has zero mean. The position at $t = nT$ is clearly a random variable given by

$$X(nT) = x_1 + x_2 + \cdots + x_n \tag{C-1}$$

Suppose that after the first n tossings, k heads show, then the value of $X(nT)$ would be given by

$$X(nT) = kS - (n - k)S = (2k - n)S = rS \tag{C-2}$$

where

$$r = 2k - n \tag{C-3}$$

Since $\{X(nT) = rS\}$ is the event $\{k = \frac{r + n}{2}$ heads in n tossing$\}$ the probability is given by

$$P\{X(nT) = rS\} = P\{\frac{r + n}{2} \text{ heads}\} = \binom{n}{\frac{n + r}{2}} \frac{1}{2^n} \tag{C-4}$$

If n is large and $npq \gg 1$, Demoivre-Laplace theorem (38) is applicable for values of k in the $\sqrt{npq}$ neighborhood of its most likely value np, i.e.

$$np - \sqrt{npq} < k < np + \sqrt{npq} \tag{C-5}$$

and the approximate form of Eq. (C-4) is given by

$$P\{k \text{ heads}\} \cong \frac{1}{\sqrt{2\ npq}}\, e - \frac{(k - np)^2}{2npq} \qquad (C\text{-}6)$$

Substitution of $P = q = \frac{1}{2}$ and $k = \frac{n + r}{2}$ into Eq. (C-6) yields the following approximate expression

$$P\{X(nt) = rS\} \cong \frac{1}{\sqrt{n\ /2}}\, e - \frac{r^2}{2n} \qquad (C\text{-}7)$$

provided that r is of the order of $\sqrt{n}$.

Furthermore, it can be shown that*

$$P\{X(nT) \leq rS\} = \frac{1}{2} + \text{erf}\, \frac{r}{\sqrt{n}} \qquad (C\text{-}8)$$

Finally, the mean and variance of the random variable $X(nT)$ are easily obtained and they are as follows:

$$E[x(nT)] = 0 \qquad (C\text{-}9)$$

$$E[x^2(nT)] = nS^2 \qquad (C\text{-}10)$$

In the following discussion, Brownian motion is developed as a limiting form of the random walk. For the time

$$t = nT \qquad (C\text{-}11)$$

the mean and variance of $X(t)$ become

$$E[X(t)] = 0 \qquad (C\text{-}12)$$

$$E[X^2(t)] = \frac{tS^2}{T} \qquad (C\text{-}13)$$

---

*Athanasias Papoulis, Probability, Random Variables, and Stochastic Processes, McGraw-Hill, p. 68.

Suppose now that we keep t constant but we make S and T tend to zero. The variance of $X(t)$ will remain finite and different from zero only if S tends to zero as $\sqrt{T}$. Otherwise, $X(t)$ would be meaningless. Therefore, assuming

$$S^2 = \alpha T \tag{C-14}$$

we define the process $W(t)$ as a limit

$$W(t) = \lim_{T \to 0} X(t) \tag{C-15}$$

A family of continuous functions results for almost all outcomes, which is known as a Brownian motion or Wiener-Levy process. From Eqs. (C-9) and (C-10), the mean and variance of this process are obtained and they are

$$E[W(t)] = 0 \tag{C-16}$$

$$E[W^2(t)] = \alpha t \tag{C-17}$$

The value of random process $W(t)$ can be determined from Eq. (C-2) and given by

$$W = rS \tag{C-18}$$

In connection with Eqs. (C-11), (C-14) and (C-18), we have the following expression:

$$\frac{r}{\sqrt{n}} = \frac{W/S}{\sqrt{t/T}} = \frac{W}{\sqrt{tS^2/T}} = \frac{W}{\sqrt{\alpha t}} \tag{C-19}$$

and hence the probability distribution $F(W,t)$ is obtained as a limit of Eq. (C-8)

$$F(W,t) = P\{W(t) \leq W\} = \tfrac{1}{2} + \operatorname{erf} \frac{W}{\sqrt{\alpha t}} \tag{C-20}$$

The probability density $f(W,t)$ is readily determined from Eq. (C-20) and

is given by

$$f(\omega,t) = \frac{1}{\sqrt{2\alpha t}} \exp\left(-\frac{\omega^2}{2\alpha t}\right) \qquad \text{(C-21)}$$

Thus, the random process $W(t)$ is normal, with zero mean and variance αt.

The fact to be pointed out here is that in passing to a limit, all formulas for the process $W(t)$ remain meaningful and agree with physically significant formulas of diffusion theory which can be derived under much more general conditions by more streamlined methods (Einstein-Wiener theory and Uhlenbeck-Orstein theory). For example, the density function is obtained as a solution of the diffusion equation by Einstein (37). The same thing can be done by using the autocorrelation of the solution of the Langevine equation (36).

From Eq. (C-1), it is seen that for $t_1 > t_2$, $W(t_1) - W(t_2)$ is independent of $W(t_2) - W(0) = W(t_2)$. Hence,

$$E[\{W(t_1) - W(t_2)\}W(t_2)] = E[W(t_1) - W(t_2)]E[W(t_2)] = 0 \qquad \text{(C-22)}$$

Thus,

$$E[W(t_1)W(t_2)] - E[W^2(t_2)] = 0 \qquad \text{(C-23)}$$

Since the left hand side of Eq. (C-22) is an autocorrelation $R(t_1,t_2)$ and the right hand side is αt_2 from Eq. (C-17), the following is developed.

$$R(t_1,t_2) = \begin{cases} \alpha t_2 & \text{for } t_1 \geq t_2 \\ \alpha t_1 & \text{for } t_1 \leq t_2 \end{cases} \qquad \text{(C-24)}$$

An infinitesimal increment $d\beta_t$ of Brownian motion $W(t)$ is defined as

$$d\beta_t = W(t + e) - W(t) \qquad \text{(C-25)}$$

The covariance of $d\beta_t$ is determined from Eq. (C-24) as follows:

$$E[d\beta_t, d\beta_t] = E[\{W(t + e) - W(t)\}\{W(t + e) - W(t)\}]$$

$$= R(t + e, t + e) - R(t + e, t) = R(t, t + e) + R(t, t)$$

$$= \alpha(t + e) - \alpha t - \alpha t + \alpha t$$

$$E[d\beta_t d\beta_t] = \alpha e \quad . \tag{C-26}$$

If we formally define white gaussian process $u(t)$ as a time derivative of Brownian motion as follows:

$$u(t) = \frac{dW(t)}{dt} = \lim_{e \to 0} \frac{d\beta_t}{e} \tag{C-27}$$

Then the autocorrelation of white gaussian process $u(t)$ is of the form

$$E[u(t)u(\tau)] = \lim_{e \to 0} \frac{\alpha}{e} = \alpha\delta(t - \tau) \tag{C-29}$$

Therefore, the variance of white Gaussian process $u(t)$ is infinite, which is in agreement with the axiomatic definition.

C

APPENDIX D

MARTINGALES

A sequence of random variables $x_1, x_2, \cdots$ is called a martingale if

$$E[|x_n|] < \infty \quad , \quad n \geq 1$$

and (D-1)

$$E[x_{n+1}/x_1, \cdots, x_n] = x_n$$

with Probability 1.

A stochastic process $\{x_t, t \in T\}$ is called a martingale if

$$E[|x_t|] < \infty$$

for all t and if, whenever $n \geq 1$ and $t_1 < \cdots < t_{n+1}$

$$E[x_{t_{n+1}}/x_{t_1}, \cdots, x_{t_n}] = x_{t_n} \qquad \text{(D-2)}$$

with Probability 1.

<Theorem 1>

If $y_1, y_2, y_3, \cdots$ are defined as

$$y_1 = x_1 \ , \ y_2 = x_2 - x_1 \ , \ y_3 = x_3 - x_2 \ , \ \cdots \qquad \text{(D-3)}$$

then, if the x_n process is a martingale,

$$E[|y_n|] < \infty \ , \ E[y_{n+1}/y_1, \cdots, y_n] = 0 \ , \ n \geq 1 \ , \qquad \text{(D-4)}$$

with Probability 1. The x_n's are thus partial sums of the series $\sum_n y_n$,

where the y_n's satisfy the condition (D-4). Conversely, the partial sums of any such series constitute a martingale.

<Proof>

x_n's and y_n's are linearly related and, hence, the mapping matrix is of full rank. Therefore, the inverse of the mapping matrix exists, which implies that the conditioning $\{y_1,\cdots,y_n\}$ of (D-4) can be replaced by the conditioning $\{x_1,\cdots,x_n\}$. Thus

$$E[y_{n+1}/y_1,\cdots,y_n] = E[(x_{n+1} - x_n)/x_1,\cdots,x_n] \tag{D-5}$$

$$E[y_{n+1}/y_1,\cdots,y_n] = E[x_{n+1}/x_1,\cdots,x_n] - x_n \tag{D-6}$$

Since the x_n process is a martingale, the right hand side of Eq. (D-6) becomes identically zero and the condition (D-4) immediately follows. Let $x_n = \sum_{i=1}^{n} y_n$ and the y_n's satisfy the condition (D-4), then

$$E[x_{n+1}/x_1,\cdots,x_n] = E[y_1 + \cdots + y_{n+1}/x_1,\cdots,x_n] \tag{D-7}$$

$$E[x_{n+1}/x_1,\cdots,x_n] = E[y_1 + \cdots + y_{n+1}/y_1,\cdots,y_n] \tag{D-8}$$

$$E[x_{n+1}/x_1,\cdots,x_n] = y_1 + \cdots + y_n + E[y_{n+1}/y_1,\cdots,y_n] \tag{D-9}$$

$$E[x_{n+1}/x_1,\cdots,x_n] = y_1 + \cdots + y_n = x_n \tag{D-10}$$

Therefore, the x_n's constitute a martingale and the inverse of the theorem is proved.

<Theorem 2>

Let $\eta,\xi_1,\xi_2,\cdots$ be any random variables with

$$E[|\eta|] < \infty$$

Then, if x_n is defined by

$$x_n = E[\eta/\xi_1,\cdots,\xi_n] \tag{D-11}$$

the x_n process is a martingale.

<Proof>

By definition

$$x_{n+1} = E[\eta/\xi_1,\cdots,\xi_{n+1}] \tag{D-12}$$

Taking the conditional expectation of Eq. (D-12) given the conditioning $\{\xi_1,\cdots,\xi_n\}$, we have in fact

$$E[x_{n+1}/\xi_1,\cdots,\xi_n] = E[E\{\eta/\xi_1,\cdots,\xi_{n+1}\}/\xi_1,\cdots,\xi_n] \tag{D-13}$$

Since the σ-field generated by $\{\xi_1,\cdots,\xi_{n+1}\}$ contains the σ-field generated by $\{\xi_1,\cdots,\xi_n\}$, the smoothing property 4 of Appendix B can be applied to the right hand side of Eq. (D-13). Therefore, Eq. (D-13) becomes

$$E[x_{n+1}/\xi_1,\cdots,\xi_n] = E[\eta/\xi_1,\cdots,\xi_n] = x_n \tag{D-14}$$

with Probability 1. Since $x_1,\cdots,x_n$ are random variables on the sample space of $\xi_1,\cdots,\xi_n$,

$$E[x_{n+1}/x_1,\cdots,x_n,\xi_1,\cdots,\xi_n] = E[x_{n+1}/\xi_1,\cdots,\xi_n] = x_n \tag{D-15}$$

with Probability 1. Taking the conditional expectation of both sides of Eq. (D-15) given $\{x_1,\cdots,x_n\}$ and using the smoothing Property 4 of Appendix B, the martingale property is obtained.

$$E[E\{x_{n+1}/x_1,\cdots,x_n,\xi,\cdots,\xi_n\}/x_1,\cdots,x_n] = E[x_n/x_1,\cdots,x_n] \qquad \text{(D-16)}$$

$$E[x_{n+1}/x_1,\cdots,x_n] = x_n \qquad \text{(D-17)}$$

Therefore, Theorem 2 is proved.

APPENDIX E

TRACE OF MATRIX

Let A be an $(n \times n)$ square matrix and a_{ij} represent the element of i^{th} row and j^{th} column, then the trace of A, denoted by $tr(A)$, is the sum of the diagonal elements of A, and similarily of A^T, i.e.,

$$tr(A) = tr(A^T) = a_{11} + \cdots + a_{nn} = \sum_{i=1}^{n} a_{ii} \qquad (E\text{-}1)$$

<Theorem 3>

Let A be any $(n \times m)$ matrix and a_{ij} represent the element of i^{th} row and j^{th} column, then AA^T and A^TA are $(n \times n)$ and $(m \times m)$ square matrices respectively, and their trace is uniquely determined by the sum of square of elements, a_{ij}^2, i.e.,

$$tr(AA^T) = tr(A^TA) = \sum_{i=1}^{n} \sum_{j=1}^{m} a_{ij}^2 \qquad (E\text{-}2)$$

If A is defined to be

$$A = V - \hat{V} \qquad (E\text{-}3)$$

where V is an $(n \times m)$ matrix with elements v_{ij} and $\hat{V}$ is an approximation of V, with elements $\hat{v}_{ij}$, then A represents the approximation error with elements $(v_{ij} - \hat{v}_{ij})$ and, hence, $tr\,(AA^T)$ is the sum of the square errors, $(v_{ij} - \hat{v}_{ij})^2$. Therefore, $tr(AA^T)$ would be a sensible criteria to be minimized and the solution $\hat{V}$ is the least square error solution. If V is a matrix of random variables v_{ij} and the risk, $trE[AA^T]$ is minimized, then the solution $\hat{V}$ is the minimum variance estimate. Note that V is not necessarily a vector.

APPENDIX F

STOCHASTIC FUNDAMENTAL LEMMAS AND OPTIMALITY CONDITION

<Lemma 1>

If X is a random variable, and if

$$E[XY] = 0 \tag{F-1}$$

for every deterministic Y (or every least fine σ-field measurable random variable) then,

$$E[X] = 0 \quad a.s. \tag{F-2}$$

<Proof>

$$E[XY] = 0$$

$$E[X]Y = 0 \quad a.s.$$

since $Y \neq 0$

$$E[X] = 0 \quad a.s.$$

<Lemma 2>

If X is a random variable, and if

$$E[XY] = 0 \tag{F-3}$$

for every ω-function Y measurable with resepct to the σ-field A of the measurable ω set , then

$$E[X/A] = 0 \quad a.s. \tag{F-4}$$

<Proof>

For the convenience of notation, $\hat{X}$ denotes the conditional expectation $E[X/A]$.

$$E[XY] = E[(X - \hat{X} + \hat{X})Y] \tag{F-5}$$

Applying the smoothing property 4, Eq. (F-5) becomes

$$E[XY] = E[E\{(X - \hat{X})Y/A\}] + E[\hat{X}Y/A] \quad a.s. \tag{F-6}$$

$$E[XY] = E[\hat{X}Y] = 0 \quad a.s. \tag{F-7}$$

Since both $\hat{X}$ and Y are A measurable random variables and Y is arbitrary, it is possible to choose $Y = \hat{X}$, then Eq. (F-7) becomes

$$E[XY] = E[\hat{X}Y] = E[\hat{X}^2] = 0 \quad a.s. \tag{F-8}$$

The above is true only for $\hat{X}^2 = 0$. Therefore,

$$\hat{X} = E[X/A] = 0 \quad a.s.$$

<Lemma 3>

If $X(\omega,t)$ is a stochastic process defined on the set $[t_1,t_2]$ $t\varepsilon[t_1,t_2]$, and if

$$\int_{t_1}^{t_2} E[X(\omega,t)Y(\omega,t)]dt = 0 \tag{F-9}$$

for every random process $Y(\omega,t)$ measurable with respect to a σ-field $A(t)$, $t\varepsilon[t_1,t_2]$, then

$$E[X(\omega,t)/A(t)] = 0 \quad a.s. \tag{F-10}$$

for every t, $t\varepsilon[t_1,t_2]$.

<Proof>

$$\int_{t_1}^{t_2} E[XY]dt = 0$$

$$\int_{t_1}^{t_2} E[E\{XY/A(t)\}]dt = 0 \qquad \text{(F-11)}$$

$$\int_{t_1}^{t_2} E[E\{X/A(t)\} \cdot Y]dt = 0 \qquad \text{(F-12)}$$

Suppose that $E[X(\omega,t)/A(t)] \neq 0$. Since Y is arbitrary $A(t)$ measurable function, we can choose Y such that

$$Y(\omega,t) = E[X(\omega,t)/A(t)] \qquad \text{(F-13)}$$

Therefore, Eq. (F-12) becomes

$$\int_{t_1}^{t_2} E[\{E[X(\omega,t)/A(t)\}^2]dt = 0 \quad \text{a.s.} \qquad \text{(F-14)}$$

The above is positive unless $E[X(\omega,t)/A(t)] = 0$ for any t , $t\varepsilon[t_1,t_2]$. Therefore,

$$E[X(\omega,t)/A(t)] = 0 \quad \text{a.s.} \quad t\varepsilon[t_1,t_2] \qquad \text{(F-15)}$$

Let's consider the following risk function

$$R(g) = trE[(X - g)(X - g)^T] = E[(X - g)^T(X - g)] \qquad \text{(F-16)}$$

where X is an $n\times 1$ vector. If we want to minimize the risk (F-16) with any $\mathcal{B}$-measurable function g , then the solution $\hat{g}$ is the minimum variance estimate. In order to minimize R , we introduce a variation δg on g , i.e.

$$g = \hat{g} + \delta g \qquad \text{(F-17)}$$

Then the risk (F-16) becomes

$$R(\hat{g} + \delta g) = E[(X - \hat{g} + \delta g)^T(X - \hat{g} + \delta g)] \qquad \text{(F-18)}$$

Expanding Eq. (F-18) about $\hat{g}$, the following first variation is obtained.

$$\delta R(\hat{g}) = E[(X - \hat{g})^T \delta g] + E[\delta g^T (X - \hat{g})] \qquad \text{(F-19)}$$

For the minimum of R, the first variation δR must be zero and, hence, the following must be satisfied

$$E[(X - \hat{g})^T \delta g] = 0 \qquad \text{(F-20)}$$

Since a variation δg is an arbitrary $\mathcal{B}$-measurable function, the stochastic fundamental lemma 2 can be applied and the optimality condition therefore is obtained as follows:

$$E[(X - \hat{g})/\mathcal{B}] = 0 \quad \text{a.s.} \qquad \text{(F-21)}$$

$$\hat{g} = E[X/\mathcal{B}] \quad \text{a.s.} \qquad \text{(F-22)}$$

The solution $\hat{g}$ is the minimum variance estimate and is given as the conditional expectation of X given $\mathcal{B}$.

If we want to minimize the risk (F-16) with a linear function of Y which is an $(m \times 1)$ random variable observed, i.e.

$$g = KY \qquad \text{(F-23)}$$

instead of any $\mathcal{B}$-measurable function, then the solution $\hat{g}$ is the linear minimum variance estimate. This time we have to determine an $(n \times m)$ matrix $\hat{K}$ within a class of $\mathcal{B}$-measurable functions such that the risk (F-16) is minimized. Introducing a variation δK on K, the risk (F-16) becomes

$$R(\hat{K} + \delta K) = trE[\{X - (\hat{K} + \delta K)Y\}\{X - (\hat{K} + \delta K)Y\}^T] \qquad \text{(F-24)}$$

Expanding Eq. (F-24) about $\hat{K}$, the first variation follows, i.e.

$$\delta R(\hat{K}) = trE[(X - \hat{K}Y)Y^T \delta K^T] + trE[\delta K Y (X - \hat{K}Y)^T] = 0 \qquad \text{(F-25)}$$

Since δK is an arbitrary $\mathcal{B}$-measurable function, the stochastic fundamental Lemma 2 is applied and the optimality condition is obtained.

$$E[(X - \hat{K}Y)Y^T/\mathcal{B}] = 0 \qquad \text{a.s.} \qquad \text{(F-26)}$$

$$E[XY^T/\mathcal{B}] = \hat{K}E[YY^T/\mathcal{B}] \qquad \text{a.s.} \qquad \text{(F-27)}$$

$$\hat{K} = E[XY^T/\mathcal{B}]\{E[YY^T/\mathcal{B}]\}^{-1} \qquad \text{a.s.} \qquad \text{(F-28)}$$

Therefore, the linear minimum variance estimate is given by

$$\hat{g} = E[XY^T/\mathcal{B}]\{E[YY^T/\mathcal{B}]\}^{-1}Y \qquad \text{(F-29)}$$

For the scalar random variables X and Y, the linear minimum variance estimate $\hat{X}$ is obtained from Eq. (F-29) as follows:

$$\hat{X} = \frac{E[XY/\mathcal{B}]}{E[YY/\mathcal{B}]}\,Y \qquad \text{(F-30)}$$

If we choose K with a deterministic number which is measurable over the least fine σ-field, the conditioning becomes unconditional and the linear minimum variance estimate (F-30) becomes

$$\hat{X} = \frac{E[XY]}{E[YY]}\,Y \qquad \text{(F-31)}$$

BIBLIOGRAPHY

1. Jazwinski, A. H., "Nonlinear Filtering with Discrete Observations", AIAA 3rd Aerospace Science Meeting, AIAA Paper No. 66-38, January, 1966.

2. Jazwinski, A. H., "Filtering for Nonlinear Dynamical Systems", IEEE Trans. Automatic Control 11, 1966, 765-766.

3. Jazwinski, A. H., Stochastic Process and Filtering Theory, Academic Press, 1970.

4. Bucy, R. S., "Nonlinear Filtering Theory", IEEE Trans. On Automatic Control, Vol. 10, April, 1965, pp. 198.

5. Bucy, R. S. and Joseph, P. D., Filtering for Stochastic Processes with Applications to Guidance, Interscience Publishers, New York, 1968.

6. Kalman, R. E., "A New Approach to Linear Filtering and Prediction Problem", Trans. ASME, Ser. D, J. of Basic Engr., Vol. 82, March, 1960, pp. 34-45.

7. Kalman, R. E. and Bucy, R. S., "New Result in Linear Filtering and Prediction Problem", Trans. ASME, Ser. D, J. of Basic Engr., Vol. 83, No. 1, March, 1961, pp. 95-107.

8. Kushner, H. J., "On the Differential Equation Satisfied by Conditional Probability Densities of Markov Process with Applications", J. SIAM, Control, Ser. A, Vol. 2, No. 1, 1962.

9. Kushner, H. J., "On the Dynamic Equations of Conditional Probability Density Functions with Applications to Optimal Stochastic Control Theory", Journal of Math. Analysis and Applications, Vol. 8, No. 2, April, 1964, pp. 332-344.

10. Kushner, H. J., "Approximations to Optimal Nonlinear Filters", IEEE Trans. Automatic Control 12, 1967, 546-556.

11. Kushner, H. J., "On Stochastic Extremum Problems, Part 1, Calculus", Journal of Math. Analysis and Applications, Vol. 10, No. 2, April, 1965.

12. Stratonovich, R. L., "Conditional Markov Process", Theory of Probability and Its Applications, Vol. V, 1960.

13. Bryson A. E., Jr. and Johansen, D. E., "Linear Filtering for Time-Varying Systems Using Measurements Containing Colored Noise", IEEE Trans. on Automatic Control, January, 1965.

14. Mortenson, R. E., "Maximum-Likelihood Recursive Nonlinear Filtering", Journal of Optimization Theory and Applications, Vol. 2, No. 6, 1968.

15. Mortenson, R. E., "Mathematical Problems of Modeling Stochastic Nonlinear Systems", NASA CR-1168.

16. Meir, Lewis, "Combined Optimal Control and Estimation Theory", NASA-CR 426, April, 1966.

17. Schwartz, L. and Stear, E. B., "A Computational Comparison of Several Nonlinear Filters", IEEE Trans. Automatic Control 13, 1968, 83-86.

18. Schwartz, L. and Bass, R. W., "Extensions to Optimal Multichannel Nonlinear Filtering", Report No. SSD 60220R, Hughes Aircraft Company, Space Systems Division, February, 1966.

19. Schwartz, L., "Approximate Continuous Nonlinear Minimal-Variance Filtering", Report No. 18, SSD 60472R, Hughes Aircraft Company, Space Systems Division, December, 1966.

20. Bass, R. W., Norum, V. D. and Schwartz, L., "Optimal Multichannel Nonlinear Filtering", J. Math. Anal. Appl. 16, 1966, 152-164.

21. Detchmendy, D. M. and Sridhas, R., "Sequential Estimation of States and Parameters in Noisy Nonlinear Dynamic Systems", Proc. 1965 Joint Automatic Control Conf., Troy, New York, 1965, pp. 56-63.

22. Fisher, J. R., "Conditional Probability Density Functions and Optimal Nonlinear Estimation", Ph.D. Dissertation, Department of Engineering, University of California, Low Angeles, California, 1966.

23. Fisher, J. R. and Stear, E. B., "Optimal Nonlinear Filtering for Independent Increment Processes - Part I, II", IEEE Trans. on Information Theory, Vol. IT-3, No. 4, October, 1967.

24. Fisher, J. R., "Optimal Nonlinear Filtering", Advan. Control Systems 5, 1967, 198-301.

25. Cox, Henry, "On the Estimation of State Variables and Parameters for Noise Dynamic Systems", IEEE Trans. Automatic Control 9, 1964, 5-12.

26. Mehra, R. K., "A Comparison of Several Nonlinear Filters for Reentry Vehicle Tracking", IEEE Trans. Automatic Control, Vol. AC-16, No. 4, August, 1971.

27. Athans, M., Wishner, R. P. and Bertolini, A., "Suboptimal State for Continuous-Time Nonlinear Systems from Discrete Noise Measurements". 1968 Joint Automatic Control Conf., Ann Arbor, Michigan, June, 1968, pp. 364-382.

28. Jones, D. W., "An Analysis of Approach Navigation Accuracy and Guidance Requirements for the Grand Tour Mission to the Outer Planets", Applied Mechanics Research Laboratory Report No. AMRL-1025, The University of Texas at Austin, August, 1971.

29. Fowler, W. T., Jones, D. W. and Tapley, B. D., "A Fortran Program for Simulating the Orbit Determination Process of an Interplanetary Space Vehicle", Purchase Order No. 371448, Prepared for the General Dynamics, Fort Worth Division by Astrodynamics Research Laboratory, The University of Texas at Austin, Austin, Texas.

30. Ingram, D. S., "Orbit Determination in the Presence of Unmodeled Accelerations", Applied Mechanics Research Laboratory Report No. AMRL-1022, The University of Texas at Austin, Austin, Texas, January, 1971.

31. Alspach, D. L., "A Bayesian Approximation Technique for Estimation and Control of Time Discrete Stochastic Systems", Ph. D. Dissertation, University of California, San Diego, California, 1970.

32. Licht, B. W., "Approximations in Optimal Nonlinear Filtering", Ph.D. Dissertation, Case-Western Reserve University, Cleveland, Ohio.

33. Frost, P. A., "Nonlinear Estimation in Continuous Time Systems", Ph.D. Dissertation, Stanford University, 1968.

34. Loeve Michel, Probability Theory, D. Van Nostrand, Third Edition.

35. Dood, J. L., Stochastic Process, John Wiley and Sons, New York, 1953.

36. Papoulis, Athanasios, Probability, Random Variables and Stochastic Processes, McGraw-Hill.

37. Wax, N., Selected Papers on Noise and Stochastic Processes, Dover Publications, New York, 1954.

38. Feller, William, An Introduction to Probability Theory and Its Applications, Volume 1, John Wiley and Sons.

39. Deutsch, R., Estimation Theory, Prentice-Hall, 1965.

40. Handbook of Mathematical Functions, AMS55, National Bureau of Standards, June, 1964.

41. Lainiotis, D. G., "Joint Detection, Estimation and System Identification", Information and Control, Vol. 19, No. 1, August, 1971.

42. Lainiotis, D. G., "Optimal Nonlinear Estimation", Int. J. Control, 1971, Vol. 14, No. 6, 1137-1148.

43. Ingram, D. S. and Tapley, B. D., "Lunar Orbit Determination in the Presence of Unmodeled Accelerations", Astrodynamics Specialists Conference, 1971, August, 17-19, 1971, Ft. Lauderdale, Florida.